Charles University

Faculty of Science

Department of Biochemistry

Mgr. David Jurnečka

Structural mass spectrometry of *Bordetella* virulence factors

Strukturní hmotnostní spektrometrie faktorů virulence rodu *Bordetella*

DISSERTATION THESIS

Scientific Supervisor: Mgr. Ladislav Bumba, Ph.D.

Institute of Microbiology of the Czech Academy of Sciences

Prague, 2020

Prohlašuji, že jsem tuto práci zpracoval samostatně pod vedením školitele Mgr. Ladislava Bumby, Ph.D. a že jsem uvedl všechny použité informační zdroje a literaturu. Tato práce ani její podstatná část nebyla předložena k získání jiného nebo stejného akademického titulu.

Praha, 30.6.2020 ……

Mgr. David Jurnečka

ACKNOWLEDGEMENT

First of all, I would like to thank all members, present or past, of the Laboratory of Molecular Biology of Bacterial Pathogens of the Institute of Microbiology of the CAS led by prof. Sebo for sharing their experience, knowledge and for fruitful discussions. In particular, my gratitude belongs to Ladislav Bumba, who guided me since my bachelor studies and who shared with me his enthusiasm for science. My special thanks also belong to Petr Man, Petr Novak and Petr Pompach for their invaluable insights to the mass spectrometry techniques. Last but not least, I would like to thank to my family for their support and the patience.

ABSTRACT

The *Bordetellae* are aerobic Gram-negative coccobacilli colonizing the upper respiratory tract of mammals and thereby causing diseases with similar symptoms but different host specificity. The bacteria produce a variety of adhesins and toxins that facilitate their ability to promote infection and evade the innate immune system. Among them, the filamentous hemagglutinin (FHA) and the adenylate cyclase toxin (CyaA) are the major virulence factors providing the adherence to the host epithelial cells and the protection against bactericidal activity of phagocytic cells, respectively. Moreover, CyaA along with the *Escherichia coli* α-hemolysin (HlyA) and the *Kingella kingae* cytotoxin (RtxA) represent a prominent group of Repeats in ToXin (RTX) cytotoxins/hemolysins that undergo post-translational acylation on conserved lysine residues. Here, different mass spectrometry approaches were employed to analyze the structural features of FHA and to characterize the acylation status of the RTX toxins and their various hybrid molecules. First, the differential $^{16}O/^{18}O$ labeling revealed that the mature FHA proteins of *B. pertussis* (Bp-FHA) and the *B. bronchiseptica* (Bb-FHA) are processed at different sites, after Ala_{2348} and Lys_{2479} of the FhaB precursor, respectively. Second, the bottom-up proteomics of the acylated RTX toxins showed that the RTX-activating acyltransferases modifies the RTX protoxin by acyl chains of specific length, which are also involved in proper biological activities of the RTX toxins. Furthermore, the HlyC-activated $CyaA_{1-710}/HlyA_{411-1024}$ hybrid molecule was able to translocate the N-terminal adenylyl cyclase (AC) domain of CyaA to the cell cytosol of LFA-1-expressing cells, indicating that residues 400-710 serve as an “AC translocon” of the CyaA polypeptide.

ABSTRAKT

Bakterie rodu *Bordetella* jsou aerobní gramnegativní kokobacily, které osidlují dýchací trakt u řady savců a tím způsobují různé druhy respiračních onemocnění. Bakterie produkují velké množství adhesivních molekul a toxinů, které se výrazně podílejí na rozvoji infekce a potlačení hostitelského imunitního systému. Mezi hlavní zástupce patří filamentózní hemaglutinin (FHA), který zajišťuje přilnutí bakterie k řasinkovému epitelu hostitele, a adenylát cyklázový toxin (CyaA), který je schopen potlačit baktericidní aktivitu fagocytů. CyaA, společně s α-hemolysinem (HlyA) z *Escherichia coli* a RtxA cytotoxinem z druhu *Kingella kingae*, patří do rozsáhlé skupiny takzvaných Repeats-in-toxin (RTX) cytolysinů/hemolyzinů, které jsou post-translačně modifikovány pomocí acylace konzervovaných lyzinových zbytků. Cílem této práce je strukturně-funkční charakterizace FHA molekul a analýza post-translačních modifikací u RTX toxinů a jejich hybridních variant pomocí hmotnostní spektrometrie. Za prvé, diferenciální izotopické značení $^{16}O/^{18}O$ odhalilo, že C-koncové aminokyseliny vysoce homologních FHA proteinů z *Bordetella pertussis* a *Bordetella bronchiseptica* jsou štěpeny na různých místech, a to v pozici 2348 pro *B. pertussis* a v pozici 2479 pro *B. bronchiseptica*. Za druhé, proteomická analýza tryptických fragmentů acylovaných RTX toxinů ukázala, že post-translační aktivace RTX toxinů je řízena specifickou aktivitou acyltransferáz, které jsou schopny rozlišit různou délku acylového řetězce. Délka mastné kyseliny zároveň určuje biologickou aktivitu acylovaných RTX toxinů. Navíc, hybridní toxin $CyaA_{1-710}/HlyA_{411-1024}$, modifikovaný acyltransferázou HlyC, byl schopen dopravit svoji N-koncovou adenylyl cyklázovou (AC) doménu do cytoplazmy LFA-1-pozitivních buněk, což ukazuje, že aminokyseliny v pozicích 400 až 710 u CyaA se přímo podílí na translokaci AC domény.

TABLE OF CONTENT

LIST OF ABBREVATIONS

Ala	alanine
ACP	acyl carrier protein
ADP	adenosine diphosphate
aP	acellular pertussis vaccine
ApxIA	hemolysin from *Actinobacillus pleuropneumoniae*
ATP	adenosine triphosphate
cAMP	3',5'-cyclic adenosine monophosphate
CR3	complement receptor 3
CRD	carbohydrate recognition domain
CyaA	adenylate cyclase toxin
DNT	dermonecrotic toxin
ECT	extreme C-terminus
EDTA	ethylenediaminetetraacetic acid
Gln	glutamine
FIM	fimbriae
FHA	filamentous hemagglutinin
FT-ICR	Fourier-transform ion cyclotron resonance
HBD	heparin-binding domain
His	histidine
HlyA	α-hemolysin from *Escherichia coli*
ICAM-1	intercellular adhesion molecule 1
kDa	kilodalton
LFA-1	lymphocyte function-associated antigen 1
LOS	lipooligosaccharide
LPS	lipopolysaccharide
Lys	lysine
MALDI	matrix-assisted laser desorption/ionization
MCD	mature C-terminal domain
MS	mass spectrometry
NF-κB	nuclear factor kappa-light-chain-enhancer of activated B cells
NO	nitric oxide

NOS	nitric oxide synthase
Phe	phenylalanine
PRN	pertactin
PRR	proline-rich region
PT	pertussis toxin
RGD	arginine-glycine-aspartic acid motif
RTX	Repeats-in-toxin
RtxA	cytotoxin from *Kingella kingae*
Ser	serine
T1SS	Type 1 secretion system
TCT	tracheal cytotoxin
Th1	T helper type 1
TLR	toll-like receptor
TNF-α	tumor necrosis factor α
TOF	time-of-flight mass analyzer
wP	whole-cell pertussis vaccine

CHAPTER 1

INTRODUCTION

1.1 Bordetellae

Bordetellae are Gram-negative bacteria colonizing the respiratory tract of various animals or humans (Gross, 2010). *B. pertussis*, *B. bronchiseptica* and *B. parapertussis* are closely related species and referred to as “classical *Bordetellae*“. *B. bronchiseptica* causes chronic respiratory infections in a broad range of mammalian hosts with variable severity, but also infects immunocompromised humans [1,2]. *B. pertussis* is an exclusively human pathogen and the causative agent of whooping cough. *B. parapertussis* has two different lineages specific for humans and sheep causing pertussis-like infection with milder symptoms [3]. Both *B. pertussis* and *B. parapertussis* evolved separately from *B. bronchiseptica*-like progenitor primarily by genome reduction indicating specific niche adaptation [4-6].

1.2 Whooping cough

Whooping cough remains one of the least well controlled vaccine-preventable diseases periodically re-emerging even in the developed countries accounting for more than 40 million cases and close to 200,000 pertussis-linked deaths every year [7-9]. Moreover, pertussis constantly circulates even in populations with extremely high vaccine coverage [8,9]. Current resurgence and persistence of whooping cough in global population has been attributed to many factors such as the improvement of diagnostics, increasing number of anti-vaccination movements, rapidly waning mucosal immune response or adaptation of the bacteria to the current vaccination setup [12-14].

Typical pertussis can persist for weeks to months after initial onset and it is characterized by severe paroxysmal coughing with whooping accompanied by episodic choking and vomiting. In young infants and especially unvaccinated newborns, the disease frequently leads to serious complications, such as apnea, pneumonia or pulmonary hypertension, which require hospitalization and intensive care. Macrolide antibiotics including erythromycin or azithromycin are administered to pertussis patients to significantly shorten the duration of symptoms and period of individual contagiousness.

Pertussis caused by different *Bordetella* species can be currently diagnosed by multiple established laboratory methods. Although time-consuming, the gold standard of detection is still considered bacterial culture test followed by matrix-assisted laser

desorption/ionization-time of flight mass spectrometry (MALDI-TOF MS) identification and antimicrobial resistance testing. Real-time polymerase chain reaction (RT-PCR) is often employed due to its rapid diagnosis capacity, however specificity of insertion sequences for individual species targeted for molecular detection must be carefully evaluated due to sequence similarity. Serological tests can also be employed, but at least two weeks after onset of cough when the antibody titers are highest.

Before the introduction of vaccination, whooping cough was the leading cause of infant death, responsible for almost 13% cases in 1930s in children below 10 years of age [12]. First whole-cell pertussis vaccine (wP), which consisted of a suspension of killed *B. pertussis* cells, introduced in the 1950s, significantly decreased the incidence of pertussis infection and infant mortality rate [13]. However, the endotoxin component of the wP vaccine was associated with increased reactogenicity leading to fever, local swelling or eczema. Due to the accumulated public pressure on vaccine manufacturers, a less reactogenic acellular pertussis vaccine (aP) was developed in Japan in 1981 and subsequently introduced to most of the developed countries after year 2000 [4,14]. Current aP vaccines contain up to five different *Bordetella* antigens including pertussis toxin (PT), filamentous hemagglutinin (FHA), pertactin (PRN) and fimbrial proteins (FIM2,3). These antigens were selected to mimic the immune response of a whole-cell vaccine without any adverse effects. Consequently, multiple strains isolated during the last decade have lost the production of pertussis toxin, pertactin or FHA conceivably trying to avoid vaccine-induced clearance by immune system [16-18]. Although all recently isolated specific antigen-deficient strains were found less pathogenic for the adults, they can be still threatening for immuno-compromised patients [17]. Furthermore, aP vaccines prevent critical pulmonary pertussis but fail to induce long-lasting immune protection against infection and transmission of the pathogen [18]. Substantial increase of infection in adolescents and adults throughout the last two decades represent major problem in current pertussis epidemiology situation. Adults are often without major symptoms and provide a reservoir for transmission to the infants who are at the highest risk [19,20]. Recently, an alternative outer-membrane vesicle derived vaccine containing various membrane-bound proteins was successfully tested in mice model inducing strong antibody response [21,22]. However, introduction of a novel vaccine represents substantial

bureaucratic and financial hurdle for the vaccine producers, which rather push repetitive aP boostering.

1.3 Virulence factors of *Bordetellae*

After attachment to mucosal surface in the nasopharynx of the host, the bacteria produce a broad spectrum of virulence factor including adhesins, toxins and immune-modulating factors. Toxins include pertussis toxin (PT), adenylate cyclase toxin (ACT/CyaA), tracheal cytotoxin (TCT) and dermonecrotic toxin (DNT). Critical adhesive molecules are filamentous hemagglutinin (FHA), pertactin (PRN) and fimbriae (FIM). Among other molecules playing an important role in subversion of host immune system are complement resistance factors BrkA and Vag8, type III secretion system (T3SS) or lipooligosaccharide (LOS).

During infection, the bacterial physiology and metabolism are dynamically orchestrated to colonize, invade and survive the immune response in the harsh host environment. Tight coordination of gene expression is thus key to adapt to the site and stage of the infection. Bacteria can efficiently react to availability of various small organic and inorganic molecules, nutrients, physical properties of environment (pH, osmolarity, temperature) or fluctuations in cell-population density, so-called quorum sensing.

1.3.1. BvgAS regulon

Expression of most of the virulence factors is tightly controlled by a master regulatory two-component system BvgAS [23,24]. BvgS is a transmembrane sensor histidine kinase that contains two periplasmically located venus flytrap domains (VFT1 and VFT2), a transmembrane segment followed by a PAS domain, a histidine kinase domain (HK), a receiver domain (Rec) and a histidine phosphoryl transfer domain (Hpt) (Figure 1a). BvgA is a regulatory protein that has an N-terminal Rec and a C-terminal DNA binding helix–turn–helix domain (HTH). BvgS is able to recognize changes in environmental conditions and transduces a signal through a phosphorylation cascade to BvgA, which activates or represses transcription of target genes [25-27]. A precise mechanism of activation of this system *in vivo* is unknown, but under in vitro conditions, the BvgAS system is active at 37°C in standard Steiner-Scholte medium (Bvg^+) and it

can be modulated (Bvg^{i}) or repressed (Bvg^{-}) in the presence of chemical modulators such as nicotinic acid or magnesium sulfate (Figure 2b)[25].

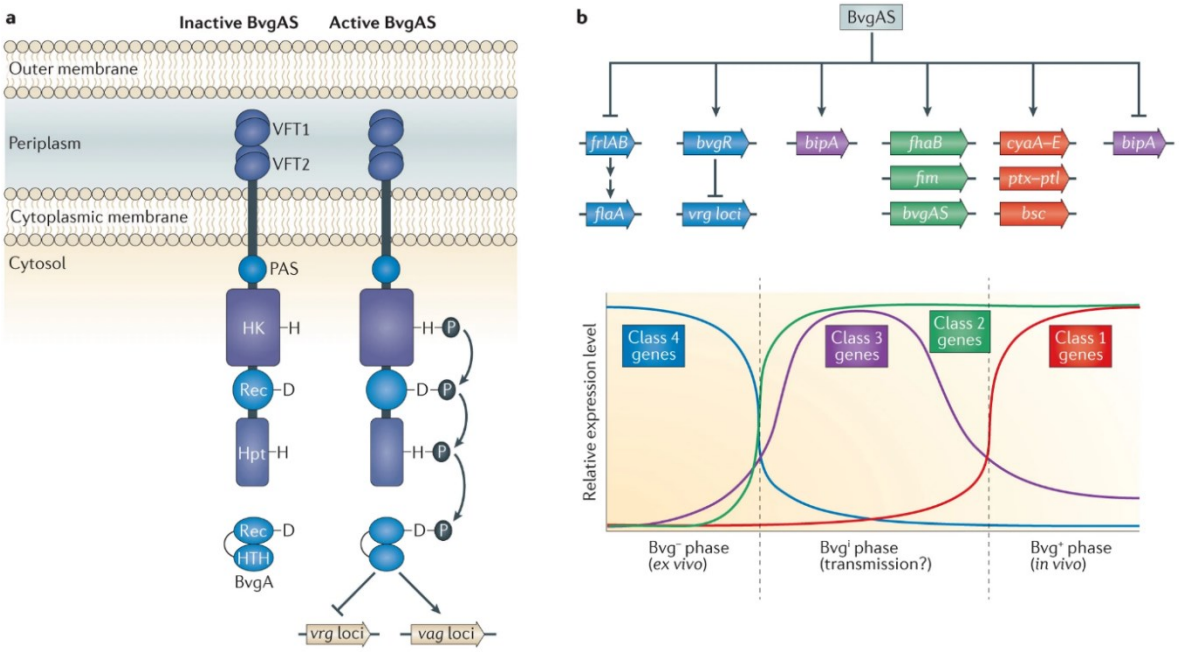

Figure 1. The BvgAS master regulatory system. a. Upon induction by a signal from an external environment, BvgS autophosphorylates and transfer the phosphate group through relay from venus fly trap domains (VFT1, VFT2) towards the Rec domain of BvgA, a DNA binding protein. Phosphorylated BvgA dimerizes and activates the expression of virulence repressed genes (vrgs) or virulence-associated genes (vags) **b.** BvgAS system controls three distinct phenotypic phases conferring four classes of genes. Early levels stages of Bvg^{+} phase enables expression class 2 genes, *fhaB* and *fim*. Higher levels of BvgAS phosphorylation brings up expression of class 1 genes, such as cyaA–E, ptx–ptl and bsc genes. The Bvg− phase occurs when phosphorylation of BvgAS system drops, class 4 genes represented by *frlAB* are inactive leading to positive regulation of motility genes and to repression of bvgR. Partial activation of BvgAS induces the Bvg^{i} phase, where expression of class 2 genes and bipA caps and class 1 and 4 descends [25].

Phosphorylation of BvgA allows its dimerization and transcriptional activation of virulence-associated genes (*vag*) promoters, a crucial step for adaptation and colonization of the host respiratory tract [26,27]. Initial levels of phosphorylation start transcription of early *vag* genes encoding adhesins, such as FHA and fimbriae. Subsequently, operons comprising genes for PT (*ptx-ptl*), ACT (*cyaA-E*) and the type III secretion system (*bsc*) are fully expressed (Bvg^{+}). Additionally, expression of *bvgR* gene maintains repression of the virulence repressed genes (*vrg*) during Bvg active state. Avirulent, Bvg^{-} phase, occurs after rapid loss of BvgA phosphorylation resulting in activation *vrg* [28,29]. Genes for flagellar apparatus, associated with the bacterial

motility, represent the most characterized *vrg* [27,28,30]. Motility was recently found to be mandatory for *B. bronchiseptica* to reach host-intracellular niche [31-33]. Furthermore, Bvg^- phase is required for growth in nutrient-limiting conditions and contributes to survival of *B. bronchiseptica* in external environments [33,34]. There is few information about intermediate state Bvg^i, when BvgS kinase active and inactive states are in equilibrium. Only expression of the *bipA* locus was found to be enhanced during Bvg^i so far. Intermediate state appears to contribute to aerosol transmission of *B. bronchiseptica*, allowing colonization of nasal cavities of various animals [35].

1.3.2. Adhesins

1.3.2.1 Filamentous hemagglutinin (FHA)

Filamentous hemagglutinin (FHA) is a key adhesive molecule mediating the adherence of bacteria to epithelial cells of the lower respiratory tract [40-43]. FHA is synthesized as an FhaB precursor that undergoes a co-secretional maturation, which yields in the release of a "mature" FHA on the cell surface [38]. However, the recent findings indicated that virulence activities of FHA can be attributed to the FhaB precursor.

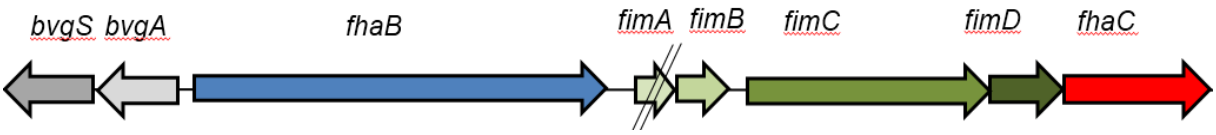

Figure2. Organization of *fha* locus. FHA is encoded by *fhab* followed downstream by *fimB-D* genes, implicated in fimbriae biogenesis. *fhaC*, located downstream of *fimD*, codes for FHA-designated outer membrane transporter. *fimA* is a pseudogene, which shows homology with major fimbrial subunits. Binding regions for the Bvg transcription factors are upstream of the *fhaB* (adapted from [39])

The FhaB preproprotein is encoded by the *fhaB* gene, the leading gene of a polycistronic operon, followed by *fimB-D* genes for fimbriae biosynthesis and *fhaC*, the two-partner secretion (TPS) outer membrane translocon (Figure 2). Albeit the genes for fimbrial subunits are located on the distinct segment of the *Bordetella* genome, *FimB-D* are crucial for their proper folding and transport to the outer membrane. It has been shown that site-directed deletion or insertion within the *fha* locus affects production of both fimbriae and FHA [40,41].

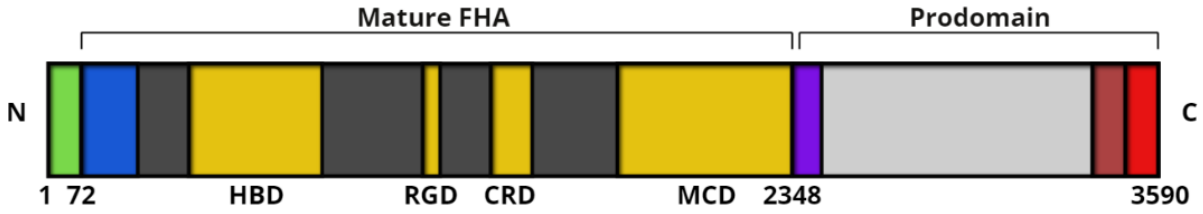

Figure 3. Schematic representation of the FhaB precursor. The very N-terminal part of precursor contains 71 residue-long N-terminal sec-dependent signal (green) followed by two-partner secretion domain (blue). Four different segments in mature FHA segment implicated in binding to various eukaryotic cells (yellow) are: heparin-binding domain (HBD), carbohydrate recognition domain (CRD), Arg-Gly-Asp (RGD) motif and mature C-terminal domain (CMD). Biologically relevant parts of prodomain are prodomain N-terminus (PNT), proline-rich region (dark red) and extreme C-terminus (light red).

FhaB gene of *B.pertussis* (Bp) and *B.bronchiseptica* (Bb) encodes precursor protein of 380 and 370 kDa, respectively (Figure 3). FhaB secretion was extensively studied as a prototypical TPS pathway where the large TpsA exoprotein (FhaB) substrate is translocated through the outer membrane pore protein TpsB (FhaC). FhaB preproprotein is transported across the cytoplasmic membrane via Sec translocon mediated by a 71-residue long N-terminal signal peptide [42]. After the maturation of this extraordinarily long Sec-dependent sequence by a leader peptidase, the N-terminal glutamine residue undergoes cyclization to pyroglutamate (Figure 4,1). Even though this modification relies on the presence of three cysteines in the signal peptide, their substitution to serine residues does not affect FHA production or its hemagglutination activities [43]. The N-terminal FhaB region carrying prototypic TPS domain then transits through periplasmic space in unfolded state to its partner protein FhaC [44,45]. FhaC belongs to an Omp85 protein family consisting of a large transmembrane C-terminal β barrel domain and an N-terminal globular periplasmic polypeptide transport associated (POTRA) domain [46]. After initial recognition of FhaB-TPS segment by FhaC-POTRA domain, FhaB proceeds through FhaC in N- to C-terminal manner keeping the N terminus anchored to POTRA in the periplasm (Figure 4,2). The first ~1800 residues of FhaB are progressively folded during the translocation process to the bacterial cell surface into a rigid β-helical structure, which is further capped by a globular domain known as a mature C-terminal domain (MCD) (Figure 4,3) [47,48]. MCD is located distally from the cell surface and was shown to mediate adherence of *Bordetella* to host cells [36]. After the translocation of MCD

domain FhaB is processed on the cell surface by an autotransporter subtilisin-type serine protease SphB1 (Figure 4,6)[49][50]. SphB1 is anchored by its N-terminal lipid moiety to the bacterial surface and its specific cleavage and subsequent release of FhaB precursor was shown to be important, but not essential, during colonization of the mouse respiratory tract. SphB1-deficient bacterial strain is still able to shed mature FHA, but with lower yields and slightly larger molecular mass [47]. However, the SphB1-mediated cleavage of FhaB does not trigger the release of mature FHA from the bacterial surface and this mechanism is yet to be determined. Mature FHA lacks the C-terminal ~1300 residues of FhaB (FhaB prodomain), which remain in the periplasm and rapidly degraded (Figure 4,5).

Prodomain N-terminus (PNT), located closely to MCD, shares a high homology to the other TpsA proteins and appears to be implicated in the intracellular retention of the FhaB prodomain (Figure 4,4). This leads to a proper maturation and folding of the MCD domain [51]. Although precise mechanism of this action is unknown PNT was proposed to either adapt conformation incompatible with transit through FhaC or control the rate of the prodomain translocation.

Very C-terminal FhaB subdomains are proline-rich region (PRR) and extreme C-terminus (ECT) (Figure 3). PRR contains 27% proline residues and shares 92% similarity, whereas ECT shares 100% homology in all *Bordetella* strains. While PRR and ECT-deficient mutant strains of *B. bronchiseptica* produce equivalent amount of FHA compared to the wild type bacteria, they display reduced persistence in the mouse trachea and lungs upon bacterial infection [52,53]. The ΔECT strain showed accelerated conversion of FhaB to FHA revealing an important role of ECT in the dynamics of FhaB processing. Together these observations indicate, that not only mature form of FHA, but also full-length precursor play a critical role during the *Bordetella* infection [51,52]. The recently updated secretion model of FHA implemented new proteases facilitating prodomain degradation in periplasm (Figure 4,5). Strain lacking periplasmic carboxy-terminal processing protease (CtpA) produces a rather large ~280 kDa FHA intermediate polypeptide, which is conclusively processed by SphB1 on the bacterial surface. CtpA protease successfully targets a large uncharacterized prodomain region (UPD) located between PNT and PRR merely on the background of ECT-deficient mutant strain. ECT is rather conceivably structured

capping segment which has to be removed by unknown P3 protease prior to CtpA-dependent degradation of FhaB prodomain [54].

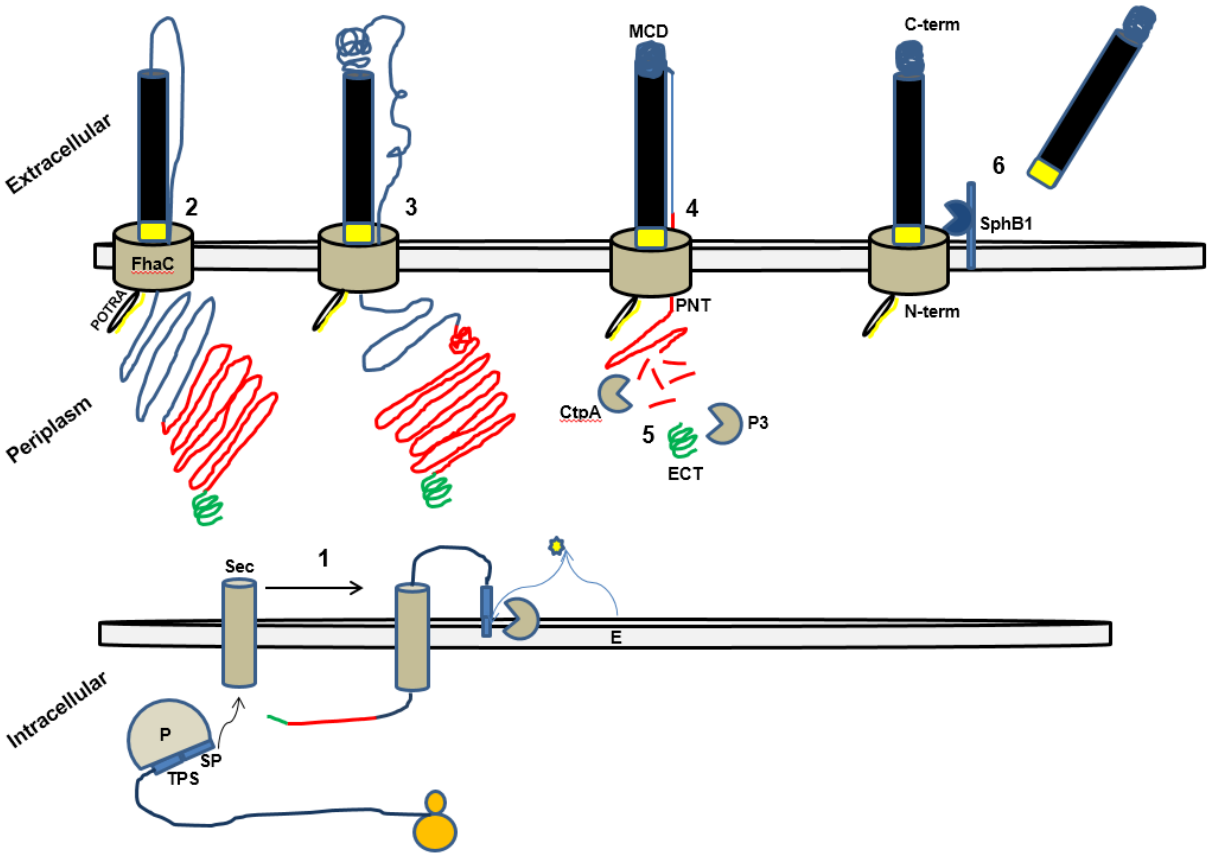

Figure 4. Schematic representation of FhaB biogenesis. FhaB is translated as a 370 kDa preproprotein that is translocated across the cytoplasmic membrane by Sec pathway (**1**). After removal of the 71 aa signal sequence and modification of N-terminal glutamine residue (E), the TPS domain of FhaB interacts with the POTRA domain of FhaC (**2**). Translocation of FhaB proceeds in N- to C- terminal manner (**3**) until stalled by the N-terminus of the prodomain (PNT, **4**). Unknown periplasmic protease (P3) clips the extreme C terminus of FhaB (ECT, green), initiating thorough degradation of the prodomain by the carboxy-terminal processing protease CtpA (**5**). FhaB is processed on the cell surface by the serine protease SphB1 (**6**) to form mature FHA polypeptide, which is either cell-associated or released to the extracellular milieu (adapted from [39]).

FHA was first described as a hairpin-shaped molecule approximately 50 nm in length and 4 nm in width (Figure 5)[48]. Mature FHA protein comprises of two extended repetitive regions R1 and R2 predicted to form β-helix containing three long parallel β-sheets and turns similarly to leucine-rich repeat domains in eukaryotic proteins with diverse functions [55,56]. Crystal structure of TPS domain revealed β-helical fold with

some extrahelical motifs and N-terminal capping formed by non-conserved regions. The solved structure also contained information about the first three repeats from R1 region thus supporting FHA structure prediction because TPS domain initiates folding adapting β-helical scaffold itself (Figure 5) [57].

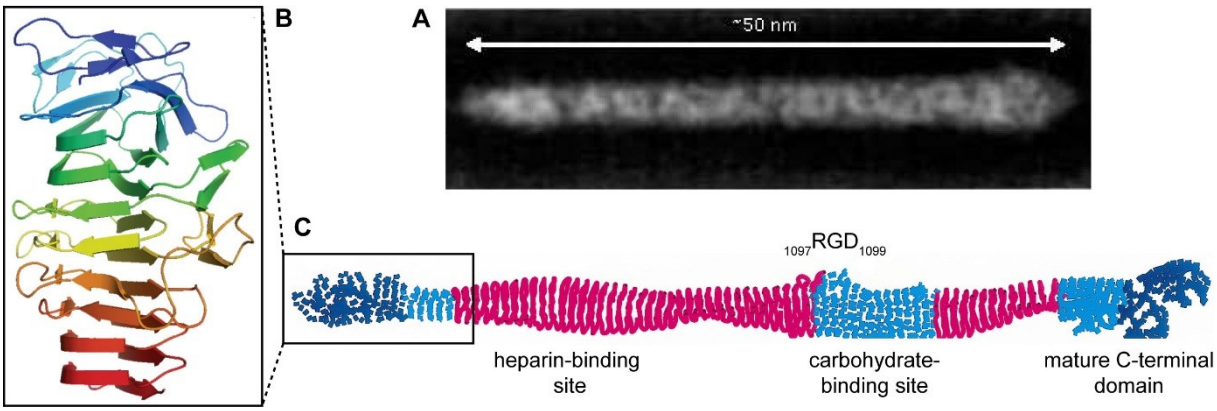

Figure 5. Structural characterization of FHA. A. Electron microscopy of negatively-stained mature FHA. **B.** Crystal structure of a secreted 30 kDa N-terminal fragment of FHA (PDB ID: 1RWR). **C.** The putative model of mature FHA generated by molecular modeling. (adapted from [48,55,57])

The mature FHA comprises four functional domains involved in binding to variety of host cells (Figure 3 in yellow, HBD, RGD, CRD, MCD). Both heparin-binding domain (HBD) and carbohydrate recognition domain (CRD) were accounted for FHA binding via glycolipids and glycoconjugates to a variety of epithelial cells [58,59]. CRD was also proposed to interact with integrin leukocyte molecules, such as the complement receptor 3 (CR3, αMβ2, Mac-1 or CD11b/CD18), the very-late antigen 5 (VLA-5, α5β1, CD49e/CD29) and the complex of the leukocyte response integrin (LRI, αVβ3, CD51/CD61) and the integrin associated protein (IAP, CD47). However, contribution of this domain to pathogenesis using in vivo models remains to be clarified. Arg-Gly-Asp (RGD) motif located around the Gly residue at position 1098 was found to bind VLA-5 fibronectin receptor and trigger NF-κB activation followed by upregulation of ICAM-1 expression and recruitment of inflammatory cells [60–62]. The latter study used epithelial cells treated by soluble FHA instead of whole bacteria showing rather dynamic response of NF-KB pathway to different cell types. Macrophages underwent initial rapid activation followed by suppression after prolonged exposure whereas in bronchial epithelial cells NF-κB pathway was blocked completely at all time points [63]. FHA was also reported to induce secretion of anti-

inflammatory IL-10 cytokine during infection of mice by *B. pertussis* resulting in down-regulation of Th1 response. Nevertheless, recent study demonstrated that high levels of IL-10 and TNF-α were abrogated by the depletion of endotoxin-associated TLR-2 ligands in FHA preparations [64].

FHA confers 90% identity between *B. pertussis* and *B. bronchiseptica* and appears to be functionally interchangeable [36]. Additionally to effects of ΔECT and ΔPRR strains during *in vivo* infections, FHA-deficient *B. bronchiseptica* strains were shown to be hyperinflammatory, causing increased cellular infiltrate around the bronchioles and rapid clearance from airways [65,66]. Moreover, co-infection experiments with the wild-type and FHA-deficient strains revealed an increased persistence in major airways [53]. Taken together, the mature FHA seems to be essential for tight adhesion of *Bordetella* in the alveoli, with the ability to suppress the innate immune response.

1.3.2.2 Fimbriae

Fimbriae, member of type 1 pili, are several hundred nm long filamentous surface-attached molecules facilitating adhesion of *Bordetella* to host cells [67]. They are composed of thousands of major pili subunits grouped into pentameric repeats of either serotype 2 or serotype 3 subunits of about 22 kDa [68]. Minor subunits, encoded by *fim*B-D genes located within FHA locus between *fhaB* and *fhaC* (Figure 6), play a crucial role during fimbriae biogenesis. Current model of pili secretion is based on a similar system extensively studied in uropathogenic *E. coli*. Major and minor subunits are first translocated to the periplasmic space by the Sec system, where a chaperone protein FimB binds the tip protein FimD and this complex is targeted to the outer membrane usher protein FimC. The chaperone then starts to stack major subunits on the gated FimD-FimC complex resulting in elongation and translocation of pili (Figure 6)[53]. Type 1 pili usually form a right-handed rod-like structure that is thought to overcome shear forces and maintain the adhesion of bacteria during the colonization of respiratory epithelia. The role of the other fimbrial subunits (FimA, FimN, FimX) in the *Bordetella* virulence is unknown.

Fimbriae comprises a heparin-binding region that interact with sulfated glucosaminoglycans presented on various mammalian cell types. Although these

regions were found to be immunodominant in both serotype 2 and 3 subunits, comparison revealed homology only on positively charged residues important for binding activity [69]. Together with the fact that *B. pertussis* is able to alter the expression of major subunits by a simple mutation in the promoter region and antibodies raised against the purified proteins show weak cross-reactivity, fimbrial phase variation might help bacteria to evade antibodies impairing binding to ciliated epithelial cells [70,71]. FIM-deficient strain of *B. bronchiseptica* displays reduced capacity to colonize mice respiratory tract, causing increased cellular infiltrate in the alveoli and induce high levels of proinflammatory cytokines and chemokines. Furthermore, FIM appears to mediate initial interaction of bacteria to ciliated epithelia of bronchi and bronchioles [53].

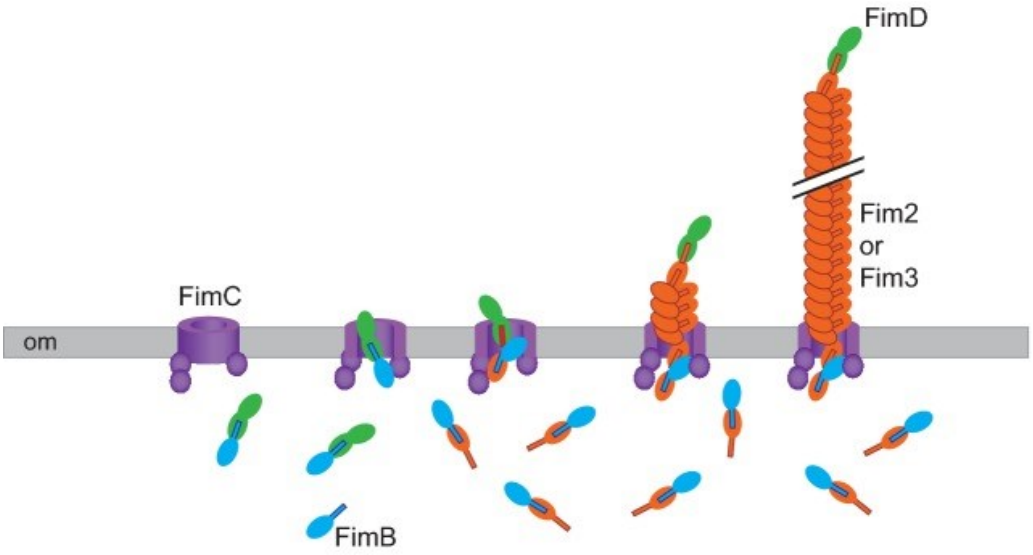

Figure 6. Major fimbrial subunits biogenesis. Upon the secretion of major and minor fimbrial subunits to the periplasm, chaperone protein FimB directs fimbrial tip subunit FimD to the transmembrane β-barrel usher protein FimC, located in the outer membrane (om). FimB then layers the major fimbrial subunits (FIM2/FIM3) on top of each other through the FimC channel, resulting in elongation of the FIM structure (adapted from [53]).

1.3.2.3 Pertactin

Pertactin is a 61 kDa surface-associated highly polymorphic protein, which belongs to a family of autotransporters. The molecular size of the precursor protein is 93 kDa and contains three distinct functional parts, the N-terminal Sec-dependent secretion signal, a central passenger domain, and the C-terminal 30 kDa segment that

form a translocon in the outer membrane. After the Sec-dependent translocation of the precursor to the periplasm, the C-terminal domain is engaged to the outer membrane and passenger domain is self-translocated to the cell surface. Both FHA and pertactin contain RGD motif previously reported to have integrin-binding activity [62,72]. Nevertheless, pertactin does not seem to be required for the colonization of *B. bronchiseptica* in rat model and does not contribute to the adherence of bacteria to macrophage-like or epithelial cell lines *in vitro* [73].

1.3.3 Toxins

1.3.3.1 Pertussis toxin

Pertussis toxin (PT) is a 105 kDa protein complex that belongs to the superfamily of AB_5 exotoxins and is exclusively produced by *B. pertussis* [74]. PT is one of the most complex bacterial toxins consisting of six different subunits defined as S1-S5. S1 is an enzymatically active A subunit sitting on pentamer of remaining B subunits S2-S5 (in ratio 1:1:2:1), which mediate binding and transport of the holotoxin (Figure 7a) [75]. Upon export of the polypeptides via the Sec system pathway, PT is assembled in the periplasm and further secreted by the type IV secretion system (T4SS) [76]. Despite the capacity of PT holotoxin to bind almost any cell-surfaced sialoglycoproteins and glycoproteins on various cells *in vitro*, specific cell types targeted by PT *in vivo* have not yet been identified [77]. Once PT enters the target cell via a receptor-mediated endocytosis, it follows a retrograde transport system to the Golgi apparatus and the endoplasmic reticulum. The S1 subunit is then disassembled from the pentamer through the ATP hydrolysis and disulfide isomerase, and then translocated across the membrane of the vesicle to the cell cytosol. Upon translocation, PT catalyzes the ADP-ribosylation of the α_i subunits of the heterotrimeric G protein. This prevents the G proteins from interacting with G protein-coupled receptors on the cell membrane, thus interfering with intracellular communication. The Gi subunits remain locked in their GDP-bound, inactive state, thus unable to inhibit adenylate cyclase activity, leading to increased cellular concentrations of cAMP (Figure 7b) [78]. Accumulation of cAMP disrupts a variety of essential biological pathways and processes eventually leading to complete dysregulation of the immune response. PT has been shown to inhibit pro-inflammatory chemokine and cytokine production,

reduce recruitment of neutrophils and delay antibody-mediated clearance of *B. pertussis* during early infection [79,80].

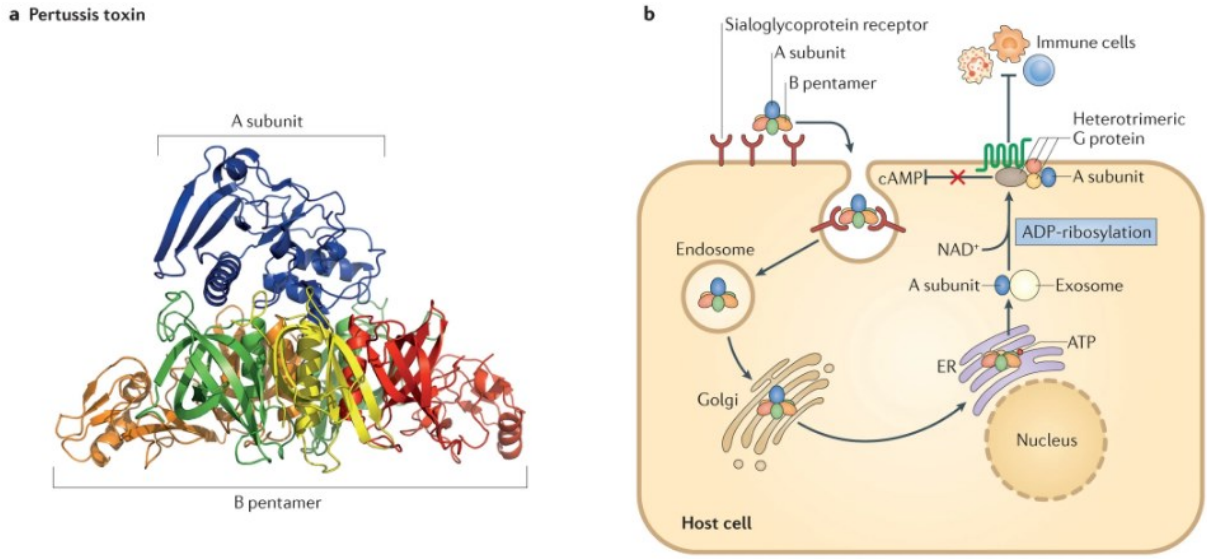

Figure 7. Structure and mechanism of pertussis toxin pathogenesis. **a.** Pertussis toxin (PDB ID: 1PRT) is an AB_5-type toxin that is composed of catalytic A subunit and pentamer of B subunits mediating membrane-binding and transport. PT is assembled in the bacterial periplasm and exported via type IV secretion system. **b.** Upon binding to a sialoglycoprotein on the surface of the host cell receptor, PT is endocytosed and transporter via the Golgi apparatus to the endoplasmic reticulum (ER). B pentamer then binds to ATP and dissociates from the A subunit. The A subunit is then carried by exosome through cytoplasm to the inner side of membrane, where it ADP-ribosylates the α-subunit of heterotrimeric G proteins. This modification inactivates the ability of G proteins to inhibit production of cyclic adenosine monophosphate (cAMP) [25].

1.3.3.2 Dermonecrotic toxin

Dermonecrotic toxin (DNT) is a 159 kDa protein released from *B. pertussis* cells upon lysis. The N-terminal 30 residue long region is essential for binding to target cells followed by putative transmembrane domain between residues 45-144. The 285 residues-long C-terminal forms an enzymatically active domain that exhibits transglutaminase activity [81,82]. Together with the cytotoxic necrotizing factor 1 (CNF1) from *E. coli*, DNT forms a unique family of CNF proteins exhibiting ability to alter host cell actin cytoskeleton. Upon binding to the target cell through its N-terminal region, DNT internalizes via dynamin-dependent endocytosis and liberates enzymatically active domain into the cytoplasm. The transglutaminase activity of the enzyme is involved in polyamination of specific glutamine residues of members of the Rho family GTPases, specifically Gln63 of Rho, Gln61 of Cdc42, and Gln61 of Rac

[83,84]. This modification triggers GTPases in constitutively active state, leading to aberrant organization of the actin cytoskeleton [85–88]. Intradermal administration of DNT into broad variety of animals including pigs, mice or rabbits causes substantial necrosis, while intravenous injection is lethal [89]. Intranasal infection of pigs by *B. bronchiseptica* strain expressing DNT induces nasal turbinate atrophy and fibrinous polyserositis of bronchial ciliated epithelial cells [90].

1.3.3.3 Endotoxin

Endotoxins are complex lipopolysaccharides (LPSs) found as major integral components in the outer membrane of gram-negative bacteria. LPS typically comprises three distinct parts: serospecific O-antigen, core oligosaccharide and the lipid A. The O-antigen is the peripheral part composed of repeating hydrophilic oligosaccharide units stabilized by divalent cations. *B. pertussis* produces distinct shorter version of LPS, called lipooligosaccharide (LOS), completely lacking O-chain [91,92]. The O-antigen of *B. bronchiseptica* and *B. parapertussis* is partially expressed during Bvg^+ phase and is host specific, with isolates from different animals or humans varying in the LOS heterogeneity [93]. Even the bacterial isolates sampled from the same human patient over two years showed variation in LOS profiles during and post-infection [94]. The core oligosaccharide essentially contains 3-deoxy-D-manno-oct-2-ulopyranosonic acid (Kdo) linked through glucosamines to the hydrophobic moiety of lipid A (Figure 8). Acylation pattern of Lipid A can vary according to the bacterial species and the length, position and modification of acyl chains heavily impacts the bacterial membrane permeability and innate immune stimulation of interacting cells [95]. Although LPS or LOS is essentially part of the outer membrane, it can be released from bacterial cell wall during cell division and death or trafficked by outer membrane vesicles. After the release, LPS binds to Toll-like receptor 4 (TLR4/MD2/CD14) presented predominantly on the surface of monocytes, macrophages, dendritic cells and B cells. Downstream signaling promotes expression of pro-inflammatory cytokines (TNF-α, IFN-β) and nitric oxide synthase (NOS), both triggering the immune defense response of the host organism [96–99].

Overall immune response depends on the host receptor structures and their ability to recognize different variants of LPS. Endotoxin of *B. pertussis* and *B. parapertussis* has been shown to stimulate mouse TLR4 receptor complex less

efficiently in comparison to *B. bronchiseptica* and human variant has been found to interact even less [25,100]. These results indicate that human-adapted strains were most probably evolved to be non-inflammatory in humans, facilitating a prolonged persistence in the respiratory tract.

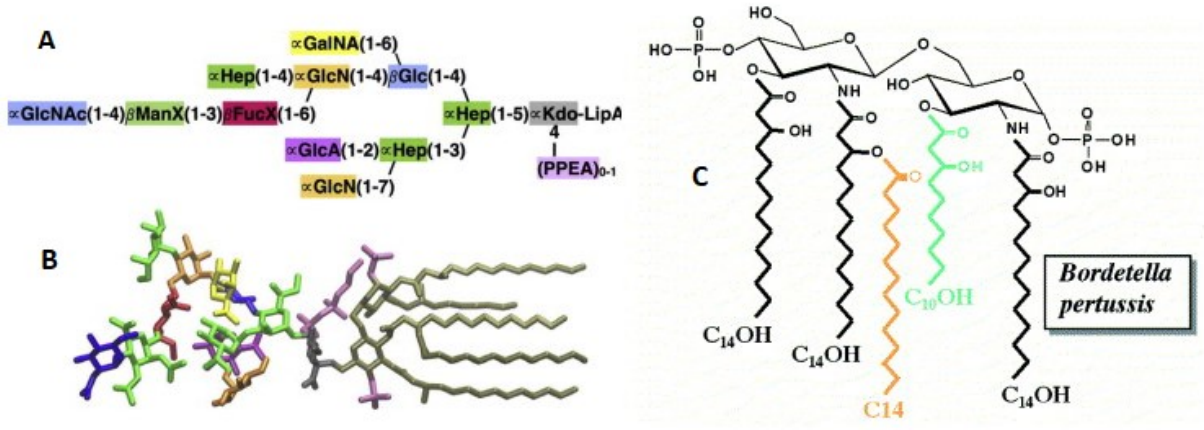

Figure 8. Structure and molecular models of *B. pertussis* LPS. A. Structure of the LPS where ManX: Man2NAc3NAcA, FucX: Fuc2NAc4NMe, GlcNac: N-acetylglukosamin, Hep: L-glycero-D-manno-heptose, GlcA: D-Glucuronic Acid and PPEA: pyrophosphoethanolamine. **B.** Molecular model of LPS (A). **C**. Lipid A structures of *B. pertussis*. Each color indicates different fatty acid.

1.3.3.4 Tracheal cytotoxin

Tracheal cytotoxin (TCT) is a disacharide-tetrapeptide monomer of peptidoglycan commonly produced by all Gram-negative bacteria during cell wall remodeling. It belongs to muramyl peptide family and is composed of N-acetylglucosaminyl-1,6anhydro-N-acetylmuramyl-(L)-alanyl-(D)-glutamyl-esodiamino pimelyl-(D)-alanine [101]. TCT is typically recycled by majority of the bacteria, but in *Bordetella,* it is released during the exponential growth independently of the BvgAS regulation system due to the lack of the integral membrane uptake protein AmpG [102]. TCT along with LOS have been shown to induce IL-1 secretion leading to production of nitrogen oxygen species [103]. High levels of NO radicals then impair the function of iron-dependent enzymes, inhibit host mitochondrial function and DNA synthesis ultimately leading to the destruction of ciliated epithelial cells [104,105]. The role of TCT during *Bordetella* infection in humans remains unknown.

1.4 RTX toxins

Repeats-in-toxin (RTX) exoproteins produced by Gram-negative bacteria represent a large family of proteins, with molecular masses ranging from about 40 to more than 600 kDa. RTX proteins exhibit a wide range of biological and biochemical activities, such as lipolytic, proteolytic, adhesive or cytolytic [106–109]. These proteins share two common characteristics. Primary sequence of RTX proteins contains calcium-binding glycine- and aspartate-rich nonapeptide repeats X-(L/I/F)-X-G-G-X-G-(N/D)-D-X (where X corresponds to any of the residues) located at the C-terminal part and unique mode of secretion via the type I secretion system (T1SS) [110,111]. High content of glycine and aspartate residues also reflects their highly acidic character with pI being around 4 and most of them also lack cysteine residues in their primary sequence.

RTX proteins require calcium ions to obtain proper conformation and activity [112,113]. Acquisition of Ca^{2+} ions by the tandem nonapeptide repeats occurs upon secretion through T1SS from Ca^{2+}-depleted cytosol (< 100nm) into the calcium-rich extracellular milieu (2-4 mM), which promotes folding of RTX blocks into β-rolls [114]. In this structure, first six residues of RTX repeat (GGxGxD) form a regular turn that binds Ca^{2+}, while the remaining three residues forms a short β-strand (Figure 9A) [115]. Calcium is then bound by conserved aspartic acids between two consecutive β-turns. Number of repeats can vary from 3 to more than 50 among different RTX proteins. The approximately 60 residues long very C-terminal part located downstream of RTX repeats, serves as a non-cleavable secretion signal for T1SS [116–118]. The T1SS-mediated secretion proceeds in a single step through a channel composed of three specific proteins: an inner membrane protein with an ABC domain (ABC), a membrane fusion protein (MFP) and an outer membrane protein (OMP) (Figure 9B). These three proteins are able to form a sealed channel-tunnel spanning across both bacterial membranes exporting RTX proteins directly to the external surface without any periplasmic intermediate [110,119]. Low calcium concentration inside cytosol allows transition of protein through a narrow channel in an unfolded state to the bacterial surface [120]. Once the C-terminal segment of the translocating substrate protein interacts with extracellular Ca^{2+}, RTX repeats start to fold into β-roll structure preventing backsliding of polypeptide inside T1SS channel [115].

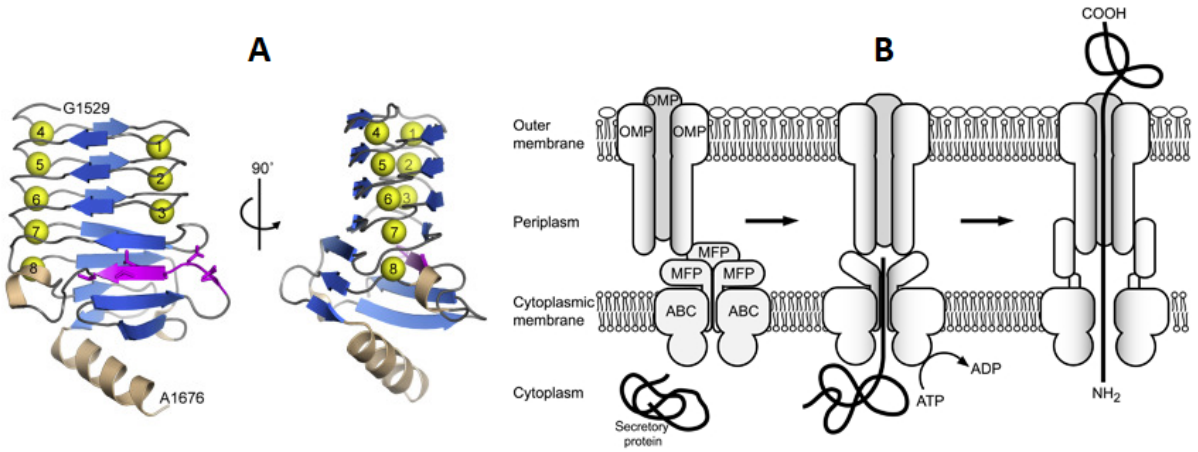

Figure 9. A. X-ray structure of CyaA$_{1529\text{-}1681}$. The N-terminal tandem nonapeptide repeats (GGxGxDxxx) are arranged in a regular right-handed helix of parallel β strands (β-roll). The first six residues of the RTX motif (GGxGxD) constitute a turn with bound calcium ion (yellow ball), while the last three non-conserved residues (xxx) form a short β strand. The TDDALTV segment, located between residues 1636 and 1642, is involved in initiation of Ca^{2+}-induced folding of the RTX domain (magenta) **B.** The schematic representation of the T1SS machinery. Upon recognition of a non-cleavable C-terminal secretion signal of RTX protein, the inner membrane complex formed by ATP binding cassette (ABC) transporter and a membrane fusion protein (MFP) associates with outer membrane protein (OMP). Complex of all three proteins creates channel-tunnel spanning from cytoplasm directly to the extracellular milieu, through which the RTX protein is exported in a single step from without periplasmic intermediate. Low concentration of calcium (< 100 nm) maintains RTX domain in an unfolded state. Upon secretion of C-terminal segment of RTX domain through T1SS channel, acquisition of extracellular calcium ions promotes gradual folding and secretion of RTX protein to the cell surface (adapted from [115,119]).

Pore-forming RTX cytotoxins are produced as inactive protoxins that undergo post-translational activation prior to export from bacterial cytosol. Activation of protoxin is carried out by specific acyltransferase, which catalyze covalent attachment of specific fatty acyl chain to ε-amino group of internal lysine residues [122–124]. Acyltransferases are well conserved among various bacterial genera and some of them were reported to acylate heterologous protoxins indicating redundancy within activation process among different bacterial species [125–128]. The overall biochemistry of activation has been analyzed in detail for the HlyC-mediated activation of the HlyA protoxin from *E. coli* and classified as a double-displacement reaction (ping-pong mechanism) [129]. First, the acyl chain is relocated from an acyl carrier protein (ACP) to the His23 of HlyC through an acyl-imidazole intermediate. Acyl chain is then transferred to the ε-amino nucleophiles of Lys546 and Lys690 of pro HlyA. His23 as well as Ser20 were found to be essential for the catalysis by HlyC and equivalent

residues are also crucial for the *B. pertussis* CyaC acyltransferase [130–132]. Although the acyl groups attached to specific lysine residues of the RTX toxins appear to be necessary for their cytolytic activities, the precise mechanism by which acylation contributes to membrane insertion and formation of pores is still unclear [133–137].

The *rtx* genes and genes encoding T1SS apparatus proteins are usually clustered within a single large *rtx* locus in designated transcriptional order – *rtxC*, *rtxA*, *rtxB* and *rtxD*. Structural gene of the toxin is encoded by *rtxA*, *rtxC* encodes specific acyltransferase, and *rtxB* and *rtxD* encode ABC transporter and MFP, respectively [120,122]. The OMP is in most cases encoded elsewhere on the bacterial chromosome (Figure 10, TolC), implying possible general function in several different transport systems. In the case of *B. pertussis*, it directly follows transcription of MFP (Figure 10, cyaE).

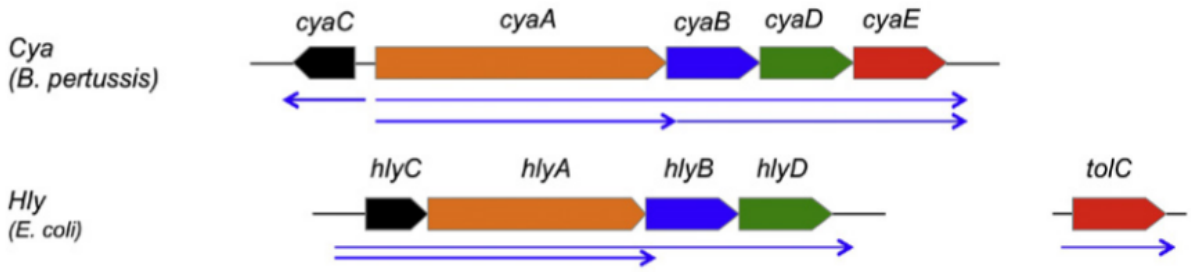

Figure 10. Genetic organization of *Cya* and *Hlya* locus. The *cyaA/HlyA* genes code for the RTX toxins (orange), the *cyaC/hlyC* encodes dedicated acyltransferases (black), the *cyaB/hlyB* genes code for the inner membrane ABC transporters (blue), the *rtxD* genes encodes membrane fusion proteins (MFPs) (green), and the *cyaE/tolC* genes encode the outer membrane proteins (OMPs) (red). The arrows indicate the different transcripts (adapted from [138]).

1.4.1 Adenylate cyclase toxin (CyaA)

Adenylate cyclase toxin (CyaA) is a 177 kDa polypeptide conserved in all pathogenic *Bordetellae* [139]. CyaA consists of an N-terminal 393 residue-long adenylyl cyclase (AC) enzyme domain linked to a 1313 residue-long hemolysin moiety (Hly), which is structurally related to other RTX toxins [140–142]. Hly segment consists of a hydrophobic domain, two post-translationally acylated lysine residues, a C-terminal calcium-binding RTX domain and a C-terminal secretion signal (Figure 11). Lysine residues at positions 860 and 983 are acylated by cognate acyltransferase predominantly by palmitic (C16) and palmitoleic acid (C16:1) [133,135,143,144].

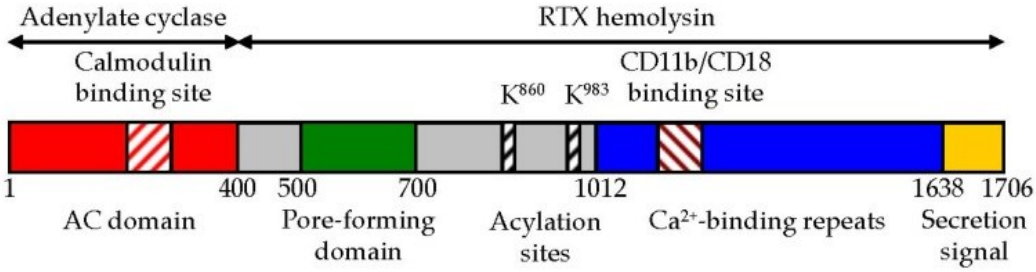

Figure 11. Schematic representation of CyaA. CyaA is a 1706 residue-long polypeptide that comprises an N-terminal AC enzyme domain (~400 residues) and a C-terminal Hly moiety (~1300 residues). The Hly segment composed of multiple functional subdomains: (i) a hydrophobic pore-forming domain (residues 500 to 700); (ii) segment harboring two post-translationally modified lysine residues (K860 and K983); (iii) a typical calcium-binding RTX domain with the CD11b/CD18-binding segment highlighted (residues 1166–1287); and (iv) a C-terminal non-cleavable secretion signal [145].

Upon secretion via the T1SS system, the region between residues 1166 and 1281 mediates binding primarily to heterodimeric integrin $\alpha_M\beta_2$ (CD11b/CD18), also known as complement receptor 3 (CR3) or macrophage-1 antigen (Mac-1) expressed on the surface of many leukocytes [146–148]. However, though with lower efficacy, the toxin can also penetrate almost any host cell without the need for receptor-mediated endocytosis [146,149,150]. After the insertion into the lipid bilayer of target cell membrane, the N-terminal AC domain is delivered directly into the cytosol, where activation by intracellular calmodulin triggers uncontrollable conversion of cellular adenosine triphosphate (ATP) into 3',5'-cyclic adenosine monophosphate (cAMP) [151,152]. Accumulation of cAMP, the key second messenger molecule, leads to subversion of protein kinase A (PKA) signaling pathway and paralysis of the various phagocytic functions, such as oxidative burst and phagocytosis [151]. In parallel, membrane-inserted Hly portion of CyaA can acquire two distinct conformations exerting different biological functions. After the delivery of AC domain, one promotes oligomerization and formation of CyaA pores provoking calcium influx into host cell cytosol, while the other is able to form small oligomeric-cation selective pores (0.6-0.8 nm in diameter) promoting potassium ion efflux and subsequent activation of MAPK signaling (Figure 12) [140,144,153,154]. Synergistic effects of different CyaA actions then lead to apoptosis or necrotic cell death of the phagocytes [150,155,156].

Proper biological activity of CyaA requires structural integrity and co-operation of all domains within Hly moiety including post-translational acylations [141,157,158].

Both the pore forming capacity, as well as ability to translocate AC domain seem to be dependent on the presence of pore-forming hydrophobic domain [141,153,159,160]. Whilst neutral swap of key glutamate residues at positions 509 and 516 had little effect on toxin activities, charge-reversing lysine substitution reduced the capacity to translocate AC domain and enhanced hemolytic and channel-forming capacity on lipid bilayer membranes [154].

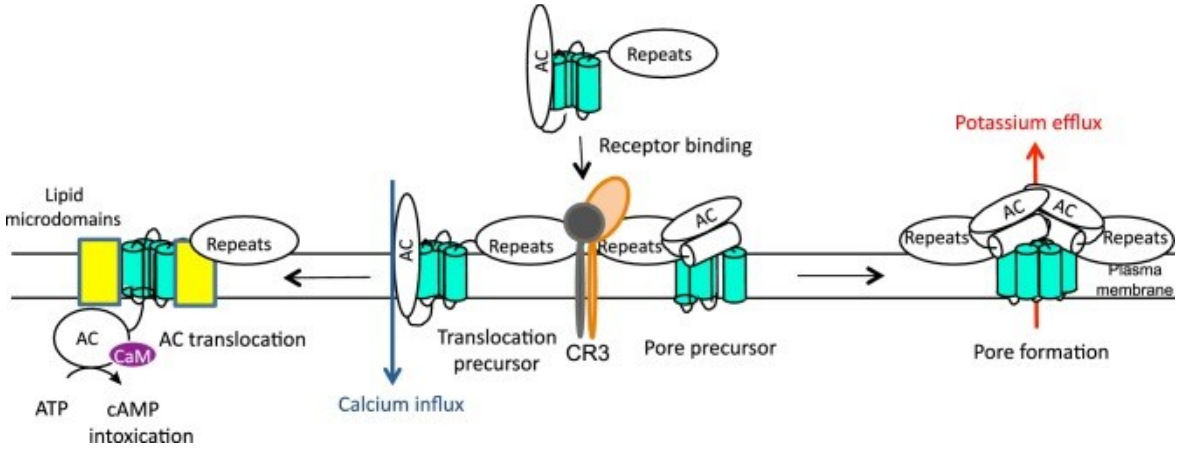

Figure 12. Schematic representation of CyaA action. CyaA initially recognizes complement receptor 3 (CR3), also known as the $\alpha_M\beta_2$, CD11b/CD18 or Mac-1, on the surface of myeloid phagocytes. CyaA employs two different conformer species to exhibit multiple activities. Upon insertion of CyaA into target membrane, one conformer forms pore precursor, allowing oligomerization and provoking potassium efflux from target cell. The other conformer forms translocation precursor, that promotes delivery of the AC domain across the membrane and provokes calcium influx of calcium ions into cell cytosol [148].

Acylation of the native CyaA purified from *B. pertussis* was initially determined by Hackett et al. as palmytoilation on the lysine residue 983 and later on the lysine 860 [143,161]. Monoacylated variants of CyaA prepared by lysine to arginine substitutions exhibited significantly reduced the toxin activity on erythrocytes [136,162]. Nevertheless, production of CyaA with co-expression of mutated variants of CyaC yielding preferentially acylated toxin molecule on either K860 or the K983 revealed, that K860 residue plays rather structural role in biological activity of CyaA independent of its acylation status [132]. Furthermore, modification of K983 as such appears to be critical for toxin activity on both erythrocytes and myeloid phagocytes [132,136].

RTX domain of CyaA is arranged into five distinct blocks (I-V) harboring the typical RTX nonapeptide repeats [163]. Bumba et al. have recently solved the structure of the block V located within residues 1529-1681 comprising the segment initiating

calcium-dependent folding. The C-terminal capping structure folds into antiparallel β strands with a short amphipathic α-helix at the tip, while the N-terminal tandem repeats (GGxGxDxxx) are arranged in a regular right-handed helix of parallel β strand (β-roll) containing buried calcium ions coordinated by carboxyl groups of the aspartic acid side chains (Figure 9A). Assembly of the β-roll structure was found to proceed in a highly cooperative calcium-dependent manner starting from C towards N terminus of the polypeptide [115]. Furthermore, deletion of homologous segments within the central conserved capping motif (Tx+xWF/Y, where + represents a basic amino acid) in other leukotoxins (HlyA, LtxA, ApxIA) abrogated calcium-dependent folding, highlighting central role of the C-terminus of the polypeptides among all RTX toxins [115].

1.4.2 α-hemolysin (HlyA)

The prototypical member of RTX family is α-hemolysin (HlyA), secreted via the T1SS machinery by uropathogenic strains of *E. coli* (UPEC) [164–166]. The *hlyA* gene is a part of the *rtxCABD* operon that encodes the HlyaA protoxin (A), the HlyC acyltransferase (C) and two subunits of the T1SS (B and D) (Figure 10). HlyA is a 110 kDa polypeptide composed of the N-terminal hydrophobic region and the C-terminal RTX segment of 11-17 calcium-binding nonapeptide repeats, responsible for the initial docking to the target cell membrane [167]. The central part of the toxin harbors two lysine residues at positions 564 and 690 that are acylated by myristoylation (C14:0) and hydroxymyristoylation (C14:0-OH) [123,124,168]. Hydrophobic domain is predicted to contain several amphiphilic α-helical structures, which are thought to mediate insertion of HlyA into target cell membrane and involved in formation of transmembrane pores of 2-3 nm in diameter [169]. HlyA has been shown to bind glycophorins presented on the surface of erythrocytes and $\alpha_L\beta_2$ integrin LFA-1 (CD11a/CD18) on macrophages, T- and B-cells and neutrophils [127]. HlyaA can also permeabilize epithelial cell, lipid vesicles and planar lipid membranes showing some degree of promiscuity known for other RTX toxins [169]. HlyA was also reported to enhance exfoliation of the bladder epithelial cells, inducing kidney inflammation and proteolysis of host proteins leading to disruption of cell adhesion and survival pathways [166].

1.4.3 Other RTX toxins

RTX toxins are also produced by other Gram-negative pathogens and commensals of vertebrates belonging to the genus of *Actinobacillus*, *Aggregatibacter*, *Kingella*, *Moraxella*, *Morganella, Photorhabdus*, *Proteus* and *Vibrio*.

Hemolysins homologous to HlyA have been identified in *Morganella morganii*, *Proteus mirabilis* and *Proteus vulgaris*. *Proteus* species are opportunistic human pathogens commonly found in gastrointestinal tract, but also widely distributed in water or manure soil. They are frequently associated with lung and urinary tract infections. *Proteus* PvxA protein and MmxA protein of *M. morganii*, commensal of the intestinal tracts of humans and animals, were found to mimic HlyA pore-forming properties on erythrocytes and lipid-bilayer membranes [153,169–171]. Additionally, hemolytic strains of *M. bovis*, etiologic agent of bovine keratoconjunctivis, release a 110 kDa RTX related toxin MbxA with hemolytic and cytotoxic activities promoting corneal epithelial cell damage [172].

Actinobacillus pleuropneumoniae is a prominent Gram-negative, facultative anaerobic, coccobacillus causing severe pulmonary disease in pigs. Different serotypes of *A. pleuropneumoniae* produce variable combinations of four RTX toxins ApxI-IVA, which appear to some extend to contribute to the pathogenesis of porcine pleuropneumonia [173,174]. Apx toxins I-IIIA are about 50% identical to HlyA and show analogous structural organization displaying variable hemolytic and cytotoxic properties [175–177]. *The* ApxIA toxin is modified by different myristoyl variants (C14:0, C14:0-OH, C14:1, C14:1-OH) on two lysine residues at positions 570 and 696 (unpublished data). Inoculation of pigs with either recombinant ApxIA or ApxIIIA induced formation of hemorrhagic lesions and severe course of disease, whereas ApxIIA was unable to reproduce typical clinical signs. Sequence of ApxIVA resembles autoprocessing RTX protein FrpC from *Neisseria meningitidis*. Albeit antibodies directed against ApxIVA can be found in convalescent pig sera, the role of this protein in *A. pleuropneumoniae* virulence remains to be determined.

Kingella kingae is a facultative anaerobic Gram-negative coccobacillus found in oropharyngeal flora of young children. It has been recently reported as a leading cause of osteomyelitis, endocarditis and septic arthritis in infants [178]. RtxA toxin of *K. kingae* is a 101-kDa protein encoded in the *rtxCABD-TolC* locus [134,179]. RtxA possesses

the typical hydrophobic pore-forming domain, two post-translationally modified lysine residues at positions 558 and 689, the calcium-binding nonapeptide repeats and the very C-terminal T1SS signal. RtxA is able to target and rapidly lyse various human cell types in cholesterol-dependent manner. The cytotoxic activity of RtxA is also tightly linked to the acylation of two lysine residues in the central region of the polypeptide [134].

Most of the RTX toxins target a wide array of mammalian cell lines, however toxins produced by *Aggregatibacter actinomycetemcomitans* and *Pasteurella haemolytica* seem to be very selective. The LtxA leukotoxin of *A. actinomycetemcomitans*, a Gram-negative facultative nonmotile bacterium associated with aggressive periodontitis, kills only leukocytes from humans, rodents and Old world primates [180,181]. LtxA is a 144-kDa polypeptide, identical with ~50% to HlyA, encoded together with its LtxC acyltransferase in the *ltx*CABD operon. LtxA is cell associated in rough and secreted into the culture supernatant by smooth strains of *A. actinomycetemcomitans* [182]. Secretion of LtxA can be completely abolished by free iron or modulated by pH or anaerobic conditions [183]. It is also the only known RTX toxin with basic pI of 8.9. LtxA comprises only of a short RTX domain, post-translationally modified lysine residues at positions 562 and 687 and an N-terminal hydrophobic domain, which contains cholesterol-binding CRAC motifs. Recognition of lymphocytes is facilitated both through membrane lipids and the LFA-1 glycoprotein receptor followed by induction of cell death by variety of mechanisms [184–186]. *M. haemolytica* is a Gram-negative, anaerobic, nonmotile pathogen associated with pneumonia and septicemia in domestic ruminants [187]. It secretes the LktA leukotoxin, a 105 kDa protein largely restricted to ruminant leukocytes and platelets [187–190]. LktA is from 62% identical to HlyA and from 43 % to LktA, sharing all common RTX proteins characteristics. LktA is only monoacylated on the lysine residue at position 554. LktA binds to CD18 subunit of β2 integrin of bovine leukocytes and induces formation of transmembrane pores and cell death [191]. Despite neither the N-terminal hydrophobic segment nor the post-translational acylation is required for binding, they are crucial for cytotoxic activity.

The MARTX represents a unique group of very large RTX toxins found in *Vibrio*, *Aeromonas*, *Proteus*, *Photorhadbus* or *Yersinia* [120,192,193]. They differ from classical RTX toxins by the organization of *rtx* gene cluster, molecular structure and

overall mode of action. The MARTX gene cluster consists of two divergent operons encoding RtxHCA and RtxBDE proteins. RtxA is a large >300 kDa toxin molecule, RtxC is a putative acyltransferase and RtxH is a MARTX-conserved protein of unknown function. RtxB and RtxE are putative ABC transporters, which together with RtxD protein (MFP) and TolC constitute unorthodox T1SS apparatus [194–196]. MARTX toxins contain two RTX motifs with about unusually long repeats located at both the N- and C-termini of the polypeptides. MARTXs do not appear to be functionally dependent on the post-translational modification, but the central part of the proteins contains several effector domains with cysteine protease domain (CPD) being the very C-terminal. Upon translocation to the cytosol of target cell, inositol hexakisphosphate activates CPD, which liberates different effector domains triggering the cytotoxic effects of MARTX, such as cell rounding triggered by actin depolymerization [192,197].

1.5 Mass Spectrometry

Mass spectrometry (MS) is a powerful analytical technique that can ionize a sample and determine the mass-to-charge ratio of the resulting ions. Despite the simplicity of this definition, MS nowadays became steadily growing field utilizing cutting-edge technology for identification of foreign compounds, quantification of unknown materials or studying molecular structure and chemical properties of different molecules. This versatility is given by the fact, that samples in minuscule amounts can be analyzed from the gas, liquid or solid state, and the range of masses that can be studied vary from single atom to multimeric protein complexes. The first mass spectrometer was constructed by J.J. Thompson in 1912, who together with F.W. Aston first measured deviation of mass-to-charge (m/z) ratio of stable isotopes of elements. Gradual implementation of different ionization and fragmentation techniques in the 1960-90s eventually enabled not only identification of larger organic compounds, but also detail determination of their molecular structure [198–203].

Most modern mass spectrometers contain at least three fundamental components: an ion source, a mass analyzer and a detection system. Internal components are maintained under high vacuum to facilitate ion travel, limit possible unwanted ion collision and interference from air molecules (Figure 13). Although there are multiple variations of possible MS instrumentation including home-made

modifications, mostly techniques used to gather datasets implemented within attached manuscripts will be discussed in detail.

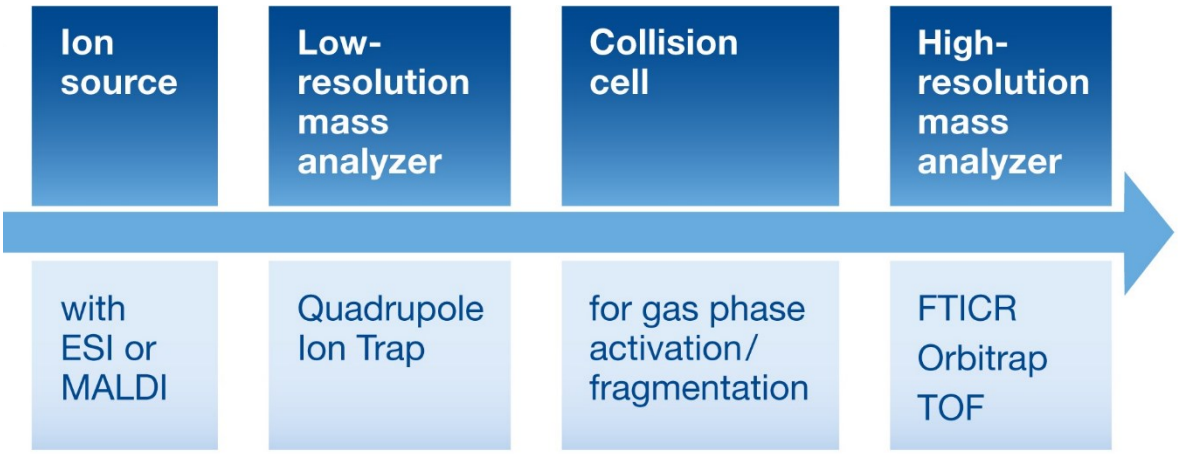

Figure13. Essential components of a mass spectrometer. The ion source facilitates the transfer of the analyte into the gas phase. The low-resolution mass analyzer enables mass selection of specific analyte ion species and, in case of ion traps, may also be utilized for ion activation/fragmentation. Otherwise, gas-phase fragmentation, for example, using CID, HCD, or ETD, takes place in the collision cell. Finally, a high-resolution FT-ICR, TOF, or Orbitrap mass analyzer facilitates precise and accurate mass measurements [204].

The two most widely used methods for ionization of proteins and peptides are matrix-assisted laser desorption/ionization (MALDI) and electrospray ionization (ESI) (Figure 14A). In MALDI, the sample is mixed on a metal target plate with organic matrix molecules, such as α-cyano-4-hydroxycinnamic acid (CAA),2,5-dihydroxybenzoic acid (DHB) or 3,5-dimethoxy4-hydroxycinnamic acid (SA). Desorption and ionization of sample is then induced by laser, generating predominantly single charged ions. In an ESI source, the sample is dissolved in a volatile buffer and inserted into a small capillary that has a high voltage applied to it. The analyte is ionized by desolvation, while passing through heated capillary, ultimately forming multiply charged ions. After the initial ionization of the sample, ions are focused and lead up into a mass analyzer, which separates the ions according to their mass-to-charge ratio. There are many types of mass analyzers with very different operating characteristics each having some tradeoffs. However, the benchmark to select the right instrument for different application depends upon mass resolving power, mass accuracy, scan rate and mass

range. Currently, the most used high-resolution analyzers in biology and biochemistry involve time-of-flight (TOF) tubes, Orbitraps and Fourier transform ion cyclotron resonance (FT-ICR) traps. Despite employing different principles of measurement, all mentioned above can comfortably separate individual masses into the different peptide isotopes, thus determine the peptide charge state. TOF separates ions in time as they travel within flight tube and directly determine their m/z. In FT-ICR MS, the ions are trapped in a magnetic field combined with electric field perpendicular to each other (Penning trap) and excited to perform a cyclotron movement. The cyclotron frequency depends directly on the m/z of the ions. The ion cyclotron resonance signal is then converted to a frequency spectrum using Fourier transformation, which can be calibrated to obtain m/z. Orbitrap instrument is similar to FT-ICR, however, it does not require a magnetic field. Ions are trapped in an electric field generated around spindle-like shaped electrode producing image current converted by Fourier transformation to the m/z. Often two or more mass analyzers are coupled together with some form of fragmentation step to elucidate structural details of analyte, for example, the amino acid sequence of peptide. Fragmentation can occur in the ion source as an undesirable effect, but intentional takes place in a collision cell located between two mass analyzers or within one of them (FT-ICR, ion trap). Current fragmentation methods usually facilitate interaction of precursor ion with neutral particles, photons or electrons leading to homo- or heterolytic cleavage. Fragmentation

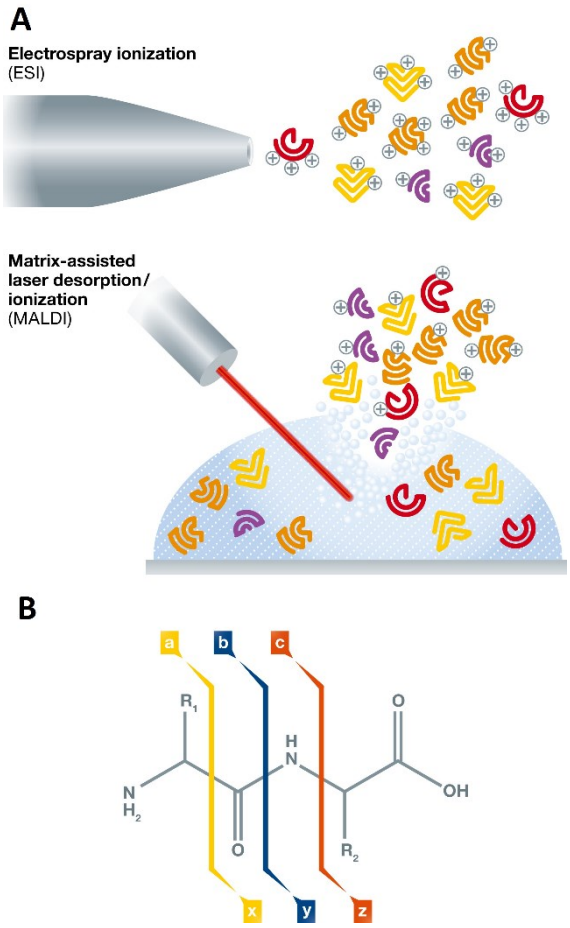

Figure 14. A. The most commonly used ionization techniques in biomolecular MS. ESI produces multiply charged analyte ions (shown in yellow, orange, red, and purple) directly from a sample solution. In MALDI, a laser is used to ablate a mixture of matrix (shown in blue) and analyte molecules from a metal plate into the mass spectrometer, yielding predominantly singly charged ions. **B.** Nomenclature of peptide fragment ions according to Roepstorff and Fohlman [205]. (adapted from [204])

of peptides and denatured proteins typically generates specific backbone cleavage generating a-/x-, b-/y- or c-/z- ion series [205] (Figure 14B). Carbohydrates and nucleic acid create other defined fragmentation patterns [206]. Some of the most popular ion activation/fragmentation techniques are collision-induced dissociation (CID), higher-energy collisional dissociation (HCD) or electron transfer dissociation (ETD). CID and HCD depends on consecutive collisions of accelerated ions with neutral gas (nitrogen, argon, xenon) yielding predominantly b- ions, whereas ETD induces fragmentation of cations by transferring electrons to them producing mostly c- and z- type ions. Fragmentation methods are also widely used for identification of post-translational modifications (PTM). CID/HCD works well for identification of stable PTMs such as acetylation, methylation and glycation, while ETD is recommended for volatile modifications including phosphorylation, glycosylation and ubiquitination. The detector is the final part of MS instrumentation. It generally records either impact of an ion on its surface which is subsequently amplified (micro-channel plate) or, in the case of FT-ICR and Orbitraps, electrical signal of ions passing through pair of electrode plates.

Combination of MS with a range of separation methods contributed to development of two major workflows to identify and characterize proteins. While the “top-down” approach enables characterization of intact proteins using subsequent electron-capture/transfer dissociation, the more common “bottom-up” technique (shotgun proteomics) analyzes peptides raised from proteolytic digestion. Shotgun proteome sequencing enables global-scale protein identification and quantification of complex samples. Protein mixtures are typically digested by protease, trypsin being usually the enzyme of choice, resulting peptides are separated using high-performance liquid chromatography followed by tandem mass spectrometry (MS/MS) analysis. Separation step can be also carried by gas chromatography, capillary electrophoresis or proteins of interest can be excised from SDS-PAGE prior to analysis. Identification of proteins is based on the comparison of generated ion masses with theoretical peptide masses calculated from a database using various searching engines, such as MASCOT, PEAKS Studio or MaxQuant [207–209].

Bottom-up MS can be also coupled with chemical cross-linking (CLMS) or specific surface labeling to probe protein structure, conformation or interactions. CLMS provides direct spatial information about protein-protein interaction creating low resolution three-dimensional structure information or general topology of the protein complex structure often providing complementary information to cryogenic electron

microscopy or X-ray crystallography. Two or more amino acids can be covalently linked via functional groups (-NH_2, -COOH, -SH, -CHO) by crosslinking reagent and subjected to the proteolysis. Since cross-linked peptides constitute only a small part of the total peptide tool, they are often subjected to separation or enrichment step prior to MS/MS analysis. The resulting map of identified CL sites and linked peptides can be computationally processed to obtain structural model of a protein. Surface labeling exploits the capacity of solvent exposed parts of biomolecules to be easily modified by different probing methods, while regions buried in folded protein core remain unaffected. It can be performed by either covalent labeling of amino acid side chains or non-covalently by hydrogen-deuterium exchange (HDX-MS). Typically, HDX-MS analysis consists of three fundamental steps. First, biomolecular assembly is transferred from H_2O- to D_2O- based solution where the solvent-exposed backbone amide hydrogens starts to exchange to deuterium. This process is quenched at different time points by cooling (4°C) and acidification (pH~2.5) and acid-functional non-specific protease, most frequently immobilized pepsin, digests sample for following bottom-up analysis. In contrast to CLMS, defined mass shifts obtained through HDX only monitors overall conformational changes in proteins or protein complexes.

MS represents the very precise qualitative method but cannot be considered inherently quantitative for multiple reasons, such as differing ionization efficiencies among peptides, ion suppression, in-source fragmentation or space charge effect. Intensity of a peak in a spectrum does not reflect the actual amount of the analyte in the sample, hence comparison of intensities between multiple samples reflects relative difference in abundance. The most common approaches to quantify these changes are either label-free quantification strategy (LFQ) or incorporation of isotopic labeling. LFQ approach analyzes separately acquired data and compare them using spectral counting or peak intensity. It is the easiest and the least-time consuming method but needs to be tightly controlled to avoid bias. Stable isotope labeling with amino acids in cell culture (SILAC) is currently the most frequent technique for *in vivo* labeling. Cells are grown in the presence of heavy amino acids ($^{13}C_6$-K and/or $^{13}C_6$-R, in case of trypsin cleavage) and naturally occurring light ones. Cell lysates are combined, digested and constant mass shift between labeled versus non-labeled samples enables quantification of differences. If a sample contains already extracted proteins,

isotope-coded affinity tags (ICAT), isobaric tags (iTRAQ) or ^{18}O stable isotopes labeling is used prior to digestion or MS/MS measurement. ICAT was designed to limit the sample complexity, because the tag consists of sulfhydryl-reactive group only targeting cysteine residues. Mass difference between deuterated and hydrogenated linker segment enables relative quantification. Unlike isotopic tags, heavy and light isotopologues of isobaric tags have identical masses and chemical properties allowing co-elution from LC. They are designed to cleave at a specific linker upon CID, generating different-sized fragments. Another alternative is using protease-catalyzed replacement of two heave oxygen atoms from $H_2{}^{18}O$ on the -COOH group of every newly digested peptide. Drawback of this method is possible non-homogenous labeling of peptides and slow back-exchange of incorporated isotopes after mixing. Absolute quantification using MS can be achieved via spiking known concentration of heavy isotopologues of target peptides into the measured sample. Concentration of the target peptide can be then calculated based on calibration curve determined via single reaction monitoring (SRM).

Concerning general usage of different MS setups across academic and commercial sphere, Orbitrap-based MS systems are predominantly used for high-throughput lipidomics, metabolomics and proteomics studies due to the rapid acquisition of MS/MS spectra. FT-ICR instruments on the other hand offer approximately order of magnitude higher resolution enabling identification of substances in partially defined analytes only based on the precursor m/z. The MALDI-TOF analysis is usually used for rapid identification of biomolecules in rather uncomplex samples or as a diagnostic tool in medicine or microbiology.

CHAPTER 2

RESEARCH AIMS

- To identify the C-terminus of mature FHA proteins from *B. pertussis* and *B. bronchiseptica*

- To develop a new strategy for purification of endotoxin-free RTX toxins

- To determine specificity of RTX-activating acyltransferases during post-translational modification of the RTX protoxins and their hybrid variants

CHAPTER 3

PUBLICATIONS

Publications included in the dissertation thesis

Jurnecka D, Man P, Sebo P, Bumba L. 2018 "*Bordetella pertussis and Bordetella bronchiseptica filamentous hemagglutinins are processed at different sites*." FEBS Open Bio. 2018 Jun 20;8(8):1256-1266. doi: 10.1002/2211-5463.12474.

Stanek O, Masin J, Osicka R, **Jurnecka D**, Osickova A, Sebo P. 2019 "*Rapid Purification of Endotoxin-Free RTX Toxins.*" Toxins (Basel). 2019 Jun 12;11(6):336. doi: 10.3390/toxins11060336.

Osickova A, Khaliq H, Masin J, **Jurnecka D**, Sukova A, Fiser R, Holubova J, Stanek O, Sebo P, Osicka R. 2020 "*Acyltransferase-mediated selection of the length of the fatty acyl chain and of the acylation site governs activation of bacterial RTX toxins.*" J Biol Chem. 2020 May 27: jbc.RA120.014122. doi: 10.1074/jbc.RA120.014122.

Masin J, Osickova A, **Jurnecka D**, Klimova N, Khaliq H, Sebo P, Osicka R. 2020 "*Retargeting from the CR3 to the LFA-1 receptor uncovers the adenylyl cyclase enzyme-translocating segment of Bordetella adenylate cyclase toxin.*" J Biol Chem. 2020 May 11: jbc.RA120.013630. doi: 10.1074/jbc.RA120.013630.

Publications not included in the dissertation thesis

Bayram J, Malcova I, Sinkovec L, Holubova J, Streparola G, **Jurnecka D**, Kucera J, Sedlacek R, Sebo P, Kamanova J "*Cytotoxicity of the effector protein BteA was attenuated in Bordetella pertussis by insertion of an alanine residue*" bioRxiv 2020 April 3: doi: https://doi.org/10.1101/2020.04.03.023549.

CHAPTER 4

Bordetella pertussis and *Bordetella bronchiseptica* filamentous hemagglutinins are processed at different sites

Jurnecka D, Man P, Sebo P, Bumba L.

FEBS Open Bio. 2018 Jun 20;8(8):1256-1266. doi: 10.1002/2211-5463.12474.

4.1 Background

B. pertussis and *B. bronchiseptica* are phylogenetically closely related pathogenic bacteria colonizing the respiratory tract of a wide variety of mammals. While *B. pertussis* is a strictly human-adapted pathogen, *B. bronchiseptica* infects animals, such as rodents, dogs, pigs etc. Among the various virulence factors, both *B. pertussis* and *B. bronchiseptica* produce filamentous hemagglutinin (FHA), an adhesive molecule that is required for attachment of bacteria to host cells.

FHA is first synthesized as a 367 kDa FhaB precursor that is exported from bacterial cytoplasm to the extracellular milieu via the two-partner secretion system (TPS). The general secretion (Sec) pathway facilitates transport to the periplasm using an unusually 71 residue long N-terminal signal sequence [42]. Following the Sec-dependent signal removal, the newly revealed TPS domain interacts with the periplasmic polypeptide transport-associated (POTRA) domain of the outer protein FhaC, initiating the translocation of the FhaB precursor to the cell surface in an N- to C-terminal fashion [46]. During translocation, the FhaB polypeptide is gradually folded into a rigid β-helical structure. FhaB is then processed by a surface-exposed serine protease SphB1, which yields the release of a “mature” FHA into the extracellular milieu [210]. The SphB1-dependent processing was proposed to occur within PLFETRIKFID sequence (residues 2362-2372 of the B. pertussis FhaB precursor), but the exact cleavage site had not been identified [210].

Here, we employed bottom-up proteomic approach coupled with differential $^{16}O/^{18}O$ labeling to determine the C-terminal residues of mature FHA proteins.

4.2 Summary of the results

Affinity chromatography on Cellufine sulfate was used to purify mature FHA proteins from culture supernatants of *B. pertussis* (Bp) and *B. bronchiseptica* (Bb) (Figure 15). Unlike the Bp-FHA preparation, which was almost homogenous, the Bb-FHA preparation contained proteolytic fragments (~ 130, 100 and 75 kDa) that were recognized by a polyclonal anti-FHA antibody (data not shown). To identify the C-terminal residues of purified proteins, the individual protein bands were excised from SDS-PAGE gels and digested with AspN, LysC or trypsin. In parallel, the FHA preparations were also digested in solution and the resulting peptides were analyzed

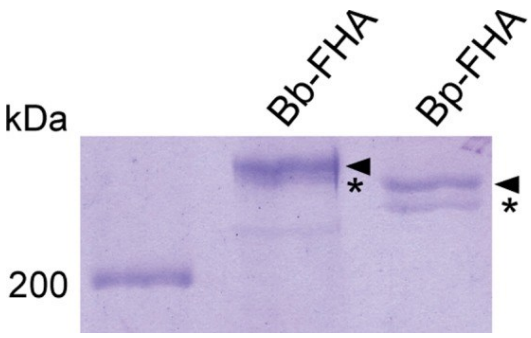

Figure 15. The SDS/PAGE analysis of FHA preparations purified from culture supernatants of *B. pertussis* (Bp-FHA) and *B. bronchiseptica* (Bb-FHA). The mature (FHA, indicated by a triangle) and alternatively processed (FHA_1, indicated by *) forms of FHA are indicated.

by LC-MS/MS followed by MASCOT search. The C-terminal peptides of FHA proteins were determined as peptides that did not match the highly specific cleavage pattern of the used proteases (X-↓-Asp/Glu for AspN; Lys-↓-X for LysC; and Arg/Lys-↓-X for trypsin). The C-terminal residue of Bp-FHA was identified as Ala_{2348}, based on detection of two, namely the AspN peptide $_{2335}$DQPVVAVGLEQPVA_{2348} and the tryptic peptide $_{2300}$NAQVADAGLAGPSAVAAPAVGAADVGVEPVTGDQVDQPVVAVGLEQP VA_{2348}. Similarly, the C terminus of Bp-FHA_1 was identified as Ala_{2228}, based on detection of the LysC peptide $_{2220}$RLDIDDALA_{2228} and of the AspN peptide $_{2214}$DVGL-EKRLDIDDALA_{2228}. The C-terminal residue of Bb-FHA could be identified only tentatively, as Lys_{2479} residue of $_{2446}$QPVVAVGLEQPAAAVRVAPPAV-ALPRPLFETR-IK_{2479}. While N-terminal Glu_{2446} residue of this peptide could have resulted from a rare unspecific AspN-mediated cleavage, it was very unlikely to have cleaved Lys_{2479}-Phe_{2480} bond indicating actual C-terminus of Bb-FHA protein. In contrast, the C-terminal residue of Bb-FHA_1 was unambiguously identified by detection of the $_{2335}$DALAAVLVNPHIF$_{2347}$ and $_{2331}$LDIDDALAAVLVNPHIF$_{2347}$ peptides in the AspN and tryptic digests of Bb-FHA_1.

To verify the identification of the C-terminal residues of Bp-FHA and Bb-FHA proteins, we performed differential stable $^{16}O/^{18}O$ isotope labeling. This technique relies on the enzyme-catalyzed ^{18}O-exchange of typically two ^{16}O atoms on the C-terminal carboxyl group of a newly liberated peptide. As the anticipated C-terminal residue of the digested protein remains unlabeled, the mass difference and isotopical pattern of internal proteolytic fragments permit identification of the peptide that contains the C-terminal residue of the given protein. The isotope envelopes of the $_{2335}$DQPVVAVGLEQPVA_{2348} and $_{2214}$DVGLEKRLDIDDALA_{2228} peptide peaks in

the ^{18}O-labeled AspN digests of the Bp-FHA and of the Bp-FHA$_1$ proteins were identical to that observed for the same peptides in non-labeled digests (Figure 16). The same was true for the $_{2446}$QPVVAVGLEQPAAAVRVAPPAVALPRPLFETRIK$_{2479}$ and $_{2335}$DALAAVLNPHF$_{2347}$ peptides derived from Bb-FHA and Bb-FHA$_1$. In contrast, the isotope envelopes of other peptides in the ^{18}O-labeled AspN digests of Bp-FHA/Bp-FHA$_1$ and Bb-FHA/Bb-FHA$_1$ proteins exhibited the expected mass shifts and 'double peak' patterns.

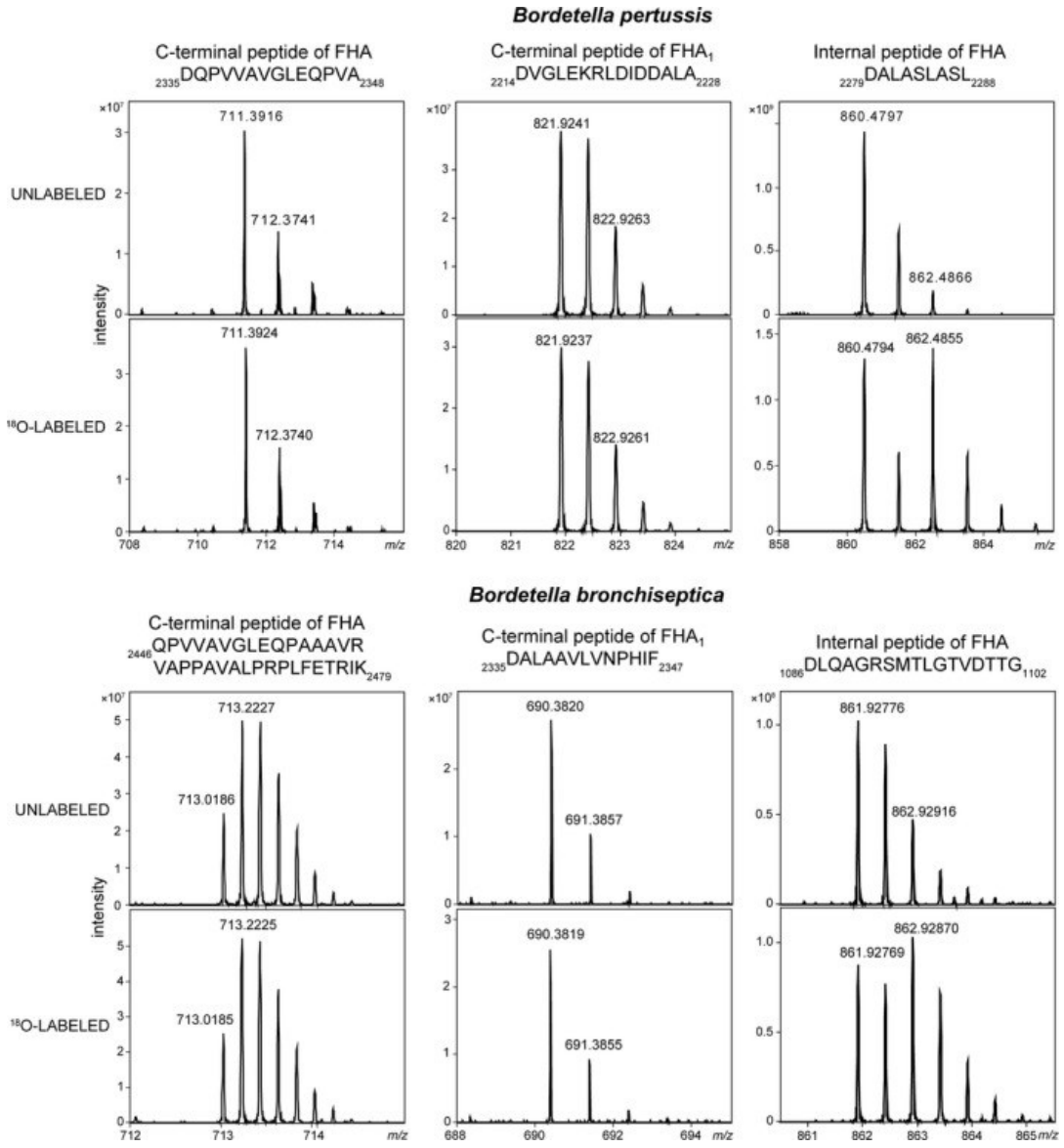

Figure 16. Isotope profiles of the C-terminal peptides of FHA and FHA 1 after enzymatic digestion of Bp-FHA (upper panel) and Bb-FHA (lower panel) with AspN in the presence of normal H_2O (unlabeled) and 50% ^{18}O water (^{18}O-labeled).

Moreover, both FHA preparations also contained peptides originating from different *Bordetella* proteins copurified as contaminants during Cellufine sulfate chromatography. Bp-FHA contained traces of the putative phospholipid-binding protein MlaC, of the toluene tolerance protein Ttg2D, and of the S4 and S5 subunits of pertussis toxin. The Bb-FHA preparation was contaminated by adenylate cyclase toxin (CyaA), the SphB1 protease, and the Bsp22, BteA, and BopD proteins secreted by the type III secretion system.

To gain insight into the specific sequence-structure relationships of the Bp-FHA and Bb-FHA proteins, we performed an on-line digestion of the two proteins on immobilized acid protease columns connected to an LC-MS/MS analyzer. Different protease columns (aspergillopepsin, pepsin, nepenthesin-1, and rhizopuspepsin) along with different times, temperatures of digestion and denaturing agents were tested. Since initial experiments gave low peptide yields with sequence coverage of only 21% (data not shown), we have performed digestion in the presence of denaturing agents to partially destabilize compact fold of FHA proteins. The quantitative analysis

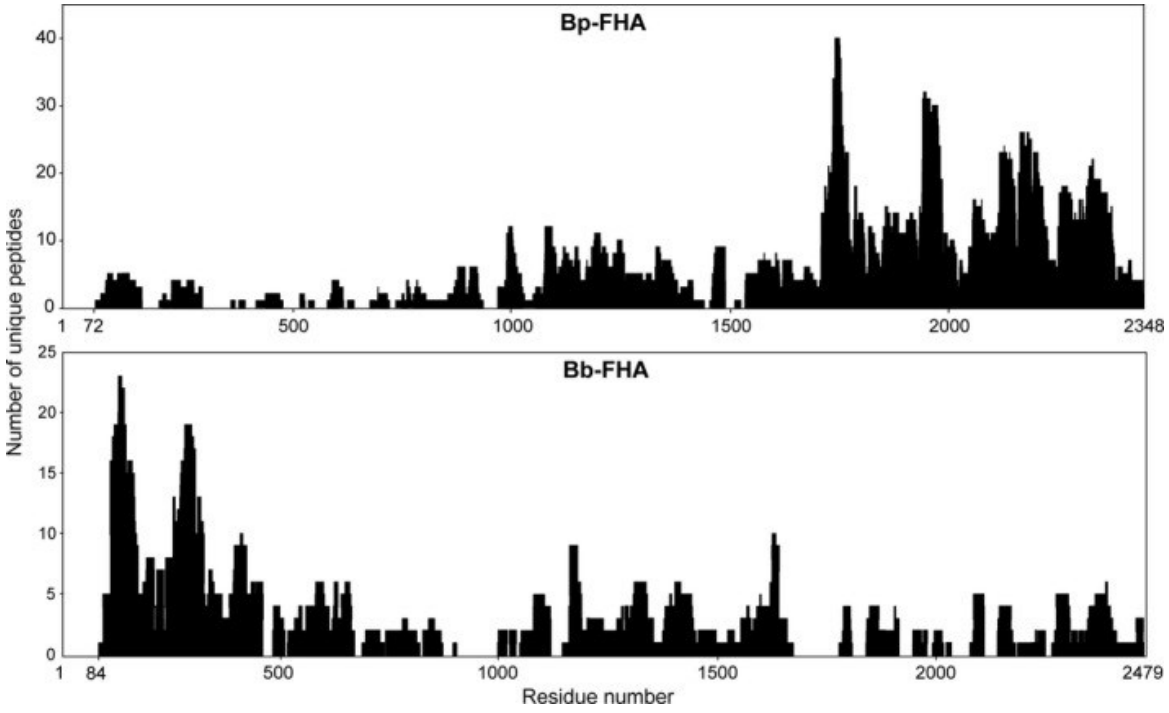

Figure 17. Surface accessibility of Bp-FHA and Bb-FHA probed by on-column (on-line) digestion. The FHA proteins were incubated in the presence of 4 M urea at 50 °C for 30 min and loaded on immobilized protease columns directly coupled to LC-MS/MS analyzer. Frequency of the appearance of individual residues in the covered sequence is plotted as the number of unique peptides against the protein sequence.

of the peptide maps revealed a striking difference in the overall distribution of unique peptides that were generated by on-line digestion of the Bp-FHA and Bb-FHA proteins (Figure 17).

Irrespectively of the protease used, importantly higher number of unique peptides were recovered from the C-terminal segment of Bp-FHA, than from its N-terminal segment, thus indicating a loosened conformation of the C-terminal segment of Bp-FHA. In contrast, the C-terminal segment yielded disproportionally low numbers of unique peptides, indicating a tightly packed structure. Substantially higher numbers of unique peptides were generated from the N-terminal segment of Bb-FHA, which revealed its loosened structure.

Even though both the Bp-FhaB and Bb-FhaB proteins and the SphB1 proteases are highly homologous proteins, we demonstrated that the processing site is not identical, and being shifted about 21 residues on FhaB polypeptides.

4.3 My contribution

I purified Bp-FHA and Bb-FHA proteins from the *Bordetella* cultures, performed in-gel and in-solution digestions and evaluated the LC-MS/MS datasets. I also contributed to the writing of the manuscript.

CHAPTER 5

Rapid Purification of Endotoxin-Free RTX Toxins

Stanek O, Masin J, Osicka R, **Jurnecka D**, Osickova A, Sebo P.

Toxins (Basel). 2019 Jun 12;11(6):336. doi: 10.3390/toxins11060336.

5.1 Background

Repeat in Toxins (RTX) leukotoxins are a large family of pore-forming and immunomodulatory proteins that are produced by Gram-negative bacteria. They share characteristic features including an N-terminal pore-forming hydrophobic domain; a central segment harboring post-translationally acylated lysine residues activated by a cognate acyltransferase; the C-terminal calcium-binding domain comprising glycine-rich nonapeptide repeats; and the non-cleavable very C-terminal secretion signal involved in the secretion of the polypeptide across the inner and outer membrane of the bacterium through the Type I secretion system (T1SS) [121]. Purification of leukotoxins from culture supernatants of respective native pathogens is often limited by their low yields. Recombinant production of RTX toxins together with their cognate activating acyltransferases often generates high amounts of toxin-loaded inclusion bodies, which can be solubilized into 8M urea buffers for further purification under denaturing conditions. Cytolysins then adopt a biologically active form upon folding of RTX domain triggered by ten-fold dilution into a calcium-containing buffer [115]. However, such preparation is typically contaminated by high amounts of *E. coli* outer membrane lipopolysaccharide (LPS). Consequently, many insufficiently purified recombinant proteins were found to trigger TLR4 signaling until their cytokine-inducing activity was associated with LPS contamination [64,211–213].

Therefore, several methods have been developed to remove LPS from protein samples, including a two-phase extraction, chromatography on LPS affinity resins, ion exchange chromatography, membrane adsorption, ultrafiltration and hydrophobic interaction chromatography [214–216]. Here we report a simplified single step purification procedure to obtain large amounts of biologically active LPS-free RTX toxins.

5.2 Summary of the results

We aimed to develop simple a procedure to purify different recombinant LPS-free RTX toxins from inclusion bodies of *E. coli* under denaturing conditions. The whole purification process is performed at room temperature without the risk of protein degradation. We exploited the high affinity interaction of the denatured His-tagged recombinant HlyA, RtxA, and ApxIA proteins with Ni-NTA agarose beads and the strong binding capacity of negatively charged CyaA (pI~4) to DEAE-Sepharose.

Protein extracts were loaded on the respective chromatographic resins and removal of LPS contamination was accomplished by subsequent washing of the columns with 10 bed volumes of either 1% (*v*/*v*) solution of the non-ionic detergents Triton X-100 or 1% (*v*/*v*) Triton X-114 in 8 M urea. The detergent was washed from the resin with 5 bed volumes of the urea buffers. The His-tagged HlyA, RtxA, or ApxIA proteins were recovered by elution with 250 mM imidazole in 8 M urea buffer, while CyaA was eluted from the column with 8 M urea buffer supplemented with 200 mM NaCl. In parallel, purifications of the toxins were also performed in the absence of the detergents.

LPS content was determined by a chromogenic Limulus amebocyte lysate (LAL) assay, yielding 4×10^5 to 1×10^6 endotoxin units (EU) per mg of the protein for control purifications. The engagement of the detergent in the purification protocol reduced the LPS content to ≤115 EU/mg and ≤25 EU/mg for Triton X-100 and Triton X-114 washing steps, respectively. Since the presence of the detergents might interfere with biological activities of the RTX toxins, residual traces of the detergents were quantified by detection of equidistant peaks of the Triton ethoxy groups (44.026 Da) in the matrix-assisted laser desorption ionization-time-of-flight (MALDI-TOF) mass spectrometry (MS) spectra. The sample was considered detergent-free provided that none of detected ions matched potential contaminant TritonX-100/TritonX-114 ion list [217]. Triton X-100 was added to the detergent-free RtxA protein sample in the range of 0.1 to 0.0001% and analyzed by MALDI-TOF MS. As shown in Figure 18 (a–d), Triton X-100 specific peaks were detected in the MALDI-TOF spectra of RtxA samples containing 0.001% or higher Triton X-100 concentrations (Figure 18a-c). In contrast, no such peaks were present in the spectra of the RTX proteins purified without the use of detergent, or in the spectra obtained for the RTX proteins that were purified using Triton X-100 in the column wash solution (Figure 18e–h). Similar MS results were observed when Triton X-114 was used to remove LPS from the RTX toxin preparations. Considering that purified toxins are diluted over 100-fold prior to biological activity assays, the overall amounts of detergent are well below the effective cytolytic concentration and should not hinder proper interpretation of toxin activity. To elucidate whether the toxins purified in the presence of the Triton detergents preserved their biological activities, we also tested the capacity of different CyaA preparations to intoxicate THP-1 monocytic cell line. Equal protein concentrations of the CyaA toxins

purified in the presence or absence of detergents showed similar capacity to deliver the AC domain and raise the concentration of cAMP in monocytes (Figure 19A,B).

Furthermore, the same set of CyaA toxin preparations demonstrated comparable capacity to bind the surface, translocate the AC domain and form hemolytic pores using erythrocytes, lacking the CD11b/CD18 integrin. The removal of LPS achieved by addition of Triton washing steps during purification of HlyA and ApxIA also did not alter their pore-forming activity on erythrocytes. In contrast, cytotoxic activity of the LPS-depleted RtxA toxins tested using the laryngeal HLaC-78 squamous cells, which are exquisitely susceptible to RtxA-mediated killing, was significantly higher than with RtxA protein purified without the use of detergent (Figure 19C). A similar effect was observed when the hemolytic capacity of purified RtxA toxin was assessed on sheep erythrocytes, where the LPS-depleted RtxA proteins were more potent as hemolysins (Figure 19D).

These results indicated that the engagement of detergent washing step represents the rapid and universal approach for purification of recombinant LPS-free RTX toxins. The toxins preserved their biological activity and can be purified to high yields to the very high homogeneity. Moreover, the removal of LPS from RtxA resulted in the increase of the cytotoxic activity of the protein.

5.3 My contribution

I prepared RTX protein samples for MS analysis, measured the MALDI-TOF spectra and interpreted the MS data. I also contributed to the writing of the manuscript.

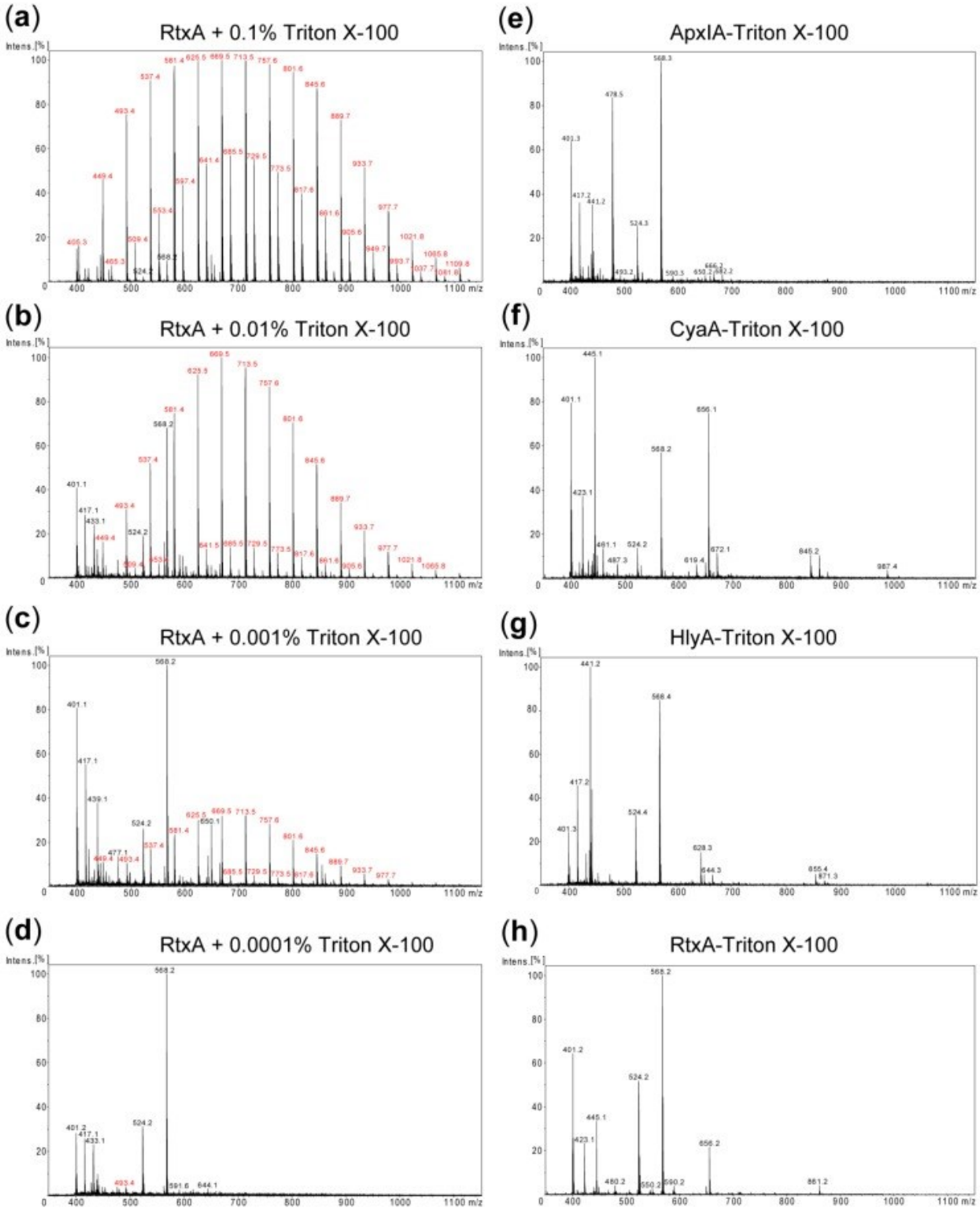

Figure 18. Detection of residual detergent in purified RTX toxin samples. **a**–**d**. RtxA (1 mg/mL) purified without the detergent was spiked with Triton X-100 at concentrations decreasing from 0.1 to 0.0001% and analyzed by matrix-assisted laser desorption ionization-time-of-flight (MALDI-TOF). **e**–**h**. MALDI-TOF spectra of the RTX toxin samples purified using the 1% Triton X-100 column wash. The m/z values of ions corresponding to Triton X-100 components are printed in red. The remaining ions represent adducts of the matrix and other small molecular mass contaminants. In each panel an ion with maximum intensity was taken as 100%.

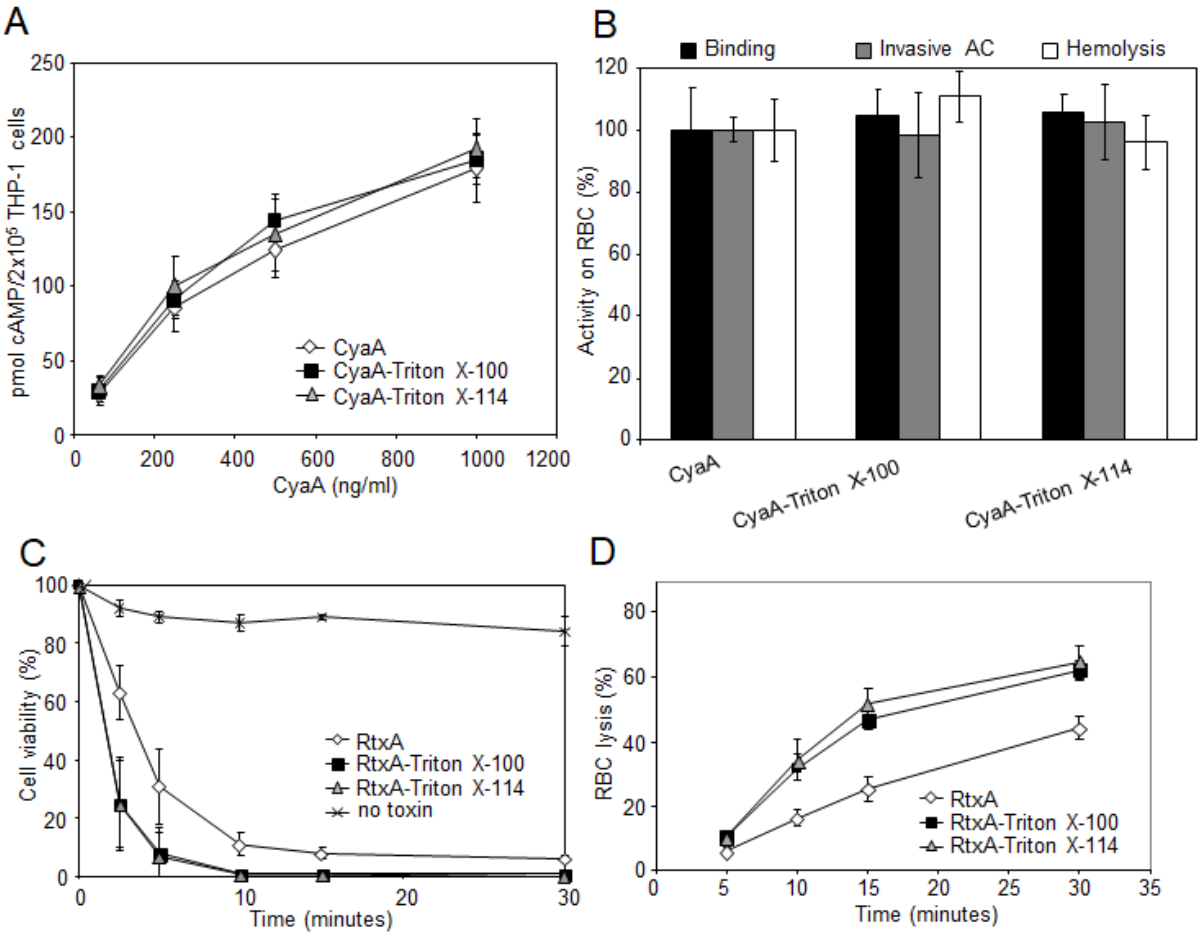

Figure 19. Toxin activities of CyaA purified in the presence or absence of detergent. **A.** CyaA toxin (62.5–1000 ng/mL) purified with or without a 1% Triton X-100 wash of the chromatographic resin was incubated with 2 × 10^5 THP-1 cells and cAMP intoxication was assessed by determining the intracellular concentration of cAMP generated in cells after 30 min of incubation with CyaA. Average values ± standard deviations from three independent experiments performed in duplicates are shown. **B.** Sheep erythrocytes were incubated at 37 °C with 1 µg/mL of the CyaA toxins and after 30 min the cell-associated adenylyl cyclase (AC) activity and the activity of the AC internalized into erythrocytes and protected against digestion by externally added trypsin was measured. For determination of hemolytic activity, sheep erythrocytes (5 × 10^8/mL) were incubated at 37 °C in the presence of 10 µg/mL of the CyaA toxins and erythrocyte lysis was measured after 3 h as the amount of released hemoglobin by photometric determination at 541 nm (A541). Each activity is expressed as percentage relative to the activity of CyaA purified in the absence of Triton and represents average value ± standard deviation from at least two independent determinations performed in duplicates with two different toxin preparations. **C.** HLaC-78 cells (1 × 10^6/mL) were incubated with 1 µg/mL of RtxA for indicated time at 37 °C. Cell viability was determined by a vital dye staining using 1 µg/mL of Hoechst 33258 followed by flow cytometry. The initial viability of cells incubated without RtxA was taken as 100%. Each point represents the mean value ± standard deviation of three independent experiments. **D.** Sheep erythrocytes (5 × 108/mL) were incubated at 37 °C in the presence of 200 ng/mL of RtxA and erythrocyte lysis was measured as above.

CHAPTER 6

Acyltransferase-mediated selection of the length of the fatty acyl chain and of the acylation site governs activation of bacterial RTX toxins

Osickova A, Khaliq H, Masin J, **Jurnecka D**, Sukova A, Fiser R, Holubova J, Stanek O, Sebo P, Osicka R.

J Biol Chem. 2020 May 27: jbc.RA120.014122. doi: 10.1074/jbc.RA120.014122.

6.1 Background

Repeats in ToXin (RTX) cytolysins, produced by a broad range of Gram-negative bacteria, form a large family of proteins that are synthesized as inactive protoxins and undergo activation by post-translational fatty-acylation on ε-amino groups of two internal conserved lysine residues [124,157,161]. The *E. coli* HlyA hemolysin and the *K. kingae* RtxA cytotoxin were found to be acylated predominantly by myristoyl chains (C14:0) on the lysine residues K564, K569 and K558, K689, respectively [134, 168]. In contrast, *B. pertussis* CyaA was found to be principally modified by palmitoylation (C16:0) or palmitoleylation (C16:1) on the internal lysine residues K860 and K983 [143,162,218]. Although acylation status of the toxin molecules seems to be essential for all their known cytotoxic activities, the molecular mechanism by which acyl chains contribute to membrane insertion and formation of pores is unknown. RTX toxin–activating acyltransferases are highly homologous and appear to be promiscuous in acylation of various RTX protoxins. For example, the HlyC-activated ApxIA hemolysin of *A. pleuropneumoniae*, as well as the ApxC-activated HlyA expressed in *E. coli*, exhibited a hemolytic activity on erythrocytes [219,220]. Comparably, the heterologously CyaC- or HlyC-modified *P. hemolytica* leukotoxin LktA exhibited the same target cell specificity and biological activity as the LktA modified by its cognate LktC acyltransferase. The activation was however not reciprocal, as the LktC-activated CyaA and HlyA produced in *E. coli* were neither cytotoxic nor hemolytic [128,221]. It is still unknown, why some RTX protoxins are efficiently cross-activated by heterologous acyltransferases and some are not.

Here we analyzed the activation of the HlyA, RtxA and CyaA toxins, each acylated by either of the three HlyC, RtxC or CyaC acyltransferases and produced in the same *E. coli* strain background, to exclude the potential effect of different bacterial acyl-ACP pools. We also examined biological properties of differently activated toxins on respective targets.

6.2 Summary of the results

To determine the fatty-acyl group and acylation site selectivity of the three homologous RTX toxin–activating acyltransferases, a total of nine pairwise combinations of the three protoxins proCyaA, proHlyA, and proRtxA with the three acyltransferase enzymes CyaC, HlyC, and RtxC were co-expressed in *E. coli*. The

individual toxin molecules were purified from the urea-solubilized inclusion bodies by affinity chromatography on calmodulin-Sepharose (CyaA proteins) or Ni-NTA agarose (HlyA and RtxA proteins) and their acylation status was analyzed by a Fourier transform ion cyclotron resonance (FT-ICR) mass spectrometry. Results of the analysis are summarized in Table 1 and Figure 21.

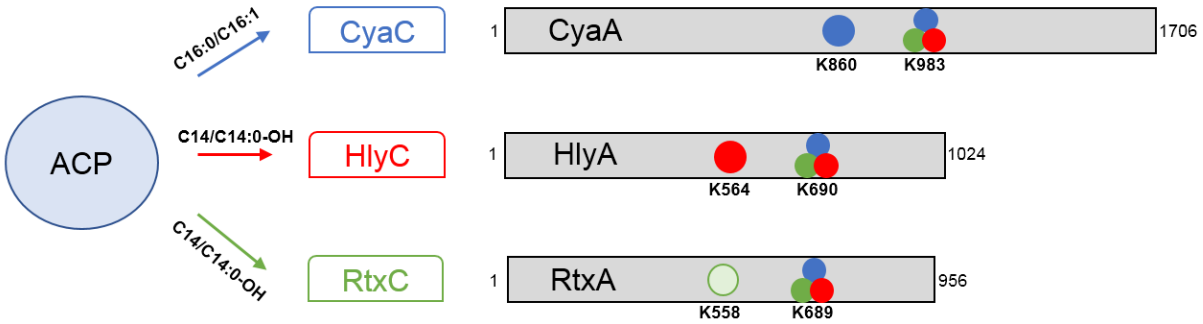

Figure 21. Schematic representation of acylation status of lysine residues of the CyaA (K860, K983), HlyA (K564, K690) and RtxA (K558, K689) proteins produced in the presence of the RTXC acyltransferases. Site selectivity of CyaC (C16:0/C16:1, blue), HlyC (C14:0/C14:0-OH, red) and RtxC (C14:0/C14:0-OH, green) for different toxin molecules is depicted as colored dots. Acylation of the K558 residue of the RtxA variants was almost negligible (feint green).

In agreement with previously published data, the $CyaA_{CyaC}$ toxin activated by its cognate acyltransferase CyaC was modified predominantly by palmitoyl (C16:0) and palmitoleyl (C16:1) chains at the K860 (~66%) and K983 (~88%) residues. In addition, minor portion of myristoyl (C14:0) and octadecenoyl (C18:1) was also detected at the K860 (~3%) and K983 (~11%) residues. While only ~31% of the K860 residues remained unacylated by CyaC, the K983 residue of $CyaA_{CyaC}$ was acylated almost completely (~99%). In contrast, when proCyaA was produced in the presence of HlyC or RtxC, the acylation of the K860 was abolished (1% in $CyaA_{HlyC}$ and 0% in $CyaA_{RtxC}$). The second acylation site, K983 residue, was successfully modified by HlyC and RtxC almost exclusively by shorter myristoyl (C14:0) and hydroxymyristoyl (C14:0-OH) chains (~77% in $CyaA_{HlyC}$ and ~85% in $CyaA_{RtxC}$). The C16:0 and C16:1 chains, native to CyaC system, formed only a minor proportion of the acyl chains linked to the K983 residue (~3% in $CyaA_{HlyC}$ and ~8% in $CyaA_{RtxC}$). The $HlyA_{HlyC}$ toxin was activated by its cognate acyltransferase HlyC with the C14:0 and C14:0-OH acyl chains at the K564 (~84%) and K690 (~93%) residues. Small portion of the K564 was modified with the C12:0, C12:0-OH, C16:0 and C16:1 chains (~6% at K564 and 7% at K690) or remained unacylated (~10%). When HlyA was activated by the heterologous acyltransferase

RtxC, the C14:0 and C14:0-OH chains were also the primary acyl groups attached to the K564 (~26%) and K690 (~95%) residues, but major portion of K564 residue remained unacylated (~73%). Intriguingly, the heterologous acyltransferase CyaC acylated the K690 residues of the HlyA molecules principally with the C16:0 and C16:1 (~90%) acyl chains and partially with C18:1 (~10%), while the K564 residue remained mostly unacylated (~93%) with small amounts of the C16:0 and C16:1 acyl groups (~7%). Finally, the RtxA cytotoxin was activated by its cognate acyltransferase RtxC, and also by the heterologous HlyC acyltransferase at the K689 residue almost exclusively with the C14:0 and C14:0-OH acyl chains (~91% in $RtxA_{RtxC}$ and ~96% in $RtxA_{HlyC}$). Similarly to $HlyA_{CyaC}$ system, CyaC promoted modification of the K689 residue of RtxA with the C16:0 and C16:1 acyl groups (~89%). In contrast, the K558 residue of the RtxA variants was activated by almost negligible amounts of the C14:0 and C14:0-OH chains (~2% in $RtxA_{RtxC}$ and ~3% in $RtxA_{HlyC}$) or remained completely unacylated ($RtxA_{CyaC}$). These results indicate that the different acyltransferases specifically select acyl groups of various lengths. CyaC selected from the *E. coli* acyl-ACP pool almost exclusively the C16:0 and C16:1 acyl chains for acylation of the protoxin substrates. On the other hand, the HlyC and RtxC acyltransferases selected predominantly the shorter C14:0 and C14:0-OH chains for activation of all three protoxin substrates. Moreover, acyltransferases seem to recognize and modify the distal, more conserved acylation sites of heterologous protoxins, more efficiently than the proximal, which was found to be almost nonacylated.

The defined acylation status of the toxin variants enabled us to resolve how the single or double acylation and the length of the attached acyl chains corelates with the biological activities of these proteins. First, we determined the capacity of differently acylated CyaA variants to bind, penetrate and lyze sheep erythrocytes, lacking the CyaA receptor CR3 (CD11b/CD18). Monoacylated variants, harboring C14:0 or C14:0-OH chains on K983 residue, exhibited reduced capacity of $CyaA_{HlyC}$ (by ~62%) and $CyaA_{RtxC}$ (by ~70%) to bind erythrocytes and cell-invasive capacity to deliver AC domain was decreased even more (by ~94%) in comparison to the fully C16:0 and/or C16:1 acylated $CyaA_{CyaC}$ protein (Figure 20A). The $CyaA_{HlyC}$ and $CyaA_{RtxC}$ proteins were also not able to provoke erythrocyte lysis, while $CyaA_{CyaC}$ was able completely lyse erythrocytes within 5 hours of incubation (Figure 20B). Moreover, lytic and invasive capacities of monoacylated variants remained very low even after 2.5-fold increase in

concentration over the $CyaA_{CyaC}$ toxin. Capacity to bind and translocate the AC domain to mouse J774A.1 macrophages that express the CyaA receptor CR3 was also significantly reduced for $CyaA_{HlyC}$ and $CyaA_{RtxC}$ toxins (Figure 20C,D). Even though very low, the binding was specific, as it could be blocked by the anti-CD11b antibody. The low cell-invasive activity of monoacylated toxins on J774A.1 cells was, most likely, caused by the presence of the shorter C14 acylation of the K983 residue, as a CyaA-K860R mutant acylated by CyaC only on the K983 residue exhibited the same biological properties as $CyaA_{CyaC}$. Although the CyaAHlyC and CyaARtxC variants displayed also a very low overall membrane activity on artificial lipid bilayers made of azolectin, the pore conductances and lifetimes measured for $CyaA_{HlyC}$ (12 pS, 1140 ms), $CyaA_{RtxC}$ (12 pS, 1129 ms) and $CyaA_{CyaC}$ (11 pS, 1083 ms) were comparable. These data suggest, that the number, length and chemical nature of attached acyl chains alter the propensity of formation but not the overall properties of the individual pores generated by the differently acylated CyaA toxin variants.

Rather contrasting effect was observed for the HlyA toxin variants modified by the CyaC, HlyC or RtxC acyltransferases. Despite the fact that the $HlyA_{CyaC}$ protein was acylated essentially only on the K690 residue by the C16:1 and C16:0 chains and the $HlyA_{RtxC}$ was modified by the C14:0 and C14:0-OH acyl chains also mostly on the K690 residue, they both exhibited a similar capacity to lyze erythrocytes as the $HlyA_{HlyC}$ toxin acylated on both K564 and K690 residues by C14:0 and C14:0-OH acyl chains (Figure 20E). Moreover, irrespective of the length or number of acylated residues, all three HlyA toxin variants were equally cytotoxic to human macrophage THP-1 cells and displayed comparable membrane activities on artificial lipid bilayers. As calculated from single-pore recordings. The $HlyA_{CyaC}$, $HlyA_{RtxC}$ and $HlyA_{HlyC}$ toxins also formed pores with similar conductances (322,384 and 405pS) and lifetimes (1788, 1654 and 1599 ms), respectively. In contrast to CyaA monoacylated variants, the partial C14 acylation of the K564 residue or the C16 acylation on the K590 residue conferred similar pore-forming and cytotoxic activity as did the naturally HlyC-mediated C14 acylation on both K564 and K690 residues in $HlyA_{HlyC}$. Analogically for $RtxA_{HlyC}$ and $RtxA_{RtxC}$, single acylation of the K689 residues by C14:0 or C14:0-OH acyl chains was sufficient for full cytolytic activity of the toxin molecules. Nevertheless, the $RtxA_{CyaC}$ toxin with almost fully modified K689 residue by the C16:0 or C16:1 acyl chains was completely inactive revealing necessity for C:14 activation in RtxA toxins (Figure 20

D). In agreement with that, the $RtxA_{HlyC}$ and $RtxA_{RtxC}$ toxins exhibited similar overall membrane activities on planar lipid bilayers, while the activity of $RtxA_{CyaC}$ protein was abolished. However, the lifetimes (968, 1002 and 1288 ms) and conductances of the most frequent pores (487, 454 and 479 pS) created by $RtxA_{CyaC}$, $RtxA_{HlyC}$ and $RtxA_{RtxC}$, respectively, were comparable.

Our results indicate, that RtxA has to be modified by C14 fatty acyl chains for proper biological activity, while activity of HlyA prevails also when modified by C16 acyl chains and CyaA is activated exclusively by C16 acyl chains. The selection of specific acyl chain by the cognate RTXC acyltransferases might reflect unique structural and functional adaptation of the respective conserved RTXA acylation site.

6.3 My contribution

I prepared the samples for MS analysis and quantified the acylation status of the toxins. I also contributed to the writing of the manuscript.

Table 1. Acylation status of the RTXA toxins modified by the RTXC acyltransferases.

Acyl chain[a]	CyaA						HlyA						RtxA					
	CyaC		HlyC		RtxC		CyaC		HlyC		RtxC		CyaC		HlyC		RtxC	
	K860	K983	K860	K983	K860	K983	K564	K690	K564	K690	K564	K690	K558	K689	K558	K689	K558	K689
None	31	1	99	20	100	7	93	0	10	0	73	0	100	1	97	0	98	0
C12:0	-	-	-	-	-	-	-	-	3	2	1	-	-	-	-	3	-	1
C12:0-OH	-	-	-	-	-	-	-	-	2	-	-	-	-	-	-	-	-	-
C14:0	-	3	-	70	-	73	-	-	13	58	10	81	-	5	1	73	1	80
C14:0-OH	-	-	1	7	-	12	-	-	71	35	16	14	-	1	2	23	1	11
C16:0	32	45	-	2	-	1	1	23	-	1	-	1	-	15	-	-	-	1
C16:1	34	43	-	1	-	7	6	67	1	4	-	4	-	74	-	1	-	7
C18:1	3	8	-	-	-	-	-	10	-	-	-	-	-	4	-	-	-	-

[a]The RTXA variants were produced in the presence of the RTXC acyltransferases in *E. coli* BL21/pMM100 cells, purified close to homogeneity and analyzed by MS. Percentage distributions of fatty acyl chains linked to the ε-amino groups of the lysine residues were estimated semiquantitatively, from the relative intensities of selected ions in reconstructed ion current chromatograms. Average values are calculated from determinations performed with two different toxin preparations. The sign "-" means that the acyl chain was not detected.

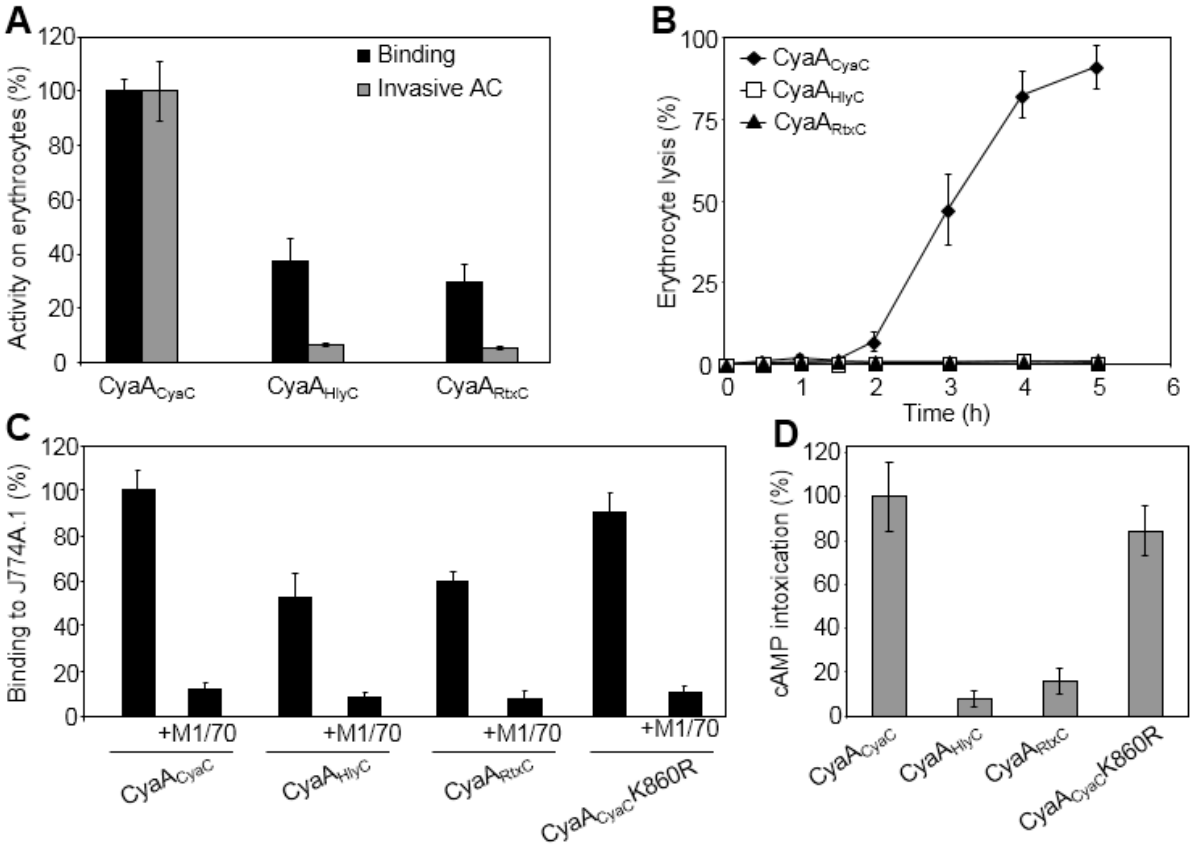

Figure 22. **A.** Sheep erythrocytes (5×10^8/ml) were incubated at 37 °C in the presence 1 µg/ml of the purified CyaA toxin variants and after 30 min, aliquots were taken for determinations of the cell-associated AC activity (Binding) and of the AC activity internalized into erythrocytes and protected against digestion by externally added trypsin (Invasive AC). Activities are expressed as percentages of intact CyaA$_{CyaC}$ activity and represent average values ± standard deviations from at least three independent determinations performed in duplicate with at least two different toxin preparations. **B.** Sheep erythrocytes (5×10^8/ml) were incubated at 37 °C in the presence of the CyaA variants (10 µg/ml). Hemolytic activity was measured as the amount of released hemoglobin by photometric determination (A_{541}), (n=3). **C.** Binding of the CyaA variants to J774A.1 cells (1×10^6) was determined as the amount of total cell-associated AC enzyme activity upon incubation of cells with 1 µg/ml of the protein for 30 min at 4 °C. To block the CR3 receptor of CyaA, J774A.1 cells (1×10^6) were preincubated for 30 min on ice with 5 µg/ml of the CD11b-specific monoclonal antibody M1/70 prior to addition of the CyaA variants (1 µg/ml). Activities are expressed as percentages of intact CyaA$_{CyaC}$ activity and represent average values ± standard deviations from at least three independent determinations performed in duplicate with two different toxin preparations. **D.** cAMP intoxication was assessed by determining the intracellular concentration of cAMP generated in cells after 30 min of incubation of J774A.1 cells (1.5×10^5) with four different toxin concentrations from within the linear range of the dose-response curve (12.5, 25, 50 and 100 ng/ml). Activities are expressed as percentages of intact CyaA$_{CyaC}$ activity and represent average values ± standard deviations from three independent determinations performed in duplicate with two different toxin preparations.

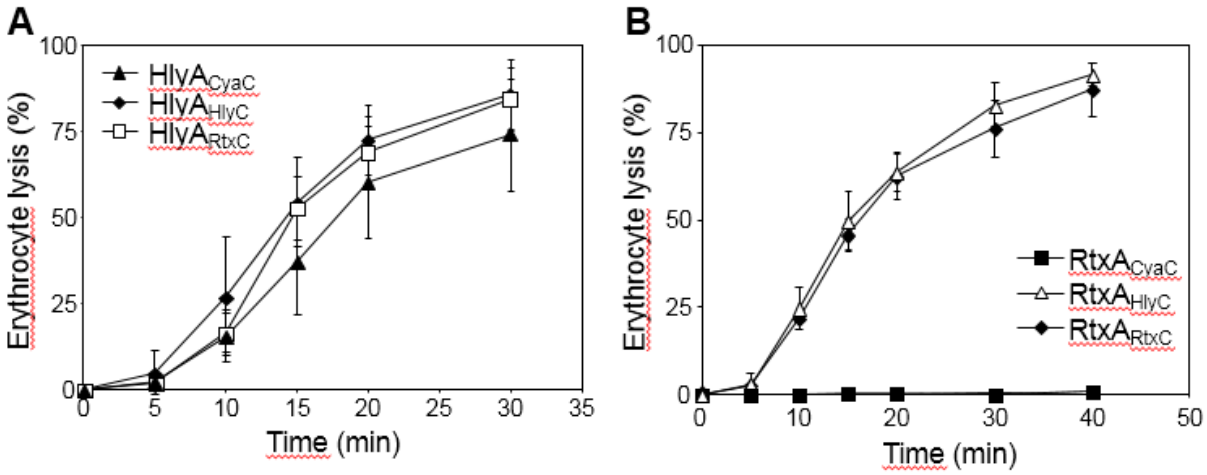

Figure 23. **A.** The HlyA variants were expressed in *E. coli* BL-21 cells and purified from urea extract on Ni-NTA agarose. Sheep erythrocytes (5×10^8/ml) were incubated at 37 °C in the presence of the HlyA variants (50 ng/ml). Hemolytic activity was measured as the amount of released hemoglobin by photometric determination (A_{541}). Activities represent average values ± standard deviations from three independent determinations performed in duplicate with three different toxin preparations. **B.** The CyaC-acylated RtxA variant is inactive. The RtxA variants were expressed in *E. coli* BL-21 cells and purified from urea extract on Ni-NTA agarose. Sheep erythrocytes (5×10^8/ml) were incubated at 37 °C in the presence of the RtxA variants (200 ng/ml). Hemolytic activity was measured as the amount of released hemoglobin by photometric determination (A_{541}), (n=3). Activities represent average values ± standard deviations from three independent determinations performed in duplicate with two different toxin preparations.

CHAPTER 7

Retargeting from the CR3 to the LFA-1 receptor uncovers the adenylyl cyclase enzyme-translocating segment of *Bordetella* adenylate cyclase toxin

Masin J, Osickova A, **Jurnecka D**, Klimova N, Khaliq H, Sebo P, Osicka R.

J Biol Chem. 2020 May 11: jbc.RA120.013630. doi: 10.1074/jbc.RA120.013630.

7.1 Background

The α-hemolysin (HlyA) of *E. coli* and the adenylate cyclase toxin-hemolysin (CyaA) of *B. pertussis* belong to the family of pore-forming Repeats in ToXin (RTX) cytotoxins, produced by a variety of Gram-negative bacteria [121]. Both proteins share overall RTX protein features but target different integrin receptor molecules presented on distinct cell types. HlyA has been shown to bind $\alpha_L\beta_2$ integrin LFA-1 (CD11a/CD18) expressed primarily on lymphocytes, whereas CyaA specifically binds myeloid phagocytic cells through their complement receptor 3 (CR3 or CD11b/CD18) and ablates their bactericidal functions [146,185]. The segment of CyaA involved in the interaction of the toxin with CR3 was previously located within the residues 1166 and 1287 at the interface of the RTX blocks II and II [222–224]. In addition, CyaA harbors an N-terminal adenylyl cyclase enzyme domain, which upon insertion of the toxin into the target cell membrane is translocated into the cell cytoplasm.

The aim of this study is to investigate, if the C-terminal hemolysin moiety of CyaA is specifically designed to support translocation of the AC domain into target cell cytosol and vice versa whether the hemolysin moiety of HlyA is capable of mediating AC domain translocation.

7.2 Summary of the results

To test the capacity of HlyA to deliver the AC enzyme across the cell membrane, a set of CyaA/HlyA fusion molecules was generated (Figure 21). Each of the recombinant CyaA/HlyA chimeric proteins was expressed in the presence of either the CyaA-activating acyltransferase CyaC, or the HlyA-activating acyltransferase HlyC (Figure 21). The proteins were purified by affinity chromatography on calmodulin and their acylation status was analyzed on tryptic digests by a Fourier transform ion cyclotron resonance (FT-ICR) mass spectrometry. The MS data showed that, CyaC modified exclusively the K690 residue of the hybrid molecules, while HlyC was able to activate both the K564 and the K690 lysine residues in all tested constructs.

In agreement with our previous observation, CyaC selected from the *E. coli* acyl-ACP pool predominantly palmitoyl (C16) and palmitoleyl (C16:1) acyl chains with minor portion of K690 residue modified by octadecenoyl (C18:1) acyl. In contrast, the HlyC acyltransferase selected for K564 and K690 residues almost exclusively the myristoyl

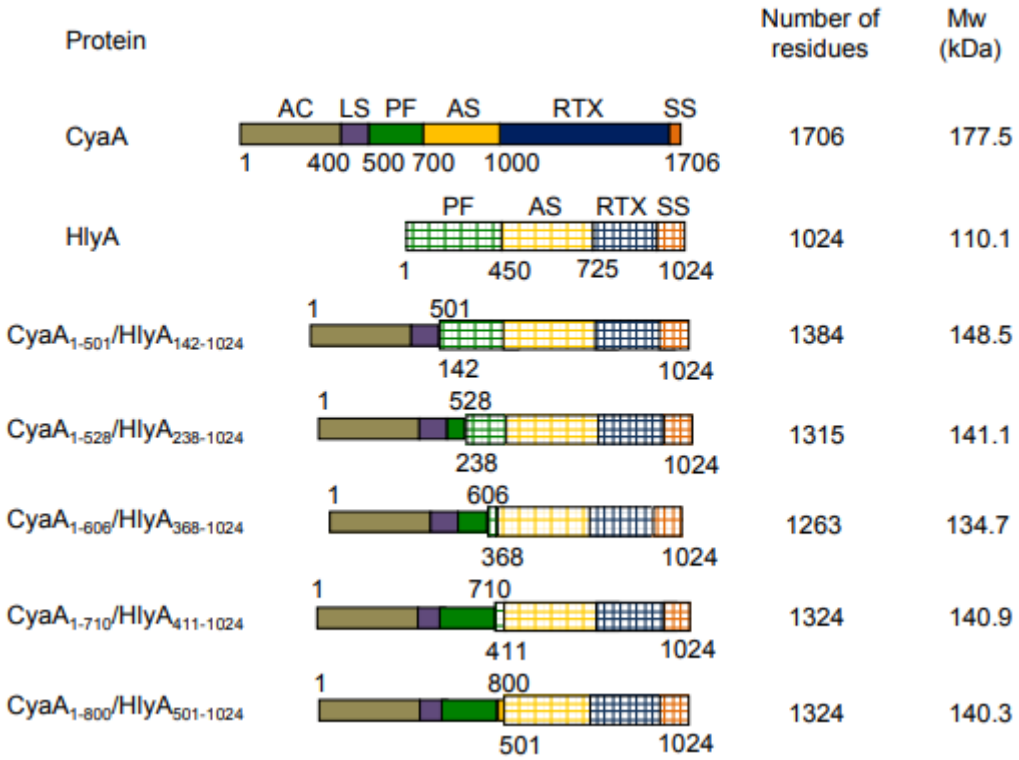

Figure 24. Schematic representation of CyaA, HlyA and hybrid CyaA/HlyA molecules. Individual domains of CyaA and HlyA are indicated by the colored rectangles. AC, adenylate cyclase domain; LS, AC-to-Hly linker segment; PF, pore-forming domain; AS, acylated segment; RTX, calcium-binding repeats; SS, secretion signal. The numbers that follow the CyaA or HlyA in the names of the CyaA/HlyA hybrid chimera represent the number of the first and of the last residue of the segment of the given protein according to the sequences of full-length CyaA and HlyA, respectively.

(C14) and hydroxymyristoyl (C14:0-OH) chains. Next, we characterized the capacity of differently acylated hybrid toxins to bind and permeabilize sheep erythrocytes, lacking receptor CR3 of CyaA and LFA-1 receptor of HlyA. All monoacylated CyaC-activated toxins exhibited reduced binding to erythrocytes (50-75%) in comparison to the fully-acylated CyaA (Figure 22C). In contrast, the doubly acylated chimeric molecules activated by HlyC interacted with erythrocytes more efficiently than their monoacylated counterparts. Binding was significantly enhanced for CyaA$_{1-501}$/HlyA$_{142-1024}$ and CyaA$_{1-528}$/HlyA$_{238-1024}$ constructs, harboring pore-forming domain of HlyA (Figure 22A). The HlyC-activated proteins were also efficient in the lysis of erythrocytes, while hemolytic activity of CyaC-activated CyaA$_{1-501}$/HlyA$_{142-1024}$ was lowered (Figure 22A,B). Replacement of up to 238 N-terminal residues of HlyA by the first 528 residues of CyaA preserved the hemolytic properties of hybrid molecules.

Since all hybrid molecules carried the N-terminal AC domain, we were also able to trace how fusion of different CyaA/HlyA segments affects the ability of hybrid toxin molecules to deliver the AC enzyme into the cytosol of erythrocytes. Aside from the capacity of the $CyaA_{1-710}/Hly_{A411-1024}$ and $CyaA_{1-800}/HlyA_{501-1024}$ HlyC-activated variants to bind erythrocytes with same efficacy as $CyaA_{CyaC}$ (Figure 22C), these two chimeras very further able to insert AC enzyme across erythrocyte membrane and elevate cellular cAMP concentrations in calcium-dependent manner to ~40% of the levels produced by the $CyaA_{CyaC}$ (Figure 22D). Intriguingly, the AC-translocating $CyaA_{1-710}/HlyA_{411-1024}$ chimeric protein was neither capable to lyse erythrocytes (Figure 22B) nor permeabilize planar azolectin lipid bilayer, even though it occasionally formed single pores with properties similar to the $CyaA_{CyaC}$ pores. This result confirmed that the delivery of the AC domain into the cytosol of target cell and formation of CyaA pores represent two separate toxin activities. Moreover, the acylated segment and the RTX domain of CyaA do not seem to play role in the process of AC domain translocation, as they both could be functionally replaced by the acylated and RTX segments of HlyA.

In addition, we examined whether swapping of RTX domains retargeted the HlyC-activated hybrid protein from CR3 to LFA-1. The $CyaA_{1-710}/HlyA_{411-1024}$ was unable to display specific binding or elevate any detectable cAMP levels in CR3 expressing J774A.1 cells in comparison to the CyaACyaC. When Jurkat lymphoblastoma T-cells that lack CR3 but express moderate amount of LFA-1 were employed, the $CyaA_{CyaC}$ exhibited approximately two times lower binding than the $CyaA_{1-710}/HlyA_{411-1024}$ chimera and both toxins produced comparable cAMP levels over a range of toxin concentrations. This result corresponded well with the assay on erythrocytes, where the efficacy of hybrid toxin to deliver AC enzyme was only ~40% of that of $CyaA_{CyaC}$. Finally, to confirm retargeting of CyaA/HlyA chimeric toxin we characterized its properties on the transfected CHO cells that expressed high levels of the LFA-1 receptor.

Compared to mock transfected cells, CHO-LFA-1 cells bound considerably higher amount of HlyC-activated $CyaA_{1-710}/HlyA_{411-1024}$ at concentrations below or equal to 5 nM (Figure 26A). Although the hybrid protein displayed high unspecific binding to mock transfected cells at 25 nM concentration, unambiguous interaction with

LFA-1 allowed efficient penetration and about ten-fold increase in cAMP levels in CHO-LFA-1 cells (Figure 26B). To further analyze which spectrum of cell types could be potentially targeted by CyaA$_{1-710}$/HlyA$_{411-1024}$ hybrid molecule, we constructed genetically detoxified (AC$^-$) HlyC-acylated toxoid (CyaA-AC$^-_{1-710}$/HlyA$_{411-1024}$) and CyaC-acylated CyaA toxoid (CyaA-AC$^-$), as a control, and labeled them by fluorescent dyes Dy495 and Dy650, respectively. The proteins were incubated with mouse splenocytes, comprising various cell types, at concentrations ranging up to 140 nM. The hybrid toxoid (CyaA-AC$^-_{1-710}$/HlyA$_{411-1024}$-Dy495) exhibited importantly higher binding to B and T lymphocytes and also non-leukocytic cells (lacking LFA-1 and CR3) in comparison to control CyaA protein (CyaA-AC—Dy650). Both proteins then shared high affinity to neutrophils and myeloid cells (macrophages, dendritic cells and monocytes) expressing comparable levels of LFA-1 and CR3 receptors.

Thus, we demonstrated that replacement of the acylated segment and the RTX domain of CyaA by HlyA counterparts retargets adenylyl cyclase toxin from its CR3 receptor to LFA-1-expressing cells. Moreover, a CyaA$_{1-710}$/HlyA$_{411-1024}$ hybrid molecule was found to bind to the LFA-1 receptor and effectively deliver the AC enzyme into the cytosol of Jurkat T cells. Finally, the CyaA domain comprising residues 400 to 710, is necessary and sufficient for accomplishing the calcium-dependent AC domain translocation across the plasma membrane of target cells.

7.3 My contribution

I prepared the samples for MS analysis and analyzed the MS results. Over 60 different constructs were tested, but only a few of them were employed in the final dataset. I also contributed to the writing of the manuscript.

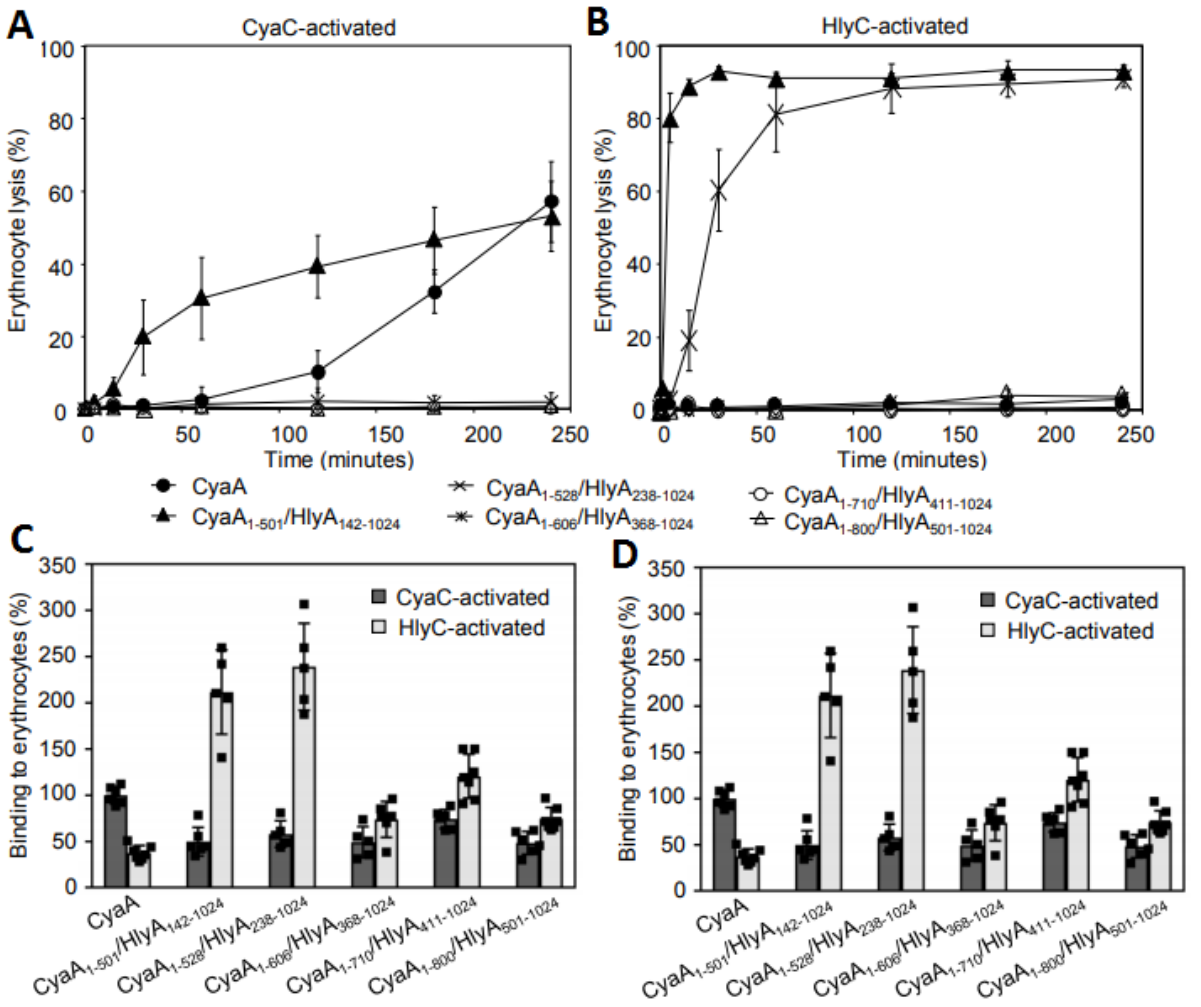

Figure. 25. 16-carbon mono- and 14-carbon doubly-acylated (CyaC- and HlyC-activated) hybrid molecules bind and lyse erythrocytes with importantly differing efficacies.Sheep erythrocytes (5×108 /ml) were incubated at 37 °C in the presence of CyaCactivated (A) or HlyC-activated (B) proteins (25 nM). Hemolytic activity was measured as the amount of released hemoglobin by photometric determination (A541), (n=3). C. Sheep erythrocytes (5×10^8 /ml) were incubated in the presence of 75 mM sucrose as osmoprotectant with 5 nM purified proteins at 37 °C and after 30 min, aliquots were taken for determinations of the cell-associated AC activity (Binding). Activities are expressed as percentages of the activity of the intact 16-carbon doubly-acylated, CyaC-activated CyaA and represent average values ± standard deviations from at least three independent determinations performed in duplicate with two different toxin preparations. (D)Sheep erythrocytes (5×108 /ml) were incubated in the presence of 2 mM calcium (+ Ca2+) or in absence of calcium and presence of 5 mM EDTA (+ EDTA) at 37 °C with 5 nM proteins. After 30 min, aliquots were taken for determinations of the cell-associated AC activity (Binding) and of the AC activity internalized into erythrocytes and protected against digestion by externally added trypsin (Invasive AC). Activities are expressed as percentages of intact CyaCactivated CyaA activity (n=3-7).

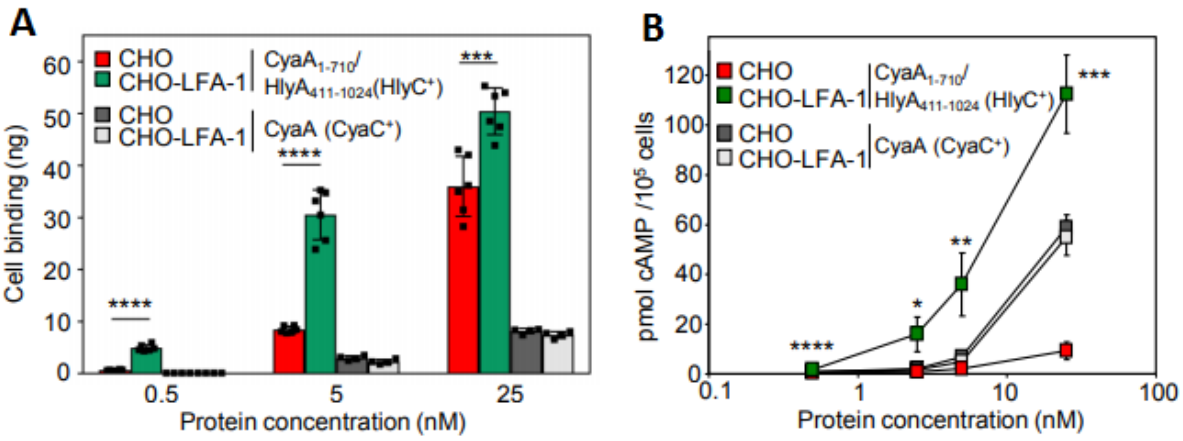

Figure 26. A. Binding of CyaA1- 710/HlyA411-1024 (HlyC+) or intact CyaA to CHO cells expressing CD11a/CD18 or mock transfected CHO cells (1×106) was determined as the amount of total cell-associated AC enzyme activity upon incubation of cells with indicated toxin concentrations for 30 min at 4 °C. Activities represent average values ± standard deviations from three independent determinations performed in duplicate with two different toxin preparations. **B.** cAMP intoxication was assessed by determining the intracellular concentration of cAMP generated in CHO cells expressing CD11a/CD18 or mock transfected CHO cells after 30 min of incubation of cells (1×10^5) with different concentrations of CyaA1-710/HlyA411-1024 ($HlyC^+$) or intact CyaA (n=4). *, statistically significant differences ($p < 0.05$); **, statistically significant differences ($p < 0.01$); ***, statistically significant differences ($p < 0.001$); ****, statistically significant differences ($p < 0.0001$).

CHAPTER 8

DISCUSSION

Proteolytic processing of proteins by specific proteolytic enzymes (peptidases) is an ubiquitous and irreversible post-translational modification that modulates the biological activity of the cleaved products. Biogenesis of the ~370 kDa *Bordetella* FhaB precursor is associated with several proteolytic steps resulting in the secretion and release of mature FHA molecules [49,51,54,225]. Here, the C-terminal residues of the mature FHA protein (FHA) and its truncated variant (FHA_1) were identified.

Up to now, the C terminus of the FHA proteins could not be accurately identified and it was only roughly estimated by mass determination of the FHA purified from *B. pertussis*. Coutte et al. reported the intact mass of Bp-FHA by MALDI-TOF analysis as 232 760 ± 558 Da, which localized the cleavage site of the *B. pertussis* FhaB precursor within the PLFETRIKFID sequence between residues 2362 and 2372 [210]. However, insufficient accuracy of intact mass analysis of very large protein did not permit identification of the C-terminal residue. The here-employed digest-based peptide mapping by FT-ICR MS, combined with post-digestion ^{18}O-labeling analysis, yielded unambiguous identification of the C-terminal residues of various forms of FHA proteins (Figure 24). First, the C-terminal residues of peptides that did not match the cleavage specificity of the used proteases indicated that the Ala_{2348} and Ala_{2228} were the *bona fide* C-terminal residues of the mature *B. pertussis* FHA and FHA_1 proteins. The Lys_{2479} and Phe_{2347} residues were then identified as the respective C-terminal residues of the *B. bronchiseptica* FHA and FHA_1 proteins. Second, the molecular masses and isotopic patterns of peptides comprising these residues remained unchanged upon post-digestion ^{18}O-exchange, while newly generated peptides displayed mass shift upon incorporation of ^{18}O isotopes to the carboxylic groups. This confirmed the assignment of the C-terminal residues.

Coutte et al (2001) have previously shown that the SphB1 protease plays an essential role in proteolytic maturation of FhaB precursor, releasing mature FHA proteins from both *B. pertussis* and *B. bronchiseptica* [210]. Although segments containing cleavage sites of the FhaB precursors from the two species exhibit a very high degree of sequence identity and both SphB1 proteases are almost identical (98 %) as well, both FhaB proteins are surprisingly processed at different sites located 21 and 9 residues apart for FHA and FHA_1 proteins, respectively (Figure 24).

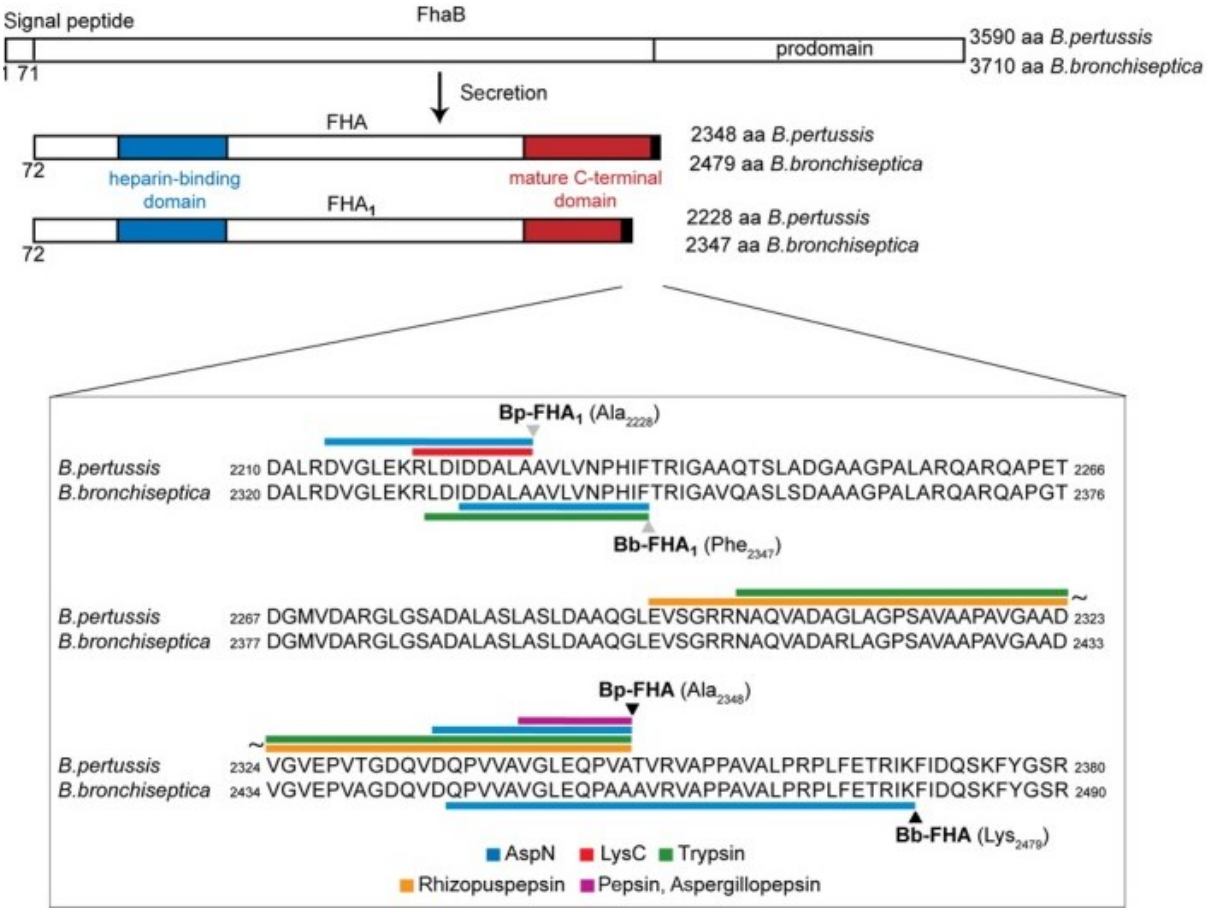

Figure 24. Schematic representation of the C termini of FHA proteins. FHA is encoded by the fhaB gene and translated as a FhaB precursor polypeptide (3590 residues in *Bordetella pertussis* and 3710 residues in *Bordetella bronchiseptica*), containing the N-terminal signal peptide (71 residues) that is removed during translocation of FhaB across the cytoplasmic membrane. FhaB is then exported from the periplasmic space through the outer membrane and processed in SphB1-dependent manner, yielding mature [C terminus at position 2348 (Bp-FHA) or 2479 (Bb-FHA)] or truncated [C terminus at position 2228 (Bp-FHA) or 2347 (Bb-FHA)] variant of FHA protruding on the cell surface. The C-terminal FhaB prodomain (130 kDa) remains in the periplasm, and is rapidly degraded. The C-terminal peptides identified by LC-MS/MS approache after digestion with AspN (blue), LysC (red), trypsin (green), rhizopuspepsin (orange), and (aspergillo) pepsin (magenta) are indicated over the Bp-FHA and Bb-FHA protein sequences aligned based on sequence homology.

Moreover, the cleavage sites possess rather different biophysical properties (Figure 24). Given the fact that in the absence of SphB1 the processing of the FhaB precursor still occurs, though generating a single slightly larger FHA protein hardly detectable on SDS-PAGE, one cannot exclude the possible role of other secreted or surface-associated protease in the FHA processing machinery. However, it is more likely that the highly conserved SphB1 protease of the two bacterial species slightly deviates in substrate specificity. The SphB1 belongs to a superfamily of subtilisin-like

serine proteases found in prokaryotes, eukaryotes and viruses [226]. The substrate specificity is largely determined by interactions of the P4-P1 residue side chains in the binding pocket of the enzyme, which usually enables the cleavage of peptide bonds on the C-terminal side of aliphatic or aromatic amino acid residues [227,228]. A closer examination of the P4-P1 residues of Bp-FHA ($QPVA_{2348}$) and Bp-FHA_1 ($DALA_{2228}$) shows certain correlation between their C-terminal sequences, in terms of side chain properties, indicating that Bp-FhaB is processed by with a well-defined substrate specificity. Despite the fact that C-terminal sequences of Bb-FHA ($TRIK_{2479}$) and Bb-FHA_1 ($PHIF_{2347}$) share the basic amino acid at P3 and isoleucine at P2 position, side chains of phenylalanine and lysine have contrasting properties, even though phenylalanine complies with the substrate specificity of a subtilisin type protease. It thus remains to be determined if the Bb-SphB1 is more promiscuous towards FHA substrate than Bp-SphB1, or another as yet unknown proteolytic step follows surface processing of the Bb-FhaB precursor.

The Bp-FHA was predicted to form rigid β-helical structure with some non-conserved regions and a globular mature C-terminal domain [47,55]. We probed the surface accessibility of Bp-FHA and Bb-FHA proteins. Irrespective of protease used, large quantity of peptides extracted predominantly from C-terminal part of Bp-FHA goes well with previously predicted model. However, whilst FHA proteins are highly homologous and functionally interchangeable, the N-terminal portion of Bb-FHA appears to be more disorganized with poor yields of proteolytic fragments from its C-terminus. *B. pertussis* is a fully human-adapted pathogen, which descended from *B. bronchiseptica*, known to infect a broad variety of animals and only very rarely humans. It will be therefore important to address whether the differences in the FhaB processing and overall susceptibility to protease treatment in these two bacterial species plays a role in the biological activity of mature FHA proteins or represents an adaptation to different host.

Finally, while mapping the FhaB precursor in search for the C-terminal processing site, we were also able to assign several peptides from Bp-FHA purificate over the very C-terminal segment of the prodomain, so called the extreme C-terminus (ECT). Intriguingly, during the analysis of *B. pertussis* secretome by SDS-PAGE, we occasionally encountered single highly abundant 12 kDa protein band, which was later

identified by MS as the ECT. The structure-function role of ECT in the *B. pertussis* infection is now under examination.

Post-translational modifications represent an essential mechanism to modulate protein function in prokaryotic and eukaryotic cells and have a ubiquitous role in a broad spectrum of cellular functions. In fact, it is estimated that 5% of the proteome comprises of enzymes that can control or direct more than 200 different types of modifications. Although less frequent in prokaryotic systems, side chains of various amino acids could still be effectively altered by phosphorylation, oxidation, acetylation, acylation or even simple forms of glycosylations [229]. In particular, bacterial RTX toxins require post-translational activation by dedicated acyltrasferases to display their full biological activity. We reported that CyaA has to be primarily activated by acylation on K983 residue by C16 fatty acyl chain, whereas RtxA is acylated on the K689 residue by C14 acyl chain. Intriguingly, HlyA can be activated by acylation with either C14 or C16 acyl chains attached to the K690 residue. Observation of native and heterologous acylation machinery on different RTX protoxins thus confirmed, that it is the acyltransferase which selects acyl chain with specific length or saturation from the acyl-ACP pool of the producing bacterium. Furthermore, the acyltransferase also determines whether the only one or both conserved acylation sites in the RTX polypeptide will be activated by fatty acyl chain.

The acylation of CyaA was initially reported on the toxin molecule purified from *B. pertussis* strain BP338 as a single amide-linked palmitoylation on the ε-amino group of K983 residue [143]. Recombinant overexpression of CyaA from a plasmid carrying the whole *cya* locus of *B. pertussis* 18323 permitted identification of an additional acylation site at K860 residue modified by palmitoylation as well [162]. The presence of the distal CyaA acylation site was further confirmed in multiple clinical isolates of *B. pertussis* and the CyaA polypeptide from *B. parapertussis* [230]. While the K860 residues of *B. pertussis* strains were almost fully palmitoylated (~70-100%), K983 residues exhibited partial myristoylation (~10-40%) as well. The second conserved acylation site of *B. parapertussis* isolates displayed near complete myristoylation (~70-90 %), which however reflected on negligible cytotoxicity towards J774A.1 cell line. First investigation of CyaA co-expressed with CyaC in the *E. coli* K12 strain XL1-Blue revealed that the recombinant toxin was activated predominantly by palmitoyl chains (~67%) at the K860 residue and palmitoyl (~87%) and myristoyl (~13%) chains at the

K983 residue [161]. Using high resolution MS instrumentation later allowed identification of additional palmitoleyl (cis Δ9 C16:1) modification on the K983 residue at a ratio of approximately 1:2 with unsaturated variant [231]. The presence of palmitoyl (K860, ~46% and K983, ~22%) and palmitoleyl (K860, ~44% and K983, ~56%) chains as the major fatty acyl chains in the recombinant CyaA purified from the E. coli K12 strain was also reported [218]. This is in agreement with our data showing that the palmitoylation (K860, ~32% and K983, ~45%) and palmitoleylation (K860, ~34% and K983, ~43%) are the two major post-translational modifications of the K860 and K983 residues in recombinant CyaA produced in the *E. coli* BL21 strain in the presence of CyaC. However, the HlyC- or RtxC-activated CyaA proteins produced in the same *E. coli* background were predominantly myristoylated and hydroxymyristoylated nearly exclusively on the K983 residue ($CyaA_{HlyC}$, ~77% and $CyaA_{RtxC}$, ~85%). The $CyaA_{HlyC}$ and $CyaA_{RtxC}$ variants exhibited slightly lower binding to the J774A.1 cells, but heavily impaired capacity to deliver the AC enzyme and elevate levels of cAMP in comparison to $CyaA_{CyaC}$. In addition, both toxins also manifested a negligible overall membrane activity on artificial lipid bilayers. Since we have demonstrated that activation of the K983 residue of monoacylated $CyaA_{CyaC}$K860R mutant was sufficient for all biological activities of the toxin on both erythrocytes and J774A.1 cells, the shorter C14:0 and C14:0-OH chains seem to be incapable to functionally replace the C16:0 and C16:1 chains at the K983 residue of CyaA (Figure 22C,D). Therefore, the presence and length of the fatty acyl chain appears to play a vital role in the membrane insertion and translocation of the CyaA polypeptide. However, once the toxin is inserted into the lipid bilayer, the short C14 acyl modification does not affect the conductance and lifetime of single pores formed by the $CyaA_{HlyC}$ and $CyaA_{RtxC}$ variants. The nature of the acyl chains linked to the CyaA molecule thus impacts only the propensity of the toxin to insert into the membrane and form oligomeric pores, but not the structure of the pores themselves.

We showed that CyaA modified by CyaC was fully acylated on the K983 residue, while ~31% of toxin molecules remained unacylated at the K860 residue (Table 1). On the contrary, when activated with HlyC or RtxC, acylation on the K860 residue was negligible. In agreement with the acylation status of the toxin in native *B. pertussis* system, CyaC acyltransferase is highly specific for C16 acyl chains and appears not to be interchangeable by other RTX toxin-activating acyltransferases.

The MS analysis of HlyA toxin purified from two different uropathogenic isolates of *E. coli*, one chromosomal (J96) and the other extrachromosomal (pHly152), revealed acylation of the K564 and K690 residues by a myristoyl chain (~68%). Intriguingly, the remaining linked acyls were then identified as the very rare C15:0 (~26%) and C17:0 (~6%) odd-carbon fatty acyl chains [168]. According to our analysis carried by the FT-ICR MS technology, the recombinant HlyC-activated HlyA toxin produced in the *E. coli* strain BL21 was acylated mostly by the C14:0 and C14:0-OH chains both at the K564 (~84%) and K690 (~93%) residue with minor modifications of C12:0, C12:0-OH, C16:0 and C16:1 chains. No odd-carbon acyl chains on HlyA were detected in our analyses. Therefore, uropathogenic *E. coli* isolates most likely employ different acyl-ACP pool composition than the *E. coli* BL21 strain. The HlyA toxin also appears to be a lot more promiscuous towards activation process than its *B. pertussis* and *K. kingae* counterparts. The $HlyA_{CyaC}$ toxin variant monoacylated on the K690 residue by the C16:0 and C16:1 (~90%) acyl chains or the $HlyA_{RtxC}$ variant acylated almost exclusively by C14:0 on the K690 residue displayed equivalent membrane properties on planar lipid bilayers along with the capacity to lyze erythrocytes and reduce viability of THP-1 cells as the completely C14-activated $HlyA_{HlyC}$ toxin. Moreover, *in vivo* affinity of the CyaC and RtxC acyltransferases was significantly higher for the segment harboring the K690 residue, whereas only ~7% or ~27% of HlyA molecules were modified on the K564 residue. In contrast, *in vitro* assays showed that HlyC acyltransferase is approximately four times more prone to modify peptide matching the K564 acylation site than the one harboring the K690 site [123]. The same group additionally reported as well that substitution of either or both of the K564 and K690 residues abolished the hemolytic activity of HlyA mutants [123]. However, the loss of the HlyA activity in the three toxin mutants was likely due to a structural role of the K564 in toxin action rather than the necessity for activation of this residue such as the $HlyA_{CyaC}$ and $HlyA_{RtxC}$ nearly without K564 modification displayed full biological activity. Indeed, a similar conclusion was reached upon substitution of the homologous K860 residue of CyaA, which is expandable for interaction of CyaA with both erythrocytes, as well as CR3-expressing cells [132,136]. Although, the specific membrane penetration activity of the CyaA-K860R on cells lacking the CR3 receptor is impaired[132,136].

Osickova et al reported that the recombinant RtxA co-expressed with RtxC in the *E. coli* BL21 was modified mainly by C14:0 and C14:0-OH acyl chains (~89%) on the K689 residue with minimal portion of the C16:1 palmitoleyl chains (~8%). Limited amount of the C14:0 and C14:0-OH acyl chains (~23%) were also found to be on the K558 residues [134]. Here, we verified acylation status of the $RtxA_{RtxC}$ toxin, while a lower level (~2%) of acylation on the K558 residue was detected. Similarly as $RtxA_{RtxC}$, the vast majority of the K689 residue of the HlyC-modified RtxA was modified by C14:0 and C14:0-OH acyl chains (~96%) and residual acylation by C14:0 and C14:0-OH chains (~3%) was observed also on the K558 residue. Both $RtxA_{HlyC}$ and $RtxA_{RtxC}$ variants exhibited capability to lyze erythrocytes and similar membrane properties on planar lipid bilayers. Unlike the fully biologically active C16-monoacylated $HlyA_{CyaC}$ toxin, the $RtxA_{CyaC}$ protein activated by CyaC on the K689 residue by the C16:0 and C16:1 acyl chains (~89%) failed to lyse erythrocytes and displayed only residual activity on planar lipid membranes.

Lower yield of the $RtxA_{RtxC}$ K558 modification in comparison to the previously detected quantity could be given either by altered physiological state of the producing bacteria or more likely by differences in LC-MS configuration used for quantification of peptides. As a matter of fact, reproducibility of MS-based peptide quantitation was shown to vary by up to 20%, depending on the sample preparation, unique characteristics of reversed-phase columns used for separation of peptides or LC-MS instrument configuration. It should be noted that the intensities of modified peptide ions do not always have to directly correlate with the actual amount of each corresponding peptide since ionization efficiency vary with different biophysical properties. However, most reported acylation modifications (myristoylation, palmitoylation, and palmitoleylation) are very similar and occur on the same amino acid, thus the ionization efficiencies should be comparable. We analyzed all samples using the cutting-edge 15T Solarix FT-ICR instrument with online calibration using Agilent tuning mix, which ensured extremely low error of measurement (~1ppm). As a result, we were able to use only survey LC-MS mode to avoid ion loss during MS/MS fragmentation securing convenient quantification of acylation sites.

In conclusion, we reported that CyaA is activated only by C16 fatty-acyl chains, while RtxA has to be modified by C14 acyl chain to be active and HlyA could be activated by either of them. These results revealed that individual RTX-activating

acyltransferases select acyl chains of specific length to modify the given RTX protoxin polypeptides.

The *B. pertussis* CyaA preferentially binds the complement receptor 3 (CR3, $\alpha_M\beta_2$, CD11b/CD18, or Mac-1) expressed on myeloid phagocytic cells whereas the *E. coli* HlyA has been shown to specifically target the $\alpha_L\beta_2$ integrin LFA-1 (CD11a/CD18) on B and T cells. Here we report that the substitution of the acylation segment of CyaA and the C-terminal RTX domain by the corresponding segments of HlyA, retargets the CyaA$_{1\text{-}710}$/HlyA$_{411\text{-}1024}$ hybrid molecule from the CR3 to the LFA-1 (Figure 25).

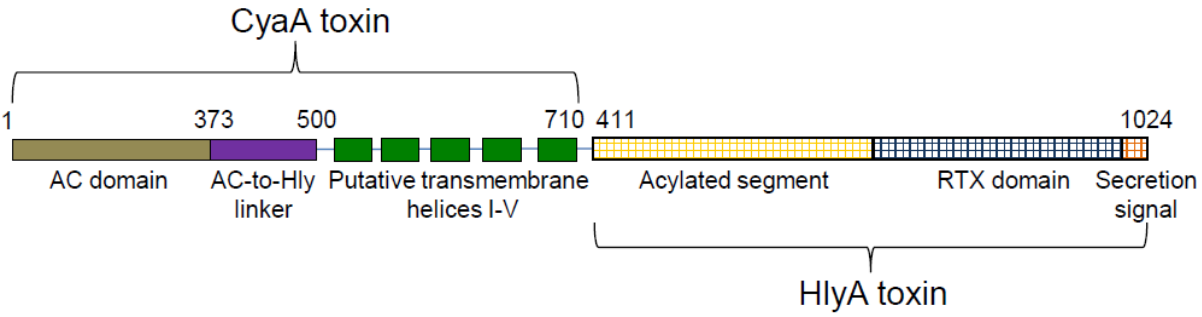

Figure 25. The AC domain of *B. pertussis* CyaA has to be fused to the adjacent AC-to-Hly linker segment and to the five predicted transmembrane α-helices for an efficient translocation across the cell membrane, while the acylated segment and the RTX domain segment of CyaA can be replaced with the corresponding segments of the *E. coli* HlyA toxin.

Furthermore, the cell-invasive capacity of the HlyC-activated CyaA$_{1\text{-}710}$/HlyA$_{411\text{-}1024}$ revealed that CyaA segments crucial for the delivery of the AC enzyme across target cell membrane are located within the residues 400 to 710 of CyaA (Figure 25). These data also revealed that the CR3 receptor as such is dispensable for membrane penetration and delivery of the AC enzyme yet accelerates the whole process. This is most likely due to imposing certain oriented topology on the receptor bound toxin molecules so that it increases the probability of their productive membrane insertion.

Westrop et al. reported that heterologous activation of *Mannheimia haemolytica* LktA leukotoxin by CyaC increases the hemolytic-to-cytotoxic ratio of the LktA but does not change specificity of the toxin, while LktC was unable to activate CyaA. The authors also constructed two hybrid molecules of the LktA and the CyaA toxin. The first, containing the N-terminal residues 1 to 687 of CyaA and the C-terminal residues 379 to 954 of LktA harboring acylation site, did not exhibit any toxic activity [128]. The

second hybrid molecule comprised the N-terminal residues 1 to 687 of CyaA linked to the residues 379 to 616 of LktA (containing the intrinsic K554 residue) and the C-terminal residues 919 to 1706 of CyaA (harboring the K983 acylation site). Although both hybrid proteins exhibited full hemolytic activity to some extent, the capacity to deliver the AC domain to the cell cytosol was negligible as compared to the intact $CyaA_{CyaC}$ [128]. In contrast, the HlyC-activated $CyaA_{1-710}$/$HlyA_{411-1024}$ hybrid molecule was able to deliver the AC domain across the membrane of cells devoid of CR3 with up to 40% efficacy of the intact CyaA. The presence of all five transmembrane α-helices, predicted between residues 502 and 698 of CyaA, thus appears to potentiate AC delivery machinery [154]. Since both hybrid molecules ultimately showed reduced efficacy of AC translocation, it is difficult to discriminate whether the actual cause were structural abnormalities within the artificial hybrid molecules or if the additional CyaA segments in our chimeric molecule facilitated the optimal function of the CyaA translocon. Indeed, the significantly shorter RTX domain of HlyA in $CyaA_{1-710}$/$HlyA_{411-1024}$ may as well yield a less appropriate positioning of the AC-to-Hly linking segment and/or of the hydrophobic domain of CyaA in respect to the membrane eventually restrict the capacity of the AC translocon.

It was previously shown that acylation of CyaA controls the overall conformation of acylated segment and consequently enhances the immunogenicity and the capacity of CyaA antigen to induce toxin/neutralizing antibodies conferring protective immunity against *Bordetella* infection [232–234]. Here we demonstrated that the acylation status of CyaA affects its capacity to deliver the AC domain across cell membrane lacking the specific integrin receptor. Although CyaC- and HlyC- activated $CyaA_{1-710}$/$HlyA_{411-1024}$ and $CyaA_{1-800}$/$HlyA_{501-1024}$ chimeric proteins bound erythrocytes with comparable efficacy, the doubly C14:0/C14:0-OH acylated variants translocated the AC enzyme into erythrocyte cytosol with efficacy of up to 40% of the intact CyaA, while the same proteins C16/C16:1 monoacylated only on the K983 residue exhibited negligible AC translocation. In fact, acylation of the proximal lysine residue was crucial for AC delivery solely on cells lacking specific receptor as the C16 monoacylated $CyaA_{1-710}$/$HlyA_{411-1024}$ toxin was able to elevate levels of cAMP in cells expressing LFA-1 on the surface. These observations indicated that in the absence of a specific β2 integrin receptor, the nature or length of acylation directly impacts the capacity to form translocon and initiate the AC domain delivery. A precedent of such a rescuing effect

of a β2 integrin receptor interaction was previously observed with the C16 monoacylated CyaA-K860R toxin molecule [136,231]. Despite both the CyaC- and HlyC-acylated $CyaA_{1-710}$/$HlyA_{411-1024}$ and $CyaA_{1-800}$/$HlyA_{501-1024}$ proteins failed to lyse erythrocytes and displayed a very limited pore-forming activity on asolectin bilayer. This is in agreement with the previous observations showing that identical conductance and cation selectivity as intact CyaA can be observed irrespectively of the differences in acylation status, truncations of CyaA variants lacking the RTX domain, or even with the CyaA protoxin [153,169]. Moreover, the pore-forming activity of CyaA is independent of the AC domain translocation event, which appears to be mediated by CyaA monomers along the electrical gradient and through a tightly sealed AC translocon formed by residues 400 to 710 of the CyaA [144,218,235].

HlyA exhibits cytotoxic activity on various cell types, such as granulocytes, monocytes, erythrocytes or endothelial cells from primates, mice and ruminants [169, [236–238]. Albeit the rather low cell specificity, HlyA binding and biological activity on erythrocytes was shown to be dependent on the presence of glycophorin [167,239]. As a matter of fact, the HlyC-activated $CyaA_{1-501}$/$HlyA_{1-1024}$ hybrid molecule bound sheep erythrocytes with a ~7 times higher efficacy than $CyaA_{CyaC}$ [167,240]. The glycophorin binding site was proposed to be localized within C-terminal RTX domain of HlyA between the residues 914 to 936 [115,239]. Remarkably, sequential deletion or shortening of the N-terminal regions of HlyA significantly reduces either cell binding or consequential hemolytic capacity of the HlyC-activated CyaA/HlyA hybrid molecules as compared to $CyaA_{1-501}$/$HlyA_{1-1024}$. Taking into account that the binding of the chimeric toxins was studied on sheep erythrocytes, while determination of the glycophorin-binding region was performed on horse and human erythrocytes, the glycophorin-mediated binding of HlyA may require the structural integrity of several toxin regions [167,239]. Another plausible explanation might be that the toxin cell-associates with the plasma membrane through its N-terminal hydrophobic region, which also modulates pore-forming activity [241,242].

The lymphocyte function-associated antigen (LFA-1, or CD11a/CD18; $\alpha_L\beta_2$ integrin) was reported to act as a receptor molecule for HlyA [184]. Monoclonal antibodies recognizing LFA-1 inhibited the binding of HlyA to cells, immobilized HlyA bound LFA-1 and in addition, the expression of LFA-1 rendered the K562 cells sensitive towards HlyA action. Valeva et al. demonstrated, however, that acylation

impaired mutants as well as wild type HlyA toxin bound to erythrocytes and granulocytes in a nonsaturable manner and also that HlyA binds nonspecifically to target cells and a receptor is involved neither in causing hemolysis nor in triggering cellular reactions [243]. Here we show that the affinity of HlyC-activated $CyaA_{1-710}$/$HlyA_{411-1024}$ to Jurkat T cells expressing LFA-1 but not CR3 was approximately two times higher than of the intact CyaA. Moreover, at low protein concentrations the chimeric molecule was able to bind and intoxicate by cAMP almost exclusively the CHO cells expressing LFA-1, suggesting specific interaction and efficient translocation of AC enzyme across cell membrane. Finally, we showed that in comparison to the enzymatically-inactive CyaA (CyaA-AC^-), the CyaA-AC^-_{1-710}/$HlyA_{411-1024}$ protein was able to bind preferably B and T lymphocytes expressing LFA-1, but not CR3. Although it should be noted that due to very high toxoid concentrations, the binding of CyaA-AC_{1-710}/$HlyA_{411-1024}$ was also considerably higher on non-leukocytic cells lacking LFA-1 and CR3. In conclusion, the HlyA appears to preferentially target cells expressing LFA-1, while at higher concentrations it exhibits more promiscuous binding and low target cell specificity.

CHAPTER 9

SUMMARY

- The mature FHA proteins of *B. pertussis* (Bp-FHA) and the *B. bronchiseptica* (Bb-FHA) are processed at different sites, after Ala_{2348} and Lys_{2479} of the FhaB precursor, respectively. The truncated variants of the mature Bp-FHA and Bb-FHA proteins terminate at Ala_{2228} and Phe_{2347}, respectively. Moreover, structural mass spectrometry approach indicates structural variations between the two highly homologous FHA proteins.

- Engagement of the detergent washing step (1% Triton X-100 or Triton X-114) significantly reduces the endotoxin content during protein purifications and enables a simple and rapid purification of endotoxin-free RTX toxins.

- The RTX-activating acyltransferases are capable of discriminating the length of acyl chains that are utilized for covalent modification of specific internal lysine residues within the RTX protoxins. The *B. pertussis* CyaA and *K. kingae* RtxA are activated exclusively by 16- and 14-carbon acyl chains, respectively, while *E. coli* HlyA appears to be promiscuous and can be modified by both C14- or 16-carbon acyl chains to exhibit its biological activity.

- C-terminal domain swapping enables retargeting of the AC enzyme-translocating segment from the CR3 to the LFA-1 receptor. In particular, the $CyaA_{1-710}$/$HlyA_{411-1024}$ chimera was found to bind and intoxicate the LFA-1-expressing Jurkat T lymphoma cells, indicating that residues 400-710 serve as an “AC translocon” of the CyaA polypeptide.

CHAPTER 10

REFERENCES

[1] R. A. Goodnow, “Biology of Bordetella bronchiseptica,” *Microbiological Reviews*. 1980, doi: 10.1128/mmbr.44.4.722-738.1980.
[2] U. Ahuja *et al.*, “Phenotypic and genomic analysis of hypervirulent human-associated bordetella bronchiseptica,” *BMC Microbiol.*, 2012, doi: 10.1186/1471-2180-12-167.
[3] C. C. Linnemann and E. B. Perry, “Bordetella parapertussis: Recent Experience and a Review of the Literature,” *Am. J. Dis. Child.*, 1977, doi: 10.1001/archpedi.1977.02120180074014.
[4] A. Preston, J. Parkhill, and D. J. Maskell, “The Bordetellae: Lessons from genomics,” *Nature Reviews Microbiology*. 2004, doi: 10.1038/nrmicro886.
[5] D. A. Diavatopoulos, C. A. Cummings, L. M. Schouls, M. M. Brinig, D. A. Relman, and F. R. Mooi, “Bordetella pertussis, the causative agent of whooping cough, evolved from a distinct, human-associated lineage of B. bronchiseptica,” *PLoS Pathog.*, 2005, doi: 10.1371/journal.ppat.0010045.
[6] J. Parkhill *et al.*, “Comparative analysis of the genome sequences of Bordetella pertussis, Bordetella parapertussis and Bordetella bronchiseptica.,” *Nat. Genet.*, vol. 35, no. 1, pp. 32–40, 2003, doi: 10.1038/ng1227.
[7] J. D. Cherry *et al.*, “Antibody response patterns to Bordetella pertussis antigens in vaccinated (primed) and unvaccinated (unprimed) young children with pertussis,” *Clin. Vaccine Immunol.*, 2010, doi: 10.1128/CVI.00469-09.
[8] H. E. de Melker, F. G. A. Versteegh, J. F. P. Schellekens, P. F. M. Teunis, and M. Kretzschmar, “The incidence of Bordetella pertussis infections estimated in the population from a combination of serological surveys,” *J. Infect.*, vol. 53, no. 2, pp. 106–113, 2006, doi: 10.1016/j.jinf.2005.10.020.
[9] J. I. Ward *et al.*, “ Bordetella Pertussis Infections in Vaccinated and Unvaccinated Adolescents and Adults, as Assessed in a National Prospective Randomized Acellular Pertussis Vaccine Trial (APERT) ,” *Clin. Infect. Dis.*, 2006, doi: 10.1086/504803.
[10] J. D. Cherry, “Why do pertussis vaccines fail?,” *Pediatrics*. 2012, doi: 10.1542/peds.2011-2594.
[11] F. R. Mooi, “Bordetella pertussis and vaccination: The persistence of a genetically monomorphic pathogen,” *Infection, Genetics and Evolution*. 2010, doi: 10.1016/j.meegid.2009.10.007.
[12] P. Stocks and M. N. Karn, “On the epidemiology of whooping cough in london,” *J. Hyg. (Lond).*, 1932, doi: 10.1017/S0022172400018301.
[13] D. de Gouw, D. A. Diavatopoulos, H. J. Bootsma, P. W. M. Hermans, and F. R. Mooi, “Pertussis: A matter of immune modulation,” *FEMS Microbiology Reviews*, vol. 35, no. 3. pp. 441–474, 2011, doi: 10.1111/j.1574-6976.2010.00257.x.
[14] Y. Sato and H. Sato, “Development of acellular pertussis vaccines.,” *Biologicals*, vol. 27, no. 2, pp. 61–69, 1999, doi: 10.1006/biol.1999.0181.
[15] S. L. Sheridan, K. Frith, T. L. Snelling, K. Grimwood, P. B. McIntyre, and S. B. Lambert, “Waning vaccine immunity in teenagers primed with whole cell and acellular pertussis vaccine: Recent epidemiology,” *Expert Review of Vaccines*. 2014, doi: 10.1586/14760584.2014.944167.
[16] M. M. Williams *et al.*, “Bordetella pertussis strain lacking pertactin and pertussis toxin,” *Emerg. Infect. Dis.*, 2016, doi: 10.3201/eid2202.151332.
[17] V. Bouchez, D. Brun, T. Cantinelli, G. Dore, E. Njamkepo, and N. Guiso, “First report and detailed characterization of B. pertussis isolates not expressing pertussis toxin or pertactin,” *Vaccine*, vol. 27, pp. 6034–6041, 2009, doi:

10.1016/j.vaccine.2009.07.074.
[18] J. M. Warfel, L. I. Zimmerman, and T. J. Merkel, “Acellular pertussis vaccines protect against disease butfail to prevent infection and transmission ina nonhuman primate model,” *Proc. Natl. Acad. Sci. U. S. A.*, 2014, doi: 10.1073/pnas.1314688110.
[19] C. H. Wirsing Von König, S. Halperin, M. Riffelmann, and N. Guiso, “Pertussis of adults and infants,” *Lancet Infectious Diseases*, vol. 2, no. 12. pp. 744–750, 2002, doi: 10.1016/S1473-3099(02)00452-8.
[20] S. M. Bisgard, Kristine M.*; Pascual, F Brian*; Ehresmann, Kristen R. RN, ; Miller, Claudia A.; Cianfrini, Christy*; Jennings, Charles E.; Rebmann, Catherine A.; Gabel, Julie; Schauer, Stephanie L.; Lett, “Infant pertussis_who was the source.pdf,” *The Pediatric infectious disease journal*, 2004. http://journals.lww.com/pidj/Abstract/2004/11000/Infant_Pertussis__Who_Was_the_Source_.2.aspx.
[21] C. J. A. Asensio *et al.*, “Outer membrane vesicles obtained from Bordetella pertussis Tohama expressing the lipid a deacylase PagL as a novel acellular vaccine candidate,” *Vaccine*, 2011, doi: 10.1016/j.vaccine.2010.12.068.
[22] D. Bottero *et al.*, “Outer membrane vesicles derived from Bordetella parapertussis as an acellular vaccine against Bordetella parapertussis and Bordetella pertussis infection,” *Vaccine*, 2013, doi: 10.1016/j.vaccine.2013.08.059.
[23] K. B. Decker, T. D. James, S. Stibitz, and D. M. Hinton, “The Bordetella pertussis model of exquisite gene control by the global transcription factor BvgA,” *Microbiol. (United Kingdom)*, vol. 158, pp. 1665–1676, 2012, doi: 10.1099/mic.0.058941-0.
[24] A. M. Stock, V. L. Robinson, and P. N. Goudreau, “Two-Component Signal Transduction,” *Annu. Rev. Biochem.*, 2000, doi: 10.1146/annurev.biochem.69.1.183.
[25] J. A. Melvin, E. V Scheller, J. F. Miller, and P. A. Cotter, “Bordetella pertussis pathogenesis: current and future challenges.,” *Nat. Rev. Microbiol.*, vol. 12, no. 4, pp. 274–88, 2014, doi: 10.1038/nrmicro3235.
[26] A. Boulanger *et al.*, “Bordetella pertussis fim3 gene regulation by bvgA: Phosphorylation controls the formation of inactive vs. active transcription complexes,” *Proc. Natl. Acad. Sci. U. S. A.*, 2015, doi: 10.1073/pnas.1421045112.
[27] G. M. De Tejada *et al.*, “Neither the Bvg- phase nor the vrg6 locus of Bordetella pertussis is required for respiratory infection in mice,” *Infect. Immun.*, 1998, doi: 10.1128/iai.66.6.2762-2768.1998.
[28] T. J. Merkel, C. Barros, and S. Stibitz, “Characterization of the bvgR locus of Bordetella pertussis,” *J. Bacteriol.*, vol. 180, no. 7, pp. 1682–1690, 1998.
[29] T. J. Merkel and S. Stibitz, “Identification of a locus required for the regulation of bvg-repressed genes in Bordetella pertussis,” *J. Bacteriol.*, 1995, doi: 10.1128/jb.177.10.2727-2736.1995.
[30] P. A. Cotter and J. F. Miller, “BvgAS-mediated signal transduction: Analysis of phase-locked regulatory mutants of Bordetella bronchiseptica in a rabbit model,” *Infect. Immun.*, 1994, doi: 10.1128/iai.62.8.3381-3390.1994.
[31] T. L. Nicholson *et al.*, “Phenotypic modulation of the virulent bvg phase is not required for pathogenesis and transmission of Bordetella bronchiseptica in swine,” *Infect. Immun.*, 2012, doi: 10.1128/IAI.06016-11.
[32] C. L. Hoffman *et al.*, “Bordetella pertussis can be motile and express flagellum-

like structures," *MBio*, 2019, doi: 10.1128/mBio.00787-19.
[33] N. Sukumar, T. L. Nicholson, M. S. Conover, T. Ganguly, and R. Deora, "Comparative analyses of a cystic fibrosis isolate of bordetella bronchiseptica reveal differences in important pathogenic phenotypes," *Infect. Immun.*, 2014, doi: 10.1128/IAI.01453-13.
[34] J. F. Porter, R. Parton, and A. C. Wardlaw, "Growth and survival of Bordetella bronchiseptica in natural waters and in buffered saline without added nutrients," *Appl. Environ. Microbiol.*, 1991, doi: 10.1128/aem.57.4.1202-1206.1991.
[35] K. E. Stockbauer, B. Fuchslocher, J. F. Miller, and P. A. Cotter, "Identification and characterization of BipA, a Bordetella Bvg-intermediate phase protein," *Mol. Microbiol.*, 2001, doi: 10.1046/j.1365-2958.2001.02191.x.
[36] S. M. Julio, C. S. Inatsuka, J. Mazar, C. Dieterich, D. a. Relman, and P. a. Cotter, "Natural-host animal models indicate functional interchangeability between the filamentous haemagglutinins of Bordetella pertussis and Bordetella bronchiseptica and reveal a role for the mature C-terminal domain, but not the RGD motif, during infection," *Mol. Microbiol.*, vol. 71, no. 6, pp. 1574–1590, 2009, doi: 10.1111/j.1365-2958.2009.06623.x.
[37] L. Ohman, R. Willén, O. H. Hultgren, and E. Hultgren Hörnquist, "Acellular Bordetella pertussis vaccine enhances mucosal interleukin-10 production, induces apoptosis of activated Th1 cells and attenuates colitis in Galphai2-deficient mice.," *Clin. Exp. Immunol.*, vol. 141, no. 1, pp. 37–46, Jul. 2005, doi: 10.1111/j.1365-2249.2005.02807.x.
[38] M. Domenighini *et al.*, "Genetic characterization of Bordetella pertussis filamentous haemagglutinin: a protein processed from an unusually large precursor," *Mol. Microbiol.*, 1990, doi: 10.1111/j.1365-2958.1990.tb00649.x.
[39] R. Villarino Romero, R. Osicka, and P. Sebo, "Filamentous hemagglutinin of Bordetella pertussis: a key adhesin with immunomodulatory properties?," *Futur. Microbiol*, vol. 9, no. 12, pp. 1339–1360, 2014, doi: 10.2217/fmb.14.77.
[40] C. Locht, P. Bertin, F. D. Menozzi, and G. Renauld, "The filamentous haemagglutinin, a multifaceted adhesion produced by virulent Bordetella spp.," *Mol. Microbiol.*, vol. 9, no. 4, pp. 653–660, 1993.
[41] R. J. L. Willems *et al.*, "Mutational analysis of the Bordetella pertussis fim/fha gene cluster: identification of a gene with sequence similarities to haemolysin accessory genes involved in export of FHA," *Mol. Microbiol.*, 1994, doi: 10.1111/j.1365-2958.1994.tb00314.x.
[42] N. Chevalier *et al.*, "Membrane targeting of a bacterial virulence factor harbouring an extended signal peptide," *J. Mol. Microbiol. Biotechnol.*, vol. 8, no. 1, pp. 7–18, 2004, doi: 10.1159/000082076.
[43] C. Lambert-Buisine, E. Willery, C. Locht, and F. Jacob-Dubuisson, "N-terminal characterization of the Bordetella pertussis filamentous haemagglutinin," *Mol. Microbiol.*, vol. 28, no. 6, pp. 1283–1293, 1998, doi: 10.1046/j.1365-2958.1998.00892.x.
[44] C. Baud *et al.*, "Role of DegP for two-partner secretion in Bordetella," *Mol. Microbiol.*, 2009, doi: 10.1111/j.1365-2958.2009.06860.x.
[45] H. Hodak *et al.*, "The Peptidyl-Prolyl Isomerase and Chaperone Par27 of Bordetella pertussis as the Prototype for a New Group of Parvulins," *J. Mol. Biol.*, 2008, doi: 10.1016/j.jmb.2007.10.088.
[46] B. Clantin *et al.*, "Structure of the membrane protein FhaC: a member of the Omp85-TpsB transporter superfamily.," *Science*, vol. 317, no. 5840, pp. 957–61, Aug. 2007, doi: 10.1126/science.1143860.

[47] J. Mazar and P. A. Cotter, “Topology and maturation of filamentous haemagglutinin suggest a new model for two-partner secretion,” *Mol. Microbiol.*, vol. 62, no. 3, pp. 641–654, 2006, doi: 10.1111/j.1365-2958.2006.05392.x.
[48] A. M. Makhov *et al.*, “Filamentous hemagglutinin of Bordetella pertussis. A bacterial adhesin formed as a 50-nm monomeric rigid rod based on a 19-residue repeat motif rich in beta strands and turns,” *J Mol Biol*, vol. 241, no. 1, pp. 110–124, 1994, doi: 10.1006/jmbi.1994.1478.
[49] L. Coutte *et al.*, “Role of adhesin release for mucosal colonization by a bacterial pathogen.,” *J. Exp. Med.*, vol. 197, no. 6, pp. 735–742, 2003, doi: 10.1084/jem.20021153.
[50] D. Jurnecka, P. Man, P. Sebo, and L. Bumba, “Bordetella pertussis and Bordetella bronchiseptica filamentous hemagglutinins are processed at different sites,” *FEBS Open Bio*, vol. 8, no. 8, pp. 1256–1266, 2018, doi: 10.1002/2211-5463.12474.
[51] C. R. Noël, J. Mazar, J. A. Melvin, J. A. Sexton, and P. A. Cotter, “The prodomain of the Bordetella two-partner secretion pathway protein FhaB remains intracellular yet affects the conformation of the mature C-terminal domain,” *Mol. Microbiol.*, vol. 86, no. 4, pp. 988–1006, 2012, doi: 10.1111/mmi.12036.
[52] J. A. Melvin, E. V. Scheller, C. R. Noël, and P. A. Cotter, “New insight into filamentous hemagglutinin secretion reveals a role for full-length FhaB in Bordetella virulence,” *MBio*, vol. 6, no. 4, pp. e01189-15, 2015, doi: 10.1128/mBio.01189-15.
[53] E. V. Scheller and P. A. Cotter, “Bordetella filamentous hemagglutinin and fimbriae: critical adhesins with unrealized vaccine potential,” *Pathogens and disease*. 2015, doi: 10.1093/femspd/ftv079.
[54] Z. M. Nash and P. A. Cotter, “Regulated, sequential processing by multiple proteases is required for proper maturation and release of Bordetella filamentous hemagglutinin,” *Mol. Microbiol.*, 2019, doi: 10.1111/mmi.14318.
[55] A. V. Kajava *et al.*, “Beta-helix model for the filamentous haemagglutinin adhesin of Bordetella pertussis and related bacterial secretory proteins,” *Mol. Microbiol.*, vol. 42, no. 2, pp. 279–292, 2001, doi: 10.1046/j.1365-2958.2001.02598.x.
[56] B. Kobe and A. V. Kajava, “When protein folding is simplified to protein coiling: The continuum of solenoid protein structures,” *Trends in Biochemical Sciences*. 2000, doi: 10.1016/S0968-0004(00)01667-4.
[57] B. Clantin, H. Hodak, E. Willery, C. Locht, F. Jacob-Dubuisson, and V. Villeret, “The crystal structure of filamentous hemagglutinin secretion domain and its implications for the two-partner secretion pathway.,” *Proc. Natl. Acad. Sci. U. S. A.*, vol. 101, no. 16, pp. 6194–6199, 2004, doi: 10.1073/pnas.0400291101.
[58] S. M. Prasad, Y. Yin, E. Rodzinski, E. I. Tuomanen, and H. R. Masure, “Identification of a carbohydrate recognition domain in filamentous hemagglutinin from Bordetella pertussis,” *Infect. Immun.*, vol. 61, no. 7, pp. 2780–2785, 1993.
[59] F. D. Menozzi *et al.*, “Heparin-inhibitable lectin activity of the filamentous hemagglutinin adhesin of Bordetella pertussis,” *Infect. Immun.*, vol. 62, no. 3, pp. 769–778, 1994.
[60] Y. Ishibashi, K. Yoshimura, A. Nishikawa, S. Claus, C. Laudanna, and D. A. Relman, “Role of phosphatidylinositol 3-kinase in the binding of Bordetella

pertussis to human monocytes," *Cell. Microbiol.*, vol. 4, no. 12, pp. 825–833, 2002.
[61] Y. Ishibashi and A. Nishikawa, "Role of nuclear factor-??B in the regulation of intercellular adhesion molecule 1 after infection of human bronchial epithelial cells by Bordetella pertussis," *Microb. Pathog.*, vol. 35, no. 4, pp. 169–177, 2003, doi: 10.1016/S0882-4010(03)00113-X.
[62] Y. Ishibashi, S. Claus, and D. A. Relman, "Bordetella pertussis filamentous hemagglutlnln interacts with a leukocyte signal transduction complex and stimulates bacterial adherence to monocyte CR3 (CD11b/CD18)," *J. Exp. Med.*, 1994, doi: 10.1084/jem.180.4.1225.
[63] T. Abramson, H. Kedem, and D. A. Relman, "Modulation of the NF-κB pathway by Bordetella pertussis filamentous hemagglutinin," *PLoS One*, 2008, doi: 10.1371/journal.pone.0003825.
[64] R. Villarino Romero *et al.*, "Bordetella pertussis filamentous hemagglutinin itself does not trigger anti-inflammatory interleukin-10 production by human dendritic cells," *Int. J. Med. Microbiol.*, vol. 306, no. 1, pp. 38–47, 2016, doi: 10.1016/j.ijmm.2015.11.003.
[65] M. W. Henderson *et al.*, "Contribution of Bordetella filamentous hemagglutinin and adenylate cyclase toxin to suppression and evasion of interleukin-17-mediated inflammation.," *Infect. Immun.*, vol. 80, no. 6, pp. 2061–75, Jun. 2012, doi: 10.1128/IAI.00148-12.
[66] S. M. Julio, C. S. Inatsuka, J. Mazar, C. Dieterich, D. A. Relman, and P. A. Cotter, "Natural-host animal models indicate functional interchangeability between the filamentous haemagglutinins of Bordetella pertussis and Bordetella bronchiseptica and reveal a role for the mature C-terminal domain, but not the RGD motif, during infection," *Mol. Microbiol.*, 2009, doi: 10.1111/j.1365-2958.2009.06623.x.
[67] M. E. Rodríguez, S. M. M. Hellwig, M. L. A. Pérez Vidakovics, G. A. M. Berbers, and J. G. J. Van De Winkel, "Bordetella pertussis attachment to respiratory epithelial cells can be impaired by fimbriae-specific antibodies," *FEMS Immunol. Med. Microbiol.*, 2006, doi: 10.1111/j.1574-695X.2005.00001.x.
[68] L. A. E. Ashworth, L. I. Irons, and A. B. Dowsett, "Antigenic relationship between serotype-specific agglutinogen and fimbriae of Bordetella pertussis," *Infect. Immun.*, vol. 37, no. 3, pp. 1278–1281, 1982.
[69] C. A. W. Geuijen, R. J. L. Willems, P. Hoogerhout, W. C. Puijk, R. H. Meloen, and F. R. Mooi, "Identification and characterization of heparin binding regions of the Fim2 subunit of Bordetella pertussis," *Infect. Immun.*, vol. 66, no. 5, pp. 2256–2263, 1998.
[70] A. Robinson, A. R. Gorringe, S. G. P. Funnell, and M. Fernandez, "Serospecific protection of mice against intranasal infection with Bordetella pertussis," *Vaccine*, 1989, doi: 10.1016/0264-410X(89)90193-X.
[71] M. F. Willems RJ, Geuijen C, van der Heide HG, Matheson M, Robinson A, Versluis LF, Ebberink R, Theelen J, "Isolation of a putative fimbrial adhesin from Bordetella pertussis and the identification of its gene," *Mol Microbiol.*, vol. 9(3), pp. 623–34.
[72] E. Leininger *et al.*, "Pertactin, an Arg-Gly-Asp-containing Bordetella pertussis surface protein that promotes adherence of mammalian cells," *Proc. Natl. Acad. Sci. U. S. A.*, 1991, doi: 10.1073/pnas.88.2.345.
[73] C. S. Inatsuka *et al.*, "Pertactin is required for Bordetella species to resist

neutrophil-mediated clearance.," *Infect. Immun.*, vol. 78, no. 7, pp. 2901–9, Jul. 2010, doi: 10.1128/IAI.00188-10.
[74] R. R. Stein PE, Boodhoo A, Armstrong GD, Cockle SA, Klein MH, "The crystal structure of pertussis toxin," *Structure.*, vol. 2(1), pp. 45-57., 1994.
[75] P. E. Stein *et al.*, "Structure of a pertussis toxin-sugar complex as a model for receptor binding.," *Nat. Struct. Biol.*, vol. 1, pp. 591–596, 1994, doi: 10.1038/nsb0994-591.
[76] S. I. Kotob, S. Z. Hausman, and D. L. Burns, "Localization of the promoter for the ptl genes of Bordetella pertussis, which encode proteins essential for secretion of pertussis toxin," *Infect. Immun.*, 1995, doi: 10.1128/iai.63.8.3227-3230.1995.
[77] C. Locht, L. Coutte, and N. Mielcarek, "The ins and outs of pertussis toxin," *FEBS Journal*, vol. 278. pp. 4668–4682, 2011, doi: 10.1111/j.1742-4658.2011.08237.x.
[78] J. Moss *et al.*, "Activation by thiol of the latent NAD glycohydrolase and ADP-ribosyltransferase activities of Bordetella pertussis toxin (islet-activating protein).," *J. Biol. Chem.*, 1983.
[79] C. Andreasen and N. H. Carbonetti, "Pertussis toxin inhibits early chemokine production to delay neutrophil recruitment in response to Bordetella pertussis respiratory tract infection in mice," *Infect. Immun.*, 2008, doi: 10.1128/IAI.00895-08.
[80] G. S. Kirimanjeswara, L. M. Agosto, M. J. Kennett, O. N. Bjornstad, and E. T. Harvill, "Pertussis toxin inhibits neutrophil recruitment to delay antibody-mediated clearance of Bordetella pertussis," *J. Clin. Invest.*, 2005, doi: 10.1172/JCI24609.
[81] G. Schmidt, P. Sehr, M. Wilm, J. Selzer, M. Mann, and K. Aktories, "Gin 63 of Rho is deamidated by Escherichia coli cytotoxic necrotizing factor-1," *Nature*, 1997, doi: 10.1038/42735.
[82] A. Fukui-Miyazaki, S. Ohnishi, S. Kamitani, H. Abe, and Y. Horiguchi, "Bordetella dermonecrotic toxin binds to target cells via the N-terminal 30 amino acids," *Microbiol. Immunol.*, 2011, doi: 10.1111/j.1348-0421.2010.00300.x.
[83] T. Matsuzawa *et al.*, "Bordetella Dermonecrotic Toxin Undergoes Proteolytic Processing to Be Translocated from a Dynamin-related Endosome into the Cytoplasm in an Acidification-independent Manner," *J. Biol. Chem.*, 2004, doi: 10.1074/jbc.M310340200.
[84] T. Matsuzawa, T. Kashimoto, J. Katahira, and Y. Horiguchi, "Identification of a receptor-binding domain of Bordetella dermonecrotic toxin," *Infect. Immun.*, 2002, doi: 10.1128/IAI.70.7.3427-3432.2002.
[85] Y. Horiguchi, "Escherichia coli cytotoxic necrotizing factors and Bordetella dermonecrotic toxin: The dermonecrosis-inducing toxins activating Rho small GTPases," *Toxicon*, 2001, doi: 10.1016/S0041-0101(01)00149-0.
[86] Y. Horiguchi, T. nakai, and K. Kume, "Effects of Bordetella bronchiseptica dermonecrotic toxin on the structure and function of osteoblastic clone MC3T3-E1 cells," *Infect. Immun.*, vol. 59, pp. 1112–1116, 1991.
[87] Y. Horiguchi, N. Sugimoto, and M. Matsuda, "Stimulation of DNA synthesis in osteoblast-like MC3T3-E1 cells by Bordetella bronchiseptica dermonecrotic toxin," *Infect. Immun.*, 1993, doi: 10.1128/iai.61.9.3611-3615.1993.
[88] Y. Horiguchi *et al.*, "Bordetella bronchiseptica dermonecrotizing toxin induces reorganization of actin stress fibers through deamidation of Gln-63 of the GTP-

binding protein Rho.," *Proc. Natl. Acad. Sci. U. S. A.*, vol. 94, pp. 11623–11626, 1997, doi: 10.1073/pnas.94.21.11623.
[89] H. Nagano, T. Nakai, Y. Horiguchi, and K. Kume, "Isolation and characterization of mutant strains of Bordetella bronchiseptica lacking dermonecrotic toxin-producing ability," *J. Clin. Microbiol.*, 1988, doi: 10.1128/jcm.26.10.1983-1987.1988.
[90] S. L. Brockmeier, K. B. Register, T. Magyar, A. J. Lax, G. D. Pullinger, and R. A. Kunkle, "Role of the dermonecrotic toxin of Bordetella bronchiseptica in the pathogenesis of respiratory disease in swine," *Infect. Immun.*, 2002, doi: 10.1128/IAI.70.2.481-490.2002.
[91] J. L. Di Fabio, M. Caroff, D. Karibian, J. C. Richards, and M. B. Perry, "Characterization of the common antigenic lipopolysaccharide O-chains produced by Bordetella bronchiseptica and Bordetella parapertussis," *FEMS Microbiol. Lett.*, 1992, doi: 10.1016/0378-1097(92)90348-R.
[92] M. Caroff, D. Karibian, J. M. Cavaillon, and N. Haeffner-Cavaillon, "Structural and functional analyses of bacterial lipopolysaccharides," *Microbes and Infection*. 2002, doi: 10.1016/S1286-4579(02)01612-X.
[93] K. Le Blay, P. Gueirard, N. Guiso, and R. Chaby, "Antigenic polymorphism of the lipopolysaccharides from human and animal isolates of Bordetella bronchiseptica," *Microbiology*, 1997, doi: 10.1099/00221287-143-4-1433.
[94] P. Gueirard, K. Le Blay, A. Le Coustumier, R. Chaby, and N. Guiso, "Variation in Bordetella bronchiseptica lipopolysaccharide during human infection," *FEMS Microbiol. Lett.*, 1998, doi: 10.1016/S0378-1097(98)00142-6.
[95] Y. Li *et al.*, "LPS remodeling is an evolved survival strategy for bacteria," *Proc. Natl. Acad. Sci. U. S. A.*, 2012, doi: 10.1073/pnas.1202908109.
[96] R. Medzhitov and C. A. Janeway, "Decoding the patterns of self and nonself by the innate immune system," *Science*. 2002, doi: 10.1126/science.1068883.
[97] G. Seyffarth, P. N. Nelson, S. J. Dunmore, N. Rodrigo, D. J. Murphy, and R. J. Carson, "Lipopolysaccharide induces nitric oxide synthase expression and platelet-activating factor increases nitric oxide production in human fetal membranes in culture," *Reprod. Biol. Endocrinol.*, 2004, doi: 10.1186/1477-7827-2-29.
[98] S. J. Kim, M. S. Ha, E. Y. Choi, J. Il Choi, and I. S. Choi, "Nitric oxide production and inducible nitric oxide synthase expression induced by Prevotella nigrescens lipopolysaccharide," *FEMS Immunol. Med. Microbiol.*, 2005, doi: 10.1016/j.femsim.2004.07.001.
[99] P. B. Mann, D. Wolfe, E. Latz, D. Golenbock, A. Preston, and E. T. Harvill, "Comparative toll-like receptor 4-mediated innate host defense to Bordetella infection," *Infect. Immun.*, 2005, doi: 10.1128/IAI.73.12.8144-8152.2005.
[100] S. C. Higgins *et al.*, " Toll-Like Receptor 4-Mediated Innate IL-10 Activates Antigen-Specific Regulatory T Cells and Confers Resistance to Bordetella pertussis by Inhibiting Inflammatory Pathology ," *J. Immunol.*, 2003, doi: 10.4049/jimmunol.171.6.3119.
[101] B. T. Cookson, A. N. Tyler, and W. E. Goldman, "Primary structure of the peptidoglycan-derived tracheal cytotoxin of Bordetella pertussis.," *Biochemistry*, vol. 28, pp. 1744–1749, 1989.
[102] N. Mielcarek *et al.*, "Attenuated Bordetella pertussis: New live vaccines for intranasal immunisation," *Vaccine*, 2006, doi: 10.1016/j.vaccine.2005.01.120.
[103] L. N. Heiss, S. A. Moser, E. R. Unanue, and W. E. Goldman, "Interleukin-1 is linked to the respiratory epithelial cytopathology of pertussis," *Infect. Immun.*,

vol. 61, pp. 3123–3128, 1993.
[104] L. N. Heiss, J. R. Lancaster, J. A. Corbett, and W. E. Goldman, “Epithelial autotoxicity of nitric oxide: Role in the respiratory cytopathology of pertussis,” *Proc. Natl. Acad. Sci. U. S. A.*, 1994, doi: 10.1073/pnas.91.1.267.
[105] T. A. Flak and W. E. Goldman, “Signalling and cellular specificity of airway nitric oxide production in pertussis,” *Cell. Microbiol.*, 1999, doi: 10.1046/j.1462-5822.1999.00004.x.
[106] P. Delepelaire and C. Wandersman, “Protease secretion by Erwinia chrysanthemi. Proteases B and C are synthesized and secreted as zymogens without a signal peptide,” *J. Biol. Chem.*, 1989.
[107] S. Létoffé, P. Delepelaire, and C. Wandersman, “Protease secretion by Erwinia chrysanthemi: the specific secretion functions are analogous to those of Escherichia coli alpha-haemolysin.,” *EMBO J.*, 1990, doi: 10.1002/j.1460-2075.1990.tb08252.x.
[108] J. M. Ghigo and C. Wandersman, “Cloning, nucleotide sequence and characterization of the gene encoding the Erwinia chrysanthemi B374 PrtA metalloprotease: a third metalloprotease secreted via a C-terminal secretion signal,” *MGG Mol. Gen. Genet.*, 1992, doi: 10.1007/BF00279652.
[109] H. Akatsuka, E. Kawai, K. Omori, S. Komatsubara, T. Shibatani, and T. Tosa, “The lipA gene of Serratia marcescens which encodes an extracellular lipase having no N-terminal signal peptide,” *J. Bacteriol.*, 1994, doi: 10.1128/jb.176.7.1949-1956.1994.
[110] P. Delepelaire, “Type I secretion in gram-negative bacteria,” *Biochimica et Biophysica Acta - Molecular Cell Research*. 2004, doi: 10.1016/j.bbamcr.2004.05.001.
[111] A. L. Pimenta, K. Racher, L. Jamieson, M. A. Blight, and I. B. Holland, “Mutations in HlyD, part of the type 1 translocator for hemolysin secretion, affect the folding of the secreted toxin,” *J. Bacteriol.*, 2005, doi: 10.1128/JB.187.21.7471-7480.2005.
[112] E. C. Short and H. J. Kurtz, “Properties of the Hemolytic Activities of Escherichia coli,” *Infect. Immun.*, 1971, doi: 10.1128/iai.3.5.678-687.1971.
[113] E. Hanski and Z. Farfel, “Bordetella pertussis invasive adenylate cyclase. Partial resolution and properties of its cellular penetration,” *J. Biol. Chem.*, 1985.
[114] U. Baumann, S. Wu, K. M. Flaherty, and D. B. McKay, “Three-dimensional structure of the alkaline protease of Pseudomonas aeruginosa: A two-domain protein with a calcium binding parallel beta roll motif,” *EMBO J.*, 1993, doi: 10.1002/j.1460-2075.1993.tb06009.x.
[115] L. Bumba *et al.*, “Calcium-Driven Folding of RTX Domain β-Rolls Ratchets Translocation of RTX Proteins through Type I Secretion Ducts,” *Mol. Cell*, 2016, doi: 10.1016/j.molcel.2016.03.018.
[116] I. Gentschev, J. Hess, and W. Goebel, “Change in the cellular localization of alkaline phosphatase by alteration of its carboxy-terminal sequence,” *MGG Mol. Gen. Genet.*, 1990, doi: 10.1007/BF00633820.
[117] P. Stanley, V. Koronakis, and C. Hughes, “Mutational analysis supports a role for multiple structural features in the C-terminal secretion signal of Escherichia coli haemolysin,” *Mol. Microbiol.*, 1991, doi: 10.1111/j.1365-2958.1991.tb02085.x.
[118] P. Šebo and D. Ladant, “Repeat sequences in the Bordetella pertussis adenylate cyclase toxin can be recognized as alternative carboxy-proximal

secretion signals by the Escherichia coliα-haemolysin translocator," *Mol. Microbiol.*, 1993, doi: 10.1111/j.1365-2958.1993.tb01229.x.
[119] V. Koronakis, J. Eswaran, and C. Hughes, "Structure and Function of TolC: The Bacterial Exit Duct for Proteins and Drugs," *Annu. Rev. Biochem.*, 2004, doi: 10.1146/annurev.biochem.73.011303.074104.
[120] J. Young and I. B. Holland, "ABC transporters: Bacterial exporters-revisited five years on," *Biochimica et Biophysica Acta - Biomembranes*. 1999, doi: 10.1016/S0005-2736(99)00158-3.
[121] I. Linhartová *et al.*, "RTX proteins: a highly diverse family secreted by a common mechanism.," *FEMS Microbiol. Rev.*, vol. 34, no. 6, pp. 1076–112, Nov. 2010, doi: 10.1111/j.1574-6976.2010.00231.x.
[122] R. A. Welch, "RTX toxin structure and function: A story of numerous anomalies and few analogies in toxin biology," *Current Topics in Microbiology and Immunology*. 2000.
[123] P. Stanley, L. C. Packman, V. Koronakis, and C. Hughes, "Fatty acylation of two internal lysine residues required for the toxic activity of escherichia coli hemolysin," *Science (80-.).*, 1994, doi: 10.1126/science.7801126.
[124] J. P. Issartel, V. Koronakis, and C. Hughes, "Activation of Escherichia coli prohaemolysin to the mature toxin by acyl carrier protein-dependent fatty acylation," *Nature*, 1991, doi: 10.1038/351759a0.
[125] C. Forestier and R. A. Welch, "Identification of RTX toxin target cell specificity domains by use of hybrid genes," *Infect. Immun.*, 1991, doi: 10.1128/iai.59.11.4212-4220.1991.
[126] S. Pellett and R. A. Welch, "Escherichia coli hemolysin mutants with altered target cell specificity," *Infect. Immun.*, 1996, doi: 10.1128/iai.64.8.3081-3087.1996.
[127] E. T. Lally, E. E. Golub, and I. R. Kieba, "Identification and immunological characterization of the domain of Actinobacillus actinomycetemcomitans leukotoxin that determines its specificity for human target cells," *J. Biol. Chem.*, 1994.
[128] G. Westrop, K. Hormozi, N. Da Costa, R. Parton, and J. Coote, "Structure-function studies of the adenylate cyclase toxin of Bordetella pertussis and the leukotoxin of Pasteurella haemolytica by heterologous C protein activation and construction of hybrid proteins," *J. Bacteriol.*, 1997, doi: 10.1128/jb.179.3.871-879.1997.
[129] K. G. Langston, L. M. S. Worsham, L. Earls, and M. Lou Ernst-Fonberg, "Activation of Hemolysin Toxin: Relationship between Two Internal Protein Sites of Acylation," *Biochemistry*, 2004, doi: 10.1021/bi035919k.
[130] M. S. Trent, L. M. S. Worsham, and M. Lou Ernst-Fonberg, "HlyC, the internal protein acyltransferase that activates hemolysin toxin: Role of conserved histidine, serine, and cysteine residues in enzymatic activity as probed by chemical modification and site-directed mutagenesis," *Biochemistry*, 1999, doi: 10.1021/bi982491u.
[131] L. M. S. Worsham, M. S. Trent, L. Earls, C. Jolly, and M. L. Ernst-Fonberg, "Insights into the catalytic mechanism of HlyC, the internal protein acyltransferase that activates Escherichia coli hemolysin toxin," *Biochemistry*, 2001, doi: 10.1021/bi011032h.
[132] T. Basar, V. Havlíček, S. Bezoušková, M. Hackett, and P. Šebo, "Acylation of lysine 983 is sufficient for toxin activity of Bordetella pertussis adenylate cyclase. Substitutions of alanine 140 modulate acylation site selectivity of the

toxin acyltransferase CyaC," *J. Biol. Chem.*, 2001, doi: 10.1074/jbc.M006463200.
[133] E. M. Barry, A. A. Weiss, I. E. Ehrmann, M. C. Gray, E. L. Hewlett, and M. S. M. Goodwin, "Bordetella pertussis adenylate cyclase toxin and hemolytic activities require a second gene, cyaC, for activation," *J. Bacteriol.*, 1991, doi: 10.1128/jb.173.2.720-726.1991.
[134] A. Osickova *et al.*, "Cytotoxic activity of Kingella kingae RtxA toxin depends on post-translational acylation of lysine residues and cholesterol binding," *Emerg. Microbes Infect.*, 2018, doi: 10.1038/s41426-018-0179-x.
[135] P. Šebo, P. Glaser, H. Sakamoto, and A. Ullmann, "High-level synthesis of active adenylate cyclase toxin of Bordetella pertussis in a reconstructed Escherichia coli system," *Gene*, 1991, doi: 10.1016/0378-1119(91)90459-O.
[136] J. Masin *et al.*, "Acylation of lysine 860 allows tight binding and cytotoxicity of Bordetella adenylate cyclase on CD11b-expressing cells," *Biochemistry*, 2005, doi: 10.1021/bi050459b.
[137] N. V. Balashova, C. Shah, J. K. Patel, S. Megalla, and S. C. Kachlany, "Aggregatibacter actinomycetemcomitans LtxC is required for leukotoxin activity and initial interaction between toxin and host cells," *Gene*, 2009, doi: 10.1016/j.gene.2009.05.002.
[138] B. A. Wilson and M. Ho, "Evolutionary aspects of toxin-producing bacteria," in *The Comprehensive Sourcebook of Bacterial Protein Toxins*, Fourth Edi., Elsevier, 2015, pp. 3–39.
[139] J. Park *et al.*, "Comparative genomics of the classical Bordetella subspecies: The evolution and exchange of virulence-associated diversity amongst closely related pathogens," *BMC Genomics*, 2012, doi: 10.1186/1471-2164-13-545.
[140] P. Glaser, H. Sakamoto, J. Bellalou, A. Ullmann, and A. Danchin, "Secretion of cyclolysin, the calmodulin-sensitive adenylate cyclase-haemolysin bifunctional protein of Bordetella pertussis.," *EMBO J.*, 1988, doi: 10.1002/j.1460-2075.1988.tb03288.x.
[141] J. Bellalou, H. Sakamoto, D. Ladant, C. Geoffroy, and A. Ullmann, "Deletions affecting hemolytic and toxin activities of Bordetella pertussis adenylate cyclase," *Infect. Immun.*, 1990, doi: 10.1128/iai.58.10.3242-3247.1990.
[142] A. Rogel, J. E. Schultz, R. M. Brownlie, J. G. Coote, R. Parton, and E. Hanski, "Bordetella pertussis adenylate cyclase: purification and characterization of the toxic form of the enzyme.," *EMBO J.*, 1989, doi: 10.1002/j.1460-2075.1989.tb08417.x.
[143] M. Hackett, L. Guo, J. Shabanowitz, D. F. Hunt, and E. L. Hewlett, "Internal lysine palmitoylation in adenylate cyclase toxin from Bordetella pertussis," *Science (80-.).*, 1994, doi: 10.1126/science.7939682.
[144] A. Osickova *et al.*, "Adenylate cyclase toxin translocates across target cell membrane without forming a pore," *Mol. Microbiol.*, 2010, doi: 10.1111/j.1365-2958.2010.07077.x.
[145] J. Novak *et al.*, "Structure–function relationships underlying the capacity of Bordetella adenylate cyclase toxin to disarm host phagocytes," *Toxins*. 2017, doi: 10.3390/toxins9100300.
[146] P. Guermonprez *et al.*, "The adenylate cyclase toxin of Bordetella pertussis binds to target cells via the alpha(M)beta(2) integrin (CD11b/CD18).," *J. Exp. Med.*, vol. 193, no. 9, pp. 1035–1044, 2001, doi: 10.1084/jem.193.9.1035.
[147] M. El-Azami-El-Idrissi *et al.*, "Interaction of Bordetella pertussis adenylate cyclase with CD11b/CD18. Role of toxin acylation and identification of the main

integrin interaction domain," *J. Biol. Chem.*, 2003, doi: 10.1074/jbc.M304387200.
[148] J. Masin, R. Osicka, L. Bumba, and P. Sebo, "Bordetella adenylate cyclase toxin: A unique combination of a pore-forming moiety with a cell-invading adenylate cyclase enzyme," *Pathogens and Disease*. 2015, doi: 10.1093/femspd/ftv075.
[149] F. GENTILE, A. RAPTIS, L. G. KNIPLING, and J. WOLFF, "Bordetella pertussis adenylate cyclase: Penetration into host cells," *Eur. J. Biochem.*, 1988, doi: 10.1111/j.1432-1033.1988.tb14215.x.
[150] M. Basler, J. Masin, R. Osicka, and P. Sebo, "Pore-forming and enzymatic activities of Bordetella pertussis adenylate cyclase toxin synergize in promoting lysis of monocytes," *Infect. Immun.*, 2006, doi: 10.1128/IAI.74.4.2207-2214.2006.
[151] J. Vojtova, J. Kamanova, and P. Sebo, "Bordetella adenylate cyclase toxin: A swift saboteur of host defense," *Current Opinion in Microbiology*, vol. 9, no. 1. pp. 69–75, 2006, doi: 10.1016/j.mib.2005.12.011.
[152] P. Guermonprez, D. Ladant, G. Karimova, A. Ullmann, and C. Leclerc, "Direct delivery of the Bordetella pertussis adenylate cyclase toxin to the MHC class I antigen presentation pathway," *J. Immunol.*, 1999.
[153] R. Benz, E. Maier, D. Ladant, A. Ullmann, and P. Sebo, "Adenylate cyclase toxin (CyaA) of Bordetella pertussis. Evidence for the formation of small ion-permeable channels and comparison with HlyA of Escherichia coli," *J. Biol. Chem.*, 1994.
[154] A. Osičková, R. Osička, E. Maier, R. Benz, and P. Šebo, "An amphipathic α-helix including glutamates 509 and 516 is crucial for membrane translocation of adenylate cyclase toxin and modulates formation and cation selectivity of its membrane channels," *J. Biol. Chem.*, 1999, doi: 10.1074/jbc.274.53.37644.
[155] M. Bachelet, M. J. Richard, D. François, and B. S. Polla, "Mitochondrial alterations precede Bordetella pertussis-induced apoptosis," *FEMS Immunol. Med. Microbiol.*, 2002, doi: 10.1016/S0928-8244(01)00289-9.
[156] N. Khelef and N. Guiso, "Induction of macrophage apoptosis by Bordetella pertussis adenylate cyclase-hemolysin," *FEMS Microbiol. Lett.*, 1995, doi: 10.1016/0378-1097(95)00375-F.
[157] M. Iwaki, A. Ullmann, and P. Šebo, "Identification by in vitro complementation of regions required for cell-invasive activity of Bordetella pertussis adenylate cyclase toxin," *Mol. Microbiol.*, 1995, doi: 10.1111/j.1365-2958.1995.mmi_17061015.x.
[158] J. Holubova *et al.*, "Delivery of large heterologous polypeptides across the cytoplasmic membrane of antigen-presenting cells by the Bordetella RTX hemolysin moiety lacking the adenylyl cyclase domain," *Infect. Immun.*, 2012, doi: 10.1128/IAI.05711-11.
[159] T. Rose, P. Sebo, J. Bellalou, and D. Ladant, "Interaction of calcium with Bordetella pertussis adenylate cyclase toxin. Characterization of multiple calcium-binding sites and calcium-induced conformational changes," *J. Biol. Chem.*, 1995, doi: 10.1074/jbc.270.44.26370.
[160] G. Szabo, M. C. Gray, and E. L. Hewlett, "Adenylate cyclase toxin from Bordetella pertussis produces ion conductance across artificial lipid bilayers in a calcium- and polarity-dependent manner," *J. Biol. Chem.*, 1994.
[161] M. Hackett *et al.*, "Hemolytic, but not cell-invasive activity, of adenylate cyclase toxin is selectively affected by differential fatty-acylation in Escherichia coli," *J.*

Biol. Chem., 1995, doi: 10.1074/jbc.270.35.20250.
[162] V. Havlícek *et al.*, “Mass spectrometric analysis of recombinant adenylate cyclase toxin from Bordetella pertussis strain 18323/pHSP9,” *J. Mass Spectrom.*, 2001, doi: 10.1002/jms.139.
[163] R. Osicka *et al.*, “Delivery of CD8(+) T-cell epitopes into major histocompatibility complex class I antigen presentation pathway by Bordetella pertussis adenylate cyclase: delineation of cell invasive structures and permissive insertion sites.,” *Infect. Immun.*, vol. 68, no. 1, pp. 247–56, Jan. 2000, [Online]. Available: http://www.pubmedcentral.nih.gov/articlerender.fcgi?artid=97128&tool=pmcentrez&rendertype=abstract.
[164] N. Johnsen *et al.*, “α-Haemolysin production, as a single factor, causes fulminant sepsis in a model of Escherichia coli-induced bacteraemia,” *Cell. Microbiol.*, 2019, doi: 10.1111/cmi.13017.
[165] M. Schwidder, L. Heinisch, and H. Schmidt, “Genetics, toxicity, and distribution of enterohemorrhagic escherichia coli hemolysin,” *Toxins*. 2019, doi: 10.3390/toxins11090502.
[166] L. C. Ristow and R. A. Welch, “Hemolysin of uropathogenic Escherichia coli: A cloak or a dagger?,” *Biochimica et Biophysica Acta - Biomembranes*. 2016, doi: 10.1016/j.bbamem.2015.08.015.
[167] A. L. Cortajarena, F. M. Goñi, and H. Ostolaza, “Glycophorin as a Receptor for Escherichia coli α-Hemolysin in Erythrocytes,” *J. Biol. Chem.*, 2001, doi: 10.1074/jbc.M006792200.
[168] K. B. Lim *et al.*, “Escherichia coli α-hemolysin (HlyA) is heterogeneously acylated in vivo with 14-, 15-, and 17-carbon fatty acids,” *J. Biol. Chem.*, 2000, doi: 10.1074/jbc.C000544200.
[169] G. Menestrina, C. Moser, S. Pellet, and R. Welch, “Pore-formation by Escherichia coli hemolysin (HlyA) and other members of the RTX toxins family,” *Toxicology*, 1994, doi: 10.1016/0300-483X(94)90254-2.
[170] B. Eberspacher, F. Hugo, M. Pohl, and S. Bhakdi, “Functional similarity between the haemolysins of Escherichia coli and Morganella morganii,” *J. Med. Microbiol.*, 1990, doi: 10.1099/00222615-33-3-165.
[171] R. Y. Lo, “Molecular characterization of cytotoxins produced by Haemophilus, Actinobacillus, Pasteurella.,” *Canadian journal of veterinary research = Revue canadienne de recherche veterinaire*. 1990.
[172] J. T. Gray, P. J. Fedorka-Cray, and D. G. Rogers, “Partial characterization of a Moraxella bovis cytolysin,” *Vet. Microbiol.*, 1995, doi: 10.1016/0378-1135(94)00084-A.
[173] J. Frey, “The role of RTX toxins in host specificity of animal pathogenic Pasteurellaceae,” *Veterinary Microbiology*. 2011, doi: 10.1016/j.vetmic.2011.05.018.
[174] Y. F. Chang, D. P. Ma, J. Shi, and M. M. Chengappa, “Molecular characterization of a leukotoxin gene from a Pasteurella haemolytica-like organism, encoding a new member of the RTX toxin family,” *Infect. Immun.*, 1993, doi: 10.1128/iai.61.5.2089-2095.1993.
[175] J. Frey *et al.*, “Actinobacillus pleuropneumoniae RTX-toxins: Uniform designation of haemolysins, cytolysins, pleurotoxin and their genes,” *J. Gen. Microbiol.*, 1993, doi: 10.1099/00221287-139-8-1723.
[176] R. Jansen, J. Briaire, E. M. Kamp, A. L. J. Gielkens, and M. A. Smits, “Structural analysis of the Actinobacillus pleuropneumoniae-RTX-toxin I (ApxI)

operon," *Infect. Immun.*, 1993, doi: 10.1128/iai.61.9.3688-3695.1993.
[177] A. Schaller *et al.*, "Characterization of apxIVA, a new RTX determinant of Actinobacillus pleuropneumoniae," *Microbiology*, 1999, doi: 10.1099/13500872-145-8-2105.
[178] P. Yagupsky and R. Dagan, "On King Saul, Two Missing Mules, and Kingella kingae: The Serendipitous Discovery of a Pediatric Pathogen," *Pediatr. Infect. Dis. J.*, 2018, doi: 10.1097/INF.0000000000002110.
[179] R. Maldonado, R. Wei, S. C. Kachlany, M. Kazi, and N. V. Balashova, "Cytotoxic effects of Kingella kingae outer membrane vesicles on human cells," *Microb. Pathog.*, 2011, doi: 10.1016/j.micpath.2011.03.005.
[180] N. S. Taichman *et al.*, "Cytopathic effects of Actinobacillus actinomycetemcomitans on monkey blood leukocytes," *J. Periodontal Res.*, 1984, doi: 10.1111/j.1600-0765.1984.tb00802.x.
[181] D. L. Simpson, P. Berthold, and N. S. Taichman, "Killing of human myelomonocytic leukemia and lymphocytic cell lines by Actinobacillus actinomycetemcomitans leukotoxin," *Infect. Immun.*, 1988, doi: 10.1128/iai.56.5.1162-1166.1988.
[182] S. C. Kachlany, D. H. Fine, and D. H. Figurski, "Secretion of RTX leukotoxin by Actinobacillus actinomycetemcomitans," *Infect. Immun.*, 2000, doi: 10.1128/IAI.68.11.6094-6100.2000.
[183] N. V. Balashova, R. Diaz, S. V. Balashov, J. A. Crosby, and S. C. Kachlany, "Regulation of Aggregatibacter (Actinobacillus) actinomycetemcomitans leukotoxin secretion by iron," *J. Bacteriol.*, 2006, doi: 10.1128/JB.01253-06.
[184] E. T. Lally *et al.*, "RTX toxins recognize a β2 integrin on the surface of human target cells," *J. Biol. Chem.*, 1997, doi: 10.1074/jbc.272.48.30463.
[185] A. C. Brown *et al.*, "Aggregatibacter actinomycetemcomitans leukotoxin utilizes a cholesterol recognition/amino acid consensus site for membrane association.," *J. Biol. Chem.*, vol. 288, no. 32, pp. 23607–21, Aug. 2013, doi: 10.1074/jbc.M113.486654.
[186] J. Korostoff, J. F. Wang, I. Kieba, M. Miller, B. J. Shenker, and E. T. Lally, "Actinobacillus actinomycetemcomitans leukotoxin induces apoptosis in HL- 60 cells," *Infect. Immun.*, 1998, doi: 10.1128/iai.66.9.4474-4483.1998.
[187] P. E. Shewen and B. N. Wilkie, "Cytotoxin of Pasteurella haemolytica acting on bovine leukocytes," *Infect. Immun.*, 1982, doi: 10.1128/iai.35.1.91-94.1982.
[188] K. L. Kaehler, R. J. F. Markham, C. C. Muscoplat, and D. W. Johnson, "Evidence of species specificity in the cytocidal effects of Pasteurella haemolytica," *Infect. Immun.*, 1980.
[189] C. A. Strathdee and R. Y. C. Lo, "Extensive homology between the leukotoxin of Pasteurella haemolytica A1 and the alpha-hemolysin of Escherichia coli," *Infect. Immun.*, 1987, doi: 10.1128/iai.55.12.3233-3236.1987.
[190] J. F. Brown, F. Leite, and C. J. Czuprynski, "Binding of Pasteurella haemolytica leukotoxin to bovine leukocytes," *Infect. Immun.*, 1997, doi: 10.1128/iai.65.9.3719-3724.1997.
[191] S. Jeyaseelan, M. S. Kannan, S. L. Hsuan, A. K. Singh, T. F. Walseth, and S. K. Maheswaran, "Pasteurella (Mannheimia) haemolytica leukotoxin-induced cytolysis of bovine leukocytes: Role of arachidonic acid and its regulation," *Microb. Pathog.*, 2001, doi: 10.1006/mpat.2000.0410.
[192] W. Lin *et al.*, "Identification of a vibrio cholerae RTX toxin gene cluster that is tightly linked to the cholera toxin prophage," *Proc. Natl. Acad. Sci. U. S. A.*, 1999, doi: 10.1073/pnas.96.3.1071.

[193] K. J. Fullner Satchell, “MARTX, multifunctional autoprocessing repeats-in-toxin toxins,” *Infection and Immunity*. 2007, doi: 10.1128/IAI.00525-07.
[194] K. J. F. Satchell, “Structure and Function of MARTX Toxins and Other Large Repetitive RTX Proteins,” *Annu. Rev. Microbiol.*, 2011, doi: 10.1146/annurev-micro-090110-102943.
[195] B. K. Boardman and K. J. Fullner Satchell, “Vibrio cholerae strains with mutations in an atypical type I secretion system accumulate RTX toxin intracellularly,” *J. Bacteriol.*, 2004, doi: 10.1128/JB.186.23.8137-8143.2004.
[196] C. L. Byung *et al.*, “Vibrio vulnificus rtxE is important for virulence, and its expression is induced by exposure to host cells,” *Infect. Immun.*, 2008, doi: 10.1128/IAI.01503-07.
[197] K. J. Fullner, “In vivo covalent cross-linking of cellular actin by the Vibrio cholerae RTX toxin,” *EMBO J.*, 2000, doi: 10.1093/emboj/19.20.5315.
[198] J. H. Beynon, R. G. Cooks, J. W. Amy, W. E. Baitinger, and T. Y. Ridley, “Design and Performance of a Mass-analyzed Ion Kinetic Energy (MIKE) Spectrometer,” *Anal. Chem.*, 1973, doi: 10.1021/ac60334a763.
[199] W. F. Haddon and F. W. McLafferty, “Metastable Ion Characteristics. VII. Collision-Induced Metastables,” *Journal of the American Chemical Society*. 1968, doi: 10.1021/ja01019a053.
[200] K. C. Kim, M. Uckotter, J. H. Beynon, and R. G. Cooks, “Collision-induced fragmentation of triatomic ions,” *Int. J. Mass Spectrom. Ion Phys.*, 1974, doi: 10.1016/0020-7381(74)80083-5.
[201] M. Barber, R. S. Bordoli, R. D. Sedgwick, and A. N. Tyler, “Fast atom bombardment of solids (F.A.B.): A new ion source for mass spectrometry,” *J. Chem. Soc. Chem. Commun.*, 1981, doi: 10.1039/C39810000325.
[202] J. B. Fenn, M. Mann, C. K. Meng, S. F. Wong, and C. M. Whitehouse, “Electrospray ionization for mass spectrometry of large biomolecules,” *Science*. 1989, doi: 10.1126/science.2675315.
[203] K. Tanaka *et al.*, “Protein and polymer analyses up to m/z 100 000 by laser ionization time-of-flight mass spectrometry,” *Rapid Commun. Mass Spectrom.*, 1988, doi: 10.1002/rcm.1290020802.
[204] P. Lössl, M. Waterbeemd, and A. J. Heck, “The diverse and expanding role of mass spectrometry in structural and molecular biology,” *EMBO J.*, 2016, doi: 10.15252/embj.201694818.
[205] P. Roepstorff and J. Fohlman, “Nomenclature for peptide ion,” *Biol. Mass Spectrom.*, 1984, doi: 10.1002/bms.1200111109.
[206] B. Domon and C. E. Costello, “A systematic nomenclature for carbohydrate fragmentations in FAB-MS/MS spectra of glycoconjugates,” *Glycoconj. J.*, 1988, doi: 10.1007/BF01049915.
[207] D. N. Perkins, D. J. C. Pappin, D. M. Creasy, and J. S. Cottrell, “Probability-based protein identification by searching sequence databases using mass spectrometry data,” 1999, doi: 10.1002/(SICI)1522-2683(19991201)20:18<3551::AID-ELPS3551>3.0.CO;2-2.
[208] J. Zhang *et al.*, “PEAKS DB: De novo sequencing assisted database search for sensitive and accurate peptide identification,” *Mol. Cell. Proteomics*, 2012, doi: 10.1074/mcp.M111.010587.
[209] J. Cox and M. Mann, “MaxQuant enables high peptide identification rates, individualized p.p.b.-range mass accuracies and proteome-wide protein quantification,” *Nat. Biotechnol.*, 2008, doi: 10.1038/nbt.1511.
[210] L. Coutte, R. Antoine, H. Drobecq, C. Locht, and F. Jacob-Dubuisson,

"Subtilisin-like autotransporter serves as maturation protease in a bacterial secretion pathway," *EMBO J.*, vol. 20, no. 18, pp. 5040–5048, 2001, doi: 10.1093/emboj/20.18.5040.
[211] C. Bache, M. Hoonakker, C. Hendriksen, K. H. Buchheit, I. Spreitzer, and T. Montag, "Workshop on Animal free Detection of Pertussis Toxin in Vaccines - Alternatives to the Histamine Sensitisation Test," 2012, doi: 10.1016/j.biologicals.2012.04.002.
[212] B. Gao and M. F. Tsan, "Recombinant human heat shock protein 60 does not induce the release of tumor necrosis factor α from murine macrophages," *J. Biol. Chem.*, 2003, doi: 10.1074/jbc.M303161200.
[213] M.-F. Tsan and B. Gao, "Endogenous ligands of Toll-like receptors," *J. Leukoc. Biol.*, 2004, doi: 10.1189/jlb.0304127.
[214] P. de Oliveira Magalhães, A. M. Lopes, P. G. Mazzola, C. Rangel-Yagui, T. C. V. Penna, and A. Pessoa, "Methods of endotoxin removal from biological preparations: A review," *Journal of Pharmacy and Pharmaceutical Sciences*. 2007.
[215] Y. Aida and M. J. Pabst, "Removal of endotoxin from protein solutions by phase separation using triton X-114," *J. Immunol. Methods*, 1990, doi: 10.1016/0022-1759(90)90029-U.
[216] A. S. Cavallaro, D. Mahony, M. Commins, T. J. Mahony, and N. Mitter, "Endotoxin-free purification for the isolation of Bovine Viral Diarrhoea Virus E2 protein from insoluble inclusion body aggregates," *Microb. Cell Fact.*, 2011, doi: 10.1186/1475-2859-10-57.
[217] Fischer, "Common Background Contamination Ions in Mass Spectrometry," [Online]. Available: https://beta-static.fishersci.ca/content/dam/fishersci/en_US/documents/programs/scientific/brochures-and-catalogs/posters/fisher-chemical-poster.pdf.
[218] J. Masin *et al.*, "The conserved tyrosine residue 940 plays a key structural role in membrane interaction of Bordetella adenylate cyclase toxin," *Sci. Rep.*, 2017, doi: 10.1038/s41598-017-09575-6.
[219] N. P. Greene, A. Crow, C. Hughes, and V. Koronakis, "Structure of a bacterial toxin-activating acyltransferase," *Proc. Natl. Acad. Sci. U. S. A.*, 2015, doi: 10.1073/pnas.1503832112.
[220] D. Gygi, J. Nicolet, J. Frey, M. Cross, V. Koronakis, and C. Hughes, "Isolation of the Actinobacillus pleuropneumoniae haemolysin gene and the activation and secretion of the prohaemolysin by the HlyC, HlyB and HlyD proteins of Escherichia coli," *Mol. Microbiol.*, 1990, doi: 10.1111/j.1365-2958.1990.tb02021.x.
[221] C. Forestier and R. A. Welch, "Nonreciprocal complementation of the hlyC and lktC genes of the Escherichia coli hemolysin and Pasteurella haemolytica leukotoxin determinants," *Infect. Immun.*, 1990, doi: 10.1128/iai.58.3.828-832.1990.
[222] R. Osicka, A. Osickova, S. Hasan, L. Bumba, J. Cerny, and P. Sebo, "Bordetella adenylate cyclase toxin is a unique ligand of the integrin complement receptor 3," *Elife*, 2015, doi: 10.7554/eLife.10766.
[223] X. Wang and J. A. Maynard, "The Bordetella adenylate cyclase repeat-in-toxin (RTX) domain is immunodominant and elicits neutralizing antibodies," *J. Biol. Chem.*, 2015, doi: 10.1074/jbc.M114.585281.
[224] X. Wang, J. A. Stapleton, J. R. Klesmith, E. L. Hewlett, T. A. Whitehead, and J. A. Maynard, "Fine Epitope Mapping of Two Antibodies Neutralizing the

Bordetella Adenylate Cyclase Toxin," *Biochemistry*, 2017, doi: 10.1021/acs.biochem.6b01163.
[225] L. Coutte *et al.*, "Role of adhesin release for mucosal colonization by a bacterial pathogen," *J. Exp. Med.*, 2003, doi: 10.1084/jem.20021153.
[226] N. D. Rawlings and A. J. Barrett, "Families of serine peptidases," *Methods Enzymol.*, 1994, doi: 10.1016/0076-6879(94)44004-2.
[227] R. J. Siezen and J. A. Leunissen, "Subtilases: the superfamily of subtilisin-like serine proteases.," *Protein Sci.*, vol. 6, no. 3, pp. 501–523, 1997, doi: 10.1002/pro.5560060301.
[228] R. J. Siezen and J. A. M. Leunissen, "Subtilases: The superfamily of subtilisin-like serine proteases," *Protein Sci.*, 2008, doi: 10.1002/pro.5560060301.
[229] B. Macek, K. Forchhammer, J. Hardouin, E. Weber-Ban, C. Grangeasse, and I. Mijakovic, "Protein post-translational modifications in bacteria," *Nature Reviews Microbiology*. 2019, doi: 10.1038/s41579-019-0243-0.
[230] V. Bouchez *et al.*, "Characterization of post-translational modifications and cytotoxic properties of the adenylate-cyclase hemolysin produced by various Bordetella pertussis and Bordetella parapertussis isolates," *Toxins (Basel).*, 2017, doi: 10.3390/toxins9100304.
[231] T. Basar, V. Havlícek, S. Bezoušková, P. Halada, M. Hackett, and P. Šebo, "The conserved lysine 860 in the additional fatty-acylation site of Bordetella pertussis adenylate cyclase is crucial for toxin function independently of its acylation status," *J. Biol. Chem.*, 1999, doi: 10.1074/jbc.274.16.10777.
[232] J. C. Karst *et al.*, "Calcium, acylation, and molecular confinement favor folding of Bordetella pertussis adenylate cyclase cyaa toxin," *J. Biol. Chem.*, 2014, doi: 10.1074/jbc.M114.580852.
[233] D. P. O'Brien *et al.*, "Post-translational acylation controls the folding and functions of the CyaA RTX toxin," *FASEB J.*, 2019, doi: 10.1096/fj.201802442RR.
[234] F. Betsou, P. Sebo, and N. Guiso, "CyaC-mediated activation is important not only for toxic but also for protective activities of Bordetella pertussis adenylate cyclase-hemolysin," *Infect. Immun.*, 1993, doi: 10.1128/iai.61.9.3583-3589.1993.
[235] J. Roderova *et al.*, "Residues 529 to 549 participate in membrane penetration and pore-forming activity of the Bordetella adenylate cyclase toxin," *Sci. Rep.*, 2019, doi: 10.1038/s41598-019-42200-2.
[236] S. Bhakdi *et al.*, "Potent leukocidal action of Escherichia coli hemolysin mediated by permeabilization of target cell membranes," *J. Exp. Med.*, 1989, doi: 10.1084/jem.169.3.737.
[237] O. V. Gadeberg and I. Orskov, "In vitro cytotoxic effect of α-hemolytic Escherichia coli on human blood granulocytes," *Infect. Immun.*, 1984, doi: 10.1128/iai.45.1.255-260.1984.
[238] H. L. Mobley *et al.*, "Pyelonephritogenic Escherichia coli and killing of cultured human renal proximal tubular epithelial cells: Role of hemolysin in some strains," *Infect. Immun.*, 1990, doi: 10.1128/iai.58.5.1281-1289.1990.
[239] A. L. Cortajarena, F. M. Goñi, and H. Ostolaza, "A receptor-binding region in Escherichia coli α-haemolysin," *J. Biol. Chem.*, 2003, doi: 10.1074/jbc.M208552200.
[240] J. Mašín, I. Konopásek, J. Svobodová, and P. Šebo, "Different structural requirements for adenylate cyclase toxin interactions with erythrocyte and liposome membranes," *Biochim. Biophys. Acta - Biomembr.*, 2004, doi:

10.1016/j.bbamem.2003.11.008.
[241] C. Hyland, L. Vuillard, C. Hughes, and V. Koronakis, “Membrane interaction of Escherichia coli hemolysin: Flotation and insertion-dependent labeling by phospholipid vesicles,” *J. Bacteriol.*, 2001, doi: 10.1128/JB.183.18.5364-5370.2001.
[242] R. Benz, E. Maier, S. Bauer, and A. Ludwig, “The deletion of several amino acid stretches of Escherichia coli alpha-hemolysin (HlyA) suggests that the channel-forming domain contains beta-strands,” *PLoS One*, 2014, doi: 10.1371/journal.pone.0112248.
[243] A. Valeva *et al.*, “Binding of Escherichia coli hemolysin and activation of the target cell is not receptor-dependent,” *J. Biol. Chem.*, 2005, doi: 10.1074/jbc.M507690200.

APPENDIX I

Bordetella pertussis and *Bordetella bronchiseptica* filamentous hemagglutinins are processed at different sites

Jurnecka D, Man P, Sebo P, Bumba L.

FEBS Open Bio. 2018 Jun 20;8(8):1256-1266. doi: 10.1002/2211-5463.12474.

FEBS openbio

FEBS PRESS science publishing by scientists

Bordetella pertussis and *Bordetella bronchiseptica* filamentous hemagglutinins are processed at different sites

David Jurnecka[1,2], Petr Man[2,3], Peter Sebo[1] and Ladislav Bumba[1]

1 Laboratory of Molecular Biology of Bacterial Pathogens, Institute of Microbiology, Czech Academy of Sciences, Prague 4, Czech Republic
2 Department of Biochemistry, Faculty of Science, Charles University in Prague, Prague 2, Czech Republic
3 BioCeV - Institute of Microbiology of the Czech Academy of Sciences, Vestec, Czech Republic

Keywords
bacterial pathogenesis; *Bordetella bronchiseptica*; *Bordetella pertussis*; mass spectrometry (MS); protein processing; serine protease

Correspondence
L. Bumba, Laboratory of Molecular Biology of Bacterial Pathogens, Institute of Microbiology, Czech Academy of Sciences, Videnska 1083, 14200 Prague 4, Czech Republic
E-mail: bumba@biomed.cas.cz

(Received 8 March 2018, revised 22 May 2018, accepted 5 June 2018)

doi:10.1002/2211-5463.12474

Filamentous hemagglutinin (FHA) mediates adherence and plays an important role in lower respiratory tract infections by pathogenic *Bordetellae*. The mature FHA proteins of *B. pertussis* (Bp-FHA) and the *B. bronchiseptica* (Bb-FHA) are generated by processing of the respective FhaB precursors by the autotransporter subtilisin-type protease SphB1. We have used bottom-up proteomics with differential $^{16}O/^{18}O$ labeling and show that despite high-sequence conservation of the corresponding FhaB segments, the mature Bp-FHA (~ 230 kDa) and Bb-FHA (~ 243 kDa) proteins are processed at different sites of FhaB, after the Ala-2348 and Lys-2479 residues, respectively. Moreover, protease surface accessibility probing by on-column (on-line) digestion of the Bp-FHA and Bb-FHA proteins yielded different peptide patterns, revealing structural differences in the N-terminal and C-terminal domains of the Bp-FHA and Bb-FHA proteins. These data indicate specific structural variations between the highly homologous FHA proteins.

The three classical species of Gram-negative *Bordetellae* cause respiratory infections in mammals. While *B. bronchiseptica* colonizes the nasopharynx and trachea of a broad range of mammalian hosts, such as rodents or dogs, *B. pertussis* is a strictly human pathogen that causes the highly contagious respiratory disease called whooping cough or pertussis. *B. parapertussis* typically infects ovines but human-adapted strains of *B. parapertussis*$_{hu}$ account for up to 20% of human whooping cough cases [1].

Introduction in the 1950s of whole-cell pertussis (wP) vaccines, composed of killed *B. pertussis* cells, led to a dramatic decrease in pertussis-related mortality and incidence of the disease [2]. Safety concerns, however, led later to the replacement of the wP vaccine with the less reactogenic acellular pertussis component vaccines (aP). The latter are composed of one to five purified pertussis proteins, including chemically inactivated pertussis toxin (PT), filamentous hemagglutinin (FHA), pertactin (PRN), and/or fimbriae of serotype 2 or 3 (FIM2, FIM3). Recent epidemiologic data show a steep increase in pertussis incidence in adolescents and adults, which is linked to the switch from the use of wP to aP vaccines in developed countries in the late 1990s [3]. While being effective in preventing clinical pertussis disease in infants, the aP vaccines appear to confer a rapidly waning protection and do not prevent bacterial colonization and transmission of the pathogen in aP-vaccinated populations [4–6].

Abbreviations
Bb-FHA, *B. bronchiseptica* filamentous hemagglutinin; Bp-FHA, *B. pertussis* filamentous hemagglutinin; ESI-FT-ICR MS, electrospray ionization Fourier transform ion cyclotron resonance mass spectrometry; FHA, filamentous hemagglutinin; HDX, hydrogen-deuterium exchange; LC-MS/MS, liquid chromatography–tandem mass spectrometry.

FEBS Open Bio **8** (2018) 1256–1266

The mature *B. pertussis* FHA is included in all but one of the used aP vaccines, as FHA was proposed to play an important role in bacterial adhesion and invasion of host epithelial and phagocytic cells [7]. It is a hairpin-shaped molecule (50 nm in length and approximately 4 nm in width) consisting predominantly of tandem repetitive β-strands arranged into a right-handed parallel β-helix [8]. Mature FHA or its FhaB precursor was found to mediate bacterial adherence to a wide range of cell lines *in vitro* and FhaB appears to play a role in colonization of the lower respiratory tract in rodents, such as rats and mice [9–11]. Four different functional domains (heparin-binding, carbohydrate recognition, Arg-Gly-Asp motif, and mature C-terminal domain) of FHA were identified and implicated in interaction of mature FHA with eukaryotic cells *in vitro*. However, the roles played by these domains in *Bordetella* infections *in vivo* are poorly defined and remain controversial [12]. In addition to a role in bacterial adherence, the FHA protein was proposed to exert immunomodulatory signaling, inducing secretion of tolerogenic IL-10 by dendritic cells [13,14]. However, this was recently shown to be due contamination of FHA preparations by endotoxin-associated TLR2 ligands [15]. Moreover, FHA was also reported to interact with the adenylate cyclase toxin, an important *Bordetella* virulence factor [16,17].

Filamentous hemagglutinin of *B. pertussis* is synthesized as a 367-kDa precursor (FhaB) that is exported across the cytoplasmic membrane by the general Sec system, using an unusually long N-terminal signal peptide comprising 71 amino acid residues. The signal peptide of FhaB contains two cysteines (Cys_{24} and Cys_{31}) that are necessary for post-translational cyclization of the N-terminal glutamine residue (Gln-72) of processed FhaB to a cyclic pyroglutamyl residue [18]. After removal of the signal sequence, the FhaB protein is secreted across the outer bacterial membrane by a two-partner secretion (TPS) pathway [19]. The N-terminal 'TPS domain' of FhaB, comprising 245 residues, initiates export across the outer membrane by interacting with the periplasmic polypeptide transport associated (POTRA) domain of FhaC, the outer membrane component of the TPS secretion pathway [20]. Translocation of FhaB proceeds in an N- to C-terminal direction, where the N terminus forms an extended hairpin through the FhaC channel and the C terminus gradually folds into a β-helix, as it emerges on the cell surface [21]. The translocated portion of FhaB is then eventually processed by the outer membrane-associated protease SphB1 to a 230-kDa mature FHA protein. The ~1300 residue-long C-terminal fragment of FhaB, called the prodomain, was recently proposed to serve as an intramolecular chaperone and appears to be rapidly degraded in bacterial periplasm [22–24].

SphB1 is a surface-exposed autotransporter protein that harbors a subtilisin-type serine protease domain. It was proposed to cleave FhaB of *B. pertussis* within the PLFETRIKFID sequence (residues 2362–2372), but the cleavage site was not identified [25]. Moreover, in SphB1-deficient (*ΔsphB1*) strains, the FhaB precursor can still be processed to a larger FHA* protein by another, as yet unknown, protease [21,23,24].

Therefore, we used differential $^{16}O/^{18}O$ labeling and proteomics to identify the C-terminal residues of FHA proteins purified from culture supernatants of wild-type *B. pertussis* and *B. bronchiseptica* strains. The results show that despite high-sequence conservation of the processed segments, the FhaB proteins from the two species are processed at different sites. Furthermore, the N- and C-terminal domains of the two resulting FHA proteins exhibit a different surface accessibility to proteolytic cleavage.

Material and methods

Bacterial strains and growth conditions

Bordetella pertussis Tohama I and *Bordetella bronchiseptica* RB50 cells were grown at 37 °C on Bordet–Gengou agar (BG) supplemented with 15% defibrinated sheep blood. For liquid cultures, the bacteria were grown in Stainer–Scholte (SS) medium supplemented with 1 $mg \cdot mL^{-1}$ (2,6-O-dimethyl)-β-cyclodextrin at 37 °C.

Purification of FHA

Bordetella cells were grown in 50 mL of SS medium for 8 h at 37 °C, diluted in fresh SS medium (200 mL and 1 l for *B. pertussis* and *B. bronchiseptica*, respectively) to OD_{600}=0.2 and cultivated for 36 or 14 h for *B. pertussis* or *B. bronchiseptica*, respectively, using a rotary shaker (160 r.p.m.) at 37 °C. The cells were spun down at 14 000 ***g*** for 25 min at 4 °C, and the supernatants were filtered through a 0.2-μm TPP Rapid Filtermax Vacuum Filtration system. The filtrates were loaded onto 5 mL bed volume of Cellufine sulfate (JNC Corporation, Japan) equilibrated with 10 mM phosphate buffer, pH 7.6 (PB), extensively washed with PB, and purified FHA proteins were eluted with PB supplemented with 700 mM NaCl. The purification procedure was performed at 4 °C. The purity of proteins was determined by sodium dodecyl sulfate–polyacrylamide gel electrophoresis (SDS/PAGE), and the protein concentrations were determined by Bradford assay using bovine serum albumin as standard. Due to low yields, *B. bronchiseptica* FHA was concentrated by

precipitation with acetone (4 : 1, v/v) at −20 °C for 12 h and collected by centrifugation at 16 000 ***g*** for 10 min at 4 °C. Protein pellets were reconstituted in phosphate-buffered saline (PBS) or PBS supplemented with 4 M urea (for on-line digestion).

Protein digest and ^{18}O stable isotope labeling

Purified FHA proteins were separated on 5% SDS/PAGE gel and stained with Coomassie brilliant blue R-250. Protein bands were excised from the gel, cut into small pieces and destained by sonication in 200 μL of Tris/HCl (pH 8.2) and 200 μL of acetonitrile (ACN). After complete destaining, the gel pieces were rinsed with 200 μL of ACN for 5 min, the liquid was discarded, and gel pieces were washed with 200 μL of H_2O. Finally, the gel was washed by 200 μL of H_2O/ACN (1 : 1) and dried under vacuum. Next, the gel was rehydrated in 50 μL of 10% ACN in 25 mM N-ethyl morpholine acetate buffer (pH 8.2) containing the protease. The buffer was prepared either with normal water, or doubly concentrated buffer was diluted 1 : 1 with $H_2{}^{18}O$. Proteins were digested at 37 °C overnight, and the proteases used were as follows: trypsin gold (enzyme-to-substrate ratio [w/w] of 1 : 75), LysC, and AspN (enzyme-to-substrate ratio [w/w] of 1 : 50 for both). After digestion, the peptides were extracted with 100 μL of 80% ACN, 0.1% trifluoroacetic acid (TFA), dried via vacuum centrifugation, and solubilized in 100 μL of 10% ACN and 0.1% TFA. Alternatively, 50 μg samples of purified FHA was dried, solubilized in 50 mM ammonium bicarbonate buffer (pH 8.2), and digested using the same proteases as described above. In-solution digestion was carried out for 6 h. Following digestion, samples were dried and reconstituted as above. Samples from in-gel and in-solution digestion were next desalted by peptide MacroTrap (Optimize Technologies) and eluted with 150 μL of 80% ACN, 0.1% TFA. Desalted peptides were dried via vacuum centrifugation and dissolved in 30 μL of 5% ACN, 0.1% TFA (v/v) prior the LC-MS/MS analysis.

Mass spectrometry

For LC-MS/MS analyses, a capillary HPLC system (1200, Agilent Technologies, Germany) connected to an ESI source of the FT-ICR mass spectrometer (15T, SolariX XR, Bruker) was used. Peptides were separated on analytical reverse phase column (MAGIC C18 AQ, 0.2 × 150 mm, Michrom Bioresources) and separated by following gradient: 1–10% *B* in 1 min, 10–40% *B* in 50 min, where solvent *A* was 0.2% formic acid, 2.5% ACN, and 2.5% isopropanol, and solvent *B* was 0.16% formic acid in 90% ACN and 5% isopropanol. The flow rate was 4 μL·min^{-1}. ESI-FT-ICR MS was calibrated externally using arginine clusters resulting in a mass accuracy below 2 p.p.m. For peptide, mapping instrument was operated in data-dependent mode, where each MS scan was followed by up to five MS/MS collision-induced fragmentations of the most intense ions.

H/D-like mapping of FHA using immobilized endopeptidase under denaturing conditions

Digestion of FHA, with immobilized porcine pepsin A, aspergillopepsin, or rhizopuspepsin under HDX compatible conditions, was performed as described previously [26]. Briefly, the system consisted of injection and switching valves mounted with immobilized protease column, trap column (peptide MicroTrap, Optimized Technologies), and analytical column (Jupiter C18, 0.5 × 50 mm, 5 μm, 300 Å, Phenomenex), with all components immersed in an ice-water bath. Digestion and desalting (4 min) were driven by a Shimadzu LC20-AD pump isocratically delivering 0.4% formic acid at a flow rate of 100–200 μL·min^{-1} depending on the protease column used. Gradient separation on the analytical column was carried out by an HPLC system (Agilent Technologies 1200) running at a flow rate of 15 μL·min^{-1} Gradient elution from 5% B to 35% B in 40 min, followed by elution with 95% B, was used for separation. Solvents used were A: 0.4% formic acid and 2% ACN; and solvent B: 0.4% formic acid in 95% ACN. The outlet of the analytical column was directly connected to an electrospray ionization (ESI) source of 15T FT-ICR mass spectrometer (Bruker Daltonics). The purified Bp-FHA or Bb-FHA (300 pmol) was diluted in 0.5 M glycine/HCl buffer (pH 2.3) and injected into the column system. Alternatively, Bp-FHA, diluted 1 : 1 with 8 M urea (to give a final urea concentration of 4 M), or Bb-FHA, resuspended in PBS containing 4 M urea, was incubated for 30 min at 50 °C before the mixture was diluted 1 : 1 with 0.5 M glycine/HCl buffer (pH 2.3) and immediately injected into the chromatography system.

Data processing

Data processing was performed using Data Analysis 4.1 (Bruker Daltonics). Peak picking was carried out by FTMS and SNAP algorithms, and two mascot generic files were created for each analysis. Data from the unlabeled samples (specific protease digestion) and from on-line aspartic protease digestion were searched using local MASCOT server (MatrixScience) against a single protein database containing the sequence of FHA from *B. pertussis* or *B. bronchiseptica* with no-enzyme specificity. Peptide tolerance was set to 10 p.p.m. and fragment ion tolerance to 0.05 Da. Identified C-terminal peptides of FHA proteins were manually searched in the ^{18}O labeled samples. The mass spectrometry proteomics data have been deposited to the ProteomeXchange Consortium via the PRIDE [27] partner repository with the dataset identifier PXD008664 and 10.6019/PXD008664.

Results

Purification of FHA proteins

Despite use of Bp-FHA in aP vaccines for two decades, the exact C-terminal sequence of FHA remained unknown. To identify the C-terminal residues of FHA of *B. pertussis* and of *B. bronchiseptica,* we have purified the mature forms of the two proteins from culture supernatants using a single-step affinity chromatography on Cellufine sulfate. SDS/PAGE analysis revealed that both *B. pertussis* (Bp-FHA) and *B. bronchiseptica* (Bb-FHA) FHA preparations contained the mature and the truncated forms of FHA [25], which migrated as double bands of >250 kDa (Fig. 1). Unlike the Bp-FHA preparation, which was almost homogenous, the Bb-FHA preparation contained proteolytic fragments (~ 130, 100 and 75 kDa) that were recognized by a polyclonal anti-FHA antibody (data not shown). This likely reflected the difficulty to purify Bb-FHA, which was obtained in about 20 times lower yields despite the use of five times larger volumes of culture supernatants. Indeed, *B. bronchiseptica* was reported to release much less FHA than *B. pertussis* [28]. The lower yield of Bb-FHA might further reflect a lower affinity for the Cellufine sulfate resin, as the heparin-binding domain sequences of Bb-FHA and Bp-FHA differ importantly.

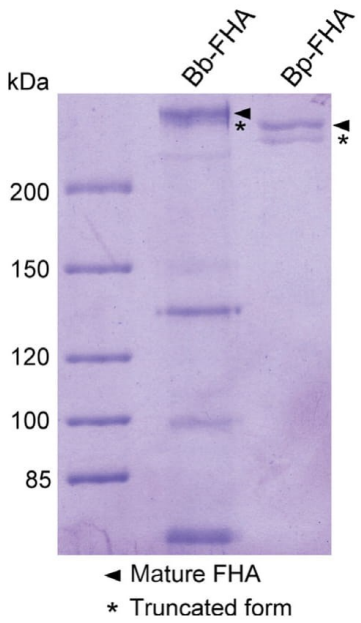

Fig. 1. The SDS/PAGE analysis of FHA preparations purified from culture supernatants of *B.pertussis* (Bp-FHA) and *B.bronchiseptica* (Bb-FHA). The mature (FHA) and alternatively processed (FHA_1) forms of FHA are indicated.

Identification of the C-terminal residue of FHA

To identify the C-terminal residues of the purified proteins, the bands corresponding to mature (FHA) and truncated (FHA_1) forms of the FHA proteins were excised from the SDS/PAGE gels and digested with trypsin, AspN, or LysC proteases. In parallel, the Bp-FHA and Bb-FHA preparations were digested in solution and the resulting peptides were analyzed by LC-MS/MS followed by MASCOT search. This yielded 94% and 96% coverage of the protein sequence of mature Bp-FHA and Bb-FHA, respectively (PRIDE Archive, project accession: PXD008664). The C-terminal peptides of FHA proteins were identified as peptides with masses that did not match the highly specific cleavage pattern of the used proteases (X-↓-Asp/Glu for AspN; Lys-↓-X for LysC; and Arg/Lys-↓-X for trypsin). The C-terminal peptides of Bp-FHA_1 and Bb-FHA_1 were further identified by peptide mapping of the in-gel digested FHA_1 bands (Fig. 1), as summarized in Table 1.

The C-terminal residue of Bp-FHA was identified as Ala_{2348}, based on detection of two peptides that partially violated the expected cleavage pattern, namely the AspN peptide $_{2335}$DQPVVAVGLEQPVA$_{2348}$ and the tryptic peptide $_{2300}$NAQVADAGLAGPSAVAAPAVGAADV GVEPVTGDQVDQPVVAVGLEQPVA$_{2348}$. The N termini of both peptides complied with the expected cleavage rules (X-↓-Asp for AspN and Arg-↓-X for trypsin) but the C-terminal Ala_{2348} residue, followed by Thr_{2349} in FhaB sequence, did not, as neither AspN nor trypsin would cleave an Ala.Thr peptide bond. Similarly, the C terminus of Bp-FHA_1 was identified as Ala_{2228}, based on detection of the LysC peptide $_{2220}$RLDIDDALA$_{2228}$ and of the AspN peptide $_{2214}$DVGLEKRLDIDDALA$_{2228}$. The N termini of these peptides complied well with LysC (Arg/Lys-↓-X) and AspN (X-↓-Asp) cleavage rules, while the C-terminal Ala_{2228} residue (followed Ala_{2229} in FhaB sequence) could not result from cleavage of an Ala.Ala bond by LysC or AspN.

It should be noted that the $_{2214}$DVGLEKRLDID-DALA$_{2228}$ peptide contains three internal aspartate residues (D) that are possible targets for AspN cleavage, while the $_{2222}$DIDDALA$_{2228}$, $_{2224}$DDALA$_{2228}$, and $_{2225}$DALA$_{2228}$ fragments were not detected. This can be understood, as the tetra- and penta-peptides were too

Table 1. The C-terminal peptides of FHA and FHA_1 proteins based on in-gel and in-solution digestions.

		Protease	Peptide position	Peptide sequence	$M_{monoisotopic}$ (calculated)	$M_{monoisotopic}$ (experimental)	Error (Δ p.p.m.)
Bordetella pertussis	FHA	AspN	2335–2348	G.DQPVVAVGLEQPVA.T	1420.7562	1420.7509	4
		trypsin	2300–2348	R.NAQVADAGLAGPSAVA APAVGAADVGVEPVTGD QVDQPVVAVGLEQPVA.T	4546.3192	4546.3249	1
	FHA_1	AspN	2214–2228	R.DVGLEKRLDIDDALA.A	1641.8573	1641.8496	5
		LysC	2220–2228	K.RLDIDDALA.A	1000.5189	1000.5251	6
Bordetella bronchiseptica	FHA	AspN	2446–2479	D.QPVVAVGLEQPAAAVRV APPAVALPRPLFETRIK.F	3560.0718	3560.0566	5
	FHA_1	AspN	2335–2347	D.DALAAVLVNPHIF.T	1378.7608	1378.7514	7
		trypsin	2331–2347	R.LDIDDALAAVLVNPHIF.T	1834.9828	1834.9818	1

small to be trapped on the desalting column and were thus not detected by MS/MS. Moreover, AspN is rather inefficient in cutting of D-D bonds and in complete processing of all the possible cleavage sites [29].

The C-terminal residue of Bb-FHA could be identified only tentatively, as Lys_{2479} residue of $_{2446}$QPVVAVGLEQPAAAVRVAPPAVALPRPLFETRIK$_{2479}$. This was the most C terminally located peptide detected in the AspN-generated digests of Bb-FHA. The N-terminal residue of this peptide could have resulted from an unspecific AspN-mediated cleavage on the N-terminal side of Gln_{2446}, but AspN was unlikely to have cleaved at the N-terminal side of the Phe_{2480} residue, which follows Lys_{2479} in Bb-FHA protein. Regrettably, no other peptides allowing confirmation of the identity of the C-terminal residue of Bb-FHA were detected.

In contrast, the C-terminal residue of $Bb\text{-}FHA_1$ was unambiguously identified by detection of the $_{2335}$DALAAVLVNPHIF$_{2347}$ and $_{2331}$LDIDDALAAVLVNPHIF$_{2347}$ peptides in the AspN and tryptic digests of $Bb\text{-}FHA_1$. Neither AspN, nor trypsin would cleave the $_{2347}$Phe.Thr$_{2348}$ bond, while AspN and trypsin would generate the Asp_{2335} and Leu_{2331} N termini, respectively.

Apart from the peptides covering the analyzed Bp-FHA and Bb-FHA proteins, the detailed analysis of MS spectra revealed that both FHA preparations contained also peptides originating from *Bordetellae* proteins other than FHA. As shown in Table 2, four and five additional proteins were identified as contaminants of the Bp-FHA and Bb-FHA preparations. Bp-FHA contained traces of the putative phospholipid-binding protein MlaC, of the toluene tolerance protein Ttg2D, and of the S4 and S5 subunits of pertussis toxin. The Bb-FHA preparation was contaminated by adenylate cyclase toxin (CyaA), the SphB1 protease, and the Bsp22, BteA, and BopD proteins secreted by the type III secretion system.

Table 2. The overall protein content in the Bp-FHA and Bb-FHA preparations.

	Protein	MW (kDa)	Isoelectric point (pI)
Bp-FHA	Filamentous hemagglutinin	367	9.2
	Pertussis toxin subunit 4	14	9.2
	Pertussis toxin subunit 5	13	5.4
	Toluene tolerance protein Ttg2D	20	9.2
	Probable phospholipid-binding protein mlaC	21	9.2
Bb-FHA	Filamentous hemagglutinin	372	8.7
	Adenylate cyclase toxin	178	4.4
	SphB1 protease	87	9.7
	T3SS protein BopD	32	6.4
	T3SS protein Bsp22	22	7.2
	T3SS protein BteA	69	5.0

To corroborate the identification of the C-terminal residues of Bp-FHA and Bb-FHA proteins, we performed differential stable ^{18}O isotope labeling. The method is based on protease-catalyzed ^{18}O replacement of two ^{16}O atoms on the carboxyl of a newly liberated C-terminal residue of a peptide that is generated by proteolytic cleavage of a protein in the presence of isotopic water ($H_2{}^{18}O$) [30]. As the carboxyl of the preexisting C-terminal residue of the digested protein remains unlabeled, the resulting mass difference between the labeled and the unlabeled peptide ions permits the identification of the peptide that contains the C-terminal residue of the given protein.

As shown in Fig. 2, the isotope envelopes of the $_{2335}$DQPVVAVGLEQPVA$_{2348}$ and $_{2214}$DVGLEKRLDIDDALA$_{2228}$ peptide peaks in the ^{18}O-labeled AspN digests of the Bp-FHA and of the $Bp\text{-}FHA_1$ proteins were identical to that observed for the same peptides

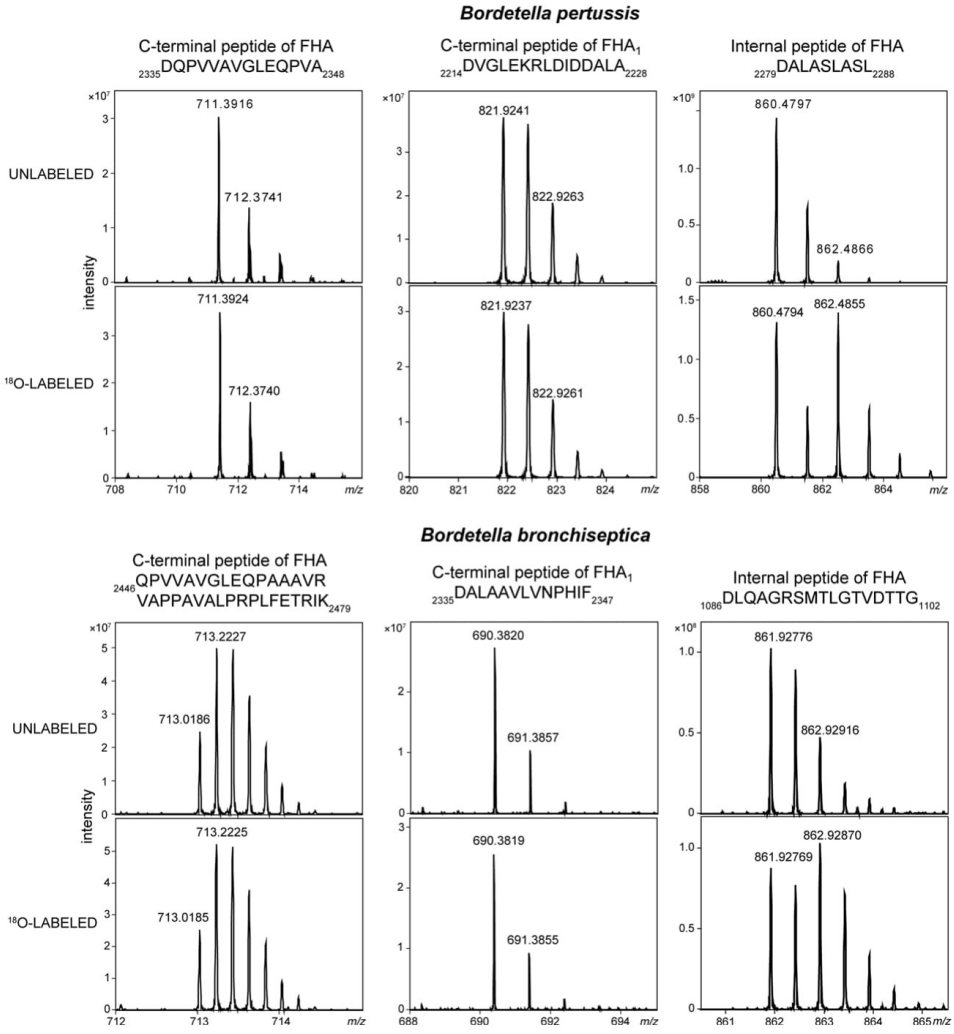

Fig. 2. Isotope profiles of the C-terminal peptides of FHA and FHA_1 after enzymatic digestion of Bp-FHA (upper panel) and Bb-FHA (lower panel) with AspN in the presence of normal H_2O (unlabeled) and 50% ^{18}O water (^{18}O-labeled).

in nonlabeled digests. The same was true for the $_{2446}$QPVVAVGLEQPAAAVRVAPPAVALPRPLFETRIK$_{2479}$ and $_{2335}$DALAAVLNPHIF$_{2347}$ peptides derived from Bb-FHA and Bb-FHA_1 (Fig. 2). In contrast, the isotope envelopes of all other peptides in the ^{18}O-labeled AspN digests of Bp-FHA/Bp-FHA_1 and Bb-FHA/Bb-FHA_1 proteins exhibited the expected shifts to 'double peaks'. These comprised strikingly enhanced intensities of the monoisotopic masses of the ^{18}O-labeled peptides, as documented in Fig. 2 for the internal $_{2279}$DALASLASL$_{2288}$ and $_{1086}$DLQAGRSMTLGTVDTTG$_{1102}$ peptides from the Bp-FHA and Bb-FHA proteins. These data thus fully confirmed that Ala_{2348} and Ala_{2228} were the C-terminal residues of

Bp-FHA and of Bp-FHA_1, while Lys_{2479} and Phe_{2347} were the C-terminal residues of Bb-FHA and of Bb-FHA_1, respectively.

Mapping of FHA surface accessibility using immobilized endopeptidase columns

To gain insight into the specific sequence-structure relationships of the Bp-FHA and Bb-FHA proteins, we performed an on-line digestion of the two proteins on immobilized acid protease columns connected to an LC-MS/MS analyzer. This instrumental setup comprises a continuous workflow system that is commonly employed for analysis of protein hydrogen/deuterium exchange (HDX) by mass spectrometry [26]. The main advantage of this protocol is the rapidity of digestion and the absence of sample handling. This minimizes sample loss and unwanted protein modifications that may occur during lengthy digestions in typical proteomic protocols.

Initial experiments with on-line digestion of Bp-FHA on an immobilized pepsin column at low pH (2.3) gave low peptide yields with sequence coverage of only 21% (data not shown). Remarkably, the recovered peptides predominantly originated from the C terminus of the mature Bp-FHA protein (residues 1600–2350), indicating that the C-terminal segment of Bp-FHA is much more susceptible to protease digestion than its N-terminal segment that exhibits a compact parallel β-helical fold [8,29]. To increase the sequence coverage of the N-terminal portion of FHA [19], the on-line digestion was performed in the presence of denaturing agents, such as 3 M guanidine chloride or 4 M urea. These conditions usually do not denature proteins, but induce a partial destabilization of compact protein folds. Moreover, such concentrations of denaturing agents do not affect the cleavage efficiency of the immobilized proteases [26]. Different protease columns (pepsin, nepenthesin-1, aspergillopepsin, and rhizopuspepsin) along with different times and temperatures of digestion were also tested. Preliminary experiments showed that the best results were obtained on columns with immobilized pepsin proteases and operated and at flow rates of 100–200 $\mu L \cdot min^{-1}$ at 50 °C.

The on-line digest peptide map acquired under such conditions covered near completely the sequence of Bp-FHA, starting from the N-terminal pyroglutamate residue 72, up to the C-terminal Ala_{2348} residue (Fig. 3). In

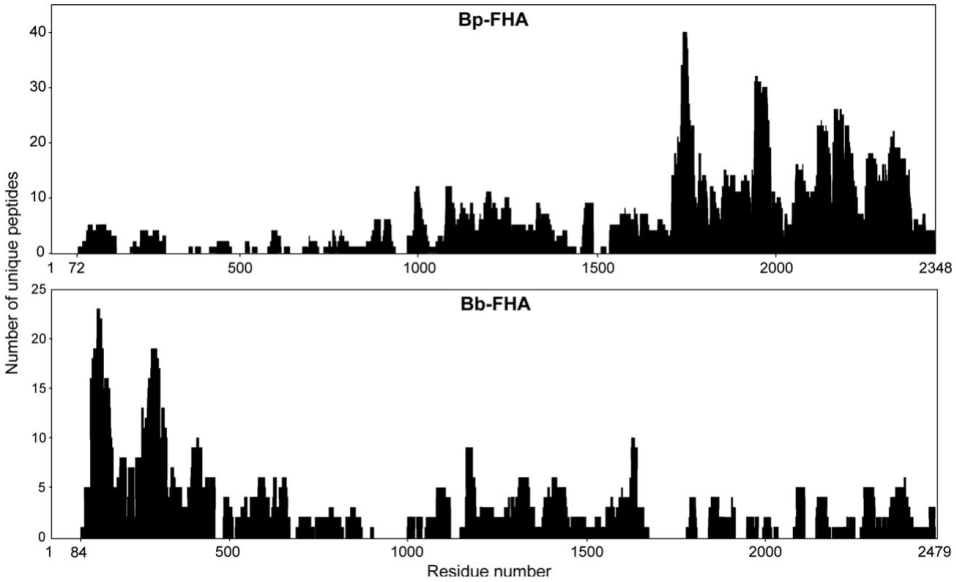

Fig. 3. Surface accessibility of Bp-FHA and Bb-FHA probed by on-column (on-line) digestion. The FHA proteins were incubated in the presence of 4 M urea at 50 °C for 30 min and loaded on immobilized protease columns directly coupled to LC-MS/MS analyzer. Frequency of the appearance of individual residues in the covered sequence is plotted as the number of unique peptides against the protein sequence. The data represent the aggregate result obtained from the on-line digests using rhizopuspepsin, pepsin A, and aspergillopepsin columns.

contrast, the sequence coverage of the on-line digest of Bb-FHA was less complete (Fig. 3). The on-line digestion was performed for a limited time under semidenaturing conditions, using proteases that mostly cleave C terminally to frequently occurring small hydrophobic residues. Therefore, the numbers of generated unique peptides, comprising a given residue of the FHA protein, reflect the accessibility of the corresponding segment to proteolytic cleavage and the compactness of its structure. The quantitative analysis of the peptide maps revealed a striking difference in the overall distribution of unique peptides that were generated by on-line digestion of the Bp-FHA and Bb-FHA proteins (Fig. 3). Irrespectively of the protease used, importantly higher number of unique peptides was recovered from the C-terminal segment of Bp-FHA, than from its N-terminal segment, thus indicating a loosened conformation of the C-terminal segment of Bp-FHA. In contrast, the C-terminal segment of Bb-FHA yielded disproportionally low numbers of unique peptides, which is indicative of a tightly packed structure. In contrast, substantially higher numbers of unique peptides were generated from the N-terminal segment of Bb-FHA, indicating its loosened structure (Fig. 3). This would go well with the fact that the N-terminal segment of Bb-FHA is about 131 residues longer than the corresponding segment of Bp-FHA. On the other hand, the C-terminal processing of the Bp-FHA and Bb-FHA proteins occurred at sites 21 residues apart within a segment of very high-sequence homology of the Bp-FHA and Bb-FHA proteins (Fig. 4).

Discussion

Release of many proteins and peptides from eukaryotic and prokaryotic cells involves proteolytic maturation of the secreted protein precursors. Production of the mature FHA protein of *Bordetella pertussis* involves processing of the 367-kDa FhaB precursor, from which the bacterial surface-anchored autotransporter subtilisin-type protease SphB1 removes the 130-kDa C-terminal prodomain [23,31,32]. Here, we have defined the C-terminal residues of the mature and alternatively processed forms of FHA from the closely related *B. pertussis* and *B. bronchiseptica* species.

Up to now, the C terminus of the mature FHA protein could not be accurately identified and it was only estimated by mass determination of purified *B. pertussis* FHA. The reported MALDI-TOF analysis indicated that mature Bp-FHA may arise from FhaB processing within the PLFETRIKFID sequence between residues 2362 and 2372 [25]. By analogy, processing of Bb-FHA was predicted to occur between residues 2472 and 2482 of Bb-FhaB. However, insufficient accuracy of mass determination of the 230-kDa protein by MALDI-TOF MS did not permit identification of its C-terminal residue. The here-employed digest-based peptide mapping by high-resolution FT-ICR-MS, combined with postdigestion ^{18}O-labeling analysis, yielded unambiguous identification of the C-terminal residues of the various forms of the FHA protein (Fig. 4). Firstly, the C-terminal residues of peptides that did not match the cleavage specificity of the used proteases indicated that the Ala_{2348} and Ala_{2228} were the *bona fide* C-terminal residues of the mature Bp-FHA/Bp-FHA_1 proteins. The Lys_{2479} and Phe_{2347} residues were then identified as the respective C-terminal residues of the Bb-FHA/Bb-FHA_1 proteins. Indeed, the molecular masses of peptides comprising these residues remained unchanged upon postdigestion ^{18}O-exchange labeling of the carboxyls of the C-terminal residues of peptides that were newly generated by *in vitro* protease digestion in $H_2{}^{18}O$. This confirmed the correct assignment of the C-terminal residues.

Mazar and Cotter (2006) have previously shown that the SphB1 protease is involved in proteolytic maturation of FhaB to FHA and FHA_1 both in *B. pertussis* and in *B. bronchiseptica*. Moreover, the processed regions of the FhaB precursors from the two species exhibit a very high degree of sequence identity (Fig. 4) and the SphB1 proteases of the two species are themselves identical to 98%. It is, therefore, intriguing that processing of the FhaB proteins from the two species was found to occur at quite different sites located 21 residues apart within the same highly conserved segment of FhaB. Moreover, the processing step involved cleavage of peptide bonds between rather different pairs of residues. The bond between a small hydrophobic Ala_{2348} and a small hydrophilic Thr_{2349} residue was cleaved in Bp-FhaB, while processing of the Bb-FhaB protein resulted from cleavage of the bond between a positively charged Lys_{2479} and a bulky aromatic Phe_{2480} residue. As a result, the C-terminal segment of the mature Bb-FHA is extended by 21 residues, compared to mature Bp-FHA. Similarly, the C-terminal sequences of Bp-FHA_1 and Bb-FHA_1 differ by 9 residues.

Albeit unlikely, it cannot be excluded that upon SphB1-mediated cleavage the C termini of FHA may be further processed by some other secreted bacterial proteases. Alternatively, these unexpected results may indicate that the substrate specificities of the highly conserved SphB1 proteases of the two bacterial species may differ. The SphB1 protease, indeed, belongs to a superfamily of subtilisin-like proteases that possess rather broad substrate specificity. This is largely

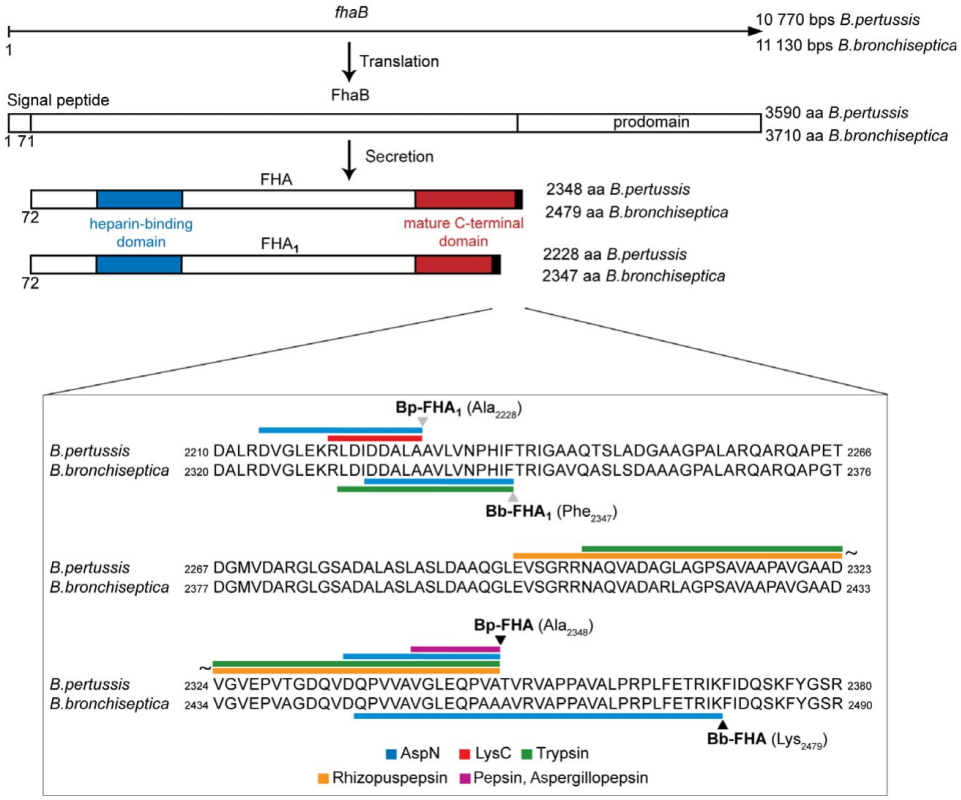

Fig. 4. Schematic representation of the C termini of FHA proteins. FHA is encoded by the *fhaB* gene and translated as a FhaB precursor polypeptide (3590 residues in *Bordetella pertussis* and 3710 residues in *Bordetella bronchiseptica*), containing the N-terminal signal peptide (71 residues) that is removed during translocation of FhaB across the cytoplasmic membrane. FhaB is then exported from the periplasmic space through the outer membrane and processed in SphB1-dependent manner, yielding mature [C terminus at position 2348 (Bp-FHA) or 2479 (Bb-FHA)] or truncated [C terminus at position 2228 (Bp-FHA) or 2347 (Bb-FHA)] variant of FHA protruding on the cell surface. The C-terminal FhaB prodomain (130 kDa) remains in the periplasm, and it is rapidly degraded. The C-terminal peptides identified by LC-MS/MS approaches after digestion with AspN (blue), LysC (red), trypsin (green), rhizopuspepsin (orange), and (aspergillo)pepsin (magenta) are indicated over the Bp-FHA and Bb-FHA protein sequences aligned based on sequence homology.

determined by interactions of the P4-P1 residue side chains in the binding pocket of the enzyme, which enables the cleavage of peptide bonds on the C-side of aliphatic or aromatic amino acid residues [33]. A closer look on the P4-P1 residues of Bp-FHA ($QPVA_{2348}$) and Bp-FHA_1 ($DALA_{2228}$) reveals a certain analogy between their C-terminal sequences, in terms of side chain properties, indicating that Bp-FhaB is processed by SphB1 with a defined substrate specificity. In contrast, the C-terminal sequences of Bb-FHA ($TRIK_{2479}$) and Bb-FHA_1 ($PHIF_{2347}$) are rather distinct and do not appear to share any similarity, even though the C-terminal residue of Bb-FHA_1 complies with the substrate specificity of subtilisin-like proteases. However, the C-terminal Lys_{2479} residue of Bb-FHA does not match the substrate specificity of a subtilisin type of protease. It thus remains to be determined if the Bb-SphB1 has a broader substrate specificity than Bp-SphB1, or another as yet unknown protease participates in the final processing of the Bb-FhaB precursor.

Even though the Bp-FHA and Bb-FHA proteins are highly homologous (90% identity) and appear to be

functionally interchangeable between *B. pertussis* and *B. bronchiseptica* [34], our data show that the C termini of mature FHA proteins differ by 21 amino acid residues. The here observed difference in the processing and protease susceptibility of the C-terminal segments of the two proteins is intriguing, as the mature C-terminal domain of FHA was proposed to play an important role in adherence and virulence of *Bordetellae* [11,24,31,34]. *B. pertussis* is a fully human-adapted pathogen, while *B. bronchiseptica* infects a broad variety of mammals. It will, hence, be important to determine whether the difference in FhaB processing in the two bacterial species plays a role in the biological activity of mature FHA proteins.

Acknowledgement

We would like to thank Petr Pompach for help with MS measurements. Access to the mass spectrometry facility was enabled through the MEYS/EU projects CZ.1.05/1.1.00.02.0109 and LM2015043 CIISB. This work was supported by the projects LM2015064 (Czech National Node to the European Infrastructure for Translational Medicine) from the Ministry of Education, Youth and Sports of the Czech Republic. The projects LQ1604 (PM), GA18-20621S (PS), and GA15-11851S (LB) are also acknowledged.

Author contributions

DJ measured and analyzed the data, PM performed and evaluated the on-line digests, LB and PS designed the project, and LB, DJ, and PS wrote the manuscript.

References

1 Diavatopoulos DA, Cummings CA, Schouls LM, Brinig MM, Relman DA and Mooi FR (2005) Bordetella pertussis, the causative agent of whooping cough, evolved from a distinct, human-associated lineage of B. bronchiseptica. *PLoS Pathog* **1**, 0373–0383.

2 Mattoo S and Cherry JD (2005) Molecular pathogenesis, epidemiology, and clinical manifestations of respiratory infections due to Bordetella pertussis and other Bordetella subspecies. *Clin Microbiol Rev* **18**, 326–382.

3 Klein NP (2014) Licensed pertussis vaccines in the United States: history and current state. *Hum Vaccines Immunother* **10**, 2684–2690.

4 Warfel JM and Edwards KM (2015) Pertussis vaccines and the challenge of inducing durable immunity. *Curr Opin Immunol* **35**, 48–54.

5 Tartof SY, Lewis M, Kenyon C, White K, Osborn A, Liko J, Zell E, Martin S, Messonnier NE, Clark TA *et al.* (2013) Waning immunity to pertussis following 5 doses of DTaP. *Pediatrics* **131**, e1047–e1052.

6 Witt MA, Arias L, Katz PH, Truong ET and Witt DJ (2013) Reduced risk of pertussis among persons ever vaccinated with whole cell pertussis vaccine compared to recipients of acellular pertussis vaccines in a large US cohort. *Clin Infect Dis* **56**, 1248–1254.

7 Hazenbos WLW, Van den Berg BM, Van't Wout JW, Mooi FR and Van Furth R (1994) Virulence factors determine attachment and ingestion of nonopsonized and opsonized Bordetella pertussis by human monocytes. *Infect Immun* **62**, 4818–4824.

8 Makhov AM, Hannah JH, Brennan MJ, Trus BL, Kocsis E, Conway JF, Wingfield PT, Simon MN and Steven AC (1994) Filamentous hemagglutinin of Bordetella pertussis. A bacterial adhesin formed as a 50-nm monomeric rigid rod based on a 19-residue repeat motif rich in beta strands and turns. *J Mol Biol* **241**, 110–124.

9 Cotter PA, Yuk MH, Mattoo S, Akerley BJ, Boschwitz J, Relman DA and Miller JF (1998) Filamentous hemagglutinin of Bordetella bronchiseptica is required for efficient establishment of tracheal colonization. *Infect Immun* **66**, 5921–5929.

10 Mattoo S, Miller JF and Cotter PA (2000) Role of Bordetella bronchiseptica fimbriae in tracheal colonization and development of a humoral immune response. *Infect Immun* **68**, 2024–2033.

11 Inatsuka CS, Julio SM and Cotter PA (2005) Bordetella filamentous hemagglutinin plays a critical role in immunomodulation, suggesting a mechanism for host specificity. *Proc Natl Acad Sci USA* **102**, 18578–18583.

12 Villarino Romero R, Osicka R and Sebo P (2014) Filamentous hemagglutinin of Bordetella pertussis: a key adhesin with immunomodulatory properties? *Future Microbiol* **9**, 1339–1360.

13 Dirix V, Mielcarek N, Debrie AS, Willery E, Alonso S, Versheure V, Mascart F and Locht C (2014) Human dendritic cell maturation and cytokine secretion upon stimulation with Bordetella pertussis filamentous haemagglutinin. *Microbes Infect* **16**, 562–570.

14 McGuirk P and Mills KHG (2002) Pathogen-specific regulatory T cells provoke a shift in the Th1/Th2 paradigm in immunity to infectious diseases. *Trends Immunol* **23**, 450–455.

15 Villarino Romero R, Hasan S, Faé K, Holubova J, Geurtsen J, Schwarzer M, Wiertsema S, Osicka R, Poolman J and Sebo P (2016) Bordetella pertussis filamentous hemagglutinin itself does not trigger anti-inflammatory interleukin-10 production by human dendritic cells. *Int J Med Microbiol* **306**, 38–47.

16 Zaretzky FR, Gray MC and Hewlett EL (2002) Mechanism of association of adenylate cyclase toxin

with the surface of Bordetella pertussis: a role for toxin-filamentous haemagglutinin interaction. *Mol Microbiol* **45**, 1589–1598.

17 Perez Vidakovics MLA, Lamberti Y, Van Der Pol WL, Yantorno O and Rodriguez ME (2006) Adenylate cyclase influences filamentous haemagglutinin-mediated attachment of Bordetella pertussis to epithelial alveolar cells. *FEMS Immunol Med Microbiol* **48**, 140–147.

18 Lambert-Buisine C, Willery E, Locht C and Jacob-Dubuisson F (1998) N-terminal characterization of the Bordetella pertussis filamentous haemagglutinin. *Mol Microbiol* **28**, 1283–1293.

19 Clantin B, Hodak H, Willery E, Locht C, Jacob-Dubuisson F and Villeret V (2004) The crystal structure of filamentous hemagglutinin secretion domain and its implications for the two-partner secretion pathway. *Proc Natl Acad Sci USA* **101**, 6194–6199.

20 Clantin B, Delattre A-SS, Rucktooa P, Saint N, Méli AC, Locht C, Françoise J-D and Villeret V (2007) Structure of the membrane protein FhaC: a member of the Omp85-TpsB transporter superfamily. *Science* **317**, 957–961.

21 Mazar J and Cotter PA (2006) Topology and maturation of filamentous haemagglutinin suggest a new model for two-partner secretion. *Mol Microbiol* **62**, 641–654.

22 Renauld-Mongénie G, Cornette J, Mielcarek N, Menozzi FD and Locht C (1996) Distinct roles of the N-terminal and C-terminal precursor domains in the biogenesis of the Bordetella pertussis filamentous hemagglutinin. *J Bacteriol* **178**, 1053–1060.

23 Noël CR, Mazar J, Melvin JA, Sexton JA and Cotter PA (2012) The prodomain of the Bordetella two-partner secretion pathway protein FhaB remains intracellular yet affects the conformation of the mature C-terminal domain. *Mol Microbiol* **86**, 988–1006.

24 Melvin JA, Scheller EV, Noël CR and Cotter PA (2015) New insight into filamentous hemagglutinin secretion reveals a role for full-length FhaB in Bordetella virulence. *MBio* **6**, e01189–15.

25 Coutte L, Antoine R, Drobecq H, Locht C and Jacob-Dubuisson F (2001) Subtilisin-like autotransporter serves as maturation protease in a bacterial secretion pathway. *EMBO J* **20**, 5040–5048.

26 Kadek A, Mrazek H, Halada P, Rey M, Schriemer DC and Man P (2014) Aspartic protease nepenthesin-1 as a tool for digestion in hydrogen/deuterium exchange mass spectrometry. *Anal Chem* **86**, 4287–4294.

27 Vizcaíno JA, Csordas A, Del-Toro N, Dianes JA, Griss J, Lavidas I, Mayer G, Perez-Riverol Y, Reisinger F, Ternent T *et al.* (2016) 2016 update of the PRIDE database and its related tools. *Nucleic Acids Res* **44**, D447–D456.

28 Jacob-Dubuisson F, Kehoe B, Willery E, Reveneau N, Locht C and Relman DA (2000) Molecular characterization of Bordetella bronchiseptica filamentous haemagglutinin and its secretion machinery. *Microbiology* **146**, 1211–1221.

29 Giansanti P, Tsiatsiani L, Low TY and Heck AJR (2016) Six alternative proteases for mass spectrometry-based proteomics beyond trypsin. *Nat Protoc* **11**, 993–1006.

30 Ye X, Luke B, Andresson T and Blonder J (2009) 18O stable isotope labeling in MS-based proteomics. *Brief Funct Genomic Proteomic* **8**, 136–144.

31 Coutte L, Alonso S, Reveneau N, Willery E, Quatannens B, Locht C and Jacob-Dubuisson F (2003) Role of adhesin release for mucosal colonization by a bacterial pathogen. *J Exp Med* **197**, 735–742.

32 Coutte L, Willery E, Antoine R, Drobecq H, Locht C and Jacob-Dubuisson F (2003) Surface anchoring of bacterial subtilisin important for maturation function. *Mol Microbiol* **49**, 529–539.

33 Siezen RJ and Leunissen JA (1997) Subtilases: the superfamily of subtilisin-like serine proteases. *Protein Sci* **6**, 501–523.

34 Julio SM, Inatsuka CS, Mazar J, Dieterich C, Relman DA and Cotter PA (2009) Natural-host animal models indicate functional interchangeability between the filamentous haemagglutinins of Bordetella pertussis and Bordetella bronchiseptica and reveal a role for the mature C-terminal domain, but not the RGD motif, during infection. *Mol Microbiol* **71**, 1574–1590.

APPENDIX II

Rapid Purification of Endotoxin-Free RTX Toxins

Stanek O, Masin J, Osicka R, **Jurnecka D**, Osickova A, Sebo P.

Toxins (Basel). 2019 Jun 12;11(6):336. doi: 10.3390/toxins11060336.

toxins

MDPI

Article

Rapid Purification of Endotoxin-Free RTX Toxins

Ondrej Stanek [1], Jiri Masin [1,*], Radim Osicka [1,*], David Jurnecka [1,2], Adriana Osickova [1,2] and Peter Sebo [1]

[1] Institute of Microbiology of the CAS, Videnska 1083, 142 20 Prague, Czech Republic; stanek@biomed.cas.cz (O.S.); david.jurnecka@biomed.cas.cz (D.J.); osickova@biomed.cas.cz (A.O.); sebo@biomed.cas.cz (P.S.)

[2] Faculty of Science, Charles University, Hlavova 2030, 128 43 Prague, Czech Republic

* Correspondence: masin@biomed.cas.cz (J.M.); osicka@biomed.cas.cz (R.O.); Tel.: +420-241-062-014 (J.M.); +420-241-062-770 (R.O.)

Received: 14 May 2019; Accepted: 7 June 2019; Published: 12 June 2019

Abstract: Cytolytic leukotoxins of the repeat in toxin (RTX) family are large proteins excreted by gram-negative bacterial pathogens through the type 1 secretion system (T1SS). Due to low yields and poor stability in cultures of the original pathogens, it is useful to purify recombinant fatty-acylated RTX cytolysins from inclusion bodies produced in *E. coli*. Such preparations are, however, typically contaminated by high amounts of *E. coli* lipopolysaccharide (LPS or endotoxin). We report a simple procedure for purification of large amounts of biologically active and endotoxin-free RTX toxins. It is based on the common feature of RTX cytolysins that are T1SS-excreted as unfolded polypeptides and fold into a biologically active toxin only upon binding of calcium ions outside of the bacterial cell. Mimicking this process, the RTX proteins are solubilized from inclusion bodies with buffered 8 M urea, bound onto a suitable chromatographic medium under denaturing conditions and the contaminating LPS is removed through extensive on-column washes with buffers containing 6 to 8 M urea and 1% Triton X-100 or Triton X-114. Extensive on-column rinsing with 8 M urea buffer removes residual detergent and the eluted highly active RTX protein preparations then contain only trace amounts of LPS. The procedure is exemplified using four prototypic RTX cytolysins, the *Bordetella pertussis* CyaA and the hemolysins of *Escherichia coli* (HlyA), *Kingella kingae* (RtxA), and *Actinobacillus pleuropneumoniae* (ApxIA).

Keywords: endotoxin; lipopolysaccharide; RTX toxins; Triton X-100; Triton X-114

Key Contribution: Protocol for purification of LPS-free and biologically active RTX toxins.

1. Introduction

Repeat in toxin (RTX) leukotoxins/cytolysins are a large family of pore-forming and immunomodulatory toxins of gram-negative pathogens belonging to the genera *Bordetella*, *Escherichia*, *Kingella*, *Moraxella*, *Morganella*, *Photorhabdus*, *Proteus*, *Vibrio*, and the *Pasteurellaceae* family. RTX toxins exert cytotoxic activities on a broad spectrum of eukaryotic host cells and share several characteristic features, such as: (i) the presence of a pore-forming hydrophobic domain; (ii) the requirement for activation by a posttranslational fatty-acyl modification accomplished by a cognate toxin activating acyltransferase (RtxC); (iii) the presence of an extensive C-terminal calcium-binding domain that consists of acidic glycine-rich repeats exhibiting a nonapeptide consensus sequence X-(L/I/F)-X-G-G-X-G-(N/D)-D; and (iv) the presence of an unprocessed C-terminal secretion signal involved in the export of the RTX protein out of the bacterial cell through a type I secretion system (T1SS) apparatus [1].

Among the best-characterized RTX toxins is the bi-functional adenylate cyclase toxin-hemolysin (CyaA) of *Bordetellae* that plays an important role in the airway colonization capacity and virulence of the whooping cough agent *Bordetella pertussis* [2,3]. The C-terminal hemolysin part of CyaA permeabilizes various host cells by cation-selective transmembrane pores, while the N-terminal adenylyl cyclase (AC) enzyme domain of CyaA translocates into cell cytosol and once activated by intracellular calmodulin, it subverts cellular signaling by catalyzing the unregulated conversion of cytosolic ATP to cAMP [4,5].

Another prototypic RTX cytolysin is α-hemolysin (HlyA), which is produced by numerous pathogenic as well as commensal *Escherichia coli* isolates. At higher toxin doses, the transmembrane pores formed by HlyA can provoke colloid-osmotic (oncotic) lysis of eukaryotic cells, while at lower concentrations the permeabilization of cells by HlyA interferes with host cell signaling pathways and can provoke apoptotic cell death [6]. Similarly, the emerging pathogen *Kingella kingae* secretes the membrane-damaging hemolysin RtxA involved in development of osteoarticular infections and infective endocarditis in children and adults [7]. *Actinobacillus pleuropneumoniae*, the etiological agent of swine pleuropneumonia, secretes the ApxIA hemolysin exhibiting strong hemolytic and cytotoxic activities [8,9].

Structural and functional studies of these RTX family cytolysins are often limited by their low yields from supernatants of cultures of the respective pathogens. An efficient method for obtaining of large quantities of the RTX toxins is their overexpression in recombinant *E. coli* cells together with their cognate RtxC toxin activating acyltransferases. This usually yields the formation of inclusion bodies from which the acylated RTX cytolysins are conveniently solubilized into 8 M urea buffers for further purification under denaturing conditions (6 to 8 M urea buffers). The biologically active cytolysins are then obtained by a more than ten-fold dilution of the urea-denatured toxin in a calcium-containing buffer. This mimics the natural process of calcium-triggered folding of the RTX cytolysin molecule upon exit of the translocating RTX polypeptide from the bacterial T1SS conduit into the calcium-rich (~2 mM Ca^{2+}) host body fluids [10]. However, high amounts of contaminating *E. coli* outer membrane lipopolysaccharide (LPS) often limit the use of such-purified RTX cytolysin preparations in cellular signaling assays or toxin immunomodulatory activity studies. Indeed, LPS is recognized by the TLR4 receptor complex [11] that triggers signal transduction leading to NF-κB activation and pro-inflammatory cytokine release by monocytes and macrophages [12]. As a result, many insufficiently purified recombinant proteins were found to trigger TLR4 signaling until their cytokine-inducing activity was attributed to contamination by LPS [13–17]. Therefore, a number of processes has been developed to remove LPS from protein samples, including a two-phase extraction, chromatography on LPS affinity resins, ultrafiltration, hydrophobic interaction chromatography, ion exchange chromatography, and membrane adsorption [18]. The most universally applicable of these processes then appears to be the two-phase LPS extraction method with Triton X-114 [19–22].

Here we report a procedure specifically devised for simple and rapid purification of large amounts of LPS-free RTX toxins.

2. Results and Discussion

2.1. Purification of LPS-free RTX Toxins

Previously, several methods for reduction of LPS contamination of purified CyaA toxin preparations were devised, including extensive washing of toxin-containing inclusion bodies with buffers containing 2 M urea or 1% (*v*/*v*) N-octyl-glucoside [23], removal of LPS from phenyl-sepharose-bound CyaA by 60% (*v*/*v*) isopropanol washes [24–26] or re-chromatography of purified CyaA on hydroxyapatite [27]. However, these purification procedures are laborious and typically reduce the yield or the specific activity of the purified toxin. Therefore, we aimed to develop a simplified single step purification procedure (Figure 1a) that would be generally applicable for removal of LPS from urea-solubilized RTX toxin preparations. We took advantage of the unique capacity of T1SS-secreted RTX proteins to undergo calcium driven folding into a biologically active

conformation upon simple dilution of the denaturant. Therefore, the entire purification process was performed under denaturing conditions in buffers containing 8 M urea and thus could be performed at room temperature without the risk of protein degradation. Use of 8 M urea buffers also provided the opportunity to exploit the strong binding of the highly negatively charged denatured CyaA (pI 4) to the positively charged groups of DEAE-Sepharose at pH 8 and the high affinity interaction of the denatured His-tagged recombinant HlyA, RtxA, and ApxIA proteins with Ni-NTA agarose beads, respectively. Following protein extract loading on the chromatographic matrices, removal of trapped LPS was achieved by washing of the toxin-loaded resins beds with 10 volumes of 1% (*v*/*v*) solution of the non-ionic detergents Triton X-100 or 1% (*v*/*v*) Triton X-114 in 8 M urea. The detergent was next removed by resin washes with 5 bed volumes of urea buffer without detergent, before CyaA was eluted in 8 M urea buffer pH 8 containing 200 mM NaCl and the HlyA, RtxA, or ApxIA proteins were eluted with 250 mM imidazole in 8 M urea buffer, respectively (Figure 1b). We also performed reference purifications, in which the resins beds were washed with 10 bed volumes of urea buffers without Triton detergents.

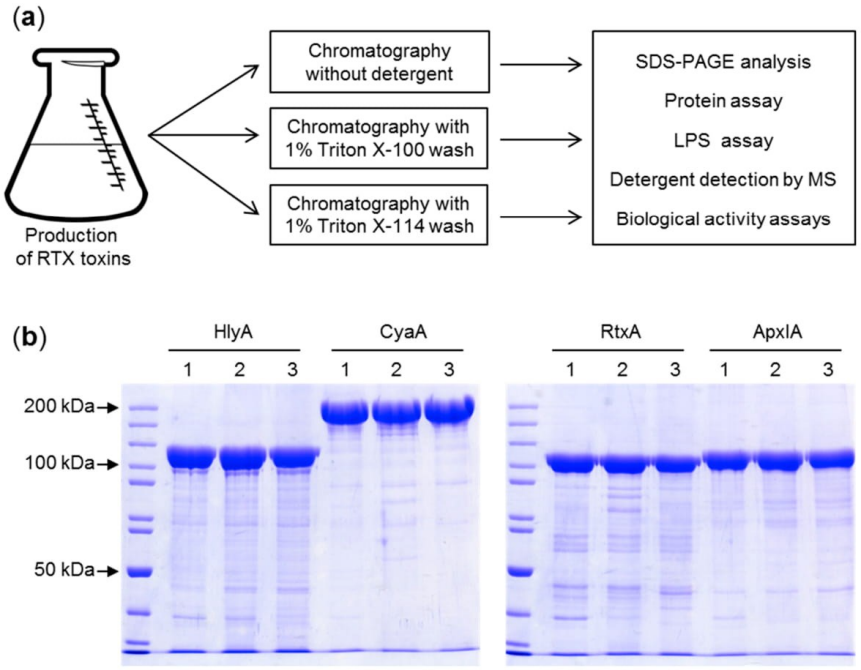

Figure 1. Purification of the repeat in toxin (RTX) toxins. (**a**) Schematic representation of the purification protocol. RTX toxin-producing *E. coli* cells were harvested, resuspended in buffer and divided in three equal aliquots that were processed in parallel, with, or without the indicated 1% detergent in the column wash buffer. (**b**) The indicated RTX toxin samples were separated by 7.5% SDS-PAGE and visualized by Coomassie blue staining. 1—purification without a detergent wash; 2—purification including a 1% Triton X-100 wash; 3—purification including a 1% Triton X-114 wash.

As shown in Table 1, when the RTX proteins were purified without including the 1% Triton X-100 or Triton X-114 detergents into the washing 8 M urea buffers, the amounts of LPS detected in the eluted toxin samples ranged from 4×10^5 to 1×10^6 endotoxin units (EU) per mg of the RTX protein, irrespective of whether a DEAE-Sepharose or Ni-NTA agarose column matrix was used. Inclusion

of 1% Triton X-100 into column wash buffer reduced the LPS amounts in the purified RTX protein samples by three to four orders of magnitude down to ≤115 EU/mg. Inclusion of 1% Triton X-114 in the wash buffer reduced the LPS content in the purified samples of the RTX proteins even more to ≤25 EU/mg (Table 1). Hence, use of either detergent in the buffer used to wash either of the two used purification matrices allowed a significant reduction of the LPS content in the final preparations of all four RTX toxins.

Table 1. RTX toxin concentrations, lipopolysaccharide (LPS) contaminations and total amounts of the proteins obtained from one liter of culture.

RTX Toxin [1]	Without Detergent Wash			1% Triton X-100 Wash			1% Triton X-114 Wash		
	Conc. [2] (mg/mL)	LPS [3] (EU/mg)	Total [4] (mg)	Conc. [2] (mg/mL)	LPS [3] (EU/mg)	Total [4] (mg)	Conc. [2] (mg/mL)	LPS [3] (EU/mg)	Total [4] (mg)
CyaA	1.3	$>4 \times 10^5$	6	1.0	12	6	1.2	8	6
RtxA	2.0	$>1 \times 10^6$	8	2.1	115	8	2.0	25	8
HlyA	1.4	$>1 \times 10^6$	4	1.3	95	4	1.4	15	4
ApxIA	1.9	$>1 \times 10^6$	8	2.1	85	8	1.6	15	8

[1] adenylate cyclase toxin-hemolysin (CyaA), RtxA, α-hemolysin (HlyA) and ApxIA toxins were purified as described in detail in Materials and Methods. [2] Protein concentration was determined by the Bradford assay. [3] LPS content was determined by the Chromogenic LAL assay. [4] Total protein amount.

Since traces of the used Triton detergents might potentially interfere with biological activities of the purified RTX toxins and confound cell cytotoxicity assays, it was important to examine whether the detergent was efficiently removed upon excessive column washing with detergent-free 8 M urea buffer. Towards this aim matrix-assisted laser desorption ionization-time-of-flight (MALDI-TOF) mass spectrometry (MS) was employed to detect any residual contamination of the purified RTX toxins by trace amounts of Triton X-100. First, the detergent-free RtxA protein sample (1 mg/mL) was spiked with Triton X-100 in the range of from 0.1 to 0.0001% and analyzed by MALDI-TOF MS. As shown in Figure 2a–d, Triton X-100-specific peaks were unambiguously detected in the MALDI-TOF spectra of RtxA samples containing 0.001% or higher Triton X-100 concentrations. In contrast, no such peaks were present in the spectra of the RTX proteins purified without the use of detergent (Figure S1), or in the spectra obtained for the RTX proteins that were purified using Triton X-100 in the column wash solution (Figure 2e–h). Similar MS results were obtained when Triton X-114 was used to remove endotoxin from the RTX toxin preparations (Figure S2). Hence, if traces of the detergent were still present in the ~10 μM protein preparations, the concentrations of remaining Triton detergent were below the detection limit of the method (~0.001%, or ~16–20 μM). Given that purified toxin stocks are further diluted over 100-fold when assayed for biological activity, protein or LPS content, such low amounts of detergent are well below the effective cytolytic concentration [28] and are very unlikely to interfere in any of these assays.

2.2. The LPS-Free RTX Toxins Are Cytotoxic on Different Cell Types

We investigated whether the RTX toxins purified in the presence of the Triton detergents preserved their biological activities. The CyaA preparations purified in the presence or absence of Triton were analyzed using human THP-1 monocytes as model cells expressing the integrin CD11b/CD18 receptor [29,30]. Sheep erythrocytes then served as model cells lacking CD11b/CD18. As summarized in Figure 3a, at equal protein concentrations the CyaA toxins purified in the presence of Triton X-100 or Triton X-114 intoxicated THP-1 monocytes by cAMP with the same capacity as the CyaA toxin purified in the absence of the detergents. Similarly, all three CyaA preparations exhibited a comparable capacity to reduce THP-1 viability, determined as the loss of mitochondrial dehydrogenase activity (Figure 3b). Finally, CyaA purified in the presence of detergents bound the surface of erythrocytes, translocated the AC domain to their cytosol, and formed hemolytic pores in the cell membrane with the same efficacy as the CyaA toxin purified in the absence of the detergents (Figure 3c). All these results demonstrate

that the detergent-involving procedure for purification of LPS-free CyaA yielded a fully biologically active toxin.

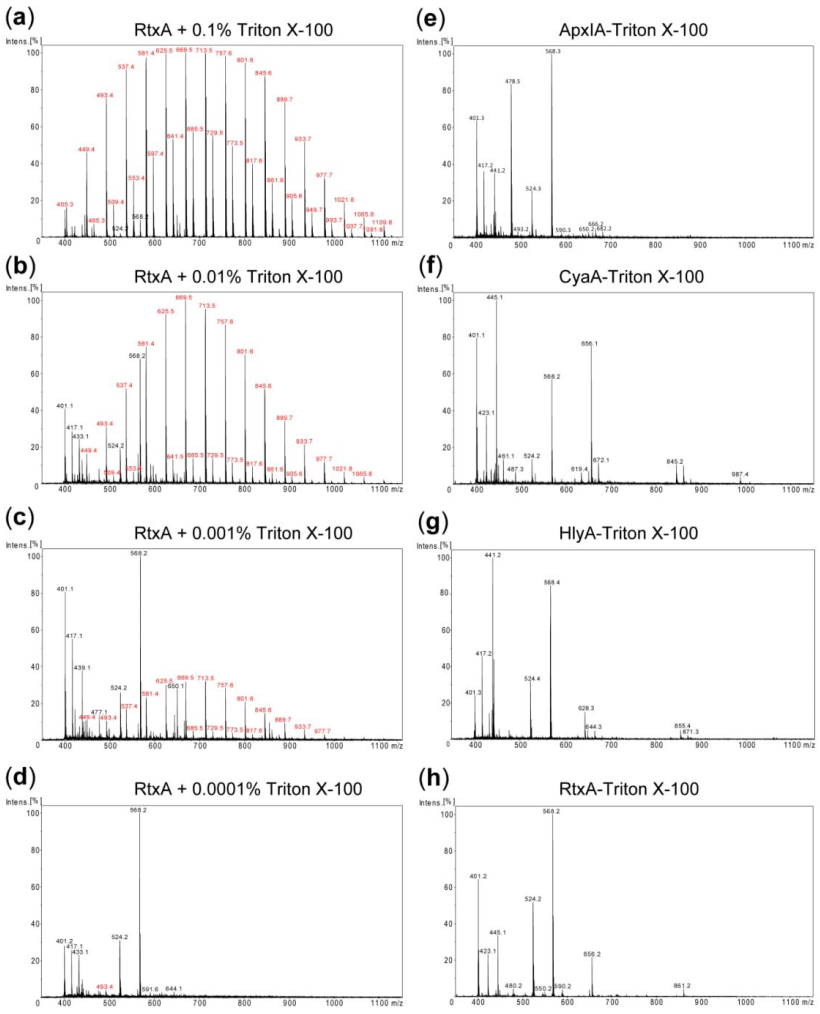

Figure 2. Detection of residual detergent in purified RTX toxin samples. (**a**–**d**) RtxA (1 mg/mL) purified without the detergent was spiked with Triton X-100 at concentrations decreasing from 0.1 to 0.0001% and analyzed by matrix-assisted laser desorption ionization-time-of-flight (MALDI-TOF). (**e**–**h**) MALDI-TOF spectra of the RTX toxin samples purified using the 1% Triton X-100 column wash. The m/z values of ions corresponding to Triton X-100 components are printed in red. The remaining ions represent adducts of the matrix and other small molecular mass contaminants. In each panel an ion with maximum intensity was taken as 100%.

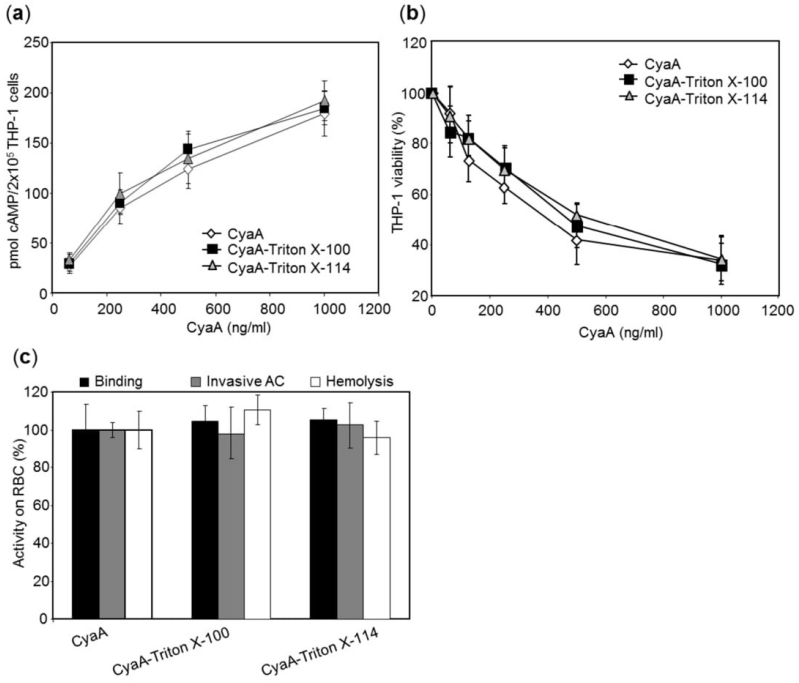

Figure 3. Toxin activities of CyaA purified in the presence or absence of detergent. (**a**) CyaA toxin (62.5–1000 ng/mL) purified with or without a 1% Triton X-100 wash of the chromatographic resin was incubated with 2×10^5 THP-1 cells in 100 µL of D-MEM medium and cAMP intoxication was assessed by determining the intracellular concentration of cAMP generated in cells after 30 min of incubation with CyaA at the indicated concentrations. Average values ± standard deviations from three independent experiments performed in duplicates are shown. (**b**) Cells were incubated with the CyaA toxins at 37 °C for 2 h and the number of viable cells was determined using the CCK-8 assay. The viability of mock-treated cells (buffer only) was taken as 100%. The percentages of viable cells represent average values ± standard deviations from two independent experiments performed in triplicates. (**c**) Sheep erythrocytes were incubated at 37 °C with 1 µg/mL of the CyaA toxins and after 30 min, aliquots were taken for determination of the cell-associated adenylyl cyclase (AC) activity and of the AC activity internalized into erythrocytes and protected against digestion by externally added trypsin. For determination of hemolytic activity, sheep erythrocytes (5×10^8/mL) were incubated at 37 °C in the presence of 10 µg/mL of the CyaA toxins and erythrocyte lysis was measured after 3 h as the amount of released hemoglobin by photometric determination at 541 nm (A_{541}). Each activity is expressed as percentage relative to the activity of CyaA purified in the absence of Triton and represents average value ± standard deviation from at least two independent determinations performed in duplicates with two different toxin preparations.

Next, we examined pore-forming (hemolytic) activity of the HlyA and ApxIA hemolysins purified in the presence or absence of Triton X-100 or of Triton X-114. As shown in Figure 4a,b, the hemolytic potency of both RTX hemolysins was not affected at all by the use of Triton X-100 or Triton X-114 detergents in column wash during toxin purification and removal of LPS from toxin preparations had no effect on their cytolytic capacities.

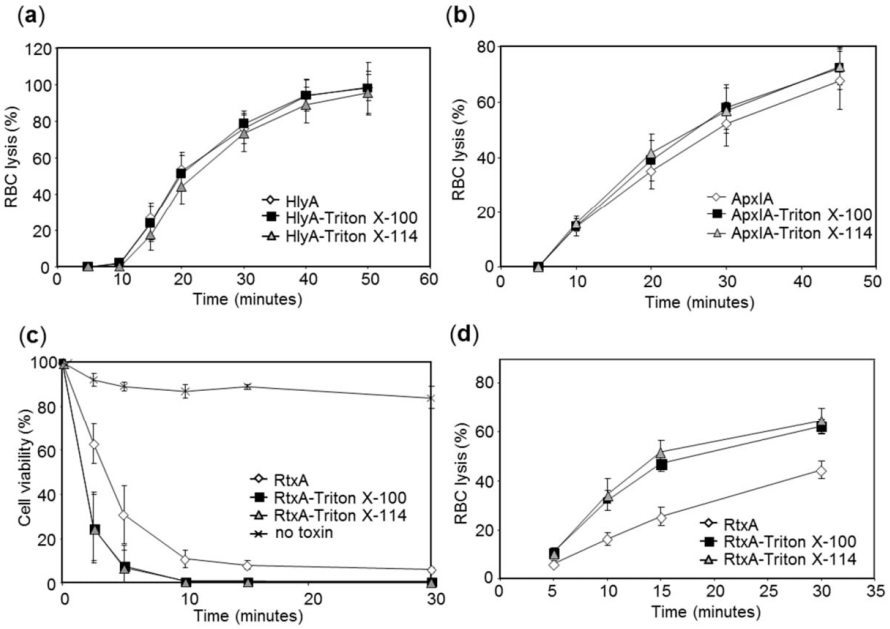

Figure 4. Cytolytic activities of purified HlyA, ApxIA, and RtxA toxins. (**a**,**b**) Washed sheep erythrocytes (5×10^8/mL) were incubated at 37 °C with 20 ng/mL of HlyA (**a**) or 1 μg/mL of ApxIA (**b**) and erythrocyte lysis was measured in time as the amount of released hemoglobin by photometric determination at 541 nm (A_{541}). Average values ± standard deviations from four independent determinations are shown. (**c**) HLaC-78 cells (1×10^6/mL) were incubated with 1 μg/mL of RtxA for indicated time at 37 °C. Cell viability was determined by a vital dye staining using 1 μg/mL of Hoechst 33258 followed by flow cytometry. The initial viability of cells incubated without RtxA was taken as 100%. Each point represents the mean value ± standard deviation of three independent experiments. (**d**) Sheep erythrocytes (5×10^8/mL) were incubated at 37 °C in the presence of 200 ng/mL of RtxA and erythrocyte lysis was measured as above.

Intriguingly, when the cytotoxic activity of purified RtxA was tested using the laryngeal HLaC-78 squamous cells, which are exquisitely susceptible to RtxA-mediated killing [31], the cytotoxic activity of the LPS-depleted RtxA-Triton X-100 and RtxA-Triton X-114 proteins (1 μg/mL) was importantly higher than the toxicity of the RtxA protein purified without the use of detergent in column washes (Figure 4c). A similar result was observed when the hemolytic capacity of purified RtxA toxin was assessed on sheep erythrocytes, where the LPS-depleted RtxA-Triton X-100 and RtxA-Triton-X114 proteins were more potent as hemolysins. Given the low residual Triton X-100 concentration (<16 μM) in the purified RtxA-Triton X-100 preparation (~10 μM) it appears unlikely that the traces of the detergent present at <16 nM concentration upon the 1000-fold dilution of the toxin stock solution into cellular suspensions could have had any stabilizing effect on the final ~10 nM RtxA protein and potentiate its activity. Rather, the presence of micromolar concentrations of contaminating *E. coli* LPS (~100–200 μg/mL or ~10–20 μM) in the RtxA sample purified without the use of detergent in column wash might have reduced toxin activity. Indeed, it was previously observed that RtxA has to be diluted from 8 M urea solutions into the assay buffer immediately before adding to cells and preincubation of the renatured toxin in the assay buffer causes a rapid loss of cytotoxic activity of RtxA [31]. It is tempting to speculate

that in the absence of chaotropic concentrations of urea the hydrophobic sites of RtxA may bind the lipid A moiety of LPS and this may affect the capacity of RtxA to interact with the target cells.

3. Conclusions

In conclusion, using four different recombinant RTX toxins as example, we present here a simple, rapid, and universal method of purification of endotoxin-depleted recombinant RTX toxins from 8 M urea extracts of *E. coli* inclusion bodies. The purification is performed at room temperature under denaturing conditions and is easily scalable. The included LPS depletion step consists in extensive on-column wash of the protein with 1% solution of Triton X-100 or Triton X-114 detergents. The detergent is effectively removed by extensive resin rinsing with 8 M urea buffer prior to RTX toxin elution, which yields concentrated RTX toxin preparations of superior homogeneity and high specific biological activity. In the case of RtxA toxin of *K. kingae* the results indicate that on-column removal of contaminating LPS by detergent wash may enhance the specific cytotoxic activity of RtxA. The described procedure opens the way to large production of endotoxin-free RTX protein preparations needed for structural and functional studies of these intriguing bacterial toxins.

4. Materials and Methods

4.1. Expression and Isolation of RTX Toxins

Plasmid pT7CACT1 was used for co-expression of the *cya*C and *cyaA* genes for production of recombinant CyaC-activated CyaA [32]. To produce the RtxC-activated RtxA toxin equipped with a C-terminal double 6xHis purification tag, the plasmid pT7rtxC-rtxA was used [31]. For production of HlyC-activated HlyA with a C-terminal double 6xHis tag, the *rtxC* and *rtxA* genes of pT7rtxC-rtxA were replaced by the *hly*C and *hlyA* genes to yield the pT7hlyC-hlyA expression vector. For production of the acylated ApxIA toxin having 6xHis tags on both the N-terminal and C-terminal ends, the pET28bapxIC-apxIA construct was used [9].

The toxins were produced in *E. coli* BL21/pMM100 (HlyA, CyaA, and RtxA) or *E. coli* Rosetta 2 (ApxIA) cells in 1000 mL cultures in MDO medium (yeast extract, 20 g/L; glycerol, 20 g/L; KH_2PO_4, 1 g/L; K_2HPO_4, 3 g/L; NH_4Cl, 2 g/L; Na_2SO_4, 0.5 g/L; and thiamine hydrochloride, 0.01 g/L) at 37 °C following IPTG induction (0.5 mM) for 3 h. The pellets of harvested bacteria were resuspended in 30 mL of 50 mM Tris-HCl pH 8.0, sonicated and split into three aliquots of 10 mL. Inclusion bodies from each aliquot were washed in 10 mL of 50 mM Tris-HCl (pH 8.0), 2 M urea buffer and then solubilized at room temperature for 30 min in 8 M urea in 5 mL of 50 mM Tris-HCl pH 8.0 containing either (i) 1% (*v*/*v*) Triton X-100 (Sigma-Aldrich, St. Louis, MO, USA), (ii) 1% (*v*/*v*) Triton X-114 (Sigma-Aldrich, St. Louis, MO, USA) or (iii) no detergent. The urea extracts were then cleared by centrifugation at 25,000× *g* for 30 min at 4 °C.

4.2. Purification of CyaA

The cleared urea extracts of CyaA were supplemented with NaCl to a final concentration of 50 mM and loaded at room temperature onto columns with 10 mL of packed DEAE-Sepharose resin pre-equilibrated with 8 M urea, 50 mM Tris-HCl pH 8.0, 120 mM NaCl buffer that contained no detergent, or was supplemented with 1% (*v*/*v*) of Triton X-100 or 1% (*v*/*v*) of Triton X-114, respectively. Contaminating *E. coli* components were removed by washing of the columns with 10 bed volumes of the respective equilibration buffer. Detergent was next removed by 5 bed volume washes with 8 M urea, 50 mM Tris-HCl pH 8, and 120 mM NaCl. Finally, CyaA was eluted with 8 M urea, 50 mM Tris-HCl pH 8, and 200 mM NaCl, and the fractions were analyzed by SDS-PAGE (Figure 1b).

4.3. Purification of HlyA, ApxIA, and RtxA

The His tag-equipped RTX hemolysins HlyA, ApxIA, and RtxA were purified by immobilized metal ion affinity chromatography on Ni-NTA agarose (GE Healthcare BioSciences, Pittsburgh, PA,

USA). The cleared urea extracts of inclusion bodies were supplemented with NaCl to 300 mM final concentration and loaded at room temperature on 5 mL Ni-NTA agarose columns equilibrated with 8 M urea, 50 mM Tris-HCl pH 8.0, 300 mM NaCl buffer without detergent, or with the same buffer containing 1% (*v*/*v*) of Triton X-100 or Triton X-114, respectively. Contaminating *E. coli* components were removed by extensive washing of the column with 10 bed volumes of the given equilibration buffers. Detergent was removed by washes with 5 bed volumes of 8 M urea, 50 mM Tris-HCl pH 8.0, 300 mM NaCl, and 30 mM imidazole, and the RTX toxins were eluted with 250 mM imidazole in the same buffer. EDTA was added to 1 mM and the pooled fractions were extensively dialyzed against 100 volumes of 8 M urea, 50 mM Tris-HCl, and 300 mM NaCl to remove imidazole and the homogeneity of the proteins was analyzed by SDS-PAGE (Figure 1b).

4.4. Determination of LPS Levels and Protein Concentrations

The LPS levels in protein samples were determined by the Chromogenic LAL assay (Charles River Endosave, Charleston, SC, USA) and protein concentration was determined by the Bradford assay using BSA as the calibration standard.

4.5. Detection of Residual Detergent

MALDI-TOF MS of protein preparations was performed using an Autoflex III (Bruker Daltonics, Bremen, Germany) instrument with mass spectra acquisition in the positive reflection mode within a scan range of 300–4000 Da. Prior to MS analysis the RTX toxin samples (50 μg) were desalted by protein MacroTrap (Optimize Technologies, Oregon City, OR, USA) and eluted with 100 μL of 80% ACN, 0.1% TFA. Desalted proteins were dried via vacuum centrifugation and dissolved in 30 μL of 5% ACN, 0.1% TFA (*v*/*v*). The samples were then mixed on the target with α-Cyano-4-hydroxycinnamic acid and dried at room temperature. Results were analyzed using Data Analysis 4.1 (Bruker Daltonics).

4.6. Determination of Hemolytic Activity on Sheep Erythrocytes

Sheep erythrocytes (LabMediaServis, Jaromer, Czech Republic) were washed, resuspended to 5×10^8/mL in 50 mM Tris-Cl, 150 mM NaCl, and 2 mM $CaCl_2$, pH 7.4 (buffer A) and incubated for 3 h with 10 μg/mL of CyaA, before the amount of released hemoglobin was measured as absorbance at 541 nm [33]. The lytic activity of CyaA purified without detergent was taken as 100%. The hemolytic activities of HlyA, RtxA, and ApxIA were measured as hemoglobin release over time of incubation of 5×10^8/mL of washed sheep erythrocytes in buffer A with 20 ng/mL of HlyA, 200 ng/mL of RtxA, or 1 μg/mL ApxIA, respectively. As a negative control, the hemolytic activity of toxins was measured in buffer containing 5 mM EDTA instead of 2 mM $CaCl_2$ and no lysis was observed (not shown).

4.7. Cell Binding and Invasive Activities of CyaA on Sheep Erythrocytes

The AC enzymatic activities of CyaA were determined in the presence of 1 μM calmodulin as previously described [34]. One unit of AC activity corresponds to 1 μmol of cAMP formed per min at 30 °C, pH 8.0. Cell invasive AC enzyme activity was measured as previously described [35], by determining the AC enzyme activity protected against externally added trypsin upon internalization into cytosol of sheep erythrocytes. Erythrocyte binding of CyaA was determined as previously described [35] by determining the amount of cell-associated (membrane bound) AC enzyme activity. Activity of CyaA purified without detergent was taken as 100%.

4.8. Human Cell Lines

Human monocytes THP-1 (ATCC, number TIB-202) and laryngeal HLaC-78 squamous cells [36] were cultured at 37 °C in a humidified air/CO_2 (19:1) atmosphere in RPMI 1640 (Sigma-Aldrich, St. Louis, MO, USA) supplemented with 10% (*v*/*v*) fetal calf serum (FCS) (GIBCO Invitrogen, Grand

Island, NY, USA) and antibiotic antimycotic solution (0.1 mg/mL streptomycin, 100 U/mL penicillin, and 0.25 mg/mL amphotericin; Sigma-Aldrich, St. Louis, MO, USA).

4.9. cAMP Elevation and Viability Assays on THP-1 Cells

Prior to assays, the RPMI 1640 medium used for THP-1 cultivation was replaced by D-MEM medium (1.9 mM Ca^{2+}) without FCS and the cells were allowed to rest in D-MEM for 1 h at 37 °C in a humidified 5% CO_2 atmosphere. For intracellular cAMP assay, 2×10^5 THP-1 cells were incubated at 37 °C with CyaA for 30 min in D-MEM, the reaction was stopped by addition of 0.2% (*v*/*v*) Tween-20 in 100 mM HCl, the samples were boiled for 15 min at 100 °C, neutralized by addition of 150 mM unbuffered imidazole and cAMP was measured by a competitive immunoassay as previously described [37]. For cell viability assay, the THP-1 (2×10^5) cells were incubated with indicated concentration of CyaA at 37 °C for 2 h in a humidified air/CO_2 atmosphere and the number of viable cells was determined as WST-8 reduction using the CCK-8 assay (Dojindo Laboratories Kamimashiki-gun, Japan). The viability of mock-treated control cells was taken as 100%.

4.10. Determination of RtxA Cytotoxicity on HLaC-78 Cells

Viability of HLaC-78 cells upon incubation with RtxA was determined as previously described [31]. Briefly, HLaC-78 cells were harvested, washed in HEPES-buffered salt solution (10 mM HEPES (pH 7.4), 140 mM NaCl, 5 mM KCl) supplemented with 2 mM $CaCl_2$, 2 mM $MgCl_2$ and diluted with the same buffer to 1×10^6 cells/mL. The cells were then incubated at 37 °C with 1 µg/mL of purified RtxA samples for the indicated times. Cell viability was determined by a vital dye staining with 1 µg/mL of Hoechst 33258 and flow cytometry on a FACS LSR II instrument (BD Biosciences, San Jose, CA, USA). Data were analyzed using the FlowJo software (Tree Star, Ashland, OR, USA) and appropriate gatings were used to exclude cell aggregates and dying/dead cells (Hoechst 33258-positive staining).

Supplementary Materials: The following are available online at http://www.mdpi.com/2072-6651/11/6/336/s1, Figure S1: MALDI-TOF spectra of the RTX toxin samples purified without the use of a detergent wash, Figure S2: Detection of residual detergent in purified RTX toxin samples.

Author Contributions: Conceptualization, O.S., J.M., R.O. and P.S.; methodology, O.S., J.M., R.O., D.J. and A.O.; validation, O.S., J.M., R.O., D.J. and A.O.; investigation, O.S., J.M., R.O., D.J. and A.O.; data curation, O.S., J.M., R.O., D.J. and A.O.; writing—original draft preparation, O.S., J.M. and R.O.; writing— review and editing, P.S.; visualization, O.S., J.M., R.O. and D.J.; supervision, O.S., J.M., R.O. and P.S.; project administration, O.S., J.M., R.O. and P.S.; funding acquisition, J.M., R.O. and P.S.

Funding: This research was funded by grants 18-18079S (R.O.), 19-04607S (J.M.), 19-12695S (R.O.) and 19-27630X (P.S.) of the Czech Science foundation.

Conflicts of Interest: The authors declare no conflict of interest.

References

1. Linhartova, I.; Bumba, L.; Masin, J.; Basler, M.; Osicka, R.; Kamanova, J.; Prochazkova, K.; Adkins, I.; Hejnova-Holubova, J.; Sadilkova, L.; et al. RTX proteins: A highly diverse family secreted by a common mechanism. *FEMS Microbiol. Rev.* **2010**, *34*, 1076–1112. [CrossRef]
2. Goodwin, M.S.; Weiss, A.A. Adenylate cyclase toxin is critical for colonization and pertussis toxin is critical for lethal infection by *Bordetella pertussis* in infant mice. *Infect. Immun.* **1990**, *58*, 3445–3447.
3. Khelef, N.; Sakamoto, H.; Guiso, N. Both adenylate cyclase and hemolytic activities are required by *Bordetella pertussis* to initiate infection. *Microb. Pathog.* **1992**, *12*, 227–235. [CrossRef]
4. Kamanova, J.; Kofronova, O.; Masin, J.; Genth, H.; Vojtova, J.; Linhartova, I.; Benada, O.; Just, I.; Sebo, P. Adenylate cyclase toxin subverts phagocyte function by RhoA inhibition and unproductive ruffling. *J. Immunol.* **2008**, *181*, 5587–5597. [CrossRef]
5. Novak, J.; Cerny, O.; Osickova, A.; Linhartova, I.; Masin, J.; Bumba, L.; Sebo, P.; Osicka, R. Structure-function relationships underlying the capacity of *Bordetella* adenylate cyclase toxin to disarm host phagocytes. *Toxins* **2017**, *9*, 300. [CrossRef]

6. Ristow, L.C.; Welch, R.A. Hemolysin of uropathogenic *Escherichia coli*: A cloak or a dagger? *Biochim. ET Biophys. Acta* **2016**, *1858*, 538–545. [CrossRef]
7. Kehl-Fie, T.E.; St Geme, J.W., 3rd. Identification and characterization of an RTX toxin in the emerging pathogen *Kingella kingae*. *J. Bacteriol.* **2007**, *189*, 430–436. [CrossRef]
8. Maier, E.; Reinhard, N.; Benz, R.; Frey, J. Channel-forming activity and channel size of the RTX toxins ApxI, ApxII, and ApxIII of *Actinobacillus pleuropneumoniae*. *Infect. Immun.* **1996**, *64*, 4415–4423.
9. Masin, J.; Fiser, R.; Linhartova, I.; Osicka, R.; Bumba, L.; Hewlett, E.L.; Benz, R.; Sebo, P. Differences in purinergic amplification of osmotic cell lysis by the pore-forming RTX toxins *Bordetella pertussis* CyaA and *Actinobacillus pleuropneumoniae* ApxIA: The role of pore size. *Infect. Immun.* **2013**, *81*, 4571–4582. [CrossRef]
10. Bumba, L.; Masin, J.; Macek, P.; Wald, T.; Motlova, L.; Bibova, I.; Klimova, N.; Bednarova, L.; Veverka, V.; Kachala, M.; et al. Calcium-driven folding of RTX domain beta-rolls ratchets translocation of RTX proteins through type I secretion ducts. *Mol. Cell* **2016**, *62*, 47–62. [CrossRef]
11. Park, B.S.; Song, D.H.; Kim, H.M.; Choi, B.S.; Lee, H.; Lee, J.O. The structural basis of lipopolysaccharide recognition by the TLR4-MD-2 complex. *Nature* **2009**, *458*, 1191–1195. [CrossRef]
12. Guha, M.; Mackman, N. LPS induction of gene expression in human monocytes. *Cell Signal.* **2001**, *13*, 85–94. [CrossRef]
13. Bache, C.; Hoonakker, M.; Hendriksen, C.; Buchheit, K.H.; Spreitzer, I.; Montag, T. Workshop on animal free detection of pertussis toxin in vaccines–alternatives to the histamine sensitisation test. *Biol. J. Int. Assoc. Biol. Stand.* **2012**, *40*, 309–311. [CrossRef]
14. Gao, B.; Tsan, M.F. Recombinant human heat shock protein 60 does not induce the release of tumor necrosis factor alpha from murine macrophages. *J. Biol. Chem.* **2003**, *278*, 22523–22529. [CrossRef]
15. Tsan, M.F.; Gao, B. Endogenous ligands of toll-like receptors. *J. Leukoc. Biol.* **2004**, *76*, 514–519. [CrossRef]
16. Villarino Romero, R.; Hasan, S.; Fae, K.; Holubova, J.; Geurtsen, J.; Schwarzer, M.; Wiertsema, S.; Osicka, R.; Poolman, J.; Sebo, P. *Bordetella pertussis* filamentous hemagglutinin itself does not trigger anti-inflammatory interleukin-10 production by human dendritic cells. *Int. J. Med. Microbiol. IJMM* **2016**, *306*, 38–47. [CrossRef]
17. Wakelin, S.J.; Sabroe, I.; Gregory, C.D.; Poxton, I.R.; Forsythe, J.L.; Garden, O.J.; Howie, S.E. "Dirty little secrets"—Endotoxin contamination of recombinant proteins. *Immunol. Lett.* **2006**, *106*, 1–7. [CrossRef]
18. Magalhaes, P.O.; Lopes, A.M.; Mazzola, P.G.; Rangel-Yagui, C.; Penna, T.C.; Pessoa, A., Jr. Methods of endotoxin removal from biological preparations: A review. *J. Pharm. Pharm. Sci.* **2007**, *10*, 388–404.
19. Aida, Y.; Pabst, M.J. Removal of endotoxin from protein solutions by phase separation using Triton X-114. *J. Immunol. Methods* **1990**, *132*, 191–195. [CrossRef]
20. Cavallaro, A.S.; Mahony, D.; Commins, M.; Mahony, T.J.; Mitter, N. Endotoxin-free purification for the isolation of bovine viral diarrhoea virus E2 protein from insoluble inclusion body aggregates. *Microb. Cell Factories* **2011**, *10*, 57. [CrossRef]
21. Liu, S.; Tobias, R.; McClure, S.; Styba, G.; Shi, Q.; Jackowski, G. Removal of endotoxin from recombinant protein preparations. *Clin. Biochem.* **1997**, *30*, 455–463. [CrossRef]
22. Reichelt, P.; Schwarz, C.; Donzeau, M. Single step protocol to purify recombinant proteins with low endotoxin contents. *Protein Expr. Purif.* **2006**, *46*, 483–488. [CrossRef]
23. Orr, B.; Douce, G.; Baillie, S.; Parton, R.; Coote, J. Adjuvant effects of adenylate cyclase toxin of *Bordetella pertussis* after intranasal immunisation of mice. *Vaccine* **2007**, *25*, 64–71. [CrossRef]
24. Franken, K.L.; Hiemstra, H.S.; van Meijgaarden, K.E.; Subronto, Y.; den Hartigh, J.; Ottenhoff, T.H.; Drijfhout, J.W. Purification of his-tagged proteins by immobilized chelate affinity chromatography: The benefits from the use of organic solvent. *Protein Expr. Purif.* **2000**, *18*, 95–99. [CrossRef]
25. Mascarell, L.; Fayolle, C.; Bauche, C.; Ladant, D.; Leclerc, C. Induction of neutralizing antibodies and Th1-polarized and CD4-independent CD8+ T-cell responses following delivery of human immunodeficiency virus type 1 Tat protein by recombinant adenylate cyclase of *Bordetella pertussis*. *J. Virol.* **2005**, *79*, 9872–9884. [CrossRef]
26. Dunne, A.; Ross, P.J.; Pospisilova, E.; Masin, J.; Meaney, A.; Sutton, C.E.; Iwakura, Y.; Tschopp, J.; Sebo, P.; Mills, K.H. Inflammasome activation by adenylate cyclase toxin directs Th17 responses and protection against *Bordetella pertussis*. *J. Immunol.* **2010**, *185*, 1711–1719. [CrossRef]
27. Prior, S.; Corbel, M.J.; Xing, D.K. Development of an approach for the laboratory toxicological evaluation of *Bordetella pertussis* adenylate cyclase genetic toxoid constructs as multipurpose vaccines. *Hum. Vaccines* **2005**, *1*, 151–159. [CrossRef]

28. Nasrin, A.; Hassan, M.; Ye, P. Inhibition of notch signaling pathway using gamma-secretase inhibitor delivered by a low dose of Triton-x100 in cultured oral cancer cells. *Biochem. Biophys. Res. Commun.* **2018**, *495*, 2118–2124. [CrossRef]
29. Guermonprez, P.; Khelef, N.; Blouin, E.; Rieu, P.; Ricciardi-Castagnoli, P.; Guiso, N.; Ladant, D.; Leclerc, C. The adenylate cyclase toxin of *Bordetella pertussis* binds to target cells via the alpha(M)beta(2) integrin (CD11b/CD18). *J. Exp. Med.* **2001**, *193*, 1035–1044. [CrossRef]
30. Osicka, R.; Osickova, A.; Hasan, S.; Bumba, L.; Cerny, J.; Sebo, P. *Bordetella* adenylate cyclase toxin is a unique ligand of the integrin complement receptor 3. *eLife* **2015**, *4*, e10766. [CrossRef]
31. Osickova, A.; Balashova, N.; Masin, J.; Sulc, M.; Roderova, J.; Wald, T.; Brown, A.C.; Koufos, E.; Chang, E.H.; Giannakakis, A.; et al. Cytotoxic activity of *Kingella kingae* RtxA toxin depends on post-translational acylation of lysine residues and cholesterol binding. *Emerg. Microbes Infect.* **2018**, *7*, 178. [CrossRef]
32. Osicka, R.; Osickova, A.; Basar, T.; Guermonprez, P.; Rojas, M.; Leclerc, C.; Sebo, P. Delivery of CD8(+) T-cell epitopes into major histocompatibility complex class I antigen presentation pathway by *Bordetella pertussis* adenylate cyclase: Delineation of cell invasive structures and permissive insertion sites. *Infect. Immun.* **2000**, *68*, 247–256.
33. Bellalou, J.; Sakamoto, H.; Ladant, D.; Geoffroy, C.; Ullmann, A. Deletions affecting hemolytic and toxin activities of *Bordetella pertussis* adenylate cyclase. *Infect. Immun.* **1990**, *58*, 3242–3247.
34. Ladant, D. Interaction of *Bordetella pertussis* adenylate cyclase with calmodulin. Identification of two separated calmodulin-binding domains. *J. Biol. Chem.* **1988**, *263*, 2612–2618.
35. Masin, J.; Osickova, A.; Sukova, A.; Fiser, R.; Halada, P.; Bumba, L.; Linhartova, I.; Osicka, R.; Sebo, P. Negatively charged residues of the segment linking the enzyme and cytolysin moieties restrict the membrane-permeabilizing capacity of adenylate cyclase toxin. *Sci. Rep.* **2016**, *6*, 29137. [CrossRef]
36. Zenner, H.P.; Lehner, W.; Herrmann, I.F. Establishment of carcinoma cell lines from larynx and submandibular gland. *Arch. Oto-Rhino-Laryngol.* **1979**, *225*, 269–277. [CrossRef]
37. Karimova, G.; Pidoux, J.; Ullmann, A.; Ladant, D. A bacterial two-hybrid system based on a reconstituted signal transduction pathway. *Proc. Natl. Acad. Sci. USA* **1998**, *95*, 5752–5756. [CrossRef]

Supporting Information: Rapid Purification of Endotoxin-Free RTX Toxins

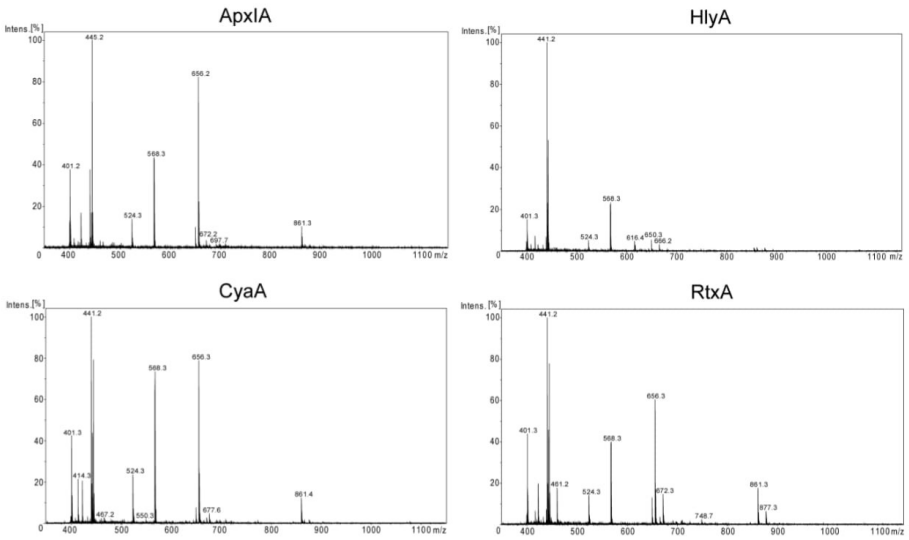

Figure S1. MALDI-TOF spectra of the RTX toxin samples purified without the use of a detergent wash. The detected ions represent adducts of the matrix and other small molecular mass contaminants. No ions corresponding to Triton X-100 were detected. In each panel an ion with maximum intensity was taken as 100%.

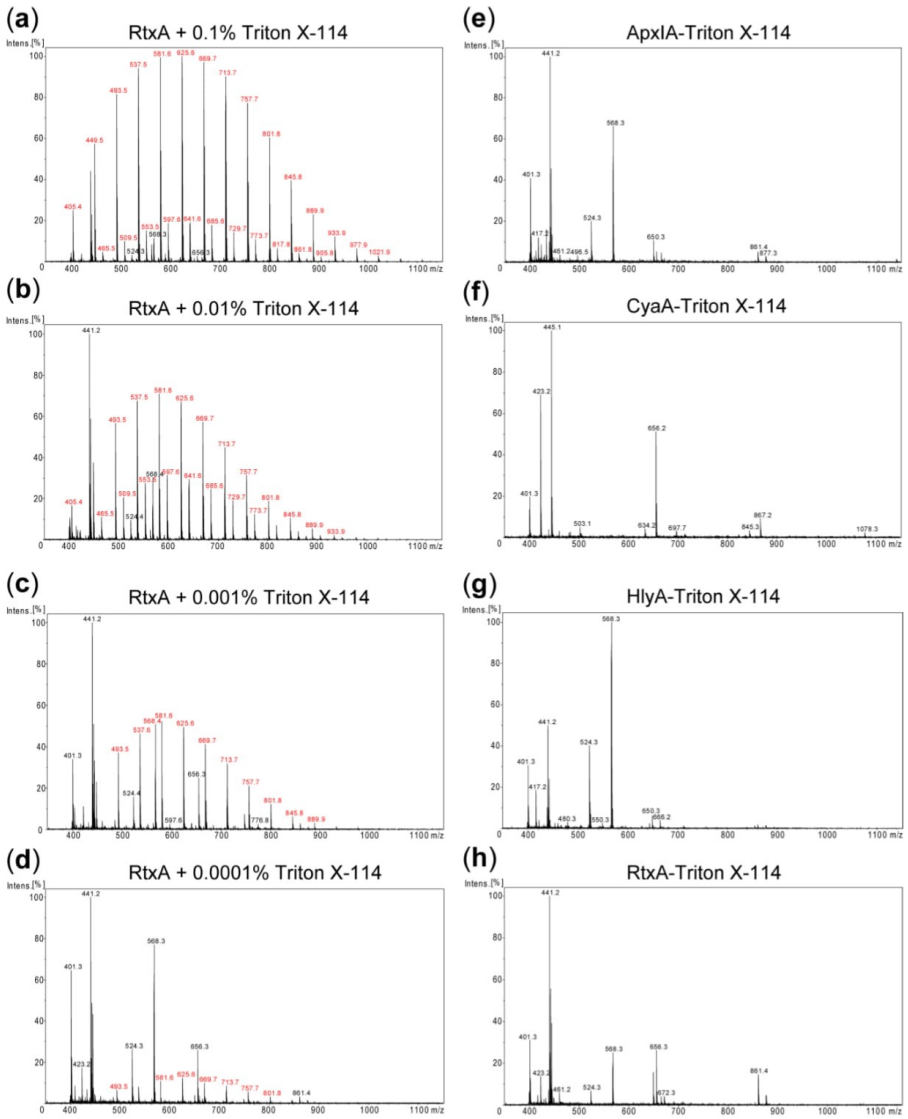

Figure S2. Detection of residual detergent in purified RTX toxin samples. (**a**–**d**) RtxA (1 mg/mL) purified without the detergent was spiked with Triton X-114 at concentrations decreasing from 0.1 to 0.0001% and analyzed by MALDI-TOF. (**e**–**h**) MALDI-TOF spectra of the RTX samples purified using the 1% Triton X-114 column wash. The *m*/*z* values of ions corresponding to Triton X-114 components are printed in red. The remaining ions represent adducts of the matrix and other small molecular mass contaminants. In each panel an ion with maximum intensity was taken as 100%.

APPENDIX III

Acyltransferase-mediated selection of the length of the fatty acyl chain and of the acylation site governs activation of bacterial RTX toxins

Osickova A, Khaliq H, Masin J, **Jurnecka D**, Sukova A, Fiser R, Holubova J, Stanek O, Sebo P, Osicka R.

J Biol Chem. 2020 May 27: jbc.RA120.014122. doi: 10.1074/jbc.RA120.014122.

J_ID: JBC Date: 18-June-20 4/Color Figure(s): F1,3,5,7 ART: RA120.014122 Page: 1 Total Pages: 15

JBC EDITORS' PICK

Acyltransferase-mediated selection of the length of the fatty acyl chain and of the acylation site governs activation of bacterial RTX toxins

Received for publication, April 29, 2020, and in revised form, May 20, 2020 Published, Papers in Press, May 27, 2020, DOI 10.1074/jbc.RA120.014122

AQ:au Adriana Osickova[1,2,‡], Humaira Khaliq[1,‡], Jiri Masin[1], David Jurnecka[1,2], Anna Sukova[1], Radovan Fiser[1,3], Jana Holubova[1], Ondrej Stanek[1], Peter Sebo[1], and Radim Osicka[1,*]

AQ:aff *From the [1]Institute of Microbiology of the Czech Academy of Sciences, Prague, Czech Republic and the Departments of [2]Biochemistry and [3]Genetics and Microbiology, Faculty of Science, Charles University in Prague, Prague, Czech Republic*

Edited by Chris Whitfield

In a wide range of organisms, from bacteria to humans, numerous proteins have to be posttranslationally acylated to become biologically active. Bacterial repeats in toxin (RTX) cytolysins form a prominent group of proteins that are synthesized as inactive protoxins and undergo posttranslational acylation on ε-amino groups of two internal conserved lysine residues by co-expressed toxin-activating acyltransferases. Here, we investigated how the chemical nature, position, and number of bound acyl chains govern the activities of *Bordetella pertussis* adenylate cyclase toxin (CyaA), *Escherichia coli* α-hemolysin (HlyA), and *Kingella kingae* cytotoxin (RtxA). We found that the three protoxins are acylated in the same *E. coli* cell background by each of the CyaC, HlyC, and RtxC acyltransferases. We also noted that the acyltransferase selects from the bacterial pool of acyl–acyl carrier proteins (ACPs) an acyl chain of a specific length for covalent linkage to the protoxin. The acyltransferase also selects whether both or only one of two conserved lysine residues of the protoxin will be posttranslationally acylated. Functional assays revealed that RtxA has to be modified by 14-carbon fatty acyl chains to be biologically active, that HlyA remains active also when modified by 16-carbon acyl chains, and that CyaA is activated exclusively by 16-carbon acyl chains. These results suggest that the RTX toxin molecules are structurally adapted to the length of the acyl chains used for modification of their acylated lysine residue in the second, more conserved acylation site.

AQ:C

The cytolytic (pore-forming) RTX toxins are important virulence factors of many Gram-negative bacterial pathogens (1). The RTX toxins permeabilize host cell membranes and share several characteristic features. These comprise (i) a C-terminal unprocessed secretion signal, recognized by the type I secretion system and mediating translocation of toxins directly from the bacterial cytosol into the extracellular milieu; (ii) characteristic C-terminal nonapeptide glycine- and aspartate-rich RTX repeats that upon binding of numerous calcium ions fold into a β-barrel structure; (iii) posttranslational modification of internal lysine residues within conserved acylated sites by covalent attachment of fatty acyl residues, and (iv) a hydrophobic pore-forming domain, respectively (1).

ZSI This article contains supporting information.

‡These authors contributed equally to this work.
* For correspondence: Radim Osicka, osicka@biomed.cas.cz.

RTX cytolysins (RTXA) are synthesized as inactive protoxins (proRTXA) and undergo a posttranslational acylation by toxin-activating acyltransferases (RTXC) co-expressed with the protoxins (2–6). As first demonstrated for the *Escherichia coli* α-hemolysin (HlyA), its cognate acyltransferase HlyC cannot use acyl-CoA as acyl chain donor and uses only fatty acyl residues carried by acyl carrier protein (ACP). Modification of proHlyA occurs through an amide-linked acylation of the ε-amino groups of the Lys-564 and Lys-690 residues of HlyA (7, 8). The two lysine residues of HlyA were found to be predominantly acylated in uropathogenic *E. coli* by myristoyl chains (C14:0; ~68%), and the remaining acyl chains were initially identified as the extremely rare odd-carbon pentadecanoyl (C15:0; ~26%) and heptadecanoyl (C17:0; ~6%) fatty acyl groups (9). The myristoyl chain was also found to be the major modification of the Lys-558 (~18%) and Lys-689 (~71%) residues of the recombinant RtxA cytotoxin of *Kingella kingae*, whereas the remaining toxin molecules were modified by hydroxymyristoyl (Lys-558, ~5%; Lys-689, ~18%), lauroyl (Lys-689, ~2%), and palmitoleyl (Lys-689, ~8%) chains (5). In contrast, the *Bordetella pertussis* RTX adenylate cyclase toxin (CyaA) was initially found to be acylated by single C16:0 palmitoylation on the Lys-983 residue (10), and when overproduced in *B. pertussis*, palmitoylation was detected also on its Lys-860 residue (11). This was recently confirmed for a number of clinical isolates producing the native CyaA (12). When CyaA was overproduced in *E. coli* together with its activating acyltransferase CyaC, a mixed acylation by predominantly palmitoyl (Lys-860, ~46%; Lys-983, ~22%) and palmitoleyl (Lys-860, ~44%; Lys-983, ~56%) chains with a low level of C14:0 myristoylation was observed (13–16).

AQ:D

Acylation of the RTX toxins appears to be crucial for all of their known cytotoxic activities (2, 5, 6, 8, 17, 18). However, the precise molecular mechanism by which the acyl chains contribute to membrane insertion and formation of pores by the toxins remains poorly understood. The presence of the acyl chains was shown to play a structural role in the folding of CyaA into a biologically active conformation (19, 20) and in a productive and irreversible interaction of CyaA with cells expressing the complement receptor 3 (CR3; also known as the integrin $\alpha_M\beta_2$, CD11b/CD18, or Mac-1) (17, 21). Acylation was also shown to be required for the irreversible insertion of HlyA to target membrane (22) and for protein-protein interaction in HlyA oligomerization within the membrane microdomains (23).

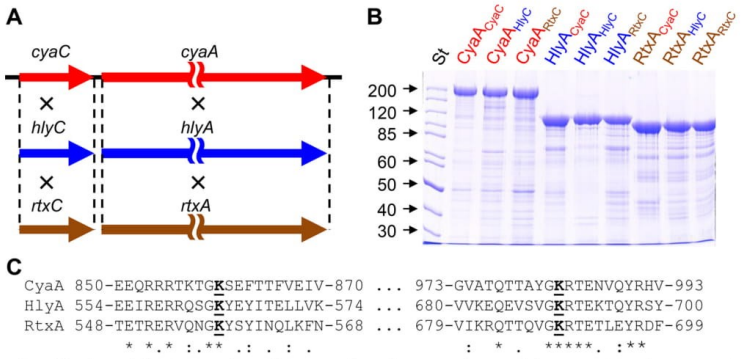

Figure 1. Expression and purification of the RTXC-activated RTXA toxin variants. *A*, scheme of the generation of constructs for the expression of the CyaA, HlyA, and RtxA toxins activated by the acyltransferase CyaC, HlyC, or RtxC, respectively. To generate the constructs, the pT7CACT1 plasmid harboring the *cyaC* and *cyaA* genes was used. The *cyaC* ORF in pT7CACT1 was replaced from its start to stop codon by *hlyC* or *rtxC*, and similarly, the *cyaA* ORF was replaced by *hlyA* or *rtxA*, respectively. *B*, a set of the nine pT7CACT1-derived constructs was used for the production of the RTXC-activated RTXA toxins in *E. coli* BL21/pMM100 cells. The proteins were purified close to homogeneity from urea-solubilized inclusion bodies by affinity chromatography on calmodulin-Sepharose (CyaA variants) or Ni-NTA agarose (HlyA and RtxA variants). The samples were analyzed on 7.5% polyacrylamide gels and stained with Coomassie Blue. *St*, molecular mass standards. *C*, ClustalW sequence alignment of acylated sites of CyaA (UniProt code: P0DKX7), HlyA (UniProt code: P08715), and RtxA (*K. kingae* isolate PYKK081) with two conserved internal lysine residues (in *boldface type* and *underlined*) whose ϵ-amino groups are posttranslationally acylated. *, identity; :, strongly similar; ., weakly similar.

The toxin-activating acyltransferase genes are highly conserved between the *rtx* loci of various bacterial genera, and some of these acyltransferases were reported to activate also heterologous protoxins. For example, the HlyC-modified *Actinobacillus pleuropneumoniae* hemolysin ApxIA, as well as the ApxC-modified HlyA expressed in *E. coli*, exhibited a hemolytic activity on erythrocytes (24, 25). Similarly, the heterologously HlyC- or CyaC-activated *Pasteurella hemolytica* leukotoxin LktA exhibited the same activity and target cell specificity as the LktA activated by its cognate LktC acyltransferase. Nevertheless, the activation was not reciprocal, as the LktC-activated HlyA and CyaA produced in *E. coli* were neither hemolytic nor cytotoxic (26, 27). However, it has not been determined why some RTX protoxins are efficiently cross-activated by heterologous acyltransferases and some are not.

Here, we analyzed the activation of the CyaA, HlyA, and RtxA AQ:E toxins, each acylated by one of the three CyaC, HlyC, or RtxC acyltransferases and produced in the same *E. coli* cell background, so as to eliminate the potential impact of differences in acyl-ACP pool composition of the original producer bacteria. The results reveal that it is the RTXC acyltransferase enzyme that selects the type of the acyl chain of adapted length that is covalently linked to the proRTXA protein, and the acyltransferase also selects whether a single lysine residue or both modification sites of proRTXA will be posttranslationally acylated, thereby conferring the biological activity on the RTX toxin.

Results

CyaC selects C16 fatty acyl chains, whereas HlyC and RtxC select C14 acyl chains and differ in recognition of acylation sites

To test the acyl residue and acylation site selectivity of the three homologous RTX toxin–activating acyltransferases, we produced the nine pairwise combinations of the three protoxins proCyaA, proHlyA, and proRtxA with the three acyltransferase enzymes CyaC, HlyC, and RtxC, respectively, in the same *E. coli* cell background. For this purpose, the expression signals of the pT7CACT1 plasmid for production of CyaC-activated CyaA toxin (28) were employed. The *cyaC* ORF in pT7CACT1 was replaced from start to stop codon by the coding sequences of the *hlyC* or *rtxC* genes, and the *cyaA* ORF was replaced by *hlyA*- or *rtxA*-coding sequences, respectively (Fig. 1*A*). In addi- F1
tion, the *hlyA* and *rtxA* genes were fused in frame at the 3′ terminus to a sequence encoding a double-hexahistidine purification tag. The obtained set of nine constructs was used to produce the nine resulting RTXC-acylated RTXA toxins in *E. coli* BL21 cells. These were purified close to homogeneity from urea-solubilized inclusion bodies by affinity chromatography on calmodulin-Sepharose (CyaA proteins) or Ni-NTA agarose (HlyA and RtxA proteins) (Fig. 1*B*).

To analyze the acylation pattern of the nine RTXA variants, digests of the purified proteins were analyzed by liquid chromatography coupled to ultrahigh-resolution Fourier transform ion cyclotron resonance MS (LC FT-ICR MS). As summarized in
Table 1, the $CyaA_{CyaC}$ toxin activated by its cognate acyltrans- T1
ferase CyaC exhibited a predominant acylation with palmitoyl (C16:0) and palmitoleyl (C16:1) chains at the Lys-860 (~66%) and Lys-983 (~88%) residues. A small proportion of the $CyaA_{CyaC}$ molecules was also modified by myristoyl (C14:0) and octadecenoyl (C18:1) chains linked to the Lys-860 (~3%) and Lys-983 (~11%) residues (Table 1). Only ~31% of the Lys-860 residues remained unacylated by CyaC, whereas the Lys-983 residue of $CyaA_{CyaC}$ was acylated nearly completely (~99%). In contrast, when proCyaA was produced in the presence of HlyC or RtxC, only minimal (1% in $CyaA_{HlyC}$) or no (0% in $CyaA_{RtxC}$) acylation of the Lys-860 residue in the first acylation site of CyaA was detected (Table 1). Hence, the heterologous acyltransferases recognized the first acylation site of CyaA (Fig. 1*C*) with negligible efficacy. In contrast, the second

J_ID: JBC Date: 18-June-20 4/Color Figure(s): F1,3,5,7 ART: RA120.014122 Page: 3 Total Pages: 15

Table 1
Acylation status of the RTXA toxins modified by the RTXC acyltransferases

	CyaA						HlyA						RtxA					
	CyaC		HlyC		RtxC		CyaC		HlyC		RtxC		CyaC		HlyC		RtxC	
Acyl chain[a]	K860	K983	K860	K983	K860	K983	K564	K690	K564	K690	K564	K690	K558	K689	K558	K689	K558	K689
None	31	1	99	20	100	7	93	0	10	0	73	0	100	1	97	0	98	0
C12:0	–	–	–	–	–	–	–	–	3	2	1	–	–	–	–	3	–	1
C12:0−OH	–	–	–	–	–	–	–	–	2	–	–	–	–	–	–	–	–	–
C14:0	–	3	–	70	–	73	–	–	13	58	10	81	–	5	1	73	1	80
C14:0−OH	–	–	1	7	–	12	–	–	71	35	16	14	–	1	2	23	1	11
C16:0	32	45	–	2	–	1	1	23	–	1	–	1	–	15	–	–	–	1
C16:1	34	43	–	1	–	7	6	67	1	4	–	4	–	74	–	1	–	7
C18:1	3	8	–	–	–	–	–	10	–	–	–	–	–	4	–	–	–	–

[a] The RTXA variants were produced in the presence of the RTXC acyltransferases in *E. coli* BL21/pMM100 cells, purified close to homogeneity and analyzed by MS. Percentage distributions of fatty acyl chains linked to the ϵ-amino groups of the lysine residues were estimated semiquantitatively, from the relative intensities of selected ions in reconstructed ion current chromatograms. Average values are calculated from determinations performed with two different toxin preparations. –, the acyl chain was not detected.

acylation site of CyaA (Fig. 1*C*) was well-recognized by HlyC and RtxC acyltransferases that efficiently acylated its Lys-983 residue. However, the HlyC and RtxC selected almost exclusively the shorter myristoyl (C14:0) and hydroxymyristoyl (C14:0-OH) chains (~77% in $CyaA_{HlyC}$ and ~85% in $CyaA_{RtxC}$) for modification of the Lys-983 residue of CyaA (Table 1). The C16:0 and C16:1 chains formed only a minor proportion of the acyl chains linked to the Lys-983 residue (~3% in $CyaA_{HlyC}$ and ~8% in $CyaA_{RtxC}$) (Table 1).

As further documented in Table 1, the $HlyA_{HlyC}$ toxin was efficiently modified by its cognate acyltransferase HlyC with the C14:0 and C14:0-OH acyl chains at the Lys-564 (~84%) and Lys-690 (~93%) residues. Only a small proportion of the $HlyA_{HlyC}$ molecules was acylated with the C12:0, C12:0-OH, C16:0, and C16:1 chains (~6% at Lys-564 and 7% at Lys-690) or remained unacylated at the Lys-564 residue (~10%) (Table 1). The C14:0 and C14:0-OH chains were also the major acyl groups attached to the Lys-564 (~26%) and Lys-690 (~95%) residues, when HlyA was modified by the heterologous acyltransferase RtxC (Table 1). However, RtxC modified the first acylation site of HlyA with lower efficiency than HlyC, and ~73% of the Lys-564 residues remained unacylated (Table 1). In contrast, the heterologous acyltransferase CyaC acylated the Lys-690 residues of the HlyA molecules almost exclusively with the C16:0 and C16:1 (~90%) acyl chains and partially with C18:1 (~10%), whereas the Lys-564 residues were partially modified with the C16:0 and C16:1 acyl groups (~7%) or remained unacylated (~93%).

Finally, the RtxA cytotoxin was efficiently modified by its cognate acyltransferase RtxC and also by the heterologous acyltransferase HlyC at the Lys-689 residue with the C14:0 and C14:0-OH acyl chains (~91% in $RtxA_{RtxC}$ and ~96% in $RtxA_{HlyC}$) (Table 1). In contrast, the heterologous acyltransferase CyaC predominantly acylated the Lys-689 residue of RtxA with the C16:0 and C16:1 acyl groups (~89%) (Table 1). On the other hand, the Lys-558 residue of the RtxA variants was only residually modified with the C14:0 and C14:0-OH chains (~2% in $RtxA_{RtxC}$ and ~3% in $RtxA_{HlyC}$) or remained completely unacylated ($RtxA_{CyaC}$) (Table 1).

All of these results demonstrated that the different RTXC acyltransferases exhibit a varying selectivity for acyls of various lengths. CyaC selected from the *E. coli* acyl-ACP pool almost exclusively the C16:0 and C16:1 acyl chains for acylation of the cognate proCyaA or of the heterologous proHlyA and proRtxA substrates. In contrast, the HlyC and RtxC acyltransferases selected nearly exclusively the shorter C14:0 and C14:0-OH chains for acylation of all three proRTXA substrates (Table 1). This reveals that it is the RTXC acyltransferase enzyme that selects the length of the acyl chain that it transfers to the RTXA substrate protein. Moreover, the data showed that the RTXC enzymes promiscuously and quite efficiently recognize and modify the second, more conserved acylation sites (Fig. 1*C*) of heterologous proRTXA substrates, whereas the recognition and acylation of the first acylation sites in heterologous proRTXA substrates was nil or inefficient.

Acylation patterns determine the levels of biological activity of the RTX toxins

The set of nine toxins with defined numbers and lengths of attached acyl chains enabled us to assess how the single or double acylation and the length of the attached acyl chains affect the biological activities of these proteins. For the three differently acylated CyaA variants, we first determined their capacity to bind, penetrate, and lyse sheep erythrocytes, respectively, using red blood cells as surrogate target cells lacking the CyaA receptor CR3. As documented in Fig. 2*A*, compared with double acylation of the $CyaA_{CyaC}$ protein by predominantly the C16:0 and/or C16:1 chains, monoacylation of the Lys-983 residue by predominantly the C14:0 or C14:0-OH chains reduced the relative capacity of $CyaA_{HlyC}$ (by ~62%) and $CyaA_{RtxC}$ (by ~70%) to bind erythrocytes. The modification by the C14 acyls decreased even more the relative cell-invasive capacity of both toxin variants (by ~94%) (Fig. 2*A*). Moreover, at the rather high concentration of 10 μg/ml that was used, the $CyaA_{HlyC}$ and $CyaA_{RtxC}$ proteins were unable to provoke any lysis of erythrocytes over time, whereas complete erythrocyte lysis was provoked by the same amount of $CyaA_{CyaC}$ within 5 h of incubation (Fig. 2*B*). The relative AC-translocating and lytic capacities of the $CyaA_{HlyC}$ and $CyaA_{RtxC}$ proteins remained low even when their input concentration was increased 2.5-fold over that of $CyaA_{CyaC}$ to achieve binding of equal amounts of the three CyaA variants to erythrocyte cells (Fig. 2, *C* and *D*). The C14:0 or C14:0-OH monoacylated $CyaA_{HlyC}$ and $CyaA_{RtxC}$ toxins bound with a reduced capacity (~53 and ~60% of $CyaA_{CyaC}$ binding) also to mouse J774A.1 macrophages that express the CyaA receptor CR3 (Fig. 2*E*). However, the binding of $CyaA_{HlyC}$

ID: yadavr Time: 15:53 I Path: //mbnas01.cadmus.com/home$/yadavr$/SB-JBCJ200128

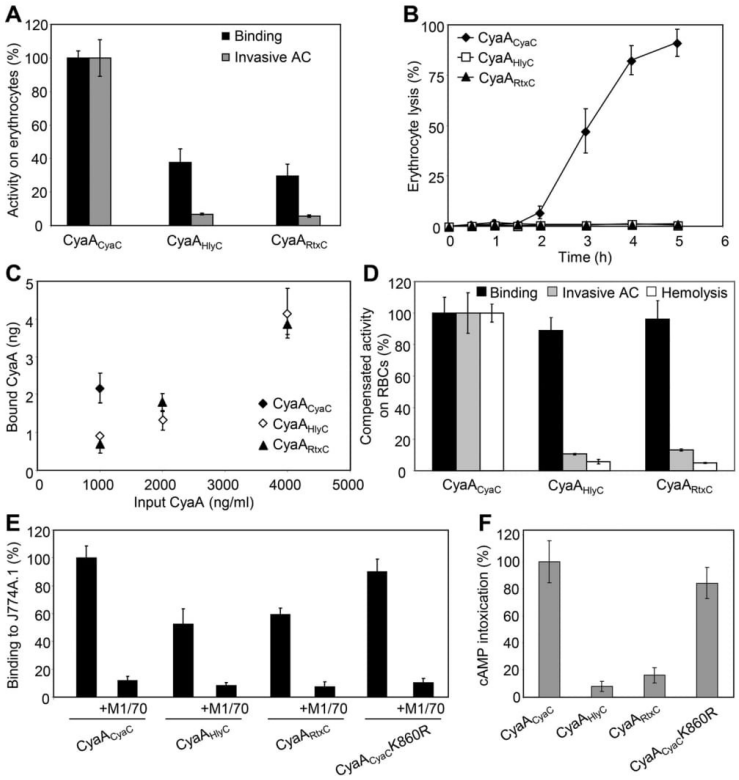

Figure 2. The HlyC- and RtxC-modified CyaA variants exhibit substantially reduced activities on erythrocytes and J774A.1 cells. *A*, sheep erythrocytes (5×10^8/ml) were incubated at 37 °C in the presence of 2 mM calcium with 1 μg/ml of the purified CyaA toxin variants, and after 30 min, aliquots were taken for determinations of the cell-associated AC activity (*Binding*) and of the AC activity internalized into erythrocytes and protected against digestion by externally added trypsin (*Invasive AC*). Activities are expressed as percentages of intact CyaA$_{CyaC}$ activity and represent average values ± S.D. (*error bars*) from at least three independent determinations performed in duplicate with at least two different toxin preparations. *B*, sheep erythrocytes (5×10^8/ml) were incubated at 37 °C in the presence of the CyaA variants (10 μg/ml). Hemolytic activity was measured as the amount of released hemoglobin by photometric determination (A_{541}) ($n = 3$). *C*, sheep erythrocytes (5×10^8/ml) were incubated with the indicated concentrations of the CyaA toxin variants (*Input CyaA*) for 30 min and washed, and the amount of cell-associated AC enzyme activity was determined. *D*, to compensate for the reduced cell-binding activity, the concentration of the CyaA$_{HlyC}$ and CyaA$_{RtxC}$ variants was increased to 2.5 μg/ml, as compared with 1 μg/ml for the intact CyaA$_{CyaC}$ toxin, allowing us to achieve binding of equal amounts of each protein per ml of erythrocytes. Binding and invasive AC of the intact CyaA$_{CyaC}$ toxin were taken as 100%. For comparison of hemolytic activity, the concentration of CyaA$_{HlyC}$ and CyaA$_{RtxC}$ was increased to 25 μg/ml, compared with 10 μg/ml for the intact CyaA$_{CyaC}$ protein. Hemolytic activity was measured after 4 h by photometric determination ($A_{541\ nm}$), and activity of intact CyaA was taken as 100%. Activities represent average values ± S.D. from three independent determinations. *E*, binding of the CyaA variants to J774A.1 cells (1×10^6) was determined as the amount of total cell-associated AC enzyme activity upon incubation of cells with 1 μg/ml of the protein for 30 min at 4 °C. To block the CR3 receptor of CyaA, J774A.1 cells (1×10^6) were preincubated for 30 min on ice with 5 μg/ml of the CD11b-specific mAb M1/70 prior to the addition of the CyaA variants (1 μg/ml). Activities are expressed as percentages of intact CyaA$_{CyaC}$ activity and represent average values ± S.D. from at least three independent determinations performed in duplicate with two different toxin preparations. *F*, cAMP intoxication was assessed by determining the intracellular concentration of cAMP generated in cells after 30 min of incubation of J774A.1 cells (1.5×10^5) with four different toxin concentrations from within the linear range of the dose-response curve (12.5, 25, 50, and 100 ng/ml). Activities are expressed as percentages of intact CyaA$_{CyaC}$ activity and represent average values ± S.D. from three independent determinations performed in duplicate with two different toxin preparations.

and CyaA$_{RtxC}$ to J774A.1 cells was CR3 receptor–specific, as it could be blocked by the competing antibody M1/70 that binds the CD11b subunit of CR3 (29, 30) (Fig. 2*E*). Nevertheless, compared with the C16 biacylated CyaA$_{CyaC}$, the C14 monoacylated CyaA$_{HlyC}$ and CyaA$_{RtxC}$ proteins were strongly impaired in their capacity to translocate the AC domain into the cytosol of J774A.1 cells to elevate the intracellular cAMP levels (Fig. 2*F*). This functional defect on J774A.1 cells was most likely not due to the lack of acylation of the Lys-860 residue of the CyaA$_{HlyC}$ and CyaA$_{RtxC}$ toxins, as a CyaA-K860R mutant acylated by CyaC only on the Lys-983 residue (17) exhibited similar capacity to bind (Fig. 2*E*) and translocate its AC domain (Fig. 2*F*) into J774A.1 cells as the intact doubly acylated CyaA$_{CyaC}$ toxin. Hence, the low cell-invasive activity of the monoacylated CyaA$_{HlyC}$ and CyaA$_{RtxC}$ proteins was rather due to the modification of the Lys-983 residue by the shorter C14 acyl chains, which conferred a much lower specific membrane penetration capacity on CyaA than the modification of the Lys-983 residue by the C16 acyl chains.

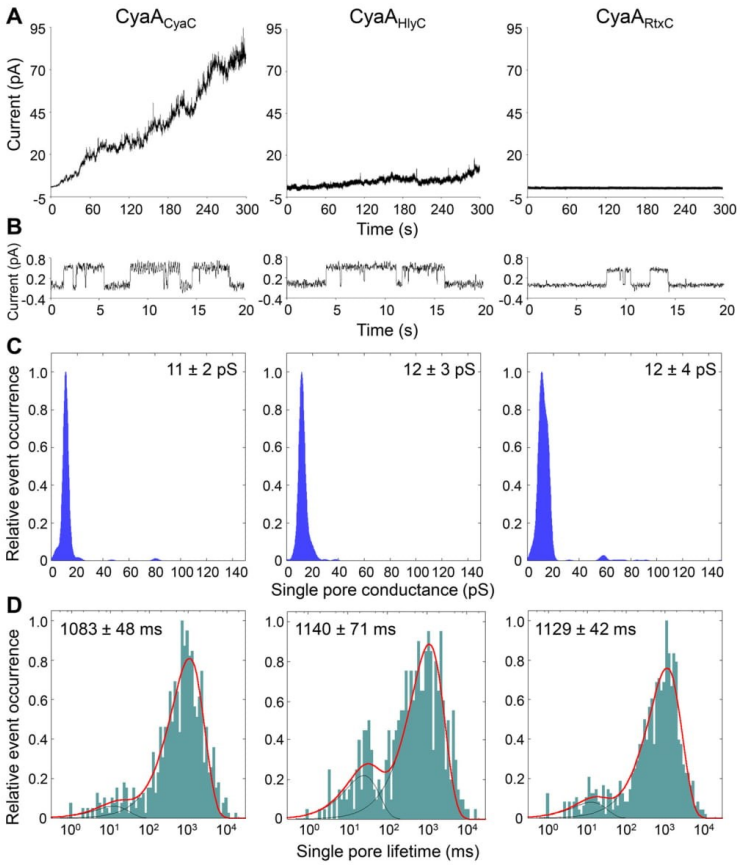

Figure 3. The CyaA variants acylated with HlyC or RtxC have substantially reduced overall membrane activity but form pores with similar single-pore conductance and pore lifetime as CyaA$_{CyaC}$. *A*, overall membrane activities of the CyaA variants on asolectin/decane:butanol (9:1) membranes in the presence of 250 pM purified proteins. The aqueous phase contained 150 mM KCl, 10 mM Tris-HCl (pH 7.4), 2 mM $CaCl_2$; the applied voltage was 50 mV; the temperature was 25 °C; and the recording was filtered at 10 Hz. *B*, single-pore recordings of asolectin membranes in the presence of 10 pM purified CyaA variants under conditions otherwise identical to those in *A*. *C*, kernel density estimation (KDE) of single-pore conductances calculated from single-pore recordings (>500 events) acquired on several different asolectin membranes with 10 pM CyaA$_{CyaC}$ or its variants under the same conditions as in *A*. The *numbers* represent the most frequent conductances ± S.D. of pores formed by the CyaA variants. *D*, for lifetime determination, ~400 individual pore openings were recorded on several different asolectin membranes with 10 pM CyaA$_{CyaC}$ or its variants under the same conditions as in *A*, and the logarithmic histogram of dwell times was fitted with a double-exponential function. The error estimates of lifetimes were obtained by bootstrap analysis. The *numbers* in each *panel* represent the most frequent values ± S.D.

In agreement with the residual cytolytic capacity on erythrocytes, the CyaA$_{HlyC}$ and CyaA$_{RtxC}$ variants exhibited also a very low overall membrane activity on artificial lipid bilayers made of 3% asolectin (Fig. 3*A*). However, as calculated from single-pore recordings (Fig. 3*B*), the most frequent conductances of pores formed by CyaA$_{HlyC}$ (12 pS) and CyaA$_{RtxC}$ (12 pS) were quite comparable with that of CyaA$_{CyaC}$ (11 pS) (Fig. 3*C*). Similarly, the most frequent lifetimes of pores formed by CyaA$_{HlyC}$ (1140 ms) and CyaA$_{RtxC}$ (1129 ms) were comparable with that of CyaA$_{CyaC}$ (1083 ms) (Fig. 3*D*). It can thus be concluded that the difference in the number (one *versus* two acylated lysine residues) and the length and chemical nature (C16:0/C16:1 *versus* C14:0/C14:0-OH) of attached acyl chains affected strongly the propensity of formation but not the overall characteristics of the individual pores generated by the differently acylated CyaA toxin variants.

A different picture was observed for the HlyA toxin variants modified by the CyaC, HlyC, or RtxC acyltransferases. As documented in Fig. 4*A*, the HlyA$_{CyaC}$ protein, acylated almost exclusively on the single Lys-690 residue by the C16:1 and C16:0 chains (Table 1), was still exhibiting a similar capacity to lyse erythrocytes as the HlyC-activated HlyA$_{HlyC}$ toxin acylated on both Lys-564 and Lys-690 residues by the shorter C14:0 and C14:0-OH acyl chains. Moreover, the RtxC-modified and predominantly monoacylated HlyA$_{RtxC}$ toxin was as hemolytic as HlyA$_{HlyC}$. Furthermore, irrespective of the length (C16 *versus*

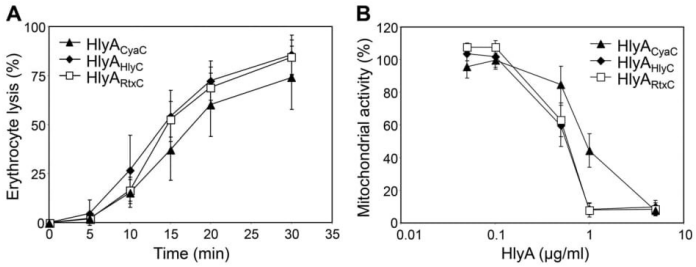

Figure 4. CyaC- and RtxC-modified HlyA variants lyse erythrocytes and reduce viability of THP-1 cells with the same efficacy as HlyA$_{HlyC}$. *A*, the HlyA variants were expressed in *E. coli* BL-21 cells and purified from urea extract on Ni-NTA agarose. Sheep erythrocytes (5×10^8/ml) were incubated at 37 °C in the presence of the HlyA variants (50 ng/ml) and in the presence of 2 mM Ca^{2+}. Hemolytic activity was measured as the amount of released hemoglobin by photometric determination (A_{541}). Activities represent average values ± S.D. (*error bars*) from three independent determinations performed in duplicate with three different toxin preparations. *B*, mitochondrial functionality in HlyA-treated THP-1 cells (1.5×10^5) was determined after 2 h as the capacity of mitochondrial dehydrogenases to reduce the tetrazolium salt WST-1 to its formazan product. Activities represent average values ± S.D. from three independent determinations performed in triplicate with two different toxin preparations.

C14) or number (one or two) of attached acyl residues, all three differently acylated HlyA toxin variants were comparably cytotoxic to human macrophage THP-1 cells, as determined by their capacity to elicit loss of capacity of mitochondrial reductases to convert the tetrazolium salt 4-[3-(4-iodophenyl)-2-(4-nitrophenyl)-2H-5-tetrazolio]-1,3-benzene disulfonate (WST-1) to formazan (Fig. 4*B*).

In line with the comparable cytolytic capacities on erythrocytes, all three HlyA variants displayed comparable overall membrane activities on artificial lipid bilayers (Fig. 5*A*). As calculated from single-pore recordings (Fig. 5*B*), the HlyA$_{HlyC}$ variant formed pores with the most frequent conductance of 405 pS that was similar to that of pores formed by the HlyA$_{CyaC}$ (322 pS) and HlyA$_{RtxC}$ (384 pS) proteins (Fig. 5*C*). The HlyA$_{CyaC}$ and HlyA$_{RtxC}$ toxin variants also formed pores with most-frequent pore lifetimes similar to those of the pores formed by the HlyA$_{HlyC}$ (1788, 1654, and 1599 ms, respectively) (Fig. 5*D*).

All of these results demonstrate that the C16 acyl chains attached to the Lys-690 residue conferred on the HlyA$_{CyaC}$ toxin a similar pore-forming and cytotoxic activity as did the naturally HlyC-mediated acylation by C14 acyl chains attached to both Lys-564 and Lys-690 residues in HlyA$_{HlyC}$ or the partial acylation of Lys-564 and full acylation of Lys-690 by C14 acyl chains in the HlyA$_{RtxC}$ toxin. This indicates that in contrast to CyaA, monoacylation of the single Lys-690 residue by either C14 or C16 acyl chains was sufficient for biological activity of HlyA.

Similarly, single acylation of the Lys-689 residue of RtxA by C14:0 or C14:0-OH acyl chains (Table 1) was sufficient for full cytolytic activity of the RtxA$_{RtxC}$ and RtxA$_{HlyC}$ toxins, acylated by RtxC or HlyC, respectively (Fig. 6). However, in contrast to HlyA, the RtxA toxin was not activated by CyaC despite almost complete modification of the Lys-689 residue by the C16:0 or C16:1 acyl chains. Hence, the biological activity of RtxA was supported only upon modification by C14 and not C16 acyl chains. In line with that, the RtxA$_{RtxC}$ and RtxA$_{HlyC}$ toxins displayed comparable overall membrane activities on planar lipid bilayers, whereas the RtxA$_{CyaC}$ protein exhibited a low membrane activity (Fig. 7*A*). Nevertheless, the formed RtxA$_{CyaC}$ pores (Fig. 7*B*) exhibited a comparable most-frequent conductance of 487 pS, like RtxA$_{HlyC}$ (454 pS) and RtxA$_{RtxC}$ (479 pS) pores, respectively (Fig. 7*C*). Similarly, the most frequent values of single-pore lifetimes of RtxA$_{CyaC}$ (968 ms) were similar to those of RtxA$_{HlyC}$ (1002 ms) and of RtxA$_{RtxC}$ (1288 ms) (Fig. 7*D*). These results indicate that the RtxA$_{CyaC}$ variant was impaired in its capacity to insert into the lipid bilayer and/or in its propensity to form oligomeric pores due to the modification by the longer C16 acyl chains.

Discussion

We report that of the three examined RTXA toxins, the CyaA toxin is only activated by predominant modification of its Lys-983 residue by C16 fatty acyl chains and the RtxA protein only by the modification of its Lys-689 residue by C14 acyl chains. Intriguingly, the HlyA toxin can be fully activated by modification with either C14 or C16 acyl chains linked to its Lys-690 residue. These results further show that it is the acyltransferase activating the RTX protoxin that selects the acyl chain of the functionally adapted length from the acyl-ACP pool of the producing bacterium. Furthermore, the acyltransferase also determines whether both or only one of the two conserved acylation sites in the respective RTX protoxin will be recognized and covalently modified by the linked acyl chains.

In the first report analyzing the acylation of CyaA, the toxin isolated from the *B. pertussis* strain BP338 was found to be modified by a single amide-linked palmitoylation on the ϵ-amino group of Lys-983 (10). However, CyaA overproduced together with CyaC in the *B. pertussis* 18-323 strain was later found to be palmitoylated on both the Lys-860 and Lys-983 residues (11), and the double acylation was recently confirmed for CyaA extracted from seven clinical isolates of *B. pertussis* (12). Most of the modifications occurring in *B. pertussis* consisted in palmitoylation of the Lys-983 (up to ~90%) and Lys-860 (~70–100%) residues. However, partial myristoylation (~10–40%) was also observed on the Lys-983 residue of the native CyaA (12). Initial analysis of CyaA produced with CyaC in the *E. coli* K12 strain XL1-Blue revealed that the recombinant toxin was acylated by palmitoyl chains (~67%) at the Lys-860 residue and palmitoyl (~87%) and myristoyl (~13%) chains at the Lys-983 residue (15). A higher-resolution MS analysis later demonstrated

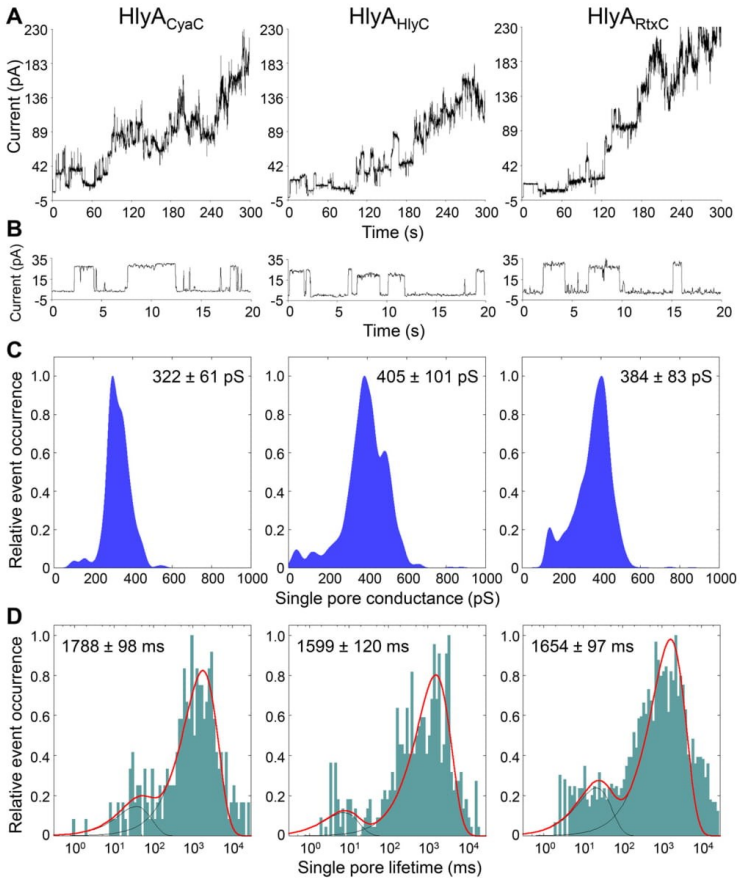

AQ:N **Figure 5. All HlyA variants exhibit similar overall membrane activities and single-pore properties.** *A*, overall membrane activities of the HlyA variants on asolectin/decane:butanol (9:1) membranes in the presence of 250 pM purified proteins. The aqueous phase contained 150 mM KCl, 10 mM Tris-HCl (pH 7.4), 2 mM $CaCl_2$; the applied voltage was 50 mV; the temperature was 25 °C; and the recording was filtered at 10 Hz. *B*, single-pore recordings of asolectin membranes in the presence of 10 pM purified HlyA variants under otherwise identical conditions as in *A*. *C*, KDE of single-pore conductances calculated from single-pore recordings (>500 events) acquired on several different asolectin membranes with 10 pM HlyA$_{HlyC}$ or its variants under the same conditions as in *A*. The *numbers* represent the most frequent conductances ± S.D. of pores formed by the HlyA variants. *D*, for lifetime determination, ~400 individual pore openings were recorded on several different asolectin membranes with 10 pM HlyA$_{HlyC}$ or its variants under the same conditions as in *A*, and the logarithmic histogram of dwell times was fitted with a double-exponential function. The error estimates of lifetimes were obtained by bootstrap analysis. The *numbers* in each *panel* represent the most frequent values ± S.D.

that the Lys-983 residue of the recombinant CyaA isolated from *E. coli* K12 was not only palmitoylated (C16:0), but also palmitoleylated (*cis* Δ9 C16:1) at a ratio of ~1:2 (14). The palmitoyl (Lys-860, ~46%; Lys-983, ~22%) and palmitoleyl (Lys-860, ~44%; Lys-983, ~56%) chains were also identified later as the major fatty acyl modifications of the recombinant CyaA purified from the *E. coli* K12 strain (16).

In line with these findings, we found here that palmitoylation (Lys-860, ~32%; Lys-983, ~45%) and palmitoleylation (Lys-860, ~34%; Lys-983, ~43%) are the two major posttranslational modifications of the Lys-860 and Lys-983 residues also when the CyaC-acylated recombinant CyaA is produced in the *E. coli* B strain BL21. In contrast, the HlyC- or RtxC-modified CyaA variants produced on the same genetic background were predominantly myristoylated and hydroxymyristoylated almost exclusively on the Lys-983 residue (CyaA$_{HlyC}$, ~77%; CyaA$_{RtxC}$, ~85%). Modification by C16:0 and C16:1 acyl chains was negligible in CyaA$_{HlyC}$ (~3%) and CyaA$_{RtxC}$ (~8%). The CyaA$_{HlyC}$ and CyaA$_{RtxC}$ variants then exhibited substantially lower biological activities than CyaA$_{CyaC}$, and this was most likely not due to the missing acylation at the Lys-860 residue of CyaA$_{HlyC}$ and CyaA$_{RtxC}$. Indeed, we have demonstrated that acylation of the Lys-983 residue of CyaA$_{CyaC}$ was necessary and sufficient for biological activities of the toxin on both CR3-negative erythrocytes (13) as well as on CR3-positive J774A.1 cells (Fig. 2 (*E* and *F*)) (17). It is therefore plausible to conclude that the 14-

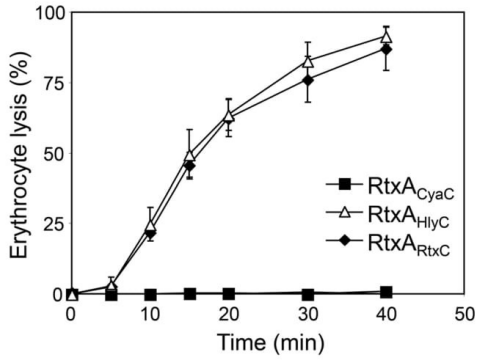

Figure 6. The CyaC-acylated RtxA variant is inactive. The RtxA variants were expressed in *E. coli* BL-21 cells and purified from urea extract on Ni-NTA agarose. Sheep erythrocytes (5×10^8/ml) were incubated at 37 °C in the presence of the RtxA variants (200 ng/ml) and in the presence of 2 mM Ca^{2+}. Hemolytic activity was measured as the amount of released hemoglobin by photometric determination (A_{541}) ($n = 3$). Activities represent average values ± S.D. (*error bars*) from three independent determinations performed in duplicate with two different toxin preparations.

carbon myristoyl and hydroxymyristoyl chains are unable to functionally replace the 16-carbon palmitoyl and palmitoleyl chains at the Lys-983 residue of CyaA. Thus, not only the absence of acylation itself, but also the length of the covalently linked acyl chains appears to play a crucial role in activation of CyaA and in conferring of biological activities on this toxin.

The specific binding of the myristoylated and hydroxymyristoylated CyaA$_{HlyC}$ and CyaA$_{RtxC}$ variants to CR3-positive J774A.1 cells was affected only mildly. However, compared with C16-acylated CyaA$_{CyaC}$, the C14 acyl-modified CyaA$_{HlyC}$ and CyaA$_{RtxC}$ variants were largely impaired in the capacity to deliver the AC enzyme across target cell membrane into the cytosol and to intoxicate cells by cAMP production. Hence, the two-carbon unit shorter C14 acyl chains were unable to adequately support the membrane insertion and translocation of the CyaA polypeptide. Indeed, the CyaA$_{HlyC}$ and CyaA$_{RtxC}$ variants exhibited a negligible overall membrane activity also on artificial lipid bilayers. This suggests that a 16-carbon-long acyl chain has to be attached to the ϵ-amino group of the side chain of the Lys-983 residue of CyaA to impose the necessary structure on the toxin molecule and enable it to effectively interact with the lipid bilayer of the target cell or of the artificial membrane. However, once the toxin has inserted into the lipid bilayer at a low frequency, the modification of CyaA with the C14 acyl chains does not affect anymore the conductance and lifetime of single pores formed by the CyaA$_{HlyC}$ and CyaA$_{RtxC}$ variants, because these exhibited quite the same properties as those formed by the C16-acylated CyaA$_{CyaC}$. This shows that differences in the number and length/chemical nature of the acyl chains linked to the CyaA molecule impact only the propensity of the toxin to insert into the membrane and form oligomeric pores and not on the structure of the pores itself.

We further demonstrated that CyaC-modified CyaA was completely acylated on the Lys-983 residue, whereas ~31% of toxin molecules remained unacylated at the Lys-860 residue (Table 1). In contrast, only residual (~1%) or no acylation was observed on Lys-860, when CyaA was modified with HlyC or RtxC, respectively. This suggests that CyaC may have a higher affinity for the Lys-860 acylation site of CyaA than the HlyC and RtxC acyltransferases. All of these results indicate that the CyaC acyltransferase co-evolved in *B. pertussis* with CyaA to modify it by C16 acyl chains and cannot be simply replaced by toxin-activating acyltransferases of other Gram-negative bacteria that preferentially select C14-bearing ACP for modification of proRTXA substrates.

Previously, fatty acyl modification of HlyA activated *in vivo* in two different uropathogenic isolates of *E. coli* (with a chromosomal (J96) and an extrachromosomal (pHly152) *hly* locus) was analyzed, and the Lys-564 and Lys-690 residues of HlyA were found to be mostly acylated by a myristoyl chain (~68%). The remaining linked acyls were then identified as the very rare C15:0 (~26%) and C17:0 (~6%) odd-carbon fatty acyl chains (9). Here, we demonstrated that the recombinant HlyC-modified HlyA toxin produced in the *E. coli* strain BL21 was acylated mostly by the C14:0 and C14:0-OH chains both at the Lys-564 (~84%) and Lys-690 (~93%) residue and partially by the C12:0, C12:0-OH, C16:0, and C16:1 chains. In contrast to the results of Lim *et al.* (9), we were unable to identify any C15:0 and C17:0 acyl groups attached to the HlyC-modified HlyA molecule despite the extreme sensitivity and accuracy of the current state-of-the-art analytical LC FT-ICR MS technology used. This indicates that uropathogenic *E. coli* isolates may have an acyl-ACP pool composition different from that of the *E. coli* B strain used here.

Intriguingly, the activation of HlyA exhibits a flexibility as to the length and nature of the attached acyl chains. When the Lys-690 residue of HlyA was predominantly acylated with the C16:0 and C16:1 (~90%) acyl chains by CyaC, the HlyA$_{CyaC}$ protein exhibited a similar capacity to reduce viability of THP-1 cells or to lyse erythrocytes, and it exhibited similar membrane properties on planar lipid bilayers as upon C14 modification on both Lys-564 and Lys-690 residues. Thus, in contrast to CyaA, the HlyA toxin can be modified by acyl chains of varying length (C14 *versus* C16) and still gains biological activity.

Previously, using deleted HlyA protoxin variants and peptides as substrates in an *in vitro* acylation assay, Stanley *et al.* (31) demonstrated that HlyC possessed an about 4 times higher affinity for the segment encompassing the Lys-564 residue of HlyA than for that harboring the Lys-690 residue, resulting in acylation of 80% Lys-564 residues and only 20% of Lys-690 residues. Moreover, substitutions of the Lys-564 and Lys-690 residues revealed that both sites were required for hemolytic activity of HlyA (8). Interestingly, our results indicate that the affinity of the CyaC and RtxC acyltransferases *in vivo* was much higher to the segment harboring the Lys-690 residue, as this was quantitatively acylated by both enzymes *in vivo*, whereas only ~7 or ~27% of HlyA molecules were modified by CyaC or RtxC on the Lys-564 residue. Despite a substantially lower extent of acylation of the Lys-564 residue, the complete acylation of the Lys-690 residue conferred on the HlyA$_{CyaC}$ and HlyA$_{RtxC}$ proteins a full capacity to lyse erythrocytes. Moreover, the HlyA$_{CyaC}$ and HlyA$_{RtxC}$ proteins also exhibited an equally high membrane activity on planar lipid bilayers as the

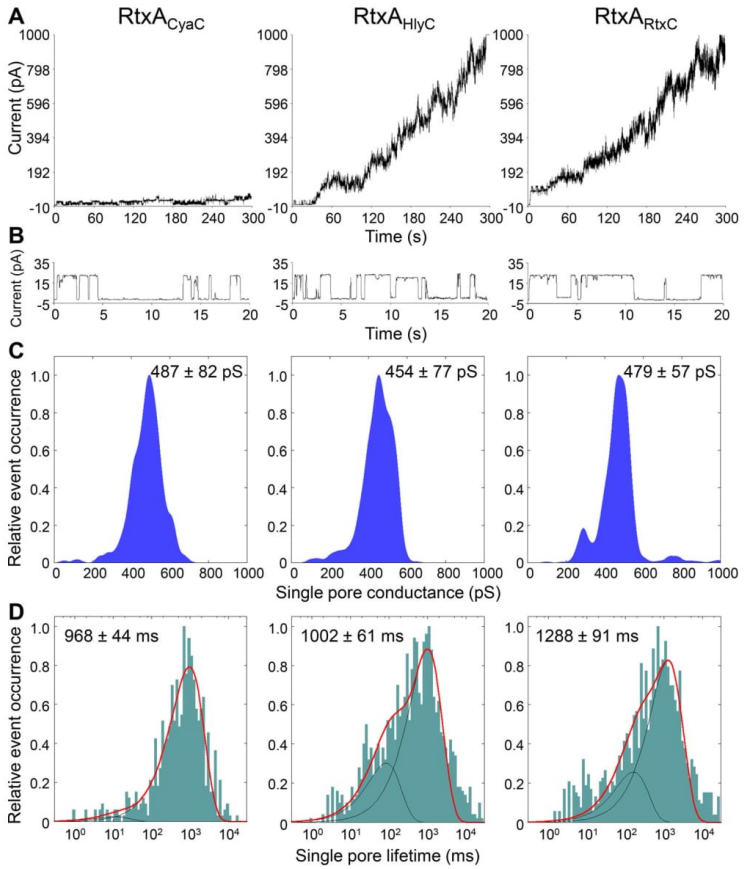

Figure 7. The CyaC-acylated RtxA variant has substantially reduced overall membrane activity but forms pores with similar single-pore conductance and pore lifetime as RtxA$_{HlyC}$ and RtxA$_{RtxC}$. *A*, overall membrane activities of the RtxA variants on asolectin/decane:butanol (9:1) membranes in the presence of 250 pM purified proteins. The aqueous phase contained 150 mM KCl, 10 mM Tris-HCl (pH 7.4), 2 mM $CaCl_2$; the applied voltage was 50 mV; the temperature was 25 °C; and the recording was filtered at 10 Hz. *B*, single-pore recordings of asolectin membranes in the presence of 10 pM purified RtxA variants under conditions otherwise identical to those in *A*. *C*, KDE of single-pore conductances calculated from single-pore recordings (>500 events) acquired on several different asolectin membranes with 10 pM RtxA$_{RtxC}$ or its variants at the same conditions as in *A*. The *numbers* represent the most frequent conductances ± S.D. of pores formed by the RtxA variants. *D*, for lifetime determination, ~400 individual pore openings were recorded on several different asolectin membranes with 10 pM RtxA$_{RtxC}$ or its variants under the same conditions as in *A*, and the logarithmic histogram of dwell times was fitted with a double-exponential function. The error estimates of lifetimes were obtained by bootstrap analysis. The *numbers* in each *panel* represent the most frequent values ± S.D.

native doubly acylated HlyA$_{HlyC}$ protein. Hence, rather than acylation of Lys-564 being essential, the activity of HlyA was likely lost upon substitution of Lys-654 because of a structural role of the Lys-564 residue in toxin activity. Indeed, a similar conclusion was reached upon substitution of the homologous Lys-860 residue of CyaA, the acylation of which is by itself dispensable for CyaA activity on both erythrocytes, as well as on CR3-expressing cells (13, 17). However, the CyaA-K860R mutant is importantly affected in its specific membrane penetration activity on cells lacking the CR3 receptor (13, 17).

Recently, we reported that the recombinant RtxA produced together with RtxC in the *E. coli* B strain BL21 was primarily modified by C14:0 and C14:0-OH acyl chains (~89%) on the Lys-689 residue (5). Only a minor proportion of the RtxA molecules (~8%) was found to be acylated on Lys-689 by C16:1 palmitoleyl chains (5). A small proportion of the RtxA molecules (~23%) was also found to be modified by C14:0 and C14:0-OH acyl chains on the Lys-558 residues (5). Here, we confirmed the type and extent of acylation of recombinant RtxA toxin on the Lys-689 residue, whereas a lower level (~2%) of modification of the Lys-558 residue was detected. This indicates that the extent of Lys-558 acylation may vary as a function of the physiological state of the producing bacteria, as discussed previously for the acylation of the Lys-860 residue of CyaA (13). Alternatively, differences in LC–MS configuration used for quantification of protein peptides between the reports may have accounted for the variation in the detected quantities of the acylated peptide (5). Indeed, reproducibility of MS-based peptide quantitation

was shown to vary by up to 20%, depending on the sample preparation, unique characteristics of reversed-phase columns used for separation of peptides, and LC–MS instrument configuration, respectively (32).

Similarly as $RtxA_{RtxC}$, the HlyC-modified RtxA was predominantly acylated by C14:0 and C14:0-OH acyl chains (~96%) on the Lys-689 residue, and only residual modification by C14:0 and C14:0-OH chains (~3%) was observed on the Lys-558 residue. The $RtxA_{RtxC}$ and $RtxA_{HlyC}$ variants with a similar acylation pattern then exhibited comparable capacities to lyse erythrocytes and similar membrane properties on planar lipid bilayers. However, unlike the fully biologically active C16-acylated $HlyA_{CyaC}$ toxin, the $RtxA_{CyaC}$ protein modified by CyaC at the Lys-689 residue by the C16:0 and C16:1 chains (~89%) was unable to lyse erythrocytes and exhibited only a residual overall membrane activity on planar lipid membranes. C16-acylated $RtxA_{CyaC}$ was most likely impaired in binding/insertion to the lipid bilayer and/or in the propensity to form oligomeric pores, as once inserted into the membrane, it formed pores exhibiting single-pore conductances and lifetimes similar to those of $RtxA_{RtxC}$. In this respect, the $RtxA_{CyaC}$ protein was similar to the unacylated proCyaA, proHlyA, and proRtxA protoxins, which despite highly decreased overall membrane activity, once inserted into the lipid bilayer, formed pores with properties similar to those of the acylated toxins (5, 17, 33, 34).

In conclusion, we report here that RtxA has to be modified by 14-carbon fatty acyl chains to be biologically active, whereas HlyA remains active also when modified by 16-carbon acyl chains and CyaA is only activated by 16-carbon acyl chains. These results reveal the selection of acyl chains of appropriate lengths by the respective cognate RTXC acyltransferase enzymes and suggest a structural adaptation of the RTXA toxin molecules to the length of the acyl chains used for modification of their crucial acylated residue in the second, more conserved acylation site.

Experimental procedures

Bacterial strains

The *E. coli* strain XL1-Blue (Stratagene, La Jolla, CA) was used throughout this work for DNA manipulations and was grown in Luria–Bertani medium at 37 °C. The *E. coli* strain BL21 (Novagen, Madison, WI) carrying the plasmid pMM100 (encoding LacI and tetracycline resistance) (35) was used for expression of the RTX proteins.

Cell lines

Murine monocytes/macrophages J774A.1 (ATCC, number TIB-67) were cultured at 37 °C in a humidified air/CO_2 (19:1) atmosphere in RPMI 1640 (Sigma–Aldrich) supplemented with 10% fetal calf serum (Gibco) and antibiotic antimycotic solution (0.1 mg/ml streptomycin, 1000 units/ml penicillin and 0.25 mg/ml amphotericin; Sigma–Aldrich).

Standard techniques

Determination of protein concentration and SDS-PAGE were performed according to standard protocols (36). PageRuler Unstained Protein Ladder (catalog no. 26614, Thermo Fisher Scientific) was used as a size standard in SDS-PAGE.

Plasmid construction

The pT7CACT1 plasmid (28), harboring the *cyaC* and *cyaA* genes under control of the isopropyl-β-D-thiogalactopyranoside–inducible *lacZp* promoter, was used to generate constructs for the expression of the CyaA, HlyA, and RtxA toxins activated by the acyltransferase CyaC, HlyC, or RtxC, respectively. For this purpose, the *cyaC* ORF in pT7CACT1 was replaced from its start to stop codon by coding sequences of *hlyC* or *rtxC*, and similarly, the *cyaA* ORF was replaced by *hlyA* or *rtxA* ORFs, respectively (Fig. 1*A*). The *hlyC* and *hlyA* genes were PCR-amplified from the plasmid pTZHly11 (37), and the *rtxC* and *rtxA* genes were amplified from the plasmid pT7*rtxC-rtxA* (5). In addition, the *hlyA* and *rtxA* genes were fused in frame at the 3′ terminus to a sequence encoding a double-hexahistidine purification tag (38).

Protein production and purification

The RTXC-activated RTXA toxins were produced in *E. coli* BL21/pMM100 cells transformed with the appropriate plasmids. 500-ml cultures were grown with shaking at 37 °C in MDO medium (20 g/liter yeast extract, 20 g/liter glycerol; 1 g/liter KH_2PO_4, 3 g/liter K_2HPO_4, 2 g/liter NH_4Cl, 0.5 g/liter Na_2SO_4, 0.01 g/liter thiamine hydrochloride) containing 150 μg/ml ampicillin and 12.5 μg/ml tetracycline. When cultures reached OD_{600} = 0.8, protein production was induced with 1 mM isopropyl-β-D-thiogalactopyranoside for an additional 4 h. For protein purification, the cells were harvested by centrifugation, washed twice with 50 mM Tris-HCl (pH 8.0), and disrupted by sonication at 4 °C, and the homogenate was centrifuged at 20,000 × *g* for 30 min at 4 °C. The inclusion bodies collected in the pellet were washed with 50 mM Tris-HCl (pH 8.0) containing 4 M urea and then solubilized with 50 mM Tris-HCl (pH 8.0) containing 8 M urea, and the urea extract was cleared at 20,000 × *g* for 30 min at 4 °C.

The urea extracts containing the HlyA and RtxA variants were loaded on an Ni-NTA agarose column (Qiagen, Germantown, MD) equilibrated with TNU buffer (50 mM Tris-HCl (pH 8.0), 200 mM NaCl, and 8 M urea). The column was washed with TNU buffer containing 20 mM imidazole, and the HlyA and RtxA variants were eluted with TNU buffer containing 600 mM imidazole. The eluted fractions of HlyA and RtxA were diluted 4 times in ice-cold 50 mM Tris-HCl (pH 8.0) containing 1 M NaCl and loaded on a phenyl-Sepharose CL-4B column (Sigma–Aldrich) equilibrated with the same buffer. The column was then washed with 50 mM Tris-HCl (pH 8.0), and the HlyA and RtxA variants were eluted with TUE buffer (50 mM Tris-HCl (pH 8.0), 8 M urea, and 2 mM EDTA).

The urea extracts containing the CyaA variants were diluted 4 times in ice-cold washing buffer (50 mM Tris-HCl (pH 8.0), 500 mM NaCl, and 2 mM $CaCl_2$) and loaded at 4 °C on a calmodulin-Sepharose 4B column (GE Healthcare) equilibrated with the same buffer. The column was washed with washing buffer, and the CyaA variants were eluted at room temperature with TUE buffer.

LC–MS analysis

The proteins were dissolved in 50 mM ammonium bicarbonate buffer (pH 8.2) to reach 4 M concentration of urea and digested with trypsin (Promega (Madison, WI), modified AQ:I sequencing grade) at a trypsin/protein ratio of 1:50 for 6 h at 30 °C. The second portion of trypsin was added to a final ratio of trypsin/protein of 1:25, and the reaction was carried out for another 6 h at 30 °C. When the reaction was complete, the concentration of the resulting peptides was adjusted by 0.1% TFA to 0.1 mg/ml, and 5 μl of the sample were injected into the LC–MS system. The LC separation was performed using a desalting column (ZORBAX C18 SB-300, 0.1 × 2 mm) at a flow rate of 40 μl/min (Shimadzu, Kyoto, Japan) of 0.1% formic acid (FA) and a separation column (ZORBAX C18 SB300, 0.2 × 150 mm) at a flow rate of 10 μl/min (Agilent 1200, Santa Clara, CA) of water/acetonitrile (MeCN) (Merck, Darmstadt, Germany) gradient: 0–1 min, 0.2% FA, 5% MeCN; 5 min, 0.2% FA, 10% MeCN; 35 min, 0.2% FA, 50% MeCN; 40 min, 0.2% FA, 95% MeCN; 40–45 min, 0.2% FA, 95% MeCN. A capillary column was directly connected to a mass analyzer. The MS analysis was performed on a commercial solariX XR FTMS instrument equipped with a 15 Tesla superconducting magnet and a Dual II ESI/MALDI ion source (Bruker Daltonics, Bremen, Germany). Mass spectra of the samples were obtained in the positive ion mode within an *m/z* range of 150–2000. The accumulation time was set at 0.2 s, LC acquisition was 45 min with a 5-min delay, and one spectrum consisted of accumulation of four experiments. The instrument was operating in survey LC–MS mode and calibrated online using Agilent tuning mix, which results in mass accuracy below 2 ppm.

Data processing and interpretation

MS data were processed by the SNAP version 2.0 algorithm of the DataAnalysis 4.4 software package (Bruker Daltonics, Billerica, MA, USA) generating a list of monoisotopic masses from deconvoluted spectra. The parameters were set as follows: export *m/z* range of 150–2000, maximum charge state of 8, signal/noise threshold of 0.75, and absolute intensity threshold 5×10^5. The extracted experimental data were searched against the FASTA of a single corresponding toxin molecule (CyaA: UniProtKB code P0DKX7; HlyA: UniProtKB code P08715; RtxA: UniprotKB code A0A1X7QNC7) using the home-built Linx software (RRID:SCR_018657). The Linx algorithm was set for fully tryptic restriction with a maximum of three missed cleavages and variable modification for methionine oxidation along with lysine acylation ranging from C12 to C18, including monosaturated and hydroxylated variants. The mass error threshold was set to ±2 ppm, and all assigned peptides used for quantification were verified manually. The acylation status of lysine residues was determined by comparison of the relative intensity ratio between acylated peptide ions and their unmodified counterparts. Only lysine residues modified at specific positions (CyaA: 860,983; HlyA: 564,690; RtxA: 558,689) according to the sequence of the full-length proteins were investigated. All assigned peptide sequences, including posttranslational modifications, along with corresponding FASTA formats used within the search algorithm are listed in the supporting MS Data. ZSI

Planar lipid bilayers

Measurements on planar lipid bilayers (black lipid membranes) (39) were performed in Teflon cells separated by a diaphragm with a circular hole (diameter 0.5 mm) bearing the membrane. The RTX proteins were prediluted in TUC buffer (50 mM Tris-HCl (pH 8.0), 8 M urea, and 2 mM $CaCl_2$) and added into the grounded cis compartment with a positive potential. The membrane was formed by the painting method using soybean lecithin in *n*-decane–butanol (9:1, v/v). Both compartments contained 150 mM KCl, 10 mM Tris-HCl (pH 7.4), and 2 mM $CaCl_2$, and the temperature was 25 °C. The membrane current was registered by Ag/AgCl electrodes (Theta) with salt bridges (applied voltage, 50 mV), amplified by AQ:J LCA-200-100G and LCA-200-10G amplifiers (Femto, Berlin, Germany), and digitized by use of a LabQuest Mini A/D convertor (Vernier, Beaverton, OR). For lifetime determination, ~400 individual pore openings were recorded, and the dwell times were determined using QuB software (40) with a 100-Hz low-pass filter. The kernel density estimation was fitted with a double-exponential function using Gnuplot software. The relevant model was selected by the χ^2 value.

Cell-binding and cell-invasive activities on sheep erythrocytes

AC enzyme activities of the CyaA variants were measured in the presence of 1 μM calmodulin as described previously (41). One unit of AC activity corresponds to 1 μmol of cAMP formed/min at 30 °C, pH 8.0. Cell-invasive AC activity was determined in TNC buffer (50 mM Tris-HCl (pH 7.4), 150 mM NaCl, and 2 mM $CaCl_2$) as the amounts of the AC enzyme protected against inactivation by externally added trypsin upon internalization into sheep erythrocytes, as described previously (42). Erythrocyte binding of the CyaA variants was determined in TNC buffer as described previously (42). Activity of CyaC-activated CyaA was taken as 100%.

Hemoglobin release assay

Sheep erythrocytes stored in Alsever's solution (Sigma–Aldrich) were repeatedly washed with TNC buffer. Washed erythrocytes (5×10^8/ml) were then incubated with various acylated CyaA, HlyA, and RtxA variants in 1 ml of TNC buffer, and hemolytic activity was measured in time by photometric determination (A_{541}) of the hemoglobin release.

Binding of CyaA to J774A.1 cells and determination of cAMP levels

Prior to assays, RPMI was replaced with DMEM (which contains 1.9 mM Ca^{2+}) without fetal calf serum, and the cells were allowed to rest in DMEM for 1 h at 37 °C in a humidified 5% CO_2 atmosphere (43). J774A.1 cells (1×10^6) were incubated in DMEM with 1 μg/ml of the CyaA variants for 30 min at 4 °C, prior to removal of unbound toxin by three washes in DMEM. After the transfer to the fresh tube, the cells were lysed with 0.1% Triton X-100 for determination of cell-bound AC enzyme

activity. For intracellular cAMP assays, 1.5×10^5 cells were incubated at 37 °C with the CyaA variants for 30 min in DMEM, the reaction was stopped by the addition of 0.2% Tween 20 in 100 mM HCl, samples were boiled for 15 min at 100 °C and neutralized by the addition of 150 mM unbuffered imidazole, and cAMP was measured by a competitive immunoassay (42). Activity of CyaC-activated CyaA was taken as 100%.

Cell viability

Cell viability following exposure to the toxin was determined as the capacity of mitochondrial reductases to convert the tetrazolium salt WST-1 to formazan, using the WST-1 assay kit (Roche Applied Science) according to the protocol of the manufacturer.

AQ:K

Data availability

The MS data have been deposited to the ProteomeXchange Consortium via the PRIDE partner repository with the data set identifier PXD018859 (44).

Acknowledgments—Sona Kozubova and Hana Lukeova are acknowledged for excellent technical help. We acknowledge CMS-Biocev Structural MS supported by MEYS CR (LM2018127).

AQ:B *Author contributions*—A. O., J. M., and R. O. conceptualization; A. O., H. K., J. M., D. J., A. S., and R. F. validation; A. O., H. K., J. M., D. J., J. H., O. S., and R. O. investigation; A. O., J. M., D. J., A. S., R. F., J. H., O. S., and R. O. methodology; H. K., J. M., and R. O. visualization; D. J. data curation; A. S., R. F., and R. O. supervision; P. S. and R. O. funding acquisition; P. S. writing-review and editing; R. O. writing-original draft; R. O. project administration.

AQ:A *Funding and additional information*—This work was supported by Grant Agency of the Czech Republic Grants 18-18079S (to R. O.), 19-12695S (to R. O.), and 19-27630X (to P.S.) and by Project LM2018133 (to R. O.) from the Ministry of Education, Youth, and Sports of the Czech Republic.

Conflict of interest—The authors declare that they have no conflicts of interest with the contents of this article.

Abbreviations—The abbreviations used are: RTX, repeats in toxin; ACP, acyl carrier protein; Ni-NTA, nickel-nitrilotriacetic acid; FT-ICR, Fourier transform ion cyclotron resonance; pS, picosiemens; FA formic acid; DMEM, Dulbecco's modified Eagle's medium; WST-1, 4-[3-(4-iodophenyl)-2-(4-nitrophenyl)-2H-5-tetrazolio]-1,3-benzene disulfonate; KDE, kernel density estimation.

References

1. Linhartová, I., Bumba, L., Mašín, J., Basler, M., Osička, R., Kamanová, J., Procházková, K., Adkins, I., Hejnová-Holubová, J., Sadílková, L., Morová, J., and Sebo, P. (2010) RTX proteins: a highly diverse family secreted by a common mechanism. *FEMS Microbiol. Rev.* **34,** 1076–1112 CrossRef Medline
2. Barry, E. M., Weiss, A. A., Ehrmann, I. E., Gray, M. C., Hewlett, E. L., and Goodwin, M. S. (1991) *Bordetella pertussis* adenylate cyclase toxin and hemolytic activities require a second gene, cyaC, for activation. *J. Bacteriol.* **173,** 720–726 CrossRef Medline
3. Goebel, W., and Hedgpeth, J. (1982) Cloning and functional characterization of the plasmid-encoded hemolysin determinant of *Escherichia coli*. *J. Bacteriol.* **151,** 1290–1298 CrossRef Medline
4. Mackman, N., Nicaud, J. M., Gray, L., and Holland, I. B. (1985) Genetical and functional organisation of the *Escherichia coli* haemolysin determinant 2001. *Mol. Gen. Genet.* **201,** 282–288 CrossRef Medline
5. Osickova, A., Balashova, N., Masin, J., Sulc, M., Roderova, J., Wald, T., Brown, A. C., Koufos, E., Chang, E. H., Giannakakis, A., Lally, E. T., and Osicka, R. (2018) Cytotoxic activity of *Kingella kingae* RtxA toxin depends on post-translational acylation of lysine residues and cholesterol binding. *Emerg. Microbes Infect.* **7,** 178 CrossRef Medline
6. Sebo, P., Glaser, P., Sakamoto, H., and Ullmann, A. (1991) High-level synthesis of active adenylate cyclase toxin of *Bordetella pertussis* in a reconstructed *Escherichia coli* system. *Gene* **104,** 19–24 CrossRef Medline
7. Issartel, J. P., Koronakis, V., and Hughes, C. (1991) Activation of *Escherichia coli* prohaemolysin to the mature toxin by acyl carrier protein-dependent fatty acylation. *Nature* **351,** 759–761 CrossRef Medline
8. Stanley, P., Packman, L. C., Koronakis, V., and Hughes, C. (1994) Fatty acylation of two internal lysine residues required for the toxic activity of *Escherichia coli* hemolysin. *Science* **266,** 1992–1996 CrossRef Medline
9. Lim, K. B., Walker, C. R., Guo, L., Pellett, S., Shabanowitz, J., Hunt, D. F., Hewlett, E. L., Ludwig, A., Goebel, W., Welch, R. A., and Hackett, M. (2000) *Escherichia coli* α-hemolysin (HlyA) is heterogeneously acylated *in vivo* with 14-, 15-, and 17-carbon fatty acids. *J. Biol. Chem.* **275,** 36698–36702 CrossRef Medline
10. Hackett, M., Guo, L., Shabanowitz, J., Hunt, D. F., and Hewlett, E. L. (1994) Internal lysine palmitoylation in adenylate cyclase toxin from *Bordetella pertussis*. *Science* **266,** 433–435 CrossRef Medline
11. Havlícek, V., Higgins, L., Chen, W., Halada, P., Sebo, P., Sakamoto, H., and Hackett, M. (2001) Mass spectrometric analysis of recombinant adenylate cyclase toxin from *Bordetella pertussis* strain 18323/pHSP9. *J Mass Spectrom* **36,** 384–391 CrossRef Medline
12. Bouchez, V., Douche, T., Dazas, M., Delaplane, S., Matondo, M., Chamot-Rooke, J., and Guiso, N. (2017) Characterization of post-translational modifications and cytotoxic properties of the adenylate-cyclase hemolysin produced by various *Bordetella pertussis* and *Bordetella parapertussis* isolates. *Toxins (Basel)* **9,** 304 CrossRef Medline
13. Basar, T., Havlícek, V., Bezouskova, S., Hackett, M., and Sebo, P. (2001) Acylation of lysine 983 is sufficient for toxin activity of *Bordetella pertussis* adenylate cyclase. Substitutions of alanine 140 modulate acylation site selectivity of the toxin acyltransferase CyaC. *J. Biol. Chem.* **276,** 348–354 CrossRef Medline
14. Basar, T., Havlícek, V., Bezousková, S., Halada, P., Hackett, M., and Sebo, P. (1999) The conserved lysine 860 in the additional fatty-acylation site of *Bordetella pertussis* adenylate cyclase is crucial for toxin function independently of its acylation status. *J. Biol. Chem.* **274,** 10777–10783 CrossRef Medline
15. Hackett, M., Walker, C. B., Guo, L., Gray, M. C., Van Cuyk, S., Ullmann, A., Shabanowitz, J., Hunt, D. F., Hewlett, E. L., and Sebo, P. (1995) Hemolytic, but not cell-invasive activity, of adenylate cyclase toxin is selectively affected by differential fatty-acylation in *Escherichia coli*. *J. Biol. Chem.* **270,** 20250–20253 CrossRef Medline
16. Masin, J., Roderova, J., Osickova, A., Novak, P., Bumba, L., Fiser, R., Sebo, P., and Osicka, R. (2017) The conserved tyrosine residue 940 plays a key structural role in membrane interaction of *Bordetella* adenylate cyclase toxin. *Sci. Rep.* **7,** 9330 CrossRef Medline
17. Masin, J., Basler, M., Knapp, O., El-Azami-El-Idrissi, M., Maier, E., Konopasek, I., Benz, R., Leclerc, C., and Sebo, P. (2005) Acylation of lysine 860 allows tight binding and cytotoxicity of *Bordetella* adenylate cyclase on CD11b-expressing cells. *Biochemistry* **44,** 12759–12766 CrossRef Medline
18. Balashova, N. V., Shah, C., Patel, J. K., Megalla, S., and Kachlany, S. C. (2009) *Aggregatibacter actinomycetemcomitans* LtxC is required for leukotoxin activity and initial interaction between toxin and host cells. *Gene* **443,** 42–47 CrossRef Medline
19. Karst, J. C., Ntsogo Enguéné, V. Y., Cannella, S. E., Subrini, O., Hessel, A., Debard, S., Ladant, D., and Chenal, A. (2014) Calcium, acylation, and

molecular confinement favor folding of *Bordetella pertussis* adenylate cyclase CyaA toxin into a monomeric and cytotoxic form. *J. Biol. Chem.* **289,** 30702–30716 CrossRef Medline

20. O'Brien, D. P., Cannella, S. E., Voegele, A., Raoux-Barbot, D., Davi, M., Douché, T., Matondo, M., Brier, S., Ladant, D., and Chenal, A. (2019) Post-translational acylation controls the folding and functions of the CyaA RTX toxin. *FASEB J.* **33,** 10065–10076 CrossRef Medline
21. El-Azami-El-Idrissi, M., Bauche, C., Loucka, J., Osicka, R., Sebo, P., Ladant, D., and Leclerc, C. (2003) Interaction of *Bordetella pertussis* adenylate cyclase with CD11b/CD18: role of toxin acylation and identification of the main integrin interaction domain. *J. Biol. Chem.* **278,** 38514–38521 CrossRef Medline
22. Herlax, V., and Bakás, L. (2003) Acyl chains are responsible for the irreversibility in the *Escherichia coli* α-hemolysin binding to membranes. *Chem. Phys. Lipids* **122,** 185–190 CrossRef Medline
23. Herlax, V., Maté, S., Rimoldi, O., and Bakás, L. (2009) Relevance of fatty acid covalently bound to *Escherichia coli* α-hemolysin and membrane microdomains in the oligomerization process. *J. Biol. Chem.* **284,** 25199–25210 CrossRef Medline
24. Greene, N. P., Crow, A., Hughes, C., and Koronakis, V. (2015) Structure of a bacterial toxin-activating acyltransferase. *Proc. Natl. Acad. Sci. U.S.A.* **112,** E3058–E3066 CrossRef Medline
25. Gygi, D., Nicolet, J., Frey, J., Cross, M., Koronakis, V., and Hughes, C. (1990) Isolation of the *Actinobacillus pleuropneumoniae* haemolysin gene and the activation and secretion of the prohaemolysin by the HlyC, HlyB and HlyD proteins of *Escherichia coli*. *Mol. Microbiol.* **4,** 123–128 CrossRef Medline
26. Forestier, C., and Welch, R. A. (1990) Nonreciprocal complementation of the *hlyC* and *lktC* genes of the *Escherichia coli* hemolysin and *Pasteurella haemolytica* leukotoxin determinants. *Infect. Immun.* **58,** 828–832 CrossRef Medline
27. Westrop, G., Hormozi, K., da Costa, N., Parton, R., and Coote, J. (1997) Structure-function studies of the adenylate cyclase toxin of *Bordetella pertussis* and the leukotoxin of *Pasteurella haemolytica* by heterologous C protein activation and construction of hybrid proteins. *J. Bacteriol.* **179,** 871–879 CrossRef Medline
28. Osicka, R., Osicková, A., Basar, T., Guermonprez, P., Rojas, M., Leclerc, C., and Sebo, P. (2000) Delivery of $CD8^+$ T-cell epitopes into major histocompatibility complex class I antigen presentation pathway by *Bordetella pertussis* adenylate cyclase: delineation of cell invasive structures and permissive insertion sites. *Infect. Immun.* **68,** 247–256 CrossRef Medline
29. Guermonprez, P., Khelef, N., Blouin, E., Rieu, P., Ricciardi-Castagnoli, P., Guiso, N., Ladant, D., and Leclerc, C. (2001) The adenylate cyclase toxin of *Bordetella pertussis* binds to target cells via the $\alpha_M\beta_2$ integrin (CD11b/CD18). *J. Exp. Med.* **193,** 1035–1044 CrossRef Medline
30. Osicka, R., Osickova, A., Hasan, S., Bumba, L., Cerny, J., and Sebo, P. (2015) *Bordetella* adenylate cyclase toxin is a unique ligand of the integrin complement receptor 3. *eLife* **4,** e10766 CrossRef Medline
31. Stanley, P., Koronakis, V., Hardie, K., and Hughes, C. (1996) Independent interaction of the acyltransferase HlyC with two maturation domains of the *Escherichia coli* toxin HlyA. *Mol. Microbiol.* **20,** 813–822 CrossRef Medline
32. Grant, R. P., and Hoofnagle, A. N. (2014) From lost in translation to paradise found: enabling protein biomarker method transfer by mass spectrometry. *Clin. Chem.* **60,** 941–944 CrossRef Medline
33. Ludwig, A., Garcia, F., Bauer, S., Jarchau, T., Benz, R., Hoppe, J., and Goebel, W. (1996) Analysis of the *in vivo* activation of hemolysin (HlyA) from *Escherichia coli*. *J. Bacteriol.* **178,** 5422–5430 CrossRef Medline
34. Benz, R., Maier, E., Ladant, D., Ullmann, A., and Sebo, P. (1994) Adenylate cyclase toxin (CyaA) of *Bordetella pertussis*: evidence for the formation of small ion-permeable channels and comparison with HlyA of *Escherichia coli*. *J. Biol. Chem.* **269,** 27231–27239 Medline
35. Laviña, M., Pugsley, A. P., and Moreno, F. (1986) Identification, mapping, cloning and characterization of a gene (*sbmA*) required for microcin B17 action on *Escherichia coli* K12. *J. Gen. Microbiol.* **132,** 1685–1693 CrossRef Medline
36. Sambrook, J., Fritsch, E. F., and Maniatis, T. (1989) *Molecular Cloning: A Laboratory Manual*, 2nd Ed., Cold Spring Harbor Laboratory, Cold Spring Harbor, NY AQ:L
37. Morova, J., Osicka, R., Masin, J., and Sebo, P. (2008) RTX cytotoxins recognize β2 integrin receptors through *N*-linked oligosaccharides. *Proc. Natl. Acad. Sci. U.S.A.* **105,** 5355–5360 CrossRef Medline
38. Khan, F., He, M., and Taussig, M. J. (2006) Double-hexahistidine tag with high-affinity binding for protein immobilization, purification, and detection on Ni-nitrilotriacetic acid surfaces. *Anal. Chem.* **78,** 3072–3079 CrossRef Medline
39. Benz, R., Janko, K., Boos, W., and Läuger, P. (1978) Formation of large, ion-permeable membrane channels by the matrix protein (porin) of *Escherichia coli*. *Biochim. Biophys. Acta* **511,** 305–319 CrossRef Medline
40. Nicolai, C., and Sachs, F. (2013) Solving ion channel kinetics with the QuB software. *Biophys. Rev. Lett.* **08,** 191–211 CrossRef
41. Ladant, D. (1988) Interaction of *Bordetella pertussis* adenylate cyclase with calmodulin. Identification of two separated calmodulin-binding domains. *J. Biol. Chem.* **263,** 2612–2618 Medline
42. Masin, J., Osickova, A., Sukova, A., Fiser, R., Halada, P., Bumba, L., Linhartova, I., Osicka, R., and Sebo, P. (2016) Negatively charged residues of the segment linking the enzyme and cytolysin moieties restrict the membrane-permeabilizing capacity of adenylate cyclase toxin. *Sci. Rep.* **6,** 29137 CrossRef Medline
43. Basler, M., Masin, J., Osicka, R., and Sebo, P. (2006) Pore-forming and enzymatic activities of *Bordetella pertussis* adenylate cyclase toxin synergize in promoting lysis of monocytes. *Infect. Immun.* **74,** 2207–2214 CrossRef Medline
44. Perez-Riverol, Y., Csordas, A., Bai, J., Bernal-Llinares, M., Hewapathirana, S., Kundu, D. J., Inuganti, A., Griss, J., Mayer, G., Eisenacher, M., Perez, E., Uszkoreit, J., Pfeuffer, J., Sachsenberg, T., Yilmaz, S., *et al.* (2019) The PRIDE database and related tools and resources in 2019: improving support for quantification data. *Nucleic Acids Res.* **47,** D442–D450 CrossRef Medline

APPENDIX IV

Retargeting from the CR3 to the LFA-1 receptor uncovers the adenylyl cyclase enzyme-translocating segment of *Bordetella* adenylate cyclase toxin

Masin J, Osickova A, **Jurnecka D**, Klimova N, Khaliq H, Sebo P, Osicka R.

J Biol Chem. 2020 May 11: jbc.RA120.013630. doi: 10.1074/jbc.RA120.013630.

J_ID: JBC Date: 12-June-20 4/Color Figure(s): F1,5-7 ART: RA120.013630 Page: 1 Total Pages: 19

JBC ARTICLE

Retargeting from the CR3 to the LFA-1 receptor uncovers the adenylyl cyclase enzyme–translocating segment of *Bordetella* adenylate cyclase toxin

Received for publication, March 27, 2020, and in revised form, May 7, 2020 Published, Papers in Press, May 11, 2020, DOI 10.1074/jbc.RA120.013630

AQ:au Jiri Masin[1,‡,*], Adriana Osickova[1,2,‡], David Jurnecka[1,2], Nela Klimova[1,2], Humaira Khaliq[1], Peter Sebo[1], and Radim Osicka[1,*]

AQ:aff *From the [1]Institute of Microbiology of the Czech Academy of Sciences, Prague, Czech Republic and the [2]Faculty of Science, Charles University in Prague, Prague, Czech Republic*

Edited by Chris Whitfield

The *Bordetella* adenylate cyclase toxin-hemolysin (CyaA) and the α-hemolysin (HlyA) of *Escherichia coli* belong to the family of cytolytic pore-forming Repeats in ToXin (RTX) cytotoxins. HlyA preferentially binds the $\alpha_L\beta_2$ integrin LFA-1 (CD11a/CD18) of leukocytes and can promiscuously bind and also permeabilize many other cells. CyaA bears an N-terminal adenylyl cyclase (AC) domain linked to a pore-forming RTX cytolysin (Hly) moiety, binds the complement receptor 3 (CR3, $\alpha_M\beta_2$, CD11b/CD18, or Mac-1) of myeloid phagocytes, penetrates their plasma membrane, and delivers the AC enzyme into the cytosol. We constructed a set of CyaA/HlyA chimeras and show that the CyaC-acylated segment and the CR3-binding RTX domain of CyaA can be functionally replaced by the HlyC-acylated segment and the much shorter RTX domain of HlyA. Instead of binding CR3, a $CyaA_{1\text{-}710}/HlyA_{411\text{-}1024}$ chimera bound the LFA-1 receptor and effectively delivered AC into Jurkat T cells. At high chimera concentrations (25 nM), the interaction with LFA-1 was not required for $CyaA_{1\text{-}710}/HlyA_{411\text{-}1024}$ binding to CHO cells. However, interaction with the LFA-1 receptor strongly enhanced the specific capacity of the bound $CyaA_{1\text{-}710}/HlyA_{411\text{-}1024}$ chimera to penetrate cells and deliver the AC enzyme into their cytosol. Hence, interaction of the acylated segment and/or the RTX domain of HlyA with LFA-1 promoted a productive membrane interaction of the chimera. These results help delimit residues 400–710 of CyaA as an "AC translocon" sufficient for translocation of the AC polypeptide across the plasma membrane of target cells.

AQ:A

The pore-forming Repeats in ToXin (RTX) cytotoxins are secreted by a broad range of pathogenic Gram-negative bacteria (1). The RTX adenylate cyclase toxin-hemolysin (CyaA, ACT, or Hly-AC) is secreted by *Bordetellae* pathogenic to mammals and acts as a "swift saboteur" of host immune cell functions (2–4). CyaA is a 1706-residue–long polypeptide (Fig. 1) that inserts directly into the plasma membrane of target cells, and without the need for endocytosis, it delivers directly into the cell cytosol an N-terminal adenylyl cyclase (AC) enzyme domain of ~400 residues (5). Within eukaryotic cells, the AC enzyme is activated by binding of cytosolic calmodulin and rapidly catalyzes unregulated conversion of intracellular ATP to the key second messenger signaling molecule cAMP (6). This near-instantaneously annihilates the bactericidal capacities of host phagocytes (2). Due to an extremely high catalytic power of the activated AC enzyme, the CyaA toxin was found to detectably bind and promiscuously elevate cytosolic cAMP concentrations in a broad array of eukaryotic cells, most likely due to a low affinity binding to glycan moieties of gangliosides and *N*-linked glycans of surface glycoproteins (7–9). However, the specific efficacy of cell binding, penetration, and cAMP intoxication of target cells by the CyaA toxin is enhanced by about 2 orders of magnitude through an interaction of CyaA with the CD11b subunit of the $\alpha_M\beta_2$ integrin receptor (CD11b/CD18), known as the complement receptor 3 (CR3), or Mac-1 of myeloid phagocytes (10). CyaA specifically binds the CD11b subunit of CR3 and does not recognize the other two highly homologous integrin heterodimers of the β_2 integrin family, namely CD11a/CD18 (LFA-1 or $\alpha_L\beta_2$) and CD11c/CD18 (CR4, $\alpha_x\beta_2$ or p150,95), which share the CD18 subunit with CD11b/CD18 (10–12). The RTX hemolysin (Hly) moiety of CyaA (~1300 carboxyl-proximal residues) is functionally independent and is itself capable to penetrate cell membranes to form small oligomeric cation-selective membrane pores in the absence of the AC domain (13–15). Hly insertion permeabilizes cell membranes for potassium efflux (16, 17) and can provoke colloid-osmotic (oncotic) lysis of cells (18–21).

The key biological role of the Hly moiety of CyaA would consist in the delivery of the AC domain into cytosol of target cells. The Hly moiety harbors all structural information involved in the translocation of the "passive passenger" AC domain polypeptide across the lipid bilayer of the cell membrane. Indeed, the Hly can deliver instead of the AC domain also large heterologous or artificial polypeptides, providing that these bear a net overall positive charge and do not adopt a stably folded tertiary structure (22–25). Furthermore, the pore-forming and the AC translocating activities associated with the Hly polypeptide appear to be functionally fully independent and occur in parallel, being most likely associated with alternative conformers of the same Hly moiety. In fact, the oligomeric pores formed by Hly appear as too small (0.6–0.8 nm in diameter) for passage of even an unfolded polypeptide chain (13). Moreover, specific nonhemolytic CyaA mutant variants, unable to form membrane

F1

ZSI This article contains supporting information.

‡These authors contributed equally to this work.

*For correspondence: Jiri Masin, masin@biomed.cas.cz; Radim Osicka, osicka@biomed.cas.cz.

Identification of the adenylate cyclase translocon

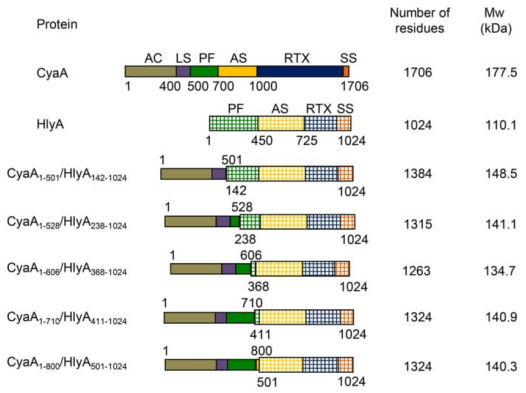

Figure 1. Schematic representation of CyaA, HlyA, and hybrid CyaA/HlyA molecules. Individual domains of CyaA and HlyA are indicated by the *colored rectangles*. *AC*, adenylate cyclase domain; *LS*, AC-to-Hly linker segment; *PF*, pore-forming domain; *AS*, acylated segment; *RTX*, calcium-binding repeats; *SS*, secretion signal. The *numbers* that follow the CyaA or HlyA in the names of the CyaA/HlyA hybrid chimera represent the number of the first and last residue of the segment of the given protein according to the sequences of full-length CyaA and HlyA, respectively. Design of the hybrid molecules: (i) in $CyaA_{1\text{-}501}/HlyA_{142\text{-}1024}$, the AC domain and the adjacent AC-to-Hly linker segment of CyaA (residues 1-501 of CyaA) are fused to a sequence beginning with the first putative transmembrane α-helix of HlyA (residues 142-1024 of HlyA); (ii) in $CyaA_{1\text{-}528}/HlyA_{238\text{-}1024}$, the AC domain, the adjacent AC-to-Hly linker segment, and the first α-helix of CyaA (residues 1-528 of CyaA) are fused to a sequence beginning with the second putative α-helix of HlyA (residues 238-1024 of HlyA); (iii) in $CyaA_{1\text{-}606}/HlyA_{368\text{-}1024}$, the AC domain, the adjacent AC-to-Hly linker segment, and the first three α-helices of CyaA (residues 1-606 of CyaA) are fused to a sequence beginning with the fourth putative α-helix of HlyA (residues 368-1024 of HlyA); (iv) in $CyaA_{1\text{-}710}/HlyA_{411\text{-}1024}$, the AC domain, the adjacent AC-to-Hly linker segment and the hydrophobic domain of CyaA (1-710 of CyaA) are fused to a sequence beginning with the acylated segment of HlyA (residues 411-1024 of HlyA); (v) in $CyaA_{1\text{-}800}/HlyA_{501\text{-}1024}$, the AC domain, the adjacent AC-to-Hly linker segment, the hydrophobic domain, and part of the acylated segment of CyaA (residues 1- 800 of CyaA) are fused to a sequence beginning with the truncated acylated segment of HlyA (residues 501-1024 of HlyA).

pores and permeabilize cellular membrane, do still efficiently deliver the AC polypeptide across the target membrane into the cytosol of cells (26). Hence, it appears that for AC polypeptide translocation across the lipid bilayer of the cell membrane it is the membrane-penetrating capacity of the hydrophobic (pore-forming) domain of the Hly moiety that is required and not its capacity to form membrane pores.

The Hly portion involved in AC domain translocation consists of several subdomains of CyaA (Fig. 1). Its most N-terminal portion forms an "AC-to-Hly linking segment" (residues ~400 to 500) that participates in membrane penetration of the toxin (27–29). This segment precedes a hydrophobic pore-forming domain (residues 500 to 700) that consists of five predicted hydrophobic and amphipathic transmembrane α-helices (30–36). This is further followed by an acylated segment (residues 700 and 1000), where the protoxin is activated through covalent acylation of the ϵ-amino groups of internal lysine residues Lys-860 and Lys-983 by the dedicated CyaC acyltransferase (32, 37–39). Adjacent is the typical calcium-binding nonapeptide repeat domain (RTX) that harbors ~40 calcium-binding sites and upon Ca^{2+} loading folds into five β-roll blocks (40–42).

In the absence of structural data, the transmembrane topology and organization of the CyaA translocon that delivers the AC polypeptide across the cell membrane remains elusive. Translocation of the AC enzyme across the cell membrane is a rapid process with a half-time of dozen of seconds (43). It occurs from cholesterol-enriched membrane lipid microdomains (lipid rafts), into which the membrane inserted CyaA laterally separates together with its receptor CD11b/CD18, once the membrane-inserted toxin has opened a transient conduit for influx of extracellular calcium ions into cells (44, 45). Mutational studies have identified a set of residues within the hydrophobic domain of Hly that appear to play a functional or structural role in the AC translocation process (20, 27–30, 32, 33, 36, 46). Recently, it was claimed that CyaA harbors an intrinsic phospholipase A activity (PLA) that would be involved in AC domain translocation (47). However, the association of PLA activity with CyaA has been disproved by two independent studies (48–50).

Among the other best-characterized pore-forming RTX toxins is the α-hemolysin (HlyA), secreted by uropathogenic and some commensal fecal isolates of *Escherichia coli* (51–53). The N-terminal hydrophobic domain of HlyA is predicted to contain amphipathic α-helices and it is assumed that this region mediates irreversible anchoring of HlyA to the plasma membrane (54, 55). The post-translational activation of HlyA involves the covalent acylation of internal Lys-564 and Lys-690 residues by the acyltransferase HlyC (56–58). The RTX domain of HlyA (residues ~724 to 852) comprises 11 to 17 calcium-binding repeats and is much shorter than the RTX domain of CyaA. HlyA was proposed to bind two different protein receptors, the glycophorin on the membrane of erythrocytes (59) and the $\alpha_L\beta_2$ integrin LFA-1 expressed on leukocytes (60, 61). However, none of these two receptors is expressed on some other cells that are effectively permeabilized by HlyA, such as the epithelial cells, indicating that HlyA, like some other RTX toxins, is to some extent competent for a promiscuous and protein receptor-independent association with cell membrane (62).

Given the unique AC enzyme domain of CyaA, it remained unclear if its C-terminal Hly moiety has evolved to specifically participate in the translocation of the N-terminal AC domain into target cells, or whether a quite different RTX cytolysin would also support the delivery of the AC enzyme domain into cells. Therefore, we constructed a set of CyaA/HlyA hybrid molecules acylated by either CyaC or HlyC acyltransferases and show that upon swapping the acylated and RTX domains of CyaA for that of HlyA, the AC toxin can be retargeted from its CR3 receptor to bind LFA-1. The AC-delivering capacity of the acylated $CyaA_{1\text{-}710}/Hly_{411\text{-}1024}$ chimera then defines the "AC translocon" as confined within the residues 400 to 710 of CyaA.

Results

Selection of different fatty acyl chains and acylation sites by the CyaC and HlyC acyltransferases differentially determines the activity of the CyaA/HlyA chimeras

To test the capacity of HlyA to support delivery of the AC domain of CyaA into cells, we have generated a set of CyaA/HlyA molecular hybrids (Fig. 1). Each of the five CyaA/HlyA chimeras was produced in *E. coli* cells in the presence of either the CyaA-

J_ID: JBC Date: 12-June-20 4/Color Figure(s): F1,5-7 ART: RA120.013630 Page: 3 Total Pages: 19

Table 1
Acylation status of the CyaA, HlyA and hybrid proteins

Protein[a]	CyaC$^+$			HlyC$^+$		
	Modification	Lys-860[b]	Lys-983[b]	Modification	Lys-860[b]	Lys-983[b]
CyaA	Nonmodified	31	1	Nonmodified	99	20
	C16:0	32	45	C14:0	0	70
	C16:1	34	43	C14:0-OH	1	7
	C18:1	3	8			
	Modification	Lys-564[b]	Lys-690[b]	Modification	Lys-564[b]	Lys-690[b]
HlyA	Nonmodified	93	0	Nonmodified	10	0
	C16:0	1	23	C14:0	13	58
	C16:1	6	67	C14:0-OH	71	35
	C18:1	0	10			
$CyaA_{1-501}/HlyA_{142-1024}$	Nonmodified	97	0	Nonmodified	2	0
	C16:0	1	44	C14:0	57	84
	C16:1	2	33	C14:0-OH	35	9
	C18:1	0	23			
$CyaA_{1-528}/HlyA_{238-1024}$	Nonmodified	98	0	Nonmodified	2	0
	C16:0	1	39	C14:0	67	83
	C16:1	1	32	C14:0-OH	26	9
	C18:1	0	27			
$CyaA_{1-606}/HlyA_{368-1024}$	Nonmodified	96	0	Nonmodified	1	0
	C16:0	1	40	C14:0	64	84
	C16:1	2	35	C14:0-OH	30	8
	C18:1	1	25			
$CyaA_{1-710}/HlyA_{411-1024}$	Nonmodified	99	0	Nonmodified	0	0
	C16:0	0	40	C14:0	72	85
	C16:1	1	32	C14:0-OH	23	8
	C18:1	0	28			
$CyaA_{1-800}/HlyA_{501-1024}$	Nonmodified	99	0	Nonmodified	0	0
	C16:0	0	39	C14:0	67	82
	C16:1	1	42	C14:0-OH	27	8
	C18:1	0	17			

[a]Proteins were produced in the *E. coli* strain BL21/pMM100 and purified close to homogeneity.
[b]Percentage distribution of fatty acid modification of the ε-amino groups of the Lys-860, Lys-983, Lys-564, and Lys-690 residues. Average values are derived from determinations performed with two different toxin preparations (one with CyaC-modified $CyaA_{1-710}/HlyA_{411-1024}$). The numbering of the acylated lysine residues is according to the sequence of the full-length CyaA or HlyA proteins. The remaining lysine residues to 100% are acylated by C12:0, C12:0-OH, C14:0, C14:1; C16:0, C16:1, and/or C16:1-OH.

activating CyaC acyltransferase, or the HlyA-activating HlyC enzyme. The 10 acylated toxin hybrids were then purified by affinity chromatography on calmodulin-Sepharose, taking advantage of the affinity of the N-terminal AC domain of CyaA for calmodulin (Fig. S1). ZSI

Because activation by posttranslational fatty acylation is crucial for activities of RTX toxins on cells (1), we first characterized the acylation state of the individual hybrid toxins by analyzing their tryptic digests by liquid chromatography coupled to ultra high-resolution Fourier transform ion cyclotron resonance MS (LC FT-ICR MS). As shown in Table 1, the CyaC acyltransferase modified only the Lys-690 residue within the HlyA segment of the CyaA/HlyA hybrids. The Lys-564 residue of HlyA was not recognized and remained largely unacylated by CyaC. In contrast, the cognate HlyC acyltransferase modified both the Lys-564 and Lys-690 lysine residues of HlyA in all tested CyaA/HlyA chimeras that contained the entire acylated segment of HlyA (Fig. 1 and Table 1). T1

Intriguingly, as documented in Table 1, the HlyC acyltransferase selected from the *E. coli* acyl-ACP pool near-exclusively the 14-carbon myristoyl (C14:0) and hydroxymyristoyl (C14:0-OH) chains for acylation of the Lys-564 and Lys-690 residues of HlyA. In contrast, the CyaC acyltransferase selected predominantly the 16-carbon palmitoyl (C16:0) and palmitoleyl (C16:1) acyl chains, with some octadecenoyl (C18:1) acyls also being used for modification of the Lys-690 residue of HlyA (Table 1). Hence, the choice of the acyltransferase determined the site at which the CyaA/HlyA hybrids were acylated and also the nature (length) of the acyl chains (14-carbon *versus* 16/18-carbon) attached to the modified lysine residues.

To characterize how this selection of the acylated site and length of the used acyl chain impacted on the activities of the hybrid toxins, we first determined the capacity of the CyaA/HlyA hybrids to bind and permeabilize sheep erythrocytes. The red blood cells were used as a convenient model of target cells that express neither the CR3 receptor of CyaA, nor the LFA-1 receptor of HlyA. Further advantage was taken of the highly active N-terminal AC enzyme domain contained in the hybrid proteins, which allowed to quantify the specific capacity of the CyaA/Hly hybrids to tightly associate with the erythrocyte membrane (binding) and enabled to follow the delivery of the AC domain into the cytosol of erythrocytes (invasive AC). In parallel, we measured the specific capacity of the CyaA/HlyA hybrids to permeabilize erythrocytes by hemolytic pores and release hemoglobin through provoking oncotic erythrocyte lysis over time. As shown in Fig. 2*A*, the CyaC-activated hybrid molecules (monoacylated by predominantly the 16-carbon acyls on Lys-690 of HlyA) bound erythrocytes with an efficacy ranging from ~50 to ~75% of intact doubly acylated CyaA (100%). The HlyC-activated CyaA/HlyA hybrids, doubly acylated by 14-carbon acyls on the Lys-564 and Lys-690 residues of the HlyA moiety, bound erythrocytes more efficiently than their CyaC-monoacylated counterparts. This was particularly apparent when a portion of the pore-forming domain of HlyA was preserved in AQ:C F2

ID: yadavr Time: 19:01 I Path: //mbnas01.cadmus.com/home$/yadavr$/SB-JBCJ200040

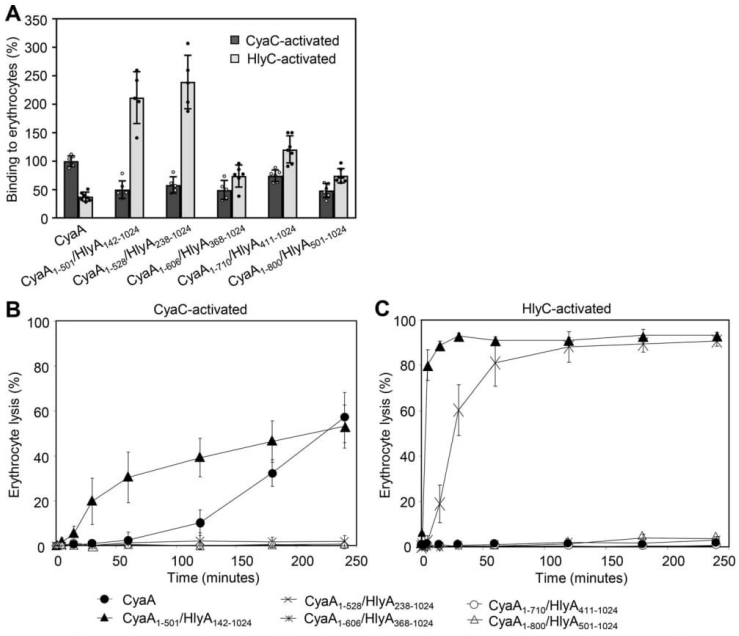

Figure 2. 16-Carbon mono- and 14-carbon doubly-acylated (CyaC- and HlyC-activated) hybrid molecules bind and lyse erythrocytes with importantly differing efficacies. *A*, sheep erythrocytes (5×10^8/ml) were incubated in the presence of 75 mM sucrose as osmoprotectant with 5 nM purified proteins at 37 °C and after 30 min, aliquots were taken for determinations of the cell-associated AC activity (*Binding*). Activities are expressed as percentages of the activity of the intact 16-carbon doubly-acylated, CyaC-activated CyaA and represent average mean ± S.D. from at least three independent determinations performed in duplicate with two different toxin preparations. Sheep erythrocytes (5×10^8/ml) were incubated at 37 °C in the presence of CyaC-activated (*B*) or HlyC-activated (*C*) proteins (25 nM). Hemolytic activity was measured as the amount of released hemoglobin by photometric determination (A541) ($n = 3$).

the CyaA/HlyA hybrid, such as in the $CyaA_{1\text{-}501}/HlyA_{142\text{-}1024}$ and $CyaA_{1\text{-}528}/HlyA_{238\text{-}1024}$ constructs, which bound to cells in several times higher amounts than the intact CyaC-activated CyaA (Fig. 2*A*). However, compared with intact CyaA, which under the conditions used provoked lysis of ~50% red blood cells in 4 h, the hybrids containing the pore-forming domain of CyaA, such as the $CyaA_{1\text{-}606}/HlyA_{368\text{-}1024}$, $CyaA_{1\text{-}710}/HlyA_{411\text{-}1024}$, and $CyaA_{1\text{-}800}/HlyA_{501\text{-}1024}$ constructs, did not exhibit any hemolytic activity. This was true irrespective of whether these proteins were monoacylated by CyaC (Fig. 2*B*), or doubly acylated by HlyC (Fig. 2*C*). Only the $CyaA_{1\text{-}501}/HlyA_{142\text{-}1024}$ chimera, with a large portion of the pore-forming domain of HlyA preserved, exhibited a rapidly manifesting HlyA-like hemolytic activity even when monoacylated by CyaC (Fig. 2*B*). Hence, the 16-carbon–monoacylated HlyA moiety was also able to form pores in erythrocyte membrane. Furthermore, its hemolytic activity, as well as the hemolytic activity of the $CyaA_{1\text{-}528}/HlyA_{238\text{-}1024}$ hybrid, was much higher when these hybrids were acylated by the HlyC-attached 14-carbon acyls on the Lys-564 and Lys-690 residues of the HlyA moiety (Fig. 2*C*). These results show that replacement of up to 238 N-terminal residues of HlyA by the first 528 residues of CyaA (comprising the AC domain, the AC-to-Hly linking segment, and the first amphipathic α-helix of the pore-forming domain of CyaA) still preserved the hemolysin function of the HlyC-activated HlyA moiety. In contrast, the other HlyC- or CyaC-acylated CyaA/HlyA hybrids were unable to properly insert into erythrocyte membrane and form hemolytic pores.

The AC-to-Hly linking segment and the intact hydrophobic domain of CyaA are necessary and sufficient for AC domain translocation into cells by a mechanism that does not provoke permeabilization of the membrane by CyaA pores

Importantly, as shown in Fig. 3*A*, whereas single acylation by CyaC was insufficient, the double modification of the Lys-564 and Lys-690 residues of the HlyA moiety with the 14-carbon acyls conferred on the nonhemolytic $CyaA_{1\text{-}710}/HlyA_{411\text{-}1024}$ and $CyaA_{1\text{-}800}/HlyA_{501\text{-}1024}$ hybrids the capacity to translocate the AC domain into erythrocytes. These two chimeras bound erythrocytes comparably well as the CyaC-acylated CyaA (Fig. 2*A*). Their specific capacity to penetrate the erythrocyte membrane and translocate the N-terminal AC enzyme domain into erythrocyte cytosol corresponded to ~35 to ~40% of the specific capacity of CyaA (Fig. 3*A*). The doubly acylated $CyaA_{1\text{-}710}/HlyA_{411\text{-}1024}$ and $CyaA_{1\text{-}800}/HlyA_{501\text{-}1024}$ hybrid proteins not only inserted the AC enzyme across the erythrocyte membrane, but the AC also became protected from degradation by externally added trypsin. The translocated AC enzyme was truly delivered into erythrocyte cytosol containing ATP and calmodulin and it catalyzed an increase of cellular cAMP concentrations to roughly ~40% of the levels produced by the CyaC-activated

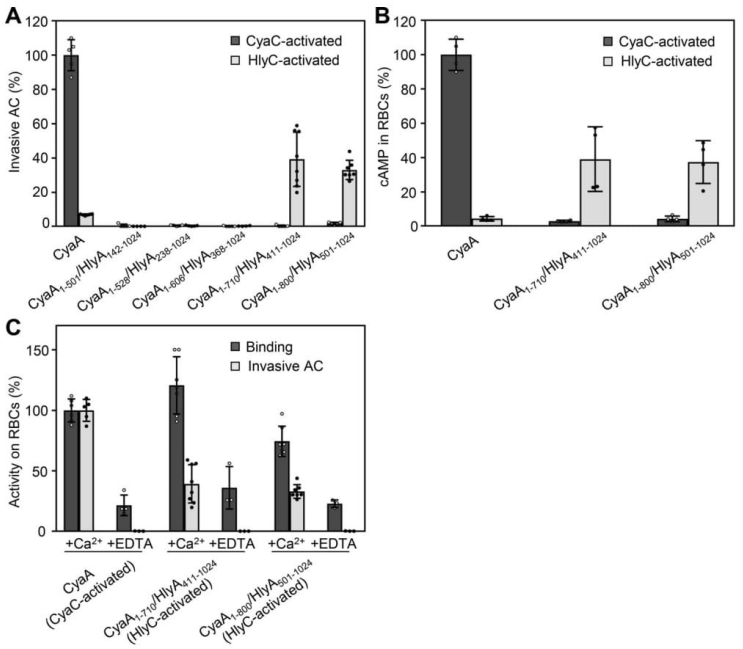

Figure 3. Nonhemolytic HlyC-activated chimeras CyaA$_{1\text{-}710}$/HlyA$_{411\text{-}1024}$, and CyaA$_{1\text{-}800}$/HlyA$_{501\text{-}1024}$ translocate the AC domain across the plasma membrane of sheep erythrocytes in a calcium-dependent manner. *A,* sheep erythrocytes (5×10^8/ml) were incubated in the presence of 75 mM sucrose as osmoprotectant with 5 nM purified proteins at 37 °C and after 30 min, aliquots were taken for determinations of the AC activity internalized into erythrocytes and protected against digestion by externally added trypsin (*Invasive AC*). Activities are expressed as the activity of the intact, 16-carbon doubly-acylated, CyaC-activated CyaA and represent average mean ± S.D. from at least three independent determinations performed in duplicate with two different toxin preparations. *B,* cAMP intoxication was assessed by determining the intracellular concentration of cAMP generated in sheep erythrocytes (5×10^8/ml) after 30 min of incubation of cells with 25 nM CyaA or the hybrid proteins. Activities are expressed as percentages of intact CyaC-activated CyaA activity and represent average mean ± S.D. from four independent determinations performed in duplicate. *C,* sheep erythrocytes (5×10^8/ml) were incubated in the presence of 2 mM calcium (+Ca^{2+}) or in absence of calcium and presence of 5 mM EDTA (+*EDTA*) at 37 °C with 5 nM proteins. After 30 min, aliquots were taken for determinations of the cell-associated AC activity (*Binding*) and AC activity internalized into erythrocytes and protected against digestion by externally added trypsin (*Invasive AC*). Activities are expressed as percentages of intact CyaC-activated CyaA activity ($n = 3$-7).

CyaA (Fig. 3*B*). Moreover, as for the intact CyaA, the erythrocyte binding and cell-invasive activity of the CyaA$_{1\text{-}710}$/HlyA$_{411\text{-}1024}$ and CyaA$_{1\text{-}800}$/HlyA$_{501\text{-}1024}$ chimeras depended fully on the presence of free (2 mM) calcium ions (Fig. 3*C*).

Since the AC-translocating CyaA$_{1\text{-}710}$/HlyA$_{411\text{-}1024}$ hybrid was not hemolytic on erythrocytes, we examined whether the hybrid proteins exhibited a capacity to permeabilize naked planar asolectin lipid bilayers with applied negative voltage. Whereas 250 pM CyaA elicited a steep increase of conductance across the planar lipid bilayer over time, the same amounts of the CyaC- or HlyC-activated CyaA$_{1\text{-}710}$/HlyA$_{411\text{-}1024}$ hybrid proteins produced negligible, if any, conductance across the black lipid membrane (Fig. 4*A*). Nevertheless, with a much reduced propensity, the hybrid protein occasionally still formed single pore conductance units that exhibited similar characteristics as the pores formed at much higher frequency by the intact CyaC-activated CyaA (Fig. 4*B* and Fig. S2). Hence, the HlyC-acylated CyaA$_{1\text{-}710}$/HlyA$_{411\text{-}1024}$ hybrid was capable to efficiently translocate the AC enzyme across the erythrocyte membrane despite a close to nil hemolytic and membrane-permeabilizing (pore-forming) capacity. This result corroborates our earlier observation that translocation of the AC enzyme polypeptide across the lipid bilayer of cell membrane does not involve the formation of oligomeric membrane-permeabilizing CyaA pores and that the translocating AC polypeptide is presumably delivered by membrane-inserted monomers of CyaA through a sealed proteolipidic translocon (26).

These results further demonstrate that the AC-to-Hly linking segment and the intact hydrophobic (pore-forming) domain, comprised between residues 400 and 710 of CyaA, are necessary and sufficient for accomplishing the calcium-dependent AC domain translocation across the cell membrane. The C-terminal portion of CyaA, containing the acylated segment and the RTX domain, does not appear to be involved in the process of AC translocation, as it could be functionally replaced with the acylated segment and the much shorter RTX domain of *E. coli* HlyA that did not evolve to deliver the AC enzyme.

Swapping of the acylated segment and the RTX domain of HlyA into CyaA retargets the adenylyl cyclase toxin from its CR3 receptor to LFA-1–expressing cells

CyaA specifically binds phagocytic cells through their $\alpha_M\beta_2$ integrin CR3 (Fig. S3*A*) and thanks to this the toxin swiftly

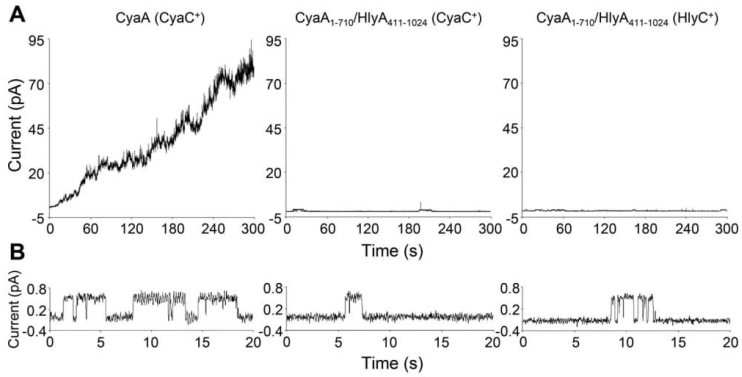

Figure 4. The cell-invasive $CyaA_{1-710}/HlyA_{411-1024}$ hybrid molecules exhibit a very low membrane-permeabilizing activity. *A*, overall membrane activities of intact CyaC-acylated CyaA and CyaC- or HlyC-activated $CyaA_{1-710}/HlyA_{411-1024}$ hybrid molecules on asolectin/decane:butanol (9:1) membranes. Conditions of measurement were: 150 mM KCl, 10 mM Tris-HCl (pH 7.4), 2 mM $CaCl_2$; the applied voltage was 50 mV; temperature was 25 °C, and the recording was filtered at 10 Hz; the protein concentration was 250 pM. *B*, single-pore recordings of asolectin membranes in the presence of 10 pM purified protein variants under otherwise identical conditions as in *A*.

exerts a complex array of cytotoxic and immunosubversive activities on host myeloid phagocytic cells (10, 11, 63–68). The segment of CyaA involved in the interaction of the toxin with CR3 was previously mapped within residues 1166 and 1287 of the RTX domain and is located at the interface of the RTX blocks II and III (11, 69–71). In the $CyaA_{1-710}/HlyA_{411-1024}$ hybrid the CR3-binding RTX domain of CyaA was replaced by the much shorter RTX domain of HlyA. It was demonstrated that HlyA preferentially targets another β_2 integrin, LFA-1 (60), but the integrin-interacting segment of HlyA is currently unknown. Therefore, we examined if the domain swap retargeted the hybrid protein from CR3 to $\alpha_L\beta_2$ LFA-1. As shown in F5 Fig. 5*A*, indeed, the HlyC-activated $CyaA_{1-710}/HlyA_{411-1024}$ hybrid bound approximately 10 times less to the CR3-expressing murine J774A.1 cells than the intact CyaC-activated CyaA. The residual binding of the hybrid to J774A.1 cells did not involve an interaction with CR3, as it was not inhibited by the mAb M1/70 that competes with CyaA for binding to the same segment of the CD11b subunit of CR3 (11). Accordingly, at the low concentrations needed for assays with CyaA (0.1–0.6 nM), the HlyC-activated $CyaA_{1-710}/HlyA_{411-1024}$ hybrid did not elevate any detectably the cAMP concentrations in the cytosol of J774A.1 cells, showing that the residual CR3-independent binding interaction to J774A.1 cells was rather unproductive (Fig. 5*B*).

We therefore assessed the cell-penetration capacity of the HlyC-acylated $CyaA_{1-710}/HlyA_{411-1024}$ hybrid using Jurkat lymphoblastoma T-cells that do not express CR3 but produce ZSI modest amounts of LFA-1 (Fig. S3*B*) (72). Higher toxin concentrations had thus to be used (5 or 50 nM) and at equal molar concentrations of the toxins, the LFA-1-expressing Jurkat cells bound about two times lower amounts of the CyaA toxin than of the $CyaA_{1-710}/HlyA_{411-1024}$ hybrid toxin (Fig. 5*C*). Furthermore, compared with intact CyaA, the hybrid produced comparable cAMP levels in Jurkat cells over a range of toxin concentrations (Fig. 5*D*). This goes well with the results of the assays on erythrocytes, where the efficacy of translocation of the HlyC-acylated cell-bound $CyaA_{1-710}/HlyA_{411-1024}$ hybrid toxin ranged between ~35 and 40% of that of cell-bound intact CyaA (*cf.* Fig. 3, *A* and *B*).

To corroborate that the swapping of the acylated segment and the RTX domain with those of HlyA retargeted AC toxin from CR3 to LFA-1, we further used transfected CHO cells that expressed high levels of the LFA-1 receptor (Fig. S3*B*). Compared to mock-transfected cells, the transfected CHO cells expressing LFA-1 on the cell surface bound much higher amounts of the HlyC-acylated $CyaA_{1-710}/HlyA_{411-1024}$ hybrid, when this was used at concentrations below or equal to 5 nM (Fig. 5*E*). At a high concentration of 25 nM the hybrid protein bound at similar levels to both mock-transfected and LFA-1–producing CHO cells (Fig. 5*E*). However, the specific interaction with LFA-1 still enabled an importantly more efficient penetration of the bound hybrid toxin across the cell membrane (Fig. 5*F*). Despite comparable amounts of the protein bound to cells, the hybrid toxin produced about 10-fold higher cAMP levels in the LFA-1-expressing cells than it produced in the mock CHO cells (Fig. 5*F*). Hence, the specific interaction with LFA-1 presumably imposed on the bound hybrid toxin an oriented and more productive topology that enhanced its capacity to penetrate cell membrane and translocate the AC domain into cytosol of LFA-1-expressing cells.

Moreover, interaction with the β_2 integrin rescued the AC translocation defect observed on erythrocytes (*cf.* Fig. 3, *A* and *B*) for the monoacylated CyaC-activated $CyaA_{1-710}/HlyA_{411-1024}$ hybrid protein (acylated only on the Lys-690 residue by 16-carbon acyls). The monoacylated protein intoxicated the LFA-1–expressing cells to the same levels as the doubly acylated HlyC-activated hybrid (*c.f.* Fig. 5*D* and Fig. S4). Hence, the ZSI interaction with LFA-1 enabled a productive interaction of the $CyaA_{1-710}/HlyA_{411-1024}$ hybrid toxin with the plasma membrane of the target cells and thereby promoted the translocation of its AC domain across the membrane even in the absence of the second acylation of the Lys-564 residue in the HlyA moiety.

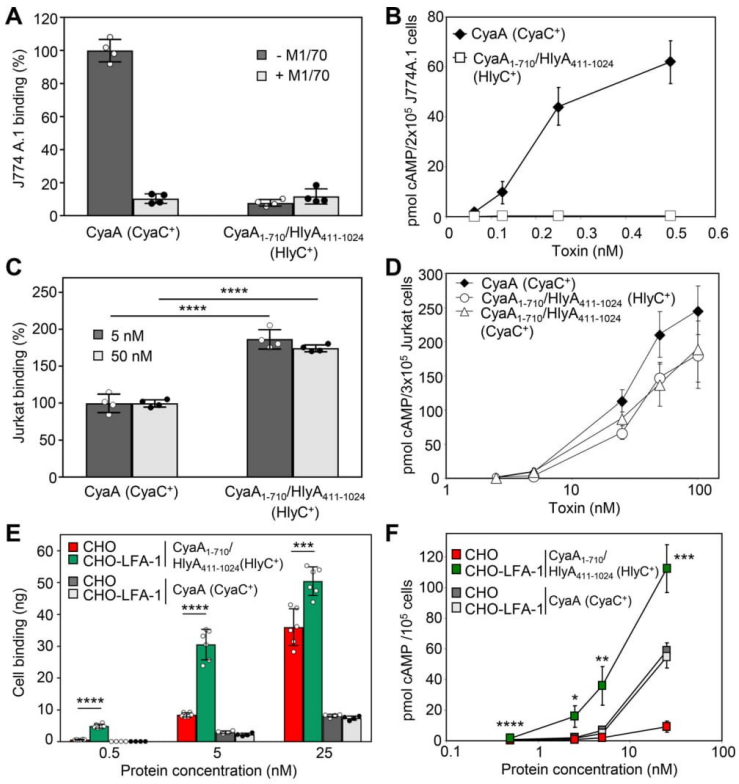

Figure 5. The CyaA$_{1\text{-}710}$/HlyA$_{411\text{-}1024}$ hybrid preferentially binds LFA-1–positive cells and monoacylation by CyaC is sufficient for AC translocating activity. *A,* binding of the intact CyaC-activated CyaA or HlyC-activated CyaA$_{1\text{-}710}$/HlyA$_{411\text{-}1024}$ hybrid variant to J774A.1 mouse macrophages (1×10^6) was determined as the amount of total cell-associated AC enzyme activity upon incubation of cells with 5 nM protein for 30 min at 4 °C. To block the binding site of CyaA on the CR3 receptor, the J774A.1 cells (1×10^6) were preincubated for 30 min on ice with 5 μg/ml of the CD11b-specific mAb M1/70 prior to addition of 5 nM CyaA (*CyaC*$^+$) or CyaA$_{1\text{-}710}$/HlyA$_{411\text{-}1024}$ (*HlyC*$^+$). Activities are expressed as percentages of intact CyaA activity in the absence of M1/70 mAb and represent average mean ± S.D. from two independent determinations performed in duplicate with two different toxin preparations. *B,* cAMP intoxication was assessed by determining the intracellular concentration of cAMP after 30 min of incubation of J774A.1 cells (2×10^5) with toxins ($n = 3$). *C,* binding of CyaA or CyaA$_{1\text{-}710}$/HlyA$_{411\text{-}1024}$ (*HlyC*$^+$) to Jurkat T-cells (1×10^6) was determined as the amount of total cell-associated AC enzyme activity upon incubation of cells with 5 and 50 nM toxin for 30 min at 4 °C. Activities are expressed as percentages of intact CyaA activity and represent average mean ± S.D. from two independent determinations performed in duplicate with two different toxin preparations. *D,* cAMP intoxication was assessed by determining the intracellular concentration of cAMP generated in Jurkat T-cells (3×10^5) after 30 min of incubation at different toxin concentrations ($n = 5$). *E,* binding of CyaA$_{1\text{-}710}$/HlyA$_{411\text{-}1024}$ (*HlyC*$^+$) or intact CyaA to CHO cells expressing CD11a/CD18 or mock-transfected CHO cells (1×10^6) was determined as the amount of total cell-associated AC enzyme activity upon incubation of cells with indicated toxin concentrations for 30 min at 4 °C. Activities represent average mean ± S.D. from three independent determinations performed in duplicate with two different toxin preparations. *F,* cAMP intoxication was assessed by determining the intracellular concentration of cAMP generated in CHO cells expressing CD11a/CD18 or mock-transfected CHO cells after 30 min of incubation of cells (1×10^5) with different concentrations of CyaA$_{1\text{-}710}$/HlyA$_{411\text{-}1024}$ (*HlyC*$^+$) or intact CyaA ($n = 4$). *, statistically significant differences ($p < 0.05$); **, statistically significant differences ($p < 0.01$); ***, statistically significant differences ($p < 0.001$); ****, statistically significant differences ($p < 0.0001$).

Swapping of the acylated segment and the RTX domain retargets the CyaA/HlyA hybrid onto a spectrum of mouse spleen cells

To analyze which cell types could be targeted by the CyaA$_{1\text{-}710}$/HlyA$_{411\text{-}1024}$ hybrid molecule following the acylated segment and the RTX domain swap, we tested *in vitro* the binding of the fluorescently labeled (Dy495) and genetically detoxified (AC$^-$) HlyC-acylated toxoid (CyaA-AC$^-_{1\text{-}710}$/HlyA$_{411\text{-}1024}$–Dy495) to mouse splenocytes comprising a broad mixture of cells of various types. A fluorescently labeled (Dy650) and CyaC-acylated CyaA toxoid (CyaA-AC$^-$–Dy650) was used as a control. At first, the CyaA-AC$^-_{1\text{-}710}$/HlyA$_{411\text{-}1024}$–Dy495 and CyaA-AC$^-$–Dy650 proteins were incubated with spleen cells separately at concentrations ranging up to 140 nM (Fig. 6*A* and Fig. S5). Although the CyaA-AC$^-$–Dy650 toxoid used at the highest concentration stained ~5% of all cells, at the same concentration the chimera stained almost 35% of splenocytes in the sample (Fig. 6*A* and Fig. S5). Because the SSC and FSC characteristics suggested binding of both proteins to different cell types (Fig. S5), a multicolor antibody panel was introduced to identify the target cell populations (Fig. S6*A*). Incubation of an equimolar mixture of the two proteins (56

F6 ZSI ZSI ZSI ZSI

Identification of the adenylate cyclase translocon

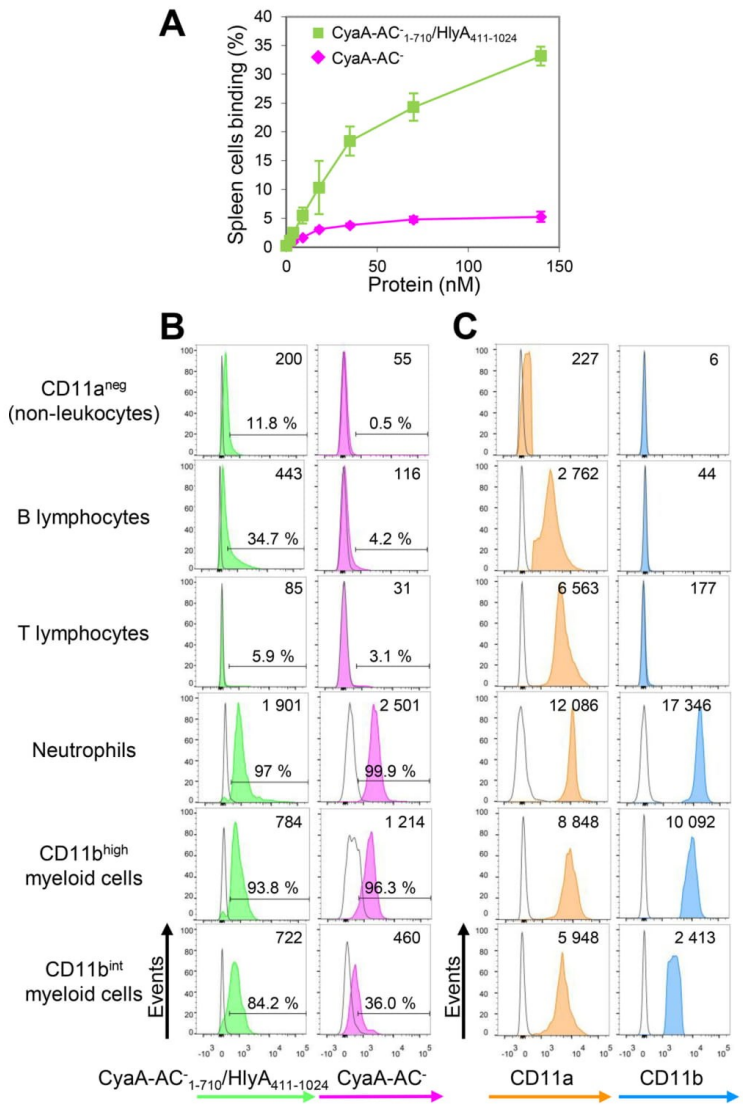

Figure 6. Binding of fluorescently labeled CyaA-AC^{-}$_{1-710}$/HlyA$_{411-1024}$ and CyaA-AC^{-} to spleen cells *in vitro*. *A*, spleen single cell suspensions (1×10^6) from 7-week–old Balb/c mice were incubated *in vitro* with a range of equimolar concentrations of separately added Dy495-labeled CyaA-AC^{-}$_{1-710}$/HlyA$_{411-1024}$ or Dy650-labeled CyaA-AC^{-} and were analyzed by flow cytometry (for gating strategy see Fig. S5). *B*, spleen single cell suspensions (1×10^6) from 7-week-old Balb/c mice were incubated with an equimolar mixture of 56 nM fluorescently-labeled or nonfluorescent CyaA-AC^{-}$_{1-710}$/HlyA$_{411-1024}$ and CyaA-AC^{-} for 30 min at 4 °C. Cells were then stained with a mixture of fluorescently-labeled antibodies against cell-surface antigens. Binding of CyaA-AC^{-}$_{1-710}$/HlyA$_{411-1024}$–Dy495 or CyaA-AC^{-}–Dy650 to nonleukocytic cells (CD11a^{-}), B lymphocytes (CD19^{+}), T lymphocytes (CD3^{+}), neutrophils (Ly-6G^{+}CD11b^{+}), CD11b^{high} myeloid cells (Lineage^{neg} CD11b^{high}) and CD11b^{int} myeloid cells (Lineage^{neg} CD11b^{int}) was determined by flow cytometry and depicted as histograms of Dy650 or Dy495 signal in each population. *Gray* histograms represent nonfluorescent CyaA-AC^{-}$_{1-710}$/HlyA$_{411-1024}$ or CyaA-AC^{-} controls. Dy650- or Dy495-positive cells in each population are shown in percentages. Values in *top right corners* indicate the mean fluorescence intensity (MFI) for each histogram with subtracted MFI of non-fluorescent controls. *C*, spleen single cell suspensions from 7-week-old Balb/c mice were stained with a mixture of fluorescently labeled antibodies against cell-surface antigens. Expression of CD11a and CD11b on corresponding cell populations was determined by flow cytometry. *Gray* histograms represent corresponding isotype control. Values in *top right corners* indicate mean fluorescent intensity for each histogram with subtracted mean fluorescent intensity of isotype controls. A result from one representative experiment is shown in each panel. *In vitro* experiment was repeated two times independently with similar results.

ZSI

J_ID: JBC Date: 12-June-20 4/Color Figure(s): F1,5-7 ART: RA120.013630 Page: 9 Total Pages: 19

nM) with cells yielded a positive detection of the CyaA-AC$^-$–Dy650 stain on 5.3% of all cells. 25.6% of the cells were stained by CyaA-AC$^-_{1\text{-}710}$/HlyA$_{411\text{-}1024}$–Dy495 when the corresponding nonfluorescent proteins were used to set the positive gates for fluorescent proteins (Fig. S6*B*). As shown in Fig. 6*B*, compared with binding of CyaA-AC$^-$–Dy650, the CyaA-AC$^-_{1\text{-}710}$/HlyA$_{411\text{-}1024}$–Dy495 toxoid exhibited importantly higher binding to nonleukocytic cells devoid of LFA-1 and CR3 (*cf.* Fig. 6*C*). Similarly, CyaA-AC$^-_{1\text{-}710}$/HlyA$_{411\text{-}1024}$–Dy495 bound better to B and T lymphocytes (Fig. 6*B*) expressing LFA-1, but lacking CR3 (Fig. 6*C*). Both proteins then bound with high affinity to neutrophils and myeloid cells (dendritic cells, monocytes, and macrophages) that express high levels of both LFA-1 and CR3 in parallel (Fig. 6, *B* and *C*). Adding the CyaA-AC$^-_{1\text{-}710}$/HlyA$_{411\text{-}1024}$–Dy495 and CyaA-AC$^-$–Dy650 proteins together or separately to spleen cells did not significantly influence their binding patterns, except for the higher binding of the individually added chimera to LFA-1–negative cells and to LFA-1–epressing B lymphocytes (Table S1). This ruled out a possible interaction of the two proteins. All these data confirm that CR3 is the *bona fide* receptor of CyaA, whereas the acylated segment and the RTX domain of HlyA swapped into the CyaA-AC$^-_{1\text{-}710}$/HlyA$_{411\text{-}1024}$ protein relocated a substantial portion of the hybrid molecules to bind cell populations expressing only LFA-1, or even to nonleukocytic cells devoid of both LFA-1 and CR3 integrins.

Discussion

We show here that swapping of the acylated segment and the RTX domain of HlyA into the CyaA toxin molecule retargets the AC toxin from the CR3 β_2 integrin for binding to the LFA-1 β_2 integrin. Moreover, the cell-invasive capacity of the doubly acylated CyaA$_{1\text{-}710}$/HlyA$_{411\text{-}1024}$ hybrid revealed that the CyaA translocon unit that delivers the AC enzyme polypeptide across the target cell membrane is formed by the structure consisting of the AC-to-Hly linking segment and the hydrophobic domain segment of CyaA comprised within residues 400 to 710 of the CyaA toxin molecule (Fig. 7*A*). This CyaA segment was necessary and sufficient to accomplish AC enzyme translocation across the lipid bilayer of target cell membrane. The results with the CyaA$_{1\text{-}710}$/HlyA$_{411\text{-}1024}$ hybrid also demonstrated that swapping of the acylated segment and the RTX domain retargeted the AC toxin from CR3-expressing myeloid phagocytic cells to LFA-1–expressing B and T leukocytes and broadened, at higher toxin concentrations, the target cell spectrum of the hybrid toxin also to nonleukocyte types of cells targeted by HlyA. More importantly, the presented data reveal that interaction with the β_2 integrin receptor is itself not crucial for membrane penetration of the CyaA translocon moiety and the delivery of the AC polypeptide across cellular membrane. As suggested by the results reported here, interaction with the β_2 integrin would only facilitate and accelerate the productive interaction of cell surface-associated toxin molecules with the lipid bilayer of the target cell membrane. This is most likely due to imposing an oriented topology on the receptor-bound toxin molecules, thus increasing the probability of their productive insertion into the lipid bilayer and the formation of a proper AC enzyme translocon unit for delivery of the AC polypeptide across the lipid bilayer of the membrane.

Previously, Westrop and co-workers (73) constructed hybrid molecules of leukotoxin (LktA) from *Mannheimia hemolytica* and the CyaA toxin. The first hybrid molecule, containing N-terminal residues 1 to 687 of CyaA and C-terminal residues 379 to 953 of LktA, showed no toxic activities (73). The second hybrid molecule, containing N-terminal residues 1 to 687 of CyaA, residues 379 to 616 of LktA, and C-terminal residues 919 to 1706 of CyaA, exhibited a hemolytic activity, but its capacity to deliver the AC domain to the cell cytosol was ~20 times lower than the activity of intact CyaA (73). Our CyaA$_{1\text{-}710}$/HlyA$_{411\text{-}1024}$ hybrid molecule was able to translocate the AC domain across the membrane of cells devoid of CR3 with a much higher efficacy of ~40% of the intact CyaA. This indicates that the presence of all five transmembrane α-helices, predicted between residues 502 and 698 of CyaA (33), may be required for translocation of the AC enzyme across the plasma membrane. However, because the CyaA$_{1\text{-}710}$/HlyA$_{411\text{-}1024}$ chimera translocated the AC domain with lower efficacy than intact CyaA, it is difficult to conclusively discriminate if the reduced translocation efficacy was due to structural constraints imposed on the AC translocon unit in the artificial hybrid molecule (assembled without any structural data guidance), or whether the additional CyaA segments participate indirectly and facilitate by structural input the optimal function of the CyaA translocon. Indeed, the calcium-binding RTX domain of CyaA$_{1\text{-}710}$/HlyA$_{411\text{-}1024}$ comes from HlyA and contains a significantly lower number of RTX repeats than CyaA (1). Thus, it can be hypothesized that the shorter RTX domain of HlyA may yield upon binding the hybrid molecule to the cell surface, a less appropriate positioning of the AC-to-Hly linking segment and/or of the hydrophobic domain of CyaA in respect to lipid bilayer of the membrane. This might reduce the efficacy of the subsequent formation and operation of the AC translocon.

Also, little is known about the role of the acylated segment of the RTX toxins in their mechanism of penetration into target membrane. In contrast to the activity on liposomes lacking membrane potential, the capacity of CyaA and HlyA to penetrate cellular membranes strictly depends on activation of their protoxins by covalent posttranslational fatty acylation (37, 58, 74–76). It was shown that acylation of CyaA alters and dictates the folding path and the overall conformation of the acylated segment of the toxin molecule (77, 78). By dictating the overall conformation of the protein, the acylation also determines the immunogenicity and the capacity of the CyaA antigen to induce toxin/neutralizing antibodies and confer protective immunity against *Bordetella* infection (79). Here we show that the acylation status of the toxin molecule also impacts on the translocation efficacy of its AC domain across the cell membrane in the absence of the integrin receptor. The doubly acylated HlyC-modified CyaA$_{1\text{-}710}$/HlyA$_{411\text{-}1024}$ and CyaA$_{1\text{-}800}$/HlyA$_{501\text{-}1024}$ variants, bearing C14:0 or C14:0-OH on the two Lys-564 and Lys-690 residues, translocated the AC domain into the erythrocyte cytosol with quite high efficacy of ~35 to 40% of intact CyaA. In contrast, the AC domain translocation capacity of the monoacylated CyaC-modified variants, acylated with a mixture of C16:0, C16:1, and C18:1 exclusively at the Lys-690, was very

ID: **yadavr** Time: 19:01 I Path: //mbnas01.cadmus.com/home$/yadavr$/SB-JBCJ200040

Identification of the adenylate cyclase translocon

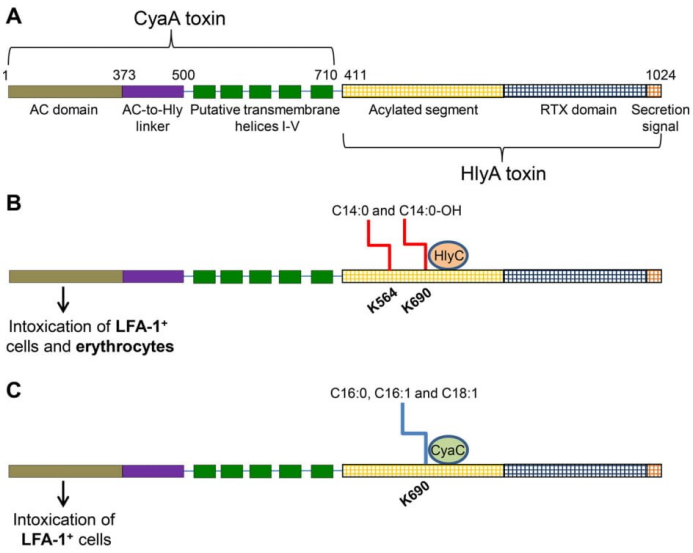

Figure 7. Schematic representation of CyaA and HlyA domains sufficient for AC translocation and LFA-1 binding. *A*, the AC domain of *Bordetella pertussis* CyaA has to be fused to the adjacent AC-to-Hly linker segment and to the five predicted transmembrane α-helices for an efficient translocation across the cell membrane, whereas the acylated segment and the RTX domain segment of CyaA can be replaced with the corresponding segments of the *E. coli* HlyA toxin. *B*, the doubly acylated HlyC-modified 14-carbon-acylated $CyaA_{1\text{-}710}/HlyA_{411\text{-}1024}$ hybrid, bearing C14:0 or C14:0-OH on the two Lys-564 and Lys-690 residues translocated the AC domain into cell cytosol of both, LFA-1–positive and LFA-1–negative cells. *C*, the monoacylated $CyaA_{1\text{-}710}/Hly_{A411\text{-}1024}$ hybrid, bearing C16:0, C16:1, and/or C18:1 on the Lys-690 residue intoxicated the LFA-1–positive cells with the same efficacy as the double acylated hybrid but was poorly active on erythrocytes lacking the β_2 integrin LFA-1. Because CyaA does not bind the LFA-1 integrin (Fig. S3), the LFA-1–binding segment of the HlyC-acylated $CyaA_{1\text{-}710}/HlyA_{411\text{-}1024}$ molecule is confined in the acylated segment and/or the RTX domain of HlyA (residues 411 to 1024).

ZSI

low when assayed on erythrocytes. Because the CyaC- and HlyC-acylated $CyaA_{1\text{-}710}/HlyA_{411\text{-}1024}$ and $CyaA_{1\text{-}800}/HlyA_{501\text{-}1024}$ variants bound erythrocytes with similar efficacy, it indicates that in the absence of interaction with the β_2 integrin receptor, which could orient the protein in respect to membrane lipid bilayer, the type and/or site of acylation of the toxin molecule directly affects its capacity to form the translocon and initiate AC domain translocation. On cells devoid of integrin receptor, the presence of two acyl chains per toxin molecule may thus be critical for the ability of the hybrid molecules to adopt a conformation that allows proper membrane insertion and subsequent AC domain translocation (Fig. 7, *B* and *C*). Indeed, interaction with the LFA-1 receptor also enabled the monoacylated CyaC-activated hybrid protein to penetrate cells and deliver its AC domain, showing that acylation of the first lysine residue (Lys-564 in HlyA and Lys-860 in CyaA) was required for toxin activity only on cells that do not express the cognate β_2 integrin receptor (*e.g.* LFA-1 or CR3, respectively) on their surface. A precedent of such a rescuing effect of a β_2 integrin receptor interaction was previously observed with the monoacylated CyaC-activated CyaA-K860R toxin variant (37, 80).

Both the CyaC-acylated and HlyC-acylated $CyaA_{1\text{-}710}/HlyA_{411\text{-}1024}$ and $CyaA_{1\text{-}800}/HlyA_{501\text{-}1024}$ variants exhibited an almost nil hemolytic capacity on erythrocytes and a very low membrane-permeabilizing activity on asolectin bilayer membranes with imposed voltage. On the other hand, the type and/or site of acylation of the $CyaA_{1\text{-}710}/HlyA_{411\text{-}1024}$ hybrid molecule did not affect characteristics of the rarely formed single pores made by these proteins. This goes well with our previous reports showing that irrespectively of the differences in acylation status, the truncated CyaA variants lacking the RTX domain, or even the nonacylated proCyaA protein can form pores that exhibit identical conductance and cation selectivity as intact CyaA and are just formed at a very much reduced frequency (13, 80). More importantly, the observations reported here show that the HlyC-acylated $CyaA_{1\text{-}710}/HlyA_{411\text{-}1024}$ and $CyaA_{1\text{-}800}/HlyA_{501\text{-}1024}$ variants can efficiently translocate the AC domain, despite being devoid of any detectable membrane-permeabilizing capacity. This corroborates our previous report that the pore-forming activity of CyaA is not involved in translocation of the AC domain across the target cell membrane (26, 32, 36). The data clearly show that AC translocation does not occur through the oligomeric CyaA pore, which is bypassed by the translocating AC enzyme polypeptide. The AC is most likely delivered across the lipid bilayer of the membrane by monomers of CyaA along the electrical gradient and through a tightly sealed proteolipid translocon formed by residues 400 to 710 of CyaA, as found here.

HlyA exhibits a limited target cell and species specificity, exhibiting a well-detectable cytotoxic activity on a broad spectrum of cell types from various species, including erythrocytes, monocytes, granulocytes, or endothelial cells from ruminants, mice, and primates (81–87). Despite the rather low cell

ID: yadavr Time: 19:01 I Path: //mbnas01.cadmus.com/home$/yadavr$/SB-JBCJ200040

specificity, HlyA binding and action on erythrocytes was shown to be dependent on the abundant glycophorin protein proposed to serve as a high-affinity receptor (59, 88). Indeed, the HlyC-activated $CyaA_{1-501}/HlyA_{1-1024}$ hybrid molecule, carrying the entire HlyA, bound sheep erythrocytes with a ~7 times higher efficacy (Fig. S7) than intact CyaA that does not bind glycophorin of erythrocytes (59, 89). The glycophorin-binding region was proposed to be located between residues 914 and 936 of HlyA (88), thus overlapping with the RTX folding center of the toxin molecule (41). This opens the possibility that mutations in this region prevented proper folding and ablated HlyA activity independently of loss of glycophorin interaction. Interestingly, sequential shortening of HlyA from its N terminus in the HlyC-acylated CyaA/HlyA hybrids, still harboring an intact putative glycophorin-binding region, resulted in a substantial reduction of their cell binding capacity, as compared with $CyaA_{1-501}/HlyA_{1-1024}$. Although the binding of the CyaA/HlyA hybrids was assessed on sheep erythrocytes, whereas identification of the glycophorin-binding region was performed on human and horse erythrocytes (59, 88), it is plausible to hypothesize that the glycophorin-dependent binding of HlyA to erythrocytes may require the structural integrity of several regions of the toxin. Another explanation may be that upon a primary interaction of residues 914 to 936 of HlyA with glycophorin, the toxin irreversibly inserts into the membrane through the N-terminal segments of the molecule. This assumption is supported by previous reports showing that HlyA is anchored to the plasma membrane through its N-terminal structures (54), which also modulate pore-forming activity (90). Moreover, the sequential deletion of the N-terminal structures of HlyA within the CyaA/HlyA hybrids, including a hydrophobic region between residues 238 and 410, also resulted in a substantial reduction of their hemolytic capacity compared with that of $CyaA_{1-501}/HlyA_{1-1024}$, most likely due to their reduced cell-association capacity.

HlyA was found to preferentially bind and target leukocytes expressing the β_2 integrin LFA-1 (60). The evidence was based on observations showing that (i) HlyA-mediated cytolysis was inhibited by mAbs recognizing the CD11a and CD18 subunits of LFA-1, (ii) immobilized HlyA bound LFA-1, and (iii) the K562 cells transfected with LFA-1 became sensitive to HlyA (60). Another study (91), however, indicated that HlyA bound to erythrocytes and granulocytes in a nonsaturable manner and competition experiments showed that the binding of HlyA to the cells was receptor-independent. Here we show that Jurkat T-cells expressing LFA-1 but not CR3 bound approximately two times more of the HlyC-acylated $CyaA_{1-710}/HlyA_{411-1024}$ than of the intact CyaA. In addition, at low protein concentrations the hybrid bound, and intoxicated by cAMP, preferentially to the CHO cells expressing LFA-1, suggesting that interaction of the acylated segment and the RTX domain of HlyA in the hybrid facilitated its productive insertion into cell membrane and fostered its capacity to deliver the AC enzyme across the cell membrane. Our results further show that compared with CyaA toxoid, the binding of CyaA-$AC^-_{1-710}/HlyA_{411-1024}$ was higher on B and T lymphocytes expressing LFA-1, but not CR3. However, due to the very high toxoid concentrations used, in the same experiment the binding of CyaA-$AC^-_{1-710}/HlyA_{411-1024}$ was also substantially higher on nonleukocytic cells lacking LFA-1 and CR3. These results further emphasize some binding "promiscuity" of HlyA and demonstrate that at low concentrations the HlyA would preferentially bind to cells expressing LFA-1, whereas at higher concentrations it exhibits promiscuous binding and low target cell specificity.

Experimental Procedures

Bacterial strains

The *E. coli* strain XL1-Blue (Stratagene, La Jolla, CA) was used throughout this work for DNA manipulations and was grown in Luria-Bertani medium at 37 °C. The *E. coli* strain BL21 (Novagen, Madison, WI) carrying the plasmid pMM100 (encoding LacI and tetracycline resistance) was used for expression of the CyaA and HlyA protein variants.

Cell lines

CHO-K1 Chinese hamster ovary cells (ATCC CCL-61) transfected with human CD11a/CD18 or mock transfected were established earlier (11). Murine monocytes/macrophages J774A.1 (ATCC, number TIB-67), human THP-1 monocytes (ATCC number TIB-202), and Jurkat human T lymphocyte cells (TIB-152) were obtained from the American Type Culture Collection (ATCC, Manassas, VA). CHO cells were grown in F12K medium (GIBCO Invitrogen) supplemented with 10% fetal calf serum (FCS) (GIBCO Invitrogen) and antibiotic antimycotic solution (ATB, 0.1 mg/ml streptomycin, 100 units/ml of penicillin, and 0.25 μg/ml of amphotericin; Sigma-Aldrich). J774A.1, THP-1, and Jurkat cells were cultured in RPMI 1640 (Sigma-Aldrich) supplemented with 10% fetal calf serum and antibiotic antimycotic solution. Prior to assays, RPMI or F12K were replaced with DMEM (1.9 mM Ca^{2+}) without FCS and the cells were allowed to rest in DMEM for 1 h at 37 °C in a humidified 5% CO_2 atmosphere.

Mice

7-Week-old female Balb/c mice were bred locally at the Institute of Microbiology of the CAS, v.v.i. All animal experiments were approved by the Animal Welfare Committee at the Institute of Microbiology of the CAS, v.v.i. in accordance with the Guidelines for the Care and Use of Laboratory Animals, the Act of the Czech National Assembly, Collection of Laws number 246/1992.

Plasmid construction

The pT7CACT1 plasmid (40), harboring the *cyaC* and *cyaA* genes under control of the isopropyl β-D-thiogalactopyranoside–inducible *lacZp* promoter, was used as a parental plasmid to generate constructs for expression of the CyaA/HlyA hybrid molecules activated by the acyltransferase CyaC or HlyC. For this purpose, the plasmid pTZHly11 (9) was used as a source of the *hlyC* and *hlyA*. First, pT7CACT1-derived plasmid expressing HlyC was constructed by replacement of the *cyaC* gene from its start to stop codon in pT7CACT1 by *hlyC*. Second, an overlapping PCR mutagenesis procedure was used to amplify DNA segments encoding required CyaA/HlyA hybrid

molecules and the PCR products were cloned instead of *cyaA* into the appropriate pT7CACT1-derived plasmid (harboring *cyaC* or *hlyC*). For production and subsequent purification of HlyC-acylated HlyA, the *cyaA* gene in the pT7CACT1-derived plasmid harboring *hlyC* was replaced from its start to stop codon by the entire *hlyA* gene, which was fused in-frame at the 3′ terminus to a sequence encoding a double hexahistidine purification tag (92). The detoxified constructs CyaA-AC$^-_{1\text{-}710}$/HlyA$_{411\text{-}1024}$ and CyaA-AC$^-$ were obtained by ablation of their catalytic activity as previously described (40).

Protein production, purification, and labeling

The intact CyaA, intact HlyA, and CyaA/HlyA hybrid molecules were produced in *E. coli* BL21/pMM100 cells transformed with the appropriate plasmids. 500-ml cultures were grown with shaking at 37 °C in MDO medium (yeast extract, 20 g/liter; glycerol, 20 g/liter; KH_2PO_4, 1 g/liter; K_2HPO_4, 3 g/liter; NH_4Cl, 2 g/liter; Na_2SO_4, 0.5 g/liter; thiamine hydrochloride, 0.01 g/liter) containing 150 μg/ml of ampicillin and 12.5 μg/ml of tetracycline. When cultures reached OD_{600} = 0.8, they were induced with 1 mM isopropyl β-D-thiogalactopyranoside and grown for an additional 4 h. For protein purification, the cells were harvested by centrifugation, washed twice with 50 mM Tris-HCl (pH 8.0), disrupted by sonication at 4 °C, and the homogenate was centrifuged at 20,000 × *g* for 30 min at 4 °C. The inclusion bodies collected in the pellet were washed with 50 mM Tris-HCl (pH 8.0) containing 4 M urea, then solubilized with 50 mM Tris-HCl (pH 8.0) containing 8 M urea, and the urea extract was cleared at 20,000 × *g* for 30 min at 4 °C.

The urea extracts containing intact CyaA or the CyaA/HlyA hybrid proteins were diluted 4 times in ice-cold TNC buffer (50 mM Tris-HCl (pH 8.0), 500 mM NaCl, and 2 mM $CaCl_2$) and loaded at 4 °C on a calmodulin-Sepharose 4B column (GE Healthcare) equilibrated with the same buffer. The column was washed with TNC buffer and the proteins were eluted at room temperature with TUE buffer (50 mM Tris-HCl (pH 8.0), 8 M urea, and 2 mM EDTA).

To prepare labeled CyaA-AC$^-_{1\text{-}710}$/HlyA$_{411\text{-}1024}$ and CyaA-AC$^-$ with low content of lipopolysaccharide for mouse experiments, the protein samples purified on calmodulin-Sepharose were diluted 4 times in ice-cold 50 mM Tris-HCl (pH 8.0) containing 1 M NaCl and loaded on phenyl-Sepharose CL-4B beads (Sigma–Aldrich). Endotoxin was removed by repeated washes of the protein-bound resin with 60% isopropyl alcohol (93). The phenyl-Sepharose column was then washed with 50 mM sodium bicarbonate (pH 8.3) containing 1 M NaCl and the beads were resuspended in the same buffer containing Dy495-NHS ester (Dyomics, Jena, Germany) for CyaA-AC$^-_{1\text{-}710}$/HlyA$_{411\text{-}1024}$ or Dy650-NHS ester for CyaA-AC$^-$ in a concentration to reach a Dyomics:protein molar ratio of ~6:1. Labeling was performed at 25 °C for 2 h and the column was subsequently washed with 50 mM Tris-HCl (pH 8.0). The labeled proteins were eluted in TU buffer (50 mM Tris-HCl (pH 8.0), 8 M urea) and concentrated on 30-kDa Ultracel membrane filters (Merck, Darmstadt, Germany). The preparations used in mouse experiments thus contained less than 0.1 EU/1 μg of the protein as determined by Limulus Amebocyte Lysate assay (QCL-1000, Lonza, Walkersville, MD).

The urea extract containing intact HlyA was loaded on a nickel-nitrilotriacetic acid-agarose column (Qiagen, Germantown, MD) equilibrated with TNU buffer (50 mM Tris-HCl (pH 8.0), 200 mM NaCl, and 8 M urea). The column was washed with TNU buffer containing 20 mM imidazole and HlyA was eluted with TNU buffer containing 600 mM imidazole. The eluted fractions of HlyA were diluted 4 times in ice-cold 50 mM Tris-HCl (pH 8.0) containing 1 M NaCl and loaded on a phenyl-Sepharose CL-4B column equilibrated with the same buffer. The column was then washed with 50 mM Tris-HCl (pH 8.0) and HlyA was eluted with TUE buffer.

Cell binding, cell invasive and hemolytic activities on sheep erythrocytes

AC enzymatic activities were measured in the presence of 1 μM calmodulin as previously described (94). One unit of AC activity corresponds to 1 μmol of cAMP formed per min at 30 °C (pH 8.0). Hemolytic activity was measured by determining the hemoglobin release in time upon toxin incubation with washed sheep erythrocytes (LabMediaServis, Jaromer, Czech Republic) (5×10^8/ml), as previously described (18). Cell invasive AC was measured by determining the AC protected against externally added trypsin upon internalization into sheep erythrocytes as previously described (27). Erythrocyte binding was measured by determining the membrane-associated AC activity as previously described (27). Activity of intact CyaA was taken as 100%.

Binding and cAMP elevation of CyaA on nucleated cells

Cells were incubated in DMEM with intact CyaA or CyaA/HlyA hybrid proteins for 30 min at 4 °C prior to removal of unbound toxin by three washes in DMEM. After transfer to a fresh tube, the cells were lysed with 0.1% Triton X-100 for determination of cell-bound AC enzyme activity. Activity of WT CyaA was taken as 100%. For intracellular cAMP assays, cells were incubated at 37 °C with CyaA or hybrid toxin for 30 min in DMEM, the reaction was stopped by addition of 0.2% Tween 20 in 100 mM HCl, samples were boiled for 15 min at 100 °C, neutralized by addition of 150 mM unbuffered imidazole, and cAMP was measured by a competitive immunoassay as previously described (24).

Detection of CD11a/CD18 on cell surface

2×10^5 Jurkat, THP-1, CHO-CD11a/CD18, and mock-transfected CHO cells were incubated for 30 min at 4 °C in 100 μl of HEPES-buffered salt solution (HBSS buffer; 10 mM HEPES, pH 7.4, 140 mM NaCl, 5 mM KCl) supplemented with 2 mM $CaCl_2$, 2 mM $MgCl_2$, 1% (w/v) glucose, and 1% (v/v) FCS (cHBSS) in 96-well culture plates (Nunc, Roskilde, Denmark) containing the anti-human CD11a-specific MEM-25 mAb (mAb) conjugated with allophycocyanin (Exbio, Vestec, Czech Republic) diluted according to the manufacturer's instructions. After washing, cells were resuspended in HBSS and analyzed by flow cytometry in the presence of 1 μg/ml of Hoechst 33258. Data were analyzed using the FlowJo software (Tree Star,

Ashland, OR) and appropriate gatings were used to exclude cell aggregates and dead cells.

Planar lipid bilayers

Measurements on planar lipid bilayers (black lipid membranes) (95) were performed in Teflon cells separated by a diaphragm with a circular hole (diameter 0.5 mm) bearing the membrane. The intact CyaA and the CyaC- or HlyC-activated $CyaA_{1\text{-}710}/HlyA_{411\text{-}1024}$ hybrid molecules were diluted in TU buffer and added into the grounded cis compartment with a positive potential. The membrane was formed by the painting method using soybean lecithin in *n*-decane–butanol (9:1, v/v). Both compartments contained 150 mM KCl, 10 mM Tris-HCl (pH 7.4), and 2 mM $CaCl_2$, the temperature was 25 °C. The membrane current was registered by Ag/AgCl electrodes (Theta) with salt bridges (applied voltage, 50 mV), amplified by LCA-200-100G amplifiers (Femto), and digitized by use of a KPCI-3108 card (Keithly). For lifetime determination, ~400 of individual pore openings were recorded and the dwell times were determined using QuB software with 10-Hz low-pass filter. The kernel density estimation was fitted with a double-exponential function using Gnuplot software. The relevant model was selected by the $\chi 2$ value. The error estimates of lifetimes were obtained by the bootstrap analysis.

LC–MS analysis

The proteins were dissolved in 50 mM ammonium bicarbonate buffer (pH 8.2) to reach 4 M concentration of urea and digested with trypsin (Promega, Madison, WI, modified sequencing grade) at a trypsin:protein ratio of 1:50 for 6 h at 30 °C. The 2nd portion of trypsin was added to a final ratio of trypsin:protein of 1:25 and the reaction was carried out for another 6 h at 30 °C. When the reaction was complete, the concentration of the resulting peptides was adjusted by 0.1% TFA (TFA) to 0.1 mg/ml and 5 μl of the sample were injected into the LC–MS system. The LC separation was performed using a desalting column (ZORBAX C18 SB-300, 0.1 × 2 mm) at a flow rate of 40 μl/min (Shimadzu, Kyoto, Japan) of 0.1% formic acid (FA) and a separation column (ZORBAX C18 SB-300, 0.2 × 150 mm) at a flow rate of 10 μl/min (Agilent 1200, Santa Clara, CA) of water/acetonitrile (MeCN) (Merck, Darmstadt, Germany) gradient: 0-1 min 0.2% FA, 5% MeCN; 5 min 0.2% FA, 10% MeCN; 35 min 0.2% FA, 50% MeCN; 40 min 0.2% FA, 95% MeCN; 40–45 min 0.2% FA, 95% MeCN. A capillary column was directly connected to a mass analyzer. The MS analysis was performed on a commercial solariX XR FTMS instrument equipped with a 15 Tesla superconducting magnet and a Dual II ESI/MALDI ion source (Bruker Daltonics, Bremen, Germany). Mass spectra of the samples were obtained in the positive ion mode within an m/z range of 150-2000. The accumulation time was set at 0.2 s, LC acquisition was 45 min with a 5-min delay, and one spectrum consisted of accumulation of four experiments. The instrument was operating in survey LC–MS mode and calibrated online using Agilent tuning mix, which results in mass accuracy below 2 ppm.

Data processing and interpretation

MS data were processed by the SNAP version 2.0 algorithm of the DataAnalysis 4.4 software package (Bruker Daltonics, Billerica, MA, USA) generating a list of monoisotopic masses from deconvoluted spectra. The parameters were set as follows: export m/z range of 150-2000, maximum charge state of 8, S/N threshold of 0.75, and absolute intensity threshold 5×10^5. The extracted experimental data were searched against the FASTA of single corresponding toxin molecule (CyaA, UniProtKB, P0DKX7; HlyA, UniProtKB, P08715, chimeric proteins: assembled from CyaA and HlyA according to the highlighted residue positions of individual molecules) using the home-built Linx software (RRID:SCR_018657). The Linx algorithm was set for fully tryptic restriction with a maximum of 3 missed cleavages and variable modification for methionine oxidation along with lysine acylation ranging from C12 to C18, including monosaturated and hydroxylated variants. The mass error threshold was set to ±2 ppm and all assigned peptides used for quantification were verified manually. The acylation status of lysine residues was determined by comparison of relative intensity ratio between acylated peptide ions and its unmodified counterparts. Only lysine residues at positions 564, 690, and 860, and 983 according to the sequence of the full-length HlyA or CyaA proteins, respectively, were investigated. All peptide sequences including post-translational modifications along with corresponding FASTA formats used within the search algorithm are listed in Supporting Information.

Tissue homogenization and single cell preparation

Mice were sacrificed by cervical dislocation and spleens were collected. Spleen single cell suspensions were obtained by homogenization in a gentleMACS™ Dissociator (Miltenyi Biotec, Bergisch Gladbach, Germany) and by enzymatic digestion with collagenase D (1 mg/ml; Roche Applied Science) in Hanks' balanced salt solution for 30 min at 37 °C. The reaction was stopped by 14 mM EDTA for 5 min, and cells were subsequently filtered through a 70-μm nylon cell strainer (Corning Costar, New York, NY). After lysing of erythrocytes by ACK lysing buffer (Life Technologies), cells were resuspended in FACS buffer (PBS, 2 mM EDTA, 2% heat-inactivated fetal bovine serum), and filtered through a 30-μm CellTrics strainer (Sysmex Partec GmbH, Görlitz, Germany).

Binding of labeled CyaA variants to spleen cells in vitro

Prior to staining, spleen cell suspensions were blocked by 10% Balb/c mouse serum and anti-mouse CD16/CD32 mAb (0.25 μg/reaction; Bioscience) in FACS buffer for 30 min at 4 °C. Aliquots of spleen cells (1×10^6) were subsequently incubated with or without $CyaA\text{-}AC^-{}_{1\text{-}710}/HlyA_{411\text{-}1024}$–Dy495 and CyaA-AC$^-$–Dy650 (or corresponding nonfluorescent proteins), added separately or in an equimolar mixture, for 30 min at 4 °C. Cells were washed once with FACS buffer and stained directly with labeled mAbs (Table S2) for 30 min in the dark at 4 °C and washed twice with FACS buffer. A Fixable Viability Dye eFluor™ 780 live/dead stain (eBioscience) was used to assess cell viability and the samples were analyzed using a BD LSRII flow cytometer. 2×10^5 events were run for each sample and

ZSI

data were analyzed using FlowJo software. Gates positive for CyaA-AC$^{-}_{1\text{-}710}$/HlyA$_{411\text{-}1024}$–Dy495 and CyaA-AC^{-}–Dy650 were set using a nonfluorescent CyaA-AC$^{-}_{1\text{-}710}$/HlyA$_{411\text{-}1024}$ and CyaA-AC^{-} as a background.

Statistical analysis

Significance of differences in values was assessed by Student's *t* test.

Data availability

The MS data have been deposited to the ProteomeXchange Consortium via the PRIDE partner repository with the data set identifier PXD018789 (96).

Acknowledgments—Sona Kozubova and Hana Lukeova are acknowledged for excellent technical help. We acknowledge CMS-Biocev Structural MS supported by MEYS CR Grant LM2018127.

Author contributions—J. M., A. O., and R. O. conceptualization; J. M. and R. O. supervision; J. M., N. K., P. S., and R. O. funding acquisition; J. M., A. O., D. J., N. K., H. K., and R. O. validation; J. M., A. O., D. J., N. K., H. K., and R. O. investigation; J. M., N. K., H. K., and R. O. visualization; J. M., A. O., D. J., N. K., and R. O. methodology; J. M., P. S., and R. O. writing-original draft; J. M. and R. O. project administration; J. M., P. S., and R. O. writing-review and editing.

Funding and additional information—This work was supported by Grants 19-04607S (to J. M.), 18-18079S (to R. O.), 19-12695S (to R. O.), and 18-20621S (to P. S.) from the Grant Agency of the Czech Republic, Project LM2018133 (to R. O.) from the Ministry of Education, Youth and Sports of the Czech Republic, and Charles University project GA UK number 507116 (to N. K.).

Conflict of interest—The authors declare no conflicts of interest in regards to this manuscript.

Abbreviations—The abbreviations used are: RTX, Repeats in ToXin; AC, adenylyl cyclase; CR3, complement receptor 3; Hly, hemolysin; PLA, phospholipase A; HlyA, α-hemolysin; CHO, Chinese hamster ovary; LktA, leukotoxin; FA, formic acid; DMEM, Dulbecco's modified Eagle's medium; FBS, fetal bovine serum.

References

1. Linhartová, I., Bumba, L., Mašín, J., Basler, M., Osička, R., Kamanova, J., Prochazkova, K., Adkins, I., Hejnová-Holubová, J., Sadilková, L., Morová, J., and Sebo, P. (2010) RTX proteins: a highly diverse family secreted by a common mechanism. *FEMS Microbiol. Rev.* **34,** 1076–1112 CrossRef Medline
2. Novak, J., Cerny, O., Osickova, A., Linhartova, I., Masin, J., Bumba, L., Sebo, P., and Osicka, R. (2017) Structure-function relationships underlying the capacity of *Bordetella* adenylate cyclase toxin to disarm host phagocytes. *Toxins* **9,** 300 CrossRef
3. Sebo, P., Osicka, R., and Masin, J. (2014) Adenylate cyclase toxin-hemolysin relevance for pertussis vaccines. *Exp. Rev. Vaccines* **13,** 1215–1227 CrossRef Medline
4. Vojtova, J., Kamanova, J., and Sebo, P. (2006) *Bordetella* adenylate cyclase toxin: a swift saboteur of host defense. *Curr. Opin. Microbiol.* **9,** 69–75 CrossRef Medline
5. Gordon, V. M., Leppla, S. H., and Hewlett, E. L. (1988) Inhibitors of receptor-mediated endocytosis block the entry of *Bacillus anthracis* adenylate cyclase toxin but not that of *Bordetella pertussis* adenylate cyclase toxin. *Infect. Immun.* **56,** 1066–1069 CrossRef Medline
6. Wolff, J., Cook, G. H., Goldhammer, A. R., and Berkowitz, S. A. (1980) Calmodulin activates prokaryotic adenylate cyclase. *Proc. Natl. Acad. Sci. U.S.A.* **77,** 3841–3844 CrossRef Medline
7. Gordon, V. M., Young, W. W., Jr., Lechler, S. M., Gray, M. C., Leppla, S. H., and Hewlett, E. L. (1989) Adenylate cyclase toxins from *Bacillus anthracis* and *Bordetella pertussis:* different processes for interaction with and entry into target cells. *J. Biol. Chem.* **264,** 14792–14796 Medline
8. Hanski, E. (1989) Invasive adenylate cyclase toxin of *Bordetella pertussis*. *Trends Biochem. Sci.* **14,** 459–463 CrossRef Medline
9. Morova, J., Osicka, R., Masin, J., and Sebo, P. (2008) RTX cytotoxins recognize β2 integrin receptors through *N*-linked oligosaccharides. *Proc. Natl. Acad. Sci. U.S.A.* **105,** 5355–5360 CrossRef Medline
10. Guermonprez, P., Khelef, N., Blouin, E., Rieu, P., Ricciardi-Castagnoli, P., Guiso, N., Ladant, D., and Leclerc, C. (2001) The adenylate cyclase toxin of *Bordetella pertussis* binds to target cells via the α(M)β(2) integrin (CD11b/CD18). *J. Exp. Med.* **193,** 1035–1044 CrossRef Medline
11. Osicka, R., Osickova, A., Hasan, S., Bumba, L., Cerny, J., and Sebo, P. (2015) *Bordetella* adenylate cyclase toxin is a unique ligand of the integrin complement receptor 3. *Elife* **4,** e10766 CrossRef Medline
12. Hasan, S., Osickova, A., Bumba, L., Novák, P., Sebo, P., and Osicka, R. (2015) Interaction of *Bordetella* adenylate cyclase toxin with complement receptor 3 involves multivalent glycan binding. *FEBS Lett.* **589,** 374–379 CrossRef Medline
13. Benz, R., Maier, E., Ladant, D., Ullmann, A., and Sebo, P. (1994) Adenylate cyclase toxin (CyaA) of *Bordetella pertussis*. Evidence for the formation of small ion-permeable channels and comparison with HlyA of *Escherichia coli*. *J. Biol. Chem.* **269,** 27231–27239 Medline
14. Sakamoto, H., Bellalou, J., Sebo, P., and Ladant, D. (1992) *Bordetella pertussis* adenylate cyclase toxin. Structural and functional independence of the catalytic and hemolytic activities. *J. Biol. Chem.* **267,** 13598–13602 Medline
15. Szabo, G., Gray, M. C., and Hewlett, E. L. (1994) Adenylate cyclase toxin from *Bordetella pertussis* produces ion conductance across artificial lipid bilayers in a calcium- and polarity-dependent manner. *J. Biol. Chem.* **269,** 22496–22499 Medline
16. Gray, M., Szabo, G., Otero, A. S., Gray, L., and Hewlett, E. (1998) Distinct mechanisms for K+ efflux, intoxication, and hemolysis by *Bordetella pertussis* AC toxin. *J. Biol. Chem.* **273,** 18260–18267 CrossRef Medline
17. Wald, T., Osickova, A., Masin, J., Liskova, P. M., Petry-Podgorska, I., Matousek, T., Sebo, P., and Osicka, R. (2016) Transmembrane segments of complement receptor 3 do not participate in cytotoxic activities but determine receptor structure required for action of *Bordetella* adenylate cyclase toxin. *Pathog. Dis.* **74,** ftw008 CrossRef
18. Bellalou, J., Sakamoto, H., Ladant, D., Geoffroy, C., and Ullmann, A. (1990) Deletions affecting hemolytic and toxin activities of *Bordetella pertussis* adenylate cyclase. *Infect. Immun.* **58,** 3242–3247 CrossRef Medline
19. Ehrmann, I. E., Gray, M. C., Gordon, V. M., Gray, L. S., and Hewlett, E. L. (1991) Hemolytic activity of adenylate cyclase toxin from *Bordetella pertussis*. *FEBS Lett.* **278,** 79–83 CrossRef Medline
20. Basler, M., Masin, J., Osicka, R., and Sebo, P. (2006) Pore-forming and enzymatic activities of *Bordetella pertussis* adenylate cyclase toxin synergize in promoting lysis of monocytes. *Infect. Immun.* **74,** 2207–2214 CrossRef Medline
21. Masin, J., Fiser, R., Linhartova, I., Osicka, R., Bumba, L., Hewlett, E. L., Benz, R., and Sebo, P. (2013) Differences in purinergic amplification of osmotic cell lysis by the pore-forming RTX toxins *Bordetella pertussis* CyaA and *Actinobacillus pleuropneumoniae* ApxIA: the role of pore size. *Infect. Immun.* **81,** 4571–4582 CrossRef Medline
22. Gmira, S., Karimova, G., and Ladant, D. (2001) Characterization of recombinant *Bordetella pertussis* adenylate cyclase toxins carrying passenger proteins. *Res. Microbiol.* **152,** 889–900 CrossRef Medline
23. Holubova, J., Kamanova, J., Jelinek, J., Tomala, J., Masin, J., Kosova, M., Stanek, O., Bumba, L., Michalek, J., Kovar, M., and Sebo, P. (2012) Delivery of large heterologous polypeptides across the cytoplasmic membrane of

J_ID: JBC Date: 12-June-20 4/Color Figure(s): F1,5-7 ART: RA120.013630 Page: 15 Total Pages: 19

antigen-presenting cells by the *Bordetella* RTX hemolysin moiety lacking the adenylyl cyclase domain. *Infect. Immun.* **80,** 1181–1192 CrossRef Medline

24. Karimova, G., Pidoux, J., Ullmann, A., and Ladant, D. (1998) A bacterial two-hybrid system based on a reconstituted signal transduction pathway. *Proc. Natl. Acad. Sci. U.S.A.* **95,** 5752–5756 CrossRef Medline
25. Sory, M. P., and Cornelis, G. R. (1994) Translocation of a hybrid YopE-adenylate cyclase from *Yersinia enterocolitica* into HeLa cells. *Mol. Microbiol.* **14,** 583–594 CrossRef Medline
26. Osickova, A., Masin, J., Fayolle, C., Krusek, J., Basler, M., Pospisilova, E., Leclerc, C., Osicka, R., and Sebo, P. (2010) Adenylate cyclase toxin translocates across target cell membrane without forming a pore. *Mol. Microbiol.* **75,** 1550–1562 CrossRef Medline
27. Masin, J., Osickova, A., Sukova, A., Fiser, R., Halada, P., Bumba, L., Linhartova, I., Osicka, R., and Sebo, P. (2016) Negatively charged residues of the segment linking the enzyme and cytolysin moieties restrict the membrane-permeabilizing capacity of adenylate cyclase toxin. *Sci. Rep.* **6,** 29137 CrossRef Medline
28. Subrini, O., Sotomayor-Pérez, A. C., Hessel, A., Spiaczka-Karst, J., Selwa, E., Sapay, N., Veneziano, R., Pansieri, J., Chopineau, J., Ladant, D., and Chenal, A. (2013) Characterization of a membrane-active peptide from the *Bordetella pertussis* CyaA toxin. *J. Biol. Chem.* **288,** 32585–32598 CrossRef Medline
29. Voegele, A., Subrini, O., Sapay, N., Ladant, D., and Chenal, A. (2017) Membrane-active properties of an amphitropic peptide from the CyaA toxin translocation region. *Toxins* **9,** 369 CrossRef
30. Basler, M., Knapp, O., Masin, J., Fiser, R., Maier, E., Benz, R., Sebo, P., and Osicka, R. (2007) Segments crucial for membrane translocation and pore-forming activity of *Bordetella* adenylate cyclase toxin. *J. Biol. Chem.* **282,** 12419–12429 CrossRef Medline
31. Juntapremjit, S., Thamwiriyasati, N., Kurehong, C., Prangkio, P., Shank, L., Powthongchin, B., and Angsuthanasombat, C. (2015) Functional importance of the Gly cluster in transmembrane helix 2 of the *Bordetella pertussis* CyaA-hemolysin: implications for toxin oligomerization and pore formation. *Toxicon* **106,** 14–19 CrossRef Medline
32. Masin, J., Roderova, J., Osickova, A., Novak, P., Bumba, L., Fiser, R., Sebo, P., and Osicka, R. (2017) The conserved tyrosine residue 940 plays a key structural role in membrane interaction of *Bordetella* adenylate cyclase toxin. *Sci. Rep.* **7,** 9330 CrossRef Medline
33. Basler, M., Knapp, O., Masin, J., Fiser, R., Maier, E., Benz, R., Sebo, P., and Osicka, R. (1999) An amphipathic alpha-helix including glutamates 509 and 516 is crucial for membrane translocation of adenylate cyclase toxin and modulates formation and cation selectivity of its membrane channels. *J. Biol. Chem.* **274,** 37644–37650 CrossRef Medline
34. Powthongchin, B., and Angsuthanasombat, C. (2009) Effects on haemolytic activity of single proline substitutions in the *Bordetella pertussis* CyaA pore-forming fragment. *Arch. Microbiol.* **191,** 1–9 CrossRef Medline
35. Prangkio, P., Juntapremjit, S., Koehler, M., Hinterdorfer, P., and Angsuthanasombat, C. (2018) Contributions of the Hydrophobic Helix 2 of the *Bordetella pertussis* CyaA-hemolysin to membrane permeabilization. *Protein Pept. Lett.* **25,** 236–243 CrossRef Medline
36. Roderova, J., Osickova, A., Sukova, A., Mikusova, G., Fiser, R., Sebo, P., Osicka, R., and Masin, J. (2019) Residues 529 to 549 participate in membrane penetration and pore-forming activity of the *Bordetella* adenylate cyclase toxin. *Sci. Rep.* **9,** 5758 CrossRef Medline
37. Basar, T., Havlíček, V., Bezoušková, S., Halada, P., Hackett, M., and Šebo, P. (1999) The conserved lysine 860 in the additional fatty-acylation site of *Bordetella pertussis* adenylate cyclase is crucial for toxin function independently of its acylation status. *J. Biol. Chem.* **274,** 10777–10783 CrossRef Medline
38. Hackett, M., Guo, L., Shabanowitz, J., Hunt, D. F., and Hewlett, E. L. (1994) Internal lysine palmitoylation in adenylate cyclase toxin from *Bordetella pertussis*. *Science* **266,** 433–435 CrossRef
39. Hackett, M., Walker, C. B., Guo, L., Gray, M. C., Van Cuyk, S., Ullmann, A., Shabanowitz, J., Hunt, D. F., Hewlett, E. L., and Sebo, P. (1995) Hemolytic, but not cell-invasive activity, of adenylate cyclase toxin is selectively affected by differential fatty-acylation in *Escherichia coli*. *J. Biol. Chem.* **270,** 20250–20253 CrossRef Medline
40. OsičKa, R., OsičKová, A., Basar, T., Guermonprez, P., Rojas, M., Leclerc, C., and Šebo, P. (2000) Delivery of CD8(+) T-cell epitopes into major histocompatibility complex class I antigen presentation pathway by *Bordetella pertussis* adenylate cyclase: delineation of cell invasive structures and permissive insertion sites. *Infect. Immun.* **68,** 247–256 CrossRef Medline
41. Bumba, L., Masin, J., Macek, P., Wald, T., Motlova, L., Bibova, I., Klimova, N., Bednarova, L., Veverka, V., Kachala, M., Svergun, D. I., Barinka, C., and Sebo, P. (2016) Calcium-driven folding of RTX domain β-rolls ratchets translocation of RTX proteins through type I secretion ducts. *Mol. Cell* **62,** 47–62 CrossRef Medline
42. Rose, T., Sebo, P., Bellalou, J., and Ladant, D. (1995) Interaction of calcium with *Bordetella pertussis* adenylate cyclase toxin: characterization of multiple calcium-binding sites and calcium-induced conformational changes. *J. Biol. Chem.* **270,** 26370–26376 CrossRef Medline
43. Rogel, A., and Hanski, E. (1992) Distinct steps in the penetration of adenylate cyclase toxin of *Bordetella pertussis* into sheep erythrocytes: translocation of the toxin across the membrane. *J. Biol. Chem.* **267,** 22599–22605 Medline
44. Bumba, L., Masin, J., Fiser, R., and Sebo, P. (2010) *Bordetella* adenylate cyclase toxin mobilizes its β2 integrin receptor into lipid rafts to accomplish translocation across target cell membrane in two steps. *PLoS Pathog.* **6,** e1000901 CrossRef Medline
45. Fiser, R., Masin, J., Basler, M., Krusek, J., Spulákova, V., Konopásek, I., and Sebo, P. (2007) Third activity of *Bordetella* adenylate cyclase (AC) toxin-hemolysin: membrane translocation of AC domain polypeptide promotes calcium influx into CD11b+ monocytes independently of the catalytic and hemolytic activities. *J. Biol. Chem.* **282,** 2808–2820 CrossRef Medline
46. Karst, J. C., Barker, R., Devi, U., Swann, M. J., Davi, M., Roser, S. J., Ladant, D., and Chenal, A. (2012) Identification of a region that assists membrane insertion and translocation of the catalytic domain of *Bordetella pertussis* CyaA toxin. *J. Biol. Chem.* **287,** 9200–9212 CrossRef Medline
47. González-Bullón, D., Uribe, K. B., Martín, C., and Ostolaza, H. (2017) Phospholipase A activity of adenylate cyclase toxin mediates translocation of its adenylate cyclase domain. *Proc. Natl. Acad. Sci. U.S.A.* **114,** E6784–E6793 CrossRef Medline
48. Bumba, L., Masin, J., Osickova, A., Osicka, R., and Sebo, P. (2018) *Bordetella pertussis* adenylate cyclase toxin does not possess a phospholipase A activity; serine 606 and aspartate 1079 residues are not involved in target cell delivery of the adenylyl cyclase enzyme domain. *Toxins* **10,** 245 CrossRef
49. Masin, J., Osicka, R., Bumba, L., and Sebo, P. (2018) Phospholipase A activity of adenylate cyclase toxin? *Proc. Natl. Acad. Sci. U.S.A.* **115,** E2489–E2490 CrossRef Medline
50. Voegele, A., Sadi, M., Raoux-Barbot, D., Douche, T., Matondo, M., Ladant, D., and Chenal, A. (2019) The adenylate cyclase (CyaA) toxin from *Bordetella pertussis* has no detectable phospholipase A (PLA) activity *in vitro*. *Toxins* **11,** 111 CrossRef
51. Johnsen, N., Hamilton, A. D. M., Greve, A. S., Christensen, M. G., Therkildsen, J. R., Wehmöller, J., Skals, M., and Praetorius, H. A. (2019) α-Haemolysin production, as a single factor, causes fulminant sepsis in a model of *Escherichia coli*-induced bacteraemia. *Cell. Microbiol.* **21,** e13017 CrossRef Medline
52. Schwidder, M., Heinisch, L., and Schmidt, H. (2019) Genetics, toxicity, and distribution of enterohemorrhagic *Escherichia coli* hemolysin. *Toxins* **11,** 502 CrossRef
53. Ristow, L. C., and Welch, R. A. (2016) Hemolysin of uropathogenic *Escherichia coli*: a cloak or a dagger? *Biochim. Biophys. Acta* **1858,** 538–545 CrossRef Medline
54. Hyland, C., Vuillard, L., Hughes, C., and Koronakis, V. (2001) Membrane interaction of *Escherichia coli* hemolysin: flotation and insertion-dependent labeling by phospholipid vesicles. *J. Bacteriol.* **183,** 5364–5370 CrossRef Medline
55. Soloaga, A., Veiga, M. P., García-Segura, L. M., Ostolaza, H., Brasseur, R., and Goñi, F. M. (1999) Insertion of *Escherichia coli* α-haemolysin in lipid bilayers as a non-transmembrane integral protein: prediction and experiment. *Mol. Microbiol.* **31,** 1013–1024 CrossRef Medline

ID: **yadavr** Time: 19:01 I Path: //mbnas01.cadmus.com/home$/yadavr$/SB-JBCJ200040

56. Issartel, J. P., Koronakis, V., and Hughes, C. (1991) Activation of *Escherichia coli* prohaemolysin to the mature toxin by acyl carrier protein-dependent fatty acylation. *Nature* **351,** 759–761 CrossRef Medline
57. Lim, K. B., Walker, C. R., Guo, L., Pellett, S., Shabanowitz, J., Hunt, D. F., Hewlett, E. L., Ludwig, A., Goebel, W., Welch, R. A., and Hackett, M. (2000) *Escherichia coli* α-hemolysin (HlyA) is heterogeneously acylated *in vivo* with 14-, 15-, and 17-carbon fatty acids. *J. Biol. Chem.* **275,** 36698–36702 CrossRef Medline
58. Stanley, P., Packman, L. C., Koronakis, V., and Hughes, C. (1994) Fatty acylation of two internal lysine residues required for the toxic activity of *Escherichia coli* hemolysin. *Science* **266,** 1992–1996 CrossRef
59. Cortajarena, A. L., Goñi, F. M., and Ostolaza, H. (2001) Glycophorin as a receptor for *Escherichia coli* α-hemolysin in erythrocytes. *J. Biol. Chem.* **276,** 12513–12519 CrossRef Medline
60. Lally, E. T., Kieba, I. R., Sato, A., Green, C. L., Rosenbloom, J., Korostoff, J., Wang, J. F., Shenker, B. J., Ortlepp, S., Robinson, M. K., and Billings, P. C. (1997) RTX toxins recognize a β2 integrin on the surface of human target cells. *J. Biol. Chem.* **272,** 30463–30469 CrossRef Medline
61. Ristow, L. C., Tran, V., Schwartz, K. J., Pankratz, L., Mehle, A., Sauer, J. D., and Welch, R. A. (2019) The extracellular domain of the β2 integrin β subunit (CD18) is sufficient for *Escherichia coli* hemolysin and *Aggregatibacter actinomycetemcomitans* leukotoxin cytotoxic activity. *mBio* **10,** e01459–19 Medline
62. Wiles, T. J., and Mulvey, M. A. (2013) The RTX pore-forming toxin α-hemolysin of uropathogenic *Escherichia coli*: progress and perspectives. *Future Microbiol.* **8,** 73–84 CrossRef Medline
63. Ahmad, J. N., Cerny, O., Linhartova, I., Masin, J., Osicka, R., and Sebo, P. (2016) cAMP signalling of *Bordetella* adenylate cyclase toxin through the SHP-1 phosphatase activates the BimEL-Bax pro-apoptotic cascade in phagocytes. *Cell. Microbiol.* **18,** 384–398 CrossRef Medline
64. Cerny, O., Anderson, K. E., Stephens, L. R., Hawkins, P. T., and Sebo, P. (2017) cAMP signaling of adenylate cyclase toxin blocks the oxidative burst of neutrophils through Epac-mediated inhibition of phospholipase C Activity. *J. Immunol.* **198,** 1285–1296 CrossRef
65. Cerny, O., Kamanova, J., Masin, J., Bibova, I., Skopova, K., and Sebo, P. (2015) *Bordetella pertussis* adenylate cyclase toxin blocks induction of bactericidal nitric oxide in macrophages through cAMP-dependent activation of the SHP-1 phosphatase. *J. Immunol.* **194,** 4901–4913 CrossRef
66. Confer, D. L., and Eaton, J. W. (1982) Phagocyte impotence caused by an invasive bacterial adenylate cyclase. *Science* **217,** 948–950 CrossRef
67. Kamanova, J., Kofronova, O., Masin, J., Genth, H., Vojtova, J., Linhartova, I., Benada, O., Just, I., and Sebo, P. (2008) Adenylate cyclase toxin subverts phagocyte function by RhoA inhibition and unproductive ruffling. *J. Immunol.* **181,** 5587–5597 CrossRef
68. Pearson, R. D., Symes, P., Conboy, M., Weiss, A. A., and Hewlett, E. L. (1987) Inhibition of monocyte oxidative responses by *Bordetella pertussis* adenylate cyclase toxin. *J. Immunol.* **139,** 2749–2754 Medline
69. El-Azami-El-Idrissi, M., Bauche, C., Loucka, J., Osicka, R., Sebo, P., Ladant, D., and Leclerc, C. (2003) Interaction of *Bordetella pertussis* adenylate cyclase with CD11b/CD18: role of toxin acylation and identification of the main integrin interaction domain. *J. Biol. Chem.* **278,** 38514–38521 CrossRef Medline
70. Wang, X., Gray, M. C., Hewlett, E. L., and Maynard, J. A. (2015) The *Bordetella* adenylate cyclase repeat-in-toxin (RTX) domain is immunodominant and elicits neutralizing antibodies. *J. Biol. Chem.* **290,** 3576–3591 CrossRef Medline
71. Wang, X., Stapleton, J. A., Klesmith, J. R., Hewlett, E. L., Whitehead, T. A., and Maynard, J. A. (2017) Fine epitope mapping of two antibodies neutralizing the *Bordetella* adenylate cyclase toxin. *Biochemistry* **56,** 1324–1336 CrossRef Medline
72. Wagner, C., Hänsch, G. M., Stegmaier, S., Denefleh, B., Hug, F., and Schoels, M. (2001) The complement receptor 3, CR3 (CD11b/CD18), on T lymphocytes: activation-dependent up-regulation and regulatory function. *Eur. J. Immunol.* **31,** 1173–1180 CrossRef Medline
73. Westrop, G., Hormozi, K., da Costa, N., Parton, R., and Coote, J. (1997) Structure-function studies of the adenylate cyclase toxin of *Bordetella pertussis* and the leukotoxin of *Pasteurella haemolytica* by heterologous C protein activation and construction of hybrid proteins. *J. Bacteriol.* **179,** 871–879 CrossRef Medline
74. Basar, T., Havlíček, V., Bezoušková, S., Hackett, M., and Šebo, P. (2001) Acylation of lysine 983 is sufficient for toxin activity of *Bordetella pertussis* adenylate cyclase: substitutions of alanine 140 modulate acylation site selectivity of the toxin acyltransferase CyaC. *J. Biol. Chem.* **276,** 348–354 CrossRef Medline
75. Rogel, A., Schultz, J. E., Brownlie, R. M., Coote, J. G., Parton, R., and Hanski, E. (1989) *Bordetella pertussis* adenylate cyclase: purification and characterization of the toxic form of the enzyme. *EMBO J.* **8,** 2755–2760 CrossRef Medline
76. Soloaga, A., Ostolaza, H., Goñi, F. M., and de la Cruz, F. (1996) Purification of *Escherichia coli* pro-haemolysin, and a comparison with the properties of mature α-haemolysin. *Eur. J. Biochem.* **238,** 418–422 CrossRef Medline
77. Karst, J. C., Ntsogo Enguene, V. Y., Cannella, S. E., Subrini, O., Hessel, A., Debard, S., Ladant, D., and Chenal, A. (2014) Calcium, acylation, and molecular confinement favor folding of *Bordetella pertussis* adenylate cyclase CyaA toxin into a monomeric and cytotoxic form. *J. Biol. Chem.* **289,** 30702–30716 CrossRef Medline
78. O'Brien, D. P., Cannella, S. E., Voegele, A., Raoux-Barbot, D., Davi, M., Douché, T., Matondo, M., Brier, S., Ladant, D., and Chenal, A. (2019) Post-translational acylation controls the folding and functions of the CyaA RTX toxin. *FASEB J.* **33,** 10065–10076 CrossRef
79. Betsou, F., Sebo, P., and Guiso, N. (1993) CyaC-mediated activation is important not only for toxic but also for protective activities of *Bordetella pertussis* adenylate cyclase-hemolysin. *Infect. Immun.* **61,** 3583–3589 CrossRef Medline
80. Masin, J., Basler, M., Knapp, O., El-Azami-El-Idrissi, M., Maier, E., Konopasek, I., Benz, R., Leclerc, C., and Sebo, P. (2005) Acylation of lysine 860 allows tight binding and cytotoxicity of *Bordetella* adenylate cyclase on CD11b-expressing cells. *Biochemistry* **44,** 12759–12766 CrossRef Medline
81. Bhakdi, S., Greulich, S., Muhly, M., Eberspächer, B., Becker, H., Thiele, A., and Hugo, F. (1989) Potent leukocidal action of *Escherichia coli* hemolysin mediated by permeabilization of target cell membranes. *J. Exp. Med.* **169,** 737–754 CrossRef Medline
82. Bhakdi, S., Muhly, M., Korom, S., and Schmidt, G. (1990) Effects of *Escherichia coli* hemolysin on human monocytes: cytocidal action and stimulation of interleukin 1 release. *J. Clin. Investig.* **85,** 1746–1753 CrossRef Medline
83. Döbereiner, A., Schmid, A., Ludwig, A., Goebel, W., and Benz, R. (1996) The effects of calcium and other polyvalent cations on channel formation by *Escherichia coli* α-hemolysin in red blood cells and lipid bilayer membranes. *Eur. J. Biochem.* **240,** 454–460 CrossRef Medline
84. Gadeberg, O. V., and Orskov, I. (1984) *In vitro* cytotoxic effect of alpha-hemolytic *Escherichia coli* on human blood granulocytes. *Infect. Immun.* **45,** 255–260 CrossRef Medline
85. Keane, W. F., Welch, R., Gekker, G., and Peterson, P. K. (1987) Mechanism of *Escherichia coli* α-hemolysin-induced injury to isolated renal tubular cells. *Am. J. Pathol.* **126,** 350–357 Medline
86. Mobley, H. L., Green, D. M., Trifillis, A. L., Johnson, D. E., Chippendale, G. R., Lockatell, C. V., Jones, B. D., and Warren, J. W. (1990) Pyelonephritogenic *Escherichia coli* and killing of cultured human renal proximal tubular epithelial cells: role of hemolysin in some strains. *Infect. Immun.* **58,** 1281–1289 CrossRef Medline
87. Suttorp, N., Flöer, B., Schnittler, H., Seeger, W., and Bhakdi, S. (1990) Effects of *Escherichia coli* hemolysin on endothelial cell function. *Infect. Immun.* **58,** 3796–3801 CrossRef Medline
88. Cortajarena, A. L., Goni, F. M., and Ostolaza, H. (2003) A receptor-binding region in *Escherichia coli* α-haemolysin. *J. Biol. Chem.* **278,** 19159–19163 CrossRef Medline
89. Masín, J., Konopásek, I., Svobodová, J., and Sebo, P. (2004) Different structural requirements for adenylate cyclase toxin interactions with erythrocyte and liposome membranes. *Biochim. Biophys. Acta* **1660,** 144–154 CrossRef Medline
90. Benz, R., Maier, E., Bauer, S., and Ludwig, A. (2014) The deletion of several amino acid stretches of *Escherichia coli* α-hemolysin (HlyA) suggests that

the channel-forming domain contains beta-strands. *PLoS One* **9,** e112248 CrossRef Medline

91. Valeva, A., Walev, I., Kemmer, H., Weis, S., Siegel, I., Boukhallouk, F., Wassenaar, T. M., Chavakis, T., and Bhakdi, S. (2005) Binding of *Escherichia coli* hemolysin and activation of the target cells is not receptor-dependent. *J. Biol. Chem.* **280,** 36657–36663 CrossRef Medline
92. Khan, F., He, M., and Taussig, M. J. (2006) Double-hexahistidine tag with high-affinity binding for protein immobilization, purification, and detection on Ni-nitrilotriacetic acid surfaces. *Anal. Chem.* **78,** 3072–3079 CrossRef Medline
93. Franken, K. L., Hiemstra, H. S., van Meijgaarden, K. E., Subronto, Y., den Hartigh, J., Ottenhoff, T. H., and Drijfhout, J. W. (2000) Purification of His-tagged proteins by immobilized chelate affinity chromatography: the benefits from the use of organic solvent. *Protein Expr. Purif.* **18,** 95–99 CrossRef Medline
94. Ladant, D. (1988) Interaction of *Bordetella pertussis* adenylate cyclase with calmodulin. Identification of two separated calmodulin-binding domains. *J. Biol. Chem.* **263,** 2612–2618 Medline
95. Benz, R., Janko, K., Boos, W., and Lauger, P. (1978) Formation of large, ion-permeable membrane channels by the matrix protein (porin) of *Escherichia coli*. *Biochim. Biophys. Acta* **511,** 305–319 CrossRef Medline
96. Pérez-Riverol, Y., Csordas, A., Bai, J., Bernal-Llinares, M., Hewapathirana, S., Kundu, D. J., Inuganti, A., Griss, J., Mayer, G., Eisenacher, M., Perez, E., Uszkoreit, J., Pfeuffer, J., Sachsenberg, T., Yilmaz, S., *et al.* (2019) The PRIDE database and related tools and resources in 2019: improving support for quantification data. *Nucleic Acids Res.* **47,** D442–D450 CrossRef Medline

Retargeting from CR3 to the LFA-1 receptor uncovers the adenylyl cyclase enzyme-translocating segment of *Bordetella* adenylate cyclase toxin

Supporting Figures and Tables

Jiri Masin[1,#,*], Adriana Osickova[1,2,#], David Jurnecka[1,2], Nela Klimova[1,2], Humaira Khaliq[1], Peter Sebo[1] and Radim Osicka[1,*]

[1]Institute of Microbiology of the Czech Academy of Sciences, 142 20 Prague, Czech Republic

[2]Faculty of Science, Charles University in Prague, 128 00 Prague, Czech Republic

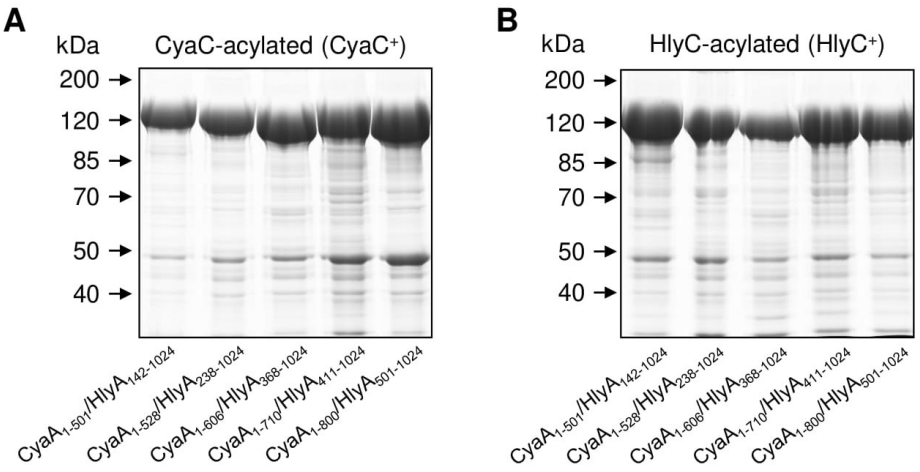

Supporting Figure S1. Expression and purification of the CyaA/HlyA hybrid variants. The CyaC-acylated **(A)** and HlyC-acylated **(B)** proteins were produced in *E. coli* BL21/pMM100 cells and purified by one-step chromatography on calmodulin agarose. The samples were analyzed on 7.5% polyacrylamide gels and stained with Coomassie blue.

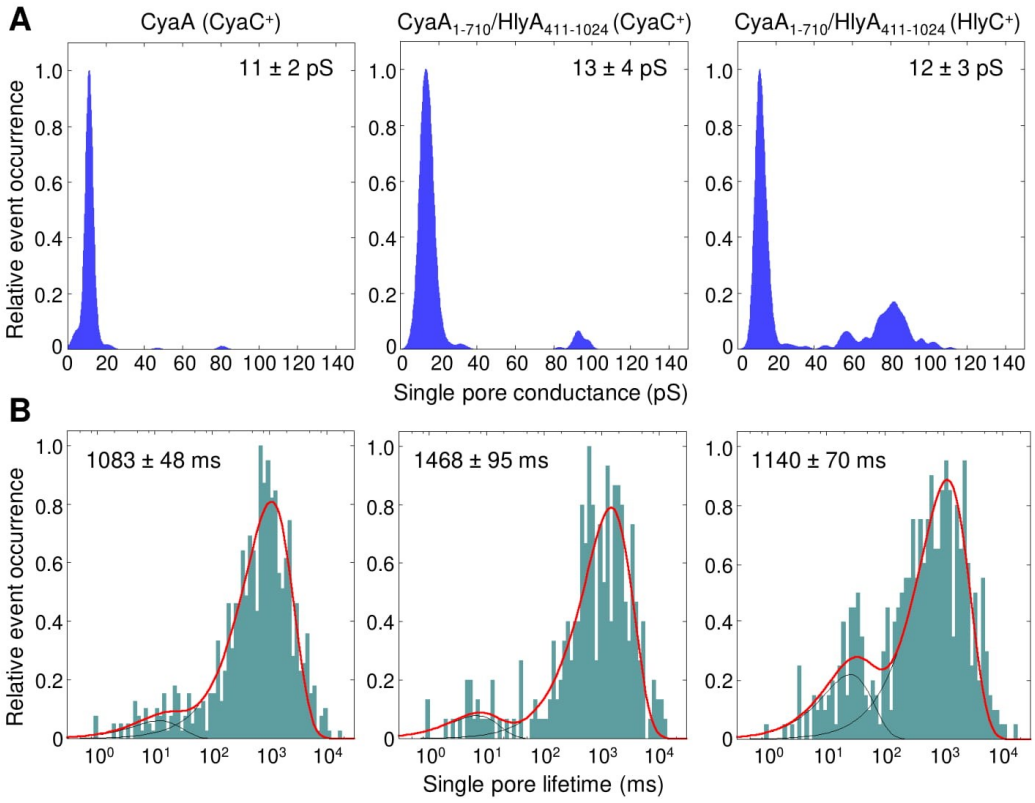

Supporting Figure S2. The hybrid proteins formed single pore conductance units that exhibited similar characteristics as the pores formed by the intact CyaA. **A.** Pore characteristics of CyaA and $CyaA_{1-710}/HlyA_{411-1024}$ variants. Kernel density estimation (KDE) of single-pore conductances of intact CyaA and the $CyaA_{1-710}/HlyA_{411-1024}$ variants calculated from single-pore recordings (>600 events) acquired on several different asolectin membranes at the same conditions as in Fig. 4A and a protein concentration of 10 pM (CyaA) or 80 pM (hybrid molecules). The numbers represent the most frequent conductances ± standard deviations of pores formed by intact CyaA and the $CyaA_{1-710}/HlyA_{411-1024}$ variants. **B.** For lifetime determination, approximately 400 of individual pore openings were recorded on several different asolectin membranes with 10 pM intact CyaA or 80 pM $CyaA_{1-710}/HlyA_{411-1024}$ variants at the same conditions as in Fig. 4A and the logarithmic histogram of dwell times was fitted with a double-exponential function. The error estimates of lifetimes were obtained by bootstrap analysis. The numbers in each panel represent the most frequent values ± standard deviations.

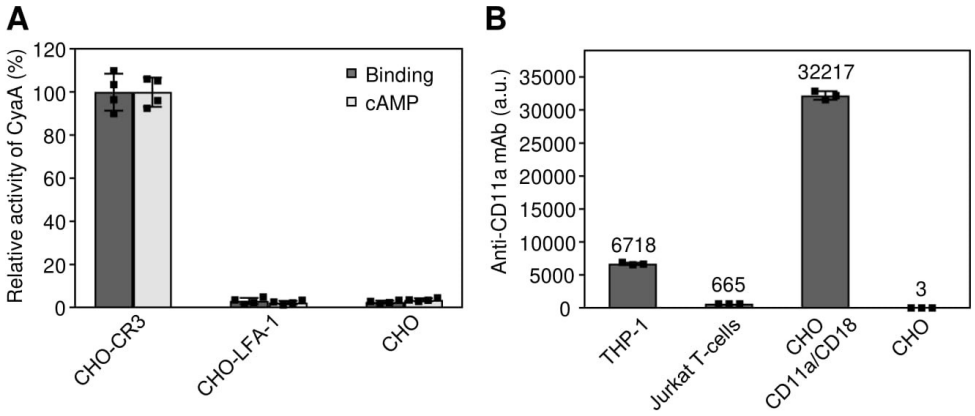

Supporting Figure S3. CyaA preferentially binds CR3-positive cells. **A.** Binding of intact CyaC-acylated CyaA to CHO cells expressing CR3 or LFA-1, or mock transfected CHO cells (1×10^6) was determined as the amount of total cell-associated AC enzyme activity upon incubation of cells with 5 nM toxin for 30 min at 4 °C. The cAMP intoxication was assessed by determining the intracellular concentration of cAMP generated in cells after 30 min of incubation of cells (1×10^5) with 0.5 nM intact CyaA. Activities are expressed as percentages of intact CyaA activity on CHO-CR3 cells and represent average values ± standard deviations from two independent determinations performed in duplicate. **B.** Expression of LFA-1 on the surface of different cell types. 2×10^5 cells were incubated with the CD11a-specific MEM-25 mAb conjugated with APC for 30 min at 4 °C and analyzed by flow cytometry. Each bar represents the mean value with standard deviation of three determinations.

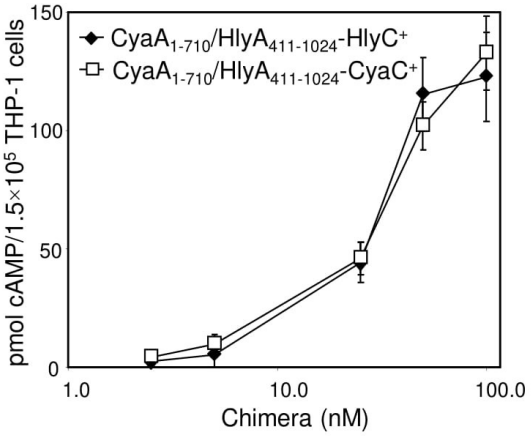

Supporting Figure S4. The monoacylated $CyaA_{1-710}/HlyA_{411-1024}$ chimera intoxicated the LFA-1-expressing THP-1 cells to the same levels as the doubly acylated HlyC-activated hybrid. cAMP intoxication was assessed by determining the intracellular concentration of cAMP after 30 min of incubation of 1.5×10^5 THP-1 cells with chimeric toxins (n=3) in D-MEM medium.

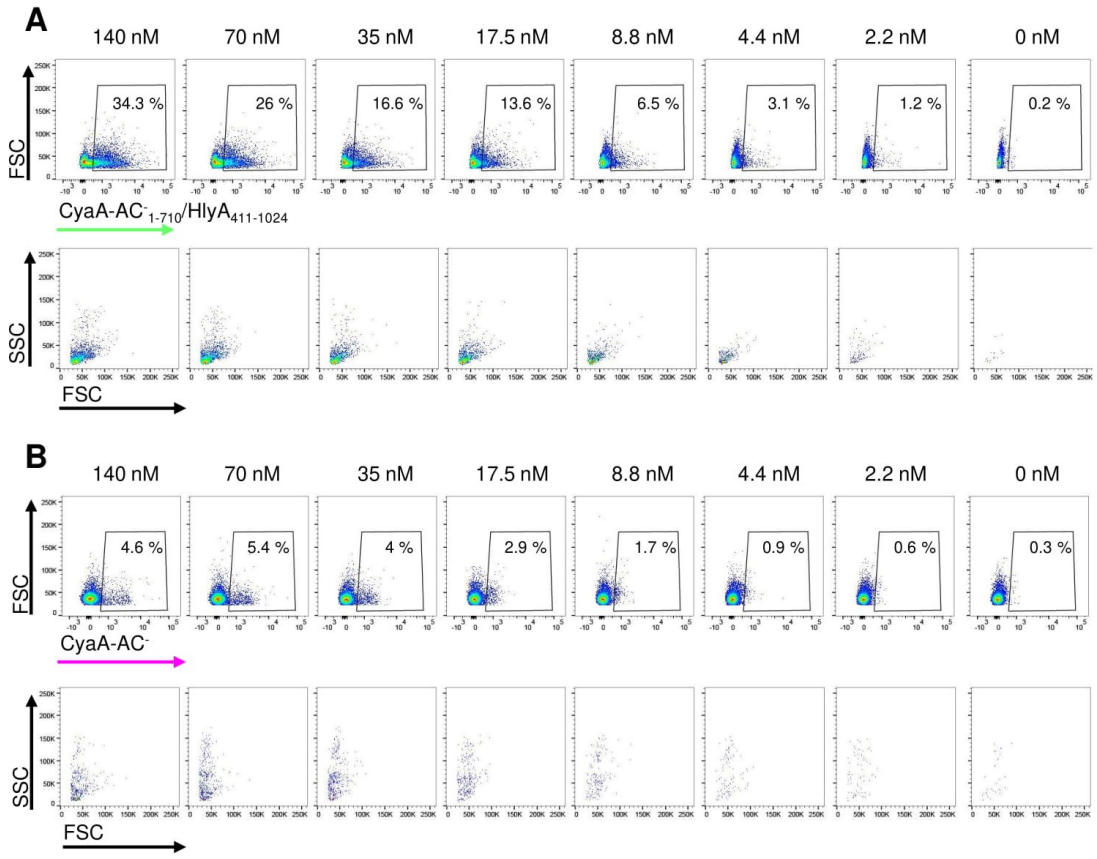

Supporting Figure S5. Titration of Dy495-labeled CyaA-AC$^{-}_{1\text{-}710}$/HlyA$_{411\text{-}1024}$ and Dy650-labeled CyaA-AC^{-} on spleen cells *in-vitro*. Spleen cell suspensions (1×10^{6}) prepared from a 7-week-old Balb/c mouse were incubated *in-vitro* with a range of equimolar concentrations of CyaA-AC$^{-}_{1\text{-}710}$/HlyA$_{411\text{-}1024}$-Dy495 or CyaA-AC^{-}-Dy650, added separately. Binding of CyaA-AC$^{-}_{1\text{-}710}$/HlyA$_{411\text{-}1024}$-Dy495 **(A)** or CyaA-AC^{-}-Dy650 **(B)**, shown as percentages of cells positive for the corresponding fluorochrome, gated out of live cells (top panels in **A**, **B**) and SSC vs. FSC dot plots of positive cells (lower panels in **A**, **B**).

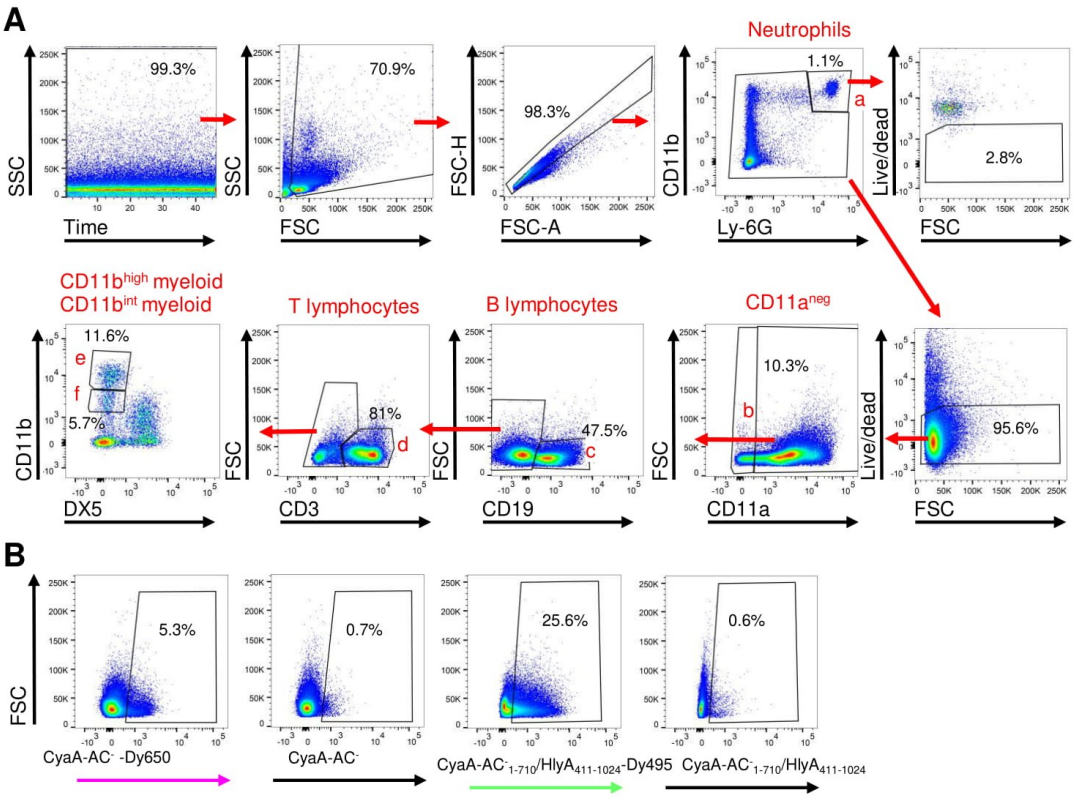

Supporting Figure S6. Gating strategy used for immunophenotyping of mouse spleen cell populations. **A.** Single cells suspensions were obtained after enzymatical digestion of mouse spleens. Cells were then stained with a cocktail of fluorescently-labeled antibodies against cell surface antigens. A sequential gating strategy was used to eliminate unstable flow of cells (SSC vs. time), debris (SSC vs. FSC) and doublets (FSC-H vs. FSC-A). Neutrophils (a) were gated out as Ly-6G^{+}CD11b^{int}, and this population was detected as dead by the FVD live/dead stain.Next, non-leucocytes were gated as CD11a^{neg} (b) out of live, non-neutrophil cells. Immune cells (CD11a^{+}) were then divided into B lymphocytes (CD19^{+}) (c) and T lymphocytes (CD3^{+}) (d). Gating on CD11b on Lineage^{neg} (CD19^{-}CD3^{-}DX5^{-}) cells allowed the separation of CD11b^{high} myeloid cells (Lin^{neg} CD11b^{high}) (e) and CD11b^{int} myeloid cells (Lin^{neg} CD11b^{int}); the two populations contain a mixture of myeloid cells (dendritic cells, macrophages, other granulocytes and monocytes). FSC, forward scatter; SSC, side scatter; lineage^{neg} cells; FVD, eBioscience™ Fixable Viability Dye eFluor™ 780. **B.** Gating of cells positive for fluorescently-labeled CyaA-AC$^{-}_{1-710}$/HlyA$_{411-1024}$-Dy495 or CyaA-AC^{-}-Dy650. Spleen single cell suspensions from a 7-week-old Balb/c mouse were incubated with an equimolar mixture of 56 nM fluorescently-labeled or of 56 nM non-fluorescent CyaA-AC$^{-}_{1-710}$/HlyA$_{411-1024}$ and CyaA-AC^{-} for 30 min at 4°C. Gates positive for CyaA-AC$^{-}_{1-710}$/HlyA$_{411-1024}$-Dy495 and CyaA-AC^{-}-Dy650 were set on live cells in order to have an equal background fluorescence in the sample stained with non-fluorescent CyaA-AC$^{-}_{1-710}$/HlyA$_{411-1024}$ and CyaA-AC^{-}.

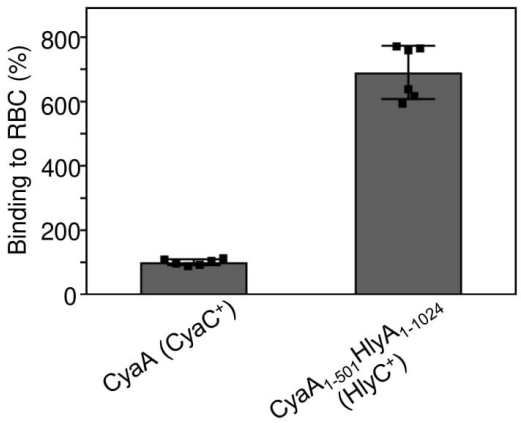

Supporting Figure S7. The HlyC-activated $CyaA_{1-501}HlyA_{1-1024}$ protein, harboring the AC domain and the adjacent membrane binding and destabilizing C-terminal segment of CyaA (residues 1-501 of CyaA) fused to a full length α-hemolysin (residues 1-1024 of HlyA) was constructed by PCR mutagenesis, expressed in *E. coli* BL-21 pMM100 and purified from urea extract by chromatography on Calmodulin Sepharose. Sheep erythrocytes (5 x 10^8/ml) were incubated in TNC (Tris-HCl 50 mM, NaCl 150 mM, $CaCl_2$ 2 mM, pH 7.4) buffer in the presence of 75 mM sucrose as osmoprotectant at 37°C with 0.5 nM purified proteins and after 30 min, aliquots were taken for determinations of the cell-associated AC activity (Binding). Binding activity of HlyC-activated $CyaA_{1-501}HlyA_{1-1024}$ was expressed as percentage of intact CyaC-activated CyaA activity and represent average values ± standard deviations from three independent determinations performed in duplicate with two different toxin preparations.

Supporting Table S1. Comparison of binding of the CyaA-AC$^{-}_{1-710}$/HlyA$_{411-1024}$ and CyaA-AC^{-} proteins added to spleen cells separately or in a mixture.

Protein	**CyaA-AC$^{-}_{1-710}$/HlyA$_{411-1024}$**		**CyaA-AC^{-}**	
Experimental set-up	**SS**	**Mix**	**SS**	**Mix**
Cell population	**Binding to cells [%]**			
CD11a^{neg}	42.7	11.8	1.1	0.5
B lymphocytes	46.6	34.7	1.4	4.2
T lymphocytes	6.6	5.9	2.7	3.1
Neutrophils	99.3	97.0	100.0	99.9
CD11b^{high} myeloid cells	97.3	93.8	98.7	96.3
CD11b^{int} myeloid cells	89.9	84.2	36.4	36.0

[a]Spleen single cell suspensions from a 7-week-old Balb/c mouse were incubated *in-vitro* with 56 nM CyaA-AC$^{-}_{1-710}$/HlyA$_{411-1024}$-Dy495 or 56 nM of CyaA-AC^{-}-Dy650 added separately (SS), or with an equimolar mixture of 56 nM CyaA-AC$^{-}_{1-710}$/HlyA$_{411-1024}$-Dy495 and CyaA-AC^{-}-Dy650 (Mix) for 30 min at 4 °C. Spleen cells were then stained with a cocktail of fluorescently-labeled antibodies against cell surface antigens and analyzed by flow cytometry. Values indicate percentages of CyaA-AC$^{-}_{1-710}$/HlyA$_{411-1024}$ -Dy495- or CyaA-AC^{-}-Dy650-positive cells in each population.

Supporting Table S2. List of used antibodies.

Antibody	Company	Reference	Target Species	Host Species	Isotype	Clone	Fluorochrome
CD3	BD Horizon	560771	Mouse	Hamster	IgG_2, κ	500A2	V500
Anti-CD49b (Integrin α2)	eBioscience	48-5971-82	Mouse	Rat	IgM, κ	DX5	eF450
CD19	eBioscience	56-0193-82	Mouse	Rat	IgG2a, κ	eBio1D3	A700
Ly-6G	Biolegend	127617	Mouse	Rat	IgG2a, κ	1A8	PE-Cy7
CD11a	eBioscience	46-0111-80	Mouse	Rat	IgG2a, κ	M17/4	PerCP-eF710
CD11b	BD Pharmingen	553311	Mouse	Rat	IgG2b, κ	M1/70	PE
IgG2a	eBioscience	46-4321-82	Mouse	Rat	IgG2a, κ	eBR2a	PerCP-eF710
IgG2b	BD Pharmingen	556925	Mouse	Rat	IgG2b, κ	A95-1	PE